Quantum Electromagnetics

A Local-Ether Wave Equation Unifying Quantum Mechanics, Electromagnetics, and Gravitation

Ching-Chuan Su

National Tsing Hua University press

Quantum Electromagnetics

Ching-Chuan Su

National Tsing Hua University press
March 2008

Quantum Electromagnetics

A Local-Ether Wave Equation Unifying Quantum Mechanics, Electromagnetics, and Gravitation

Ching-Chuan Su

Quantum Electromagnetics

A Local-Ether Wave Equation Unifying Quantum Mechanics,
Electromagnetics, and Gravitation

Ching-Chuan Su
Department of Electrical Engineering
National Tsinghua University
Hsinchu, Taiwan

ISBN 957-29880-9-3
Copyright © 2008 by
National Tsing Hua University press
Printed in Taiwan
March 2008

Printed in Taiwan

Quantum Electromagnetics

A Local-Ether Wave Equation Unifying Quantum Mechanics, Electromagnetics, and Gravitation

Ching-Chuan Su
Department of Electrical Engineering
National Tsinghua University
Hsinchu, Taiwan

ISBN 957-29880-9-3
Copyright © 2008 by
National Tsing Hua University press
Printed in Taiwan
March 2008

Printed in Taiwan

To the memory of my *agong* (grandfather),
a peasant whose lifetime perspiration in the fields inspires me.

Preface

This book presents a local-ether wave equation for electromagnetic and matter waves. From this wave equation, a time evolution equation is derived, which represents modifications of Schrödinger's equation. From this modified equation, an electromagnetic force law is derived, which represents modifications of the Lorentz force law. From the modified force law, relationships between electric and magnetic fields are derived, which represent modifications of Maxwell's equations. By refining the wave equation with a gravitational potential, the gravitational force and the mass are derived. Moreover, numerous consequences of the wave equation can account for a wide variety of important experiments in modern physics, the special relativity, and the general relativity. Thereby, the local-ether wave equation unifies quantum mechanics, electromagnetics, and gravitation.

To explore the physical origins of electromagnetic force is my dream since my undergraduate study, even though it is beyond the scope of electromagnetics. The mechanism with which a time-varying electric current affects a charged particle at a distance forms the basis of wireless communication and deeply attracts me. This electric induction force due to a time-varying current is expected to have a close relationship with the magnetic induction force due to a relative motion between a charged particle and a static current. These two induction forces together with the electrostatic and the magnetostatic force form the electromagnetic force. In a study of quantum mechanics, I learned that Schrödinger's equation incorporating the vector potential is a clue to the induction forces. And in a study of propagation properties of waveguide modes, I found a speed-dependent square-root factor quite similar to the famous one in the Lorentz mass-variation law or in the time dilation and length contraction in the special relativity. This inspired me with the idea that mass could have a connection with wave motion. Then I was endowed by myself with an ambitious plan to construct a new theory of electromagnetics in which the Lorentz force law and then Maxwell's equations are consequences of mathematical derivations from a fundamental equation. This theory had better can be constructed without resort to the intricate Lorentz transformation of space and time. However, my exploration lacked specific directions and was just like a wandering meditation for several years.

The first step in the progress of the new theory was made in the beginning years of my teaching career. In 1986 a light was shed on me that the magnetic force observed in ordinary experiments is actually due to the conduction current, rather than the convection current which has been widely adopted in the formulations since the early development of electromagnetics. The conduction current in a metal wire is actually formed by the mobile electrons electrically neutralized by the accompanying ions. For such a neutralized current, it is the drift speed of the mobile charged particles with respect to the neutralizing matrix that determines the current. Consequently, the current density in Ampère's law complies with the principle of relativity simply based on Galilean transformations. Further, the drift speed is quite low owing to collision. Thus, if the electric scalar potential is modified by incorporating an additional small part associated with the squared velocity difference between the affected and the source particles, the magnetostatic force can be derived as the corresponding modification of the electrostatic force. This idea leads to the augmented scalar potential on which the modified Lorentz force law complying with Galilean transformations is based.

Thereafter, the origin of the magnetic vector potential associated with the induction forces and the corresponding quantum theory of the electromagnetic force are the next targets of the exploration. In 1995, after numerous attempts, another important idea came to me that a plausible approach is to simply drop the magnetic vector potential. Correspondingly, Schrödinger's equation is modified by connecting the electric scalar potential with a new operator which in turn corresponds to the squared velocity difference that leads to the magnetostatic force. This idea laid the cornerstone of the quantum theory for the electromagnetic force law based on the augmented potentials. In the meantime, I found the wave equation that can lead to the modified Schrödinger equation. A quantum theory formulated in a wave equation is more appealing, since it makes matter wave closer to electromagnetic wave in nature. More specifically, from the wave equation the mass-variation factor can be derived without invoking any particular space-time transformation. In many experiments that claim to support the special relativity, the evidence merely relies on a quantity associated with this factor.

viii

Now, everything is ready, except for the keystone: how does wave propagate? This made me exhaust my imagination for years to construct and test a number of propagation models. I examined a lot of propagation experiments with several plausible models. But it appeared that no single model can fit all. One night in the spring of 1999, in a repeated examination of the effects of earth's rotational and orbital motions on terrestrial and extraterrestrial waves, one idea struck me that the classical propagation model can work if it is endowed with a characteristic of uniqueness and switchability. That is, the propagation medium is unique but not universal. The actual one depends on the location of the wave: earthbound, interplanetary, or interstellar. The medium is expected to be associated with and to move with the gravitational potential of each celestial body. Thereby, the concept of the local-ether model came out. Further, the role of the gravitational potential in the wave equation and the consequences were explored. Finally, after seemingly endless efforts to make the formulations more rigorous and compact, the arguments stricter, and the descriptions more precise, this book was brought forth.

It is something like Don Quixote's tilting at windmills to claim that this theory is correct by directly fighting against some others which have been well established for about one century. Rather, I would like to say that this book is intended to give a self-consistent and rigorous theory based on the local-ether wave equation, of which numerous consequences have been carefully examined with a wide variety of experiments. The results are encouraging. Nevertheless, the scrutiny never suffices and more consequences and some improvements are yet to be explored, such as those concerning the location and properties of the interface between the earth and the sun local ether. Further, this theory may advance with a great step forward by exploring the origin of the ether, the matter wave, or of the potentials, or by incorporating the spin into the wave equation, which are ignored so far. I sincerely expect that this book will be read or examined in a critical but open-minded manner. I also anticipate that the theory of *Quantum Electromagnetics* is breaking new ground which will attract more people to cultivate and harvest their new attempts.

Ching-Chuan Su
Hsinchu, Taiwan
February 2005

Contents

Introduction 1

I.1 Review of Conventional Electromagnetics 2
I.2 Review of Special Relativity 6
I.3 Review of Quantum Mechanics 9
I.4 Outline of Quantum Electromagnetics 10
    I.4.1 Local-ether model of wave propagation
    I.4.2 Classical theory of local-ether electromagnetics
    I.4.3 Quantum theory of electromagnetic and gravitational forces
    I.4.4 Quantum theory of speed-dependent mass and wave properties

Chapter 1 Local-Ether Model of Wave Propagation

1.1 Motivation for Local-Ether Model 19
1.2 Classical Propagation Model and Sagnac Effect 20
1.3 Propagation Mechanisms and Sagnac Effects in High-Precision Experiments 24
    1.3.1 Global positioning system
    1.3.2 Intercontinental microwave link
    1.3.3 Interplanetary radar
1.4 Discrepancy in Effects of Earth's Motions 30
1.5 Local-Ether Propagation Model 34
1.6 Reexamination of Various Propagation Phenomena 37
    1.6.1 Round-trip Sagnac effect in monostatic radar
    1.6.2 Round-trip Sagnac effect in Michelson-Morley experiment
    1.6.3 Sagnac effect in loop interferometer
    1.6.4 Constancy of speed of light
    1.6.5 Spatial isotropy in geostationary path or cavity

Contents

Introduction 1

I.1 Review of Conventional Electromagnetics 2
I.2 Review of Special Relativity 6
I.3 Review of Quantum Mechanics 9
I.4 Outline of Quantum Electromagnetics 10
  I.4.1 Local-ether model of wave propagation
  I.4.2 Classical theory of local-ether electromagnetics
  I.4.3 Quantum theory of electromagnetic and gravitational forces
  I.4.4 Quantum theory of speed-dependent mass and wave properties

Chapter 1 Local-Ether Model of Wave Propagation

1.1 Motivation for Local-Ether Model 19
1.2 Classical Propagation Model and Sagnac Effect 20
1.3 Propagation Mechanisms and Sagnac Effects in High-Precision Experiments 24
  1.3.1 Global positioning system
  1.3.2 Intercontinental microwave link
  1.3.3 Interplanetary radar
1.4 Discrepancy in Effects of Earth's Motions 30
1.5 Local-Ether Propagation Model 34
1.6 Reexamination of Various Propagation Phenomena 37
  1.6.1 Round-trip Sagnac effect in monostatic radar
  1.6.2 Round-trip Sagnac effect in Michelson-Morley experiment
  1.6.3 Sagnac effect in loop interferometer
  1.6.4 Constancy of speed of light
  1.6.5 Spatial isotropy in geostationary path or cavity

    1.6.6 Doppler effect and Roemer's observations
    1.6.7 Spatial anisotropy in CMBR
    1.6.8 Gravitational effects on wave propagation
1.7 Unsolved and Predicted Propagation Phenomena 50
    1.7.1 Stellar aberration
    1.7.2 One-way-link rotor experiment
    1.7.3 Second-order radar Doppler shift

Chapter 2 Modifications of Lorentz Force Law

2.1 Frame-Invariance of Electromagnetic Force 57
2.2 Augmented Potentials and Electromagnetic Force Law 60
2.3 Augmented Potentials under Neutralization 63
2.4 Force Law under Low-Speed Condition 64
2.5 Sagnac-Effect Deviation and Galilean Relativity 66
2.6 Extra Force Terms 69

Chapter 3 Modifications of Maxwell's Equations

3.1 Issue of Reference Frame in Electromagnetics 74
3.2 Modified Lorentz Force Law 76
3.3 Local-Ether Wave Equations for Potentials 78
3.4 Local-Ether Wave Equations for Fields 79
3.5 Reexamination of Various Interference Experiments 84
    3.5.1 Phase variation with moving medium and path
    3.5.2 Geostationary fiber-link experiment
    3.5.3 Sagnac rotating-loop experiments
    3.5.4 Fizeau's experiment with moving medium
3.6 Derivation of Modifications of Maxwell's Equations 92

Chapter 4 Modifications of Schrödinger's Equation

4.1 Force Law and Wave Equation 101
4.2 Local-Ether Wave Equation and Evolution Equation 102
4.3 Derivation of Electrostatic Force and Mass 105
4.4 Local-Ether Wave Equation with Augmentation Operator 108
4.5 Derivation of Local-Ether Electromagnetic Force 109
4.6 Augmented Potentials under Weak-Potential and Low-Speed Conditions 112
4.7 Comparison with Schrödinger's Equation 115

Chapter 5 Unified Quantum Theory of Electromagnetic and Gravitational Forces

5.1 Gravitational Effects 122
5.2 Local-Ether Wave Equation with Gravitational Potential 123
5.3 Derivation of Unified Quantum Theory 126
5.4 Reexamination of Evidence for General Relativity 128
  5.4.1 Increments of propagation time and radar echo time
  5.4.2 Gravitational deflection of light
  5.4.3 Gravitational redshift
  5.4.4 Spatial distributions of wavefunctions in gravitational redshift experiments

Chapter 6 Speed-Dependent Mass and Quantum Energy

6.1 Speed-Dependence of Atomic Clock Rate 141
6.2 Evolution Equation beyond Low-Speed Condition 142
6.3 Particle Velocity and Speed-Dependent Mass 145
6.4 Speed-Dependent Quantum Energy 147
6.5 Reexamination of Experiments with Atomic Clock Rate 150
  6.5.1 Gravitation- and speed-dependent transition frequency
  6.5.2 Clock-rate difference in Hafele-Keating experiment
  6.5.3 Clock-rate adjustment in GPS
  6.5.4 Frequency shifts in earthbound and interplanetary spacecraft microwave links
  6.5.5 Spatial isotropy in Hughes-Drever experiment

Chapter 7 Resonant Absorption between Moving Atoms

7.1 Frequency Shifts 161
7.2 Higher-Order Doppler Frequency Shift 163
7.3 Quantum Energy Variation and Resonant-Absorption Condition 165
7.4 Reexamination of Resonant-Absorption Experiments 168
  7.4.1 Ives-Stilwell experiment
  7.4.2 Output frequency from ammonia masers
  7.4.3 Mössbauer rotor experiment
  7.4.4 Spatial isotropy, terrestrial isotropy, Galilean relativity, and their breakdowns

Chapter 8 Interference of Matter Wave

8.1 Properties of Matter Wave 181
8.2 Local-Ether Wave Equation for Free Particle 182
8.3 Dispersion of Matter Wave 183
8.4 Mass, Energy, and Momentum 185
8.5 Reexamination of Matter-Wave Interference Experiments 189
  8.5.1 Bragg reflection of matter wave
  8.5.2 Predicted anisotropy in Bragg angle due to earth's rotation
  8.5.3 Effect of earth's gravity in neutron interferometry
  8.5.4 Effect of earth's rotation in neutron interferometry
  8.5.5 Matter-wave Sagnac effect in rotating loop

Epilogue 203

Appendices 207
Bibliography 215
Index 229

Introduction

The theory of *Quantum Electromagnetics* presents a wave equation which is constructed, in compliance with Galilean transformations, for electromagnetic and matter waves. A fundamental feature entirely different from the principle of relativity is that the wave equation is referred specifically to the proposed local-ether frame. For electromagnetic wave, the local-ether wave equation accounts for a wide variety of experiments on propagation and interference. For matter wave, the wave equation leads to modifications of Schrödinger's equation which in turn lead to a unified quantum theory of electromagnetic and gravitational forces in conjunction with the origin and the identity of inertial and gravitational mass. Further, it leads to modifications of the Lorentz force law and of Maxwell's equations. Moreover, the wave equation leads to the dispersion of matter wave, from which the speed-dependence in the mass of a particle and in the wavelength, angular frequency, and quantum energy of a matter wave can be derived. The consequences of the wave equation are in accord with a wide variety of experiments that are commonly ascribed to the special relativity, the general relativity, the Lorentz mass-variation law, or to the de Broglie matter wave. Thereby, the local-ether wave equation unifies quantum mechanics, electromagnetics, and gravitation.

To begin with, we review the conventional electromagnetics and discuss its fundamental difficulty with reference frames. Next, we review the special relativity and discuss how it deals with reference frames. Then we review quantum mechanics and discuss its relationship with the electromagnetic force. Finally, we outline the quantum electromagnetics by presenting the fundamental equations and their various consequences.

I.1 Review of Conventional Electromagnetics

The conventional electromagnetics starts from Maxwell's equations

$$\begin{cases} \nabla \cdot \mathbf{E}(\mathbf{r},t) = \dfrac{1}{\epsilon_0}\rho(\mathbf{r},t) & \text{(I.1a)} \\[2ex] \nabla \times \mathbf{E}(\mathbf{r},t) = -\dfrac{\partial}{\partial t}\mathbf{B}(\mathbf{r},t) & \text{(I.1b)} \\[2ex] \nabla \cdot \mathbf{B}(\mathbf{r},t) = 0 & \text{(I.1c)} \\[2ex] \nabla \times \mathbf{B}(\mathbf{r},t) = \mu_0\mathbf{J}(\mathbf{r},t) + \dfrac{1}{c^2}\dfrac{\partial}{\partial t}\mathbf{E}(\mathbf{r},t). & \text{(I.1d)} \end{cases}$$

In these equations the electric field $\mathbf{E}$ and the magnetic field $\mathbf{B}$ are related to each other and to the sources represented by the charge density ρ and the current density $\mathbf{J}$ through their spatial and temporal derivatives in a coupled way. These relations are individually known as Gauss's law for the electric field, Faraday's law, Gauss's law for the magnetic field, and Ampère's law, respectively.

It is known that in the presence of electric and magnetic fields, the electromagnetic force exerted on a particle of charge q and velocity $\mathbf{v}$ is given by the Lorentz force law

$$\mathbf{F}(\mathbf{r},t) = q\left\{\mathbf{E}(\mathbf{r},t) + \mathbf{v} \times \mathbf{B}(\mathbf{r},t)\right\}. \tag{I.2}$$

This force law and Maxwell's equations form the fundamental equations adopted by Lorentz in the early development of electromagnetics [71]. It is noted that the four relations in Maxwell's equations are not all independent, as the two Gauss's laws can be derived from the other two relations with appropriate initial conditions [107].

The conventional electromagnetics can be expressed in an alternative way, by which the Lorentz force law is given directly in terms of the scalar and the vector potential originating from the charge and the current density, respectively. It is supposed that the Lorentz force law can be given in terms of the scalar potential Φ and the vector potential $\mathbf{A}$ in the form

$$\mathbf{F}(\mathbf{r},t) = q\left\{-\nabla\Phi(\mathbf{r},t) - \frac{\partial}{\partial t}\mathbf{A}(\mathbf{r},t) + \mathbf{v} \times \nabla \times \mathbf{A}(\mathbf{r},t)\right\}. \tag{I.3}$$

The term associated with the gradient of the scalar potential, with the time derivative of the vector potential, and the one with the particle velocity are known as the electrostatic force, the electric induction force, and the magnetic force, respectively.

Quantitatively, the scalar and the vector potential are given explicitly in terms of the charge density ρ and the current density $\mathbf{J}$ respectively by the volume integrals

$$\Phi(\mathbf{r}, t) = \frac{1}{4\pi\epsilon_0} \int \frac{\rho(\mathbf{r}', t - R/c)}{R} dv' \tag{I.4}$$

and

$$\mathbf{A}(\mathbf{r}, t) = \frac{\mu_0}{4\pi} \int \frac{\mathbf{J}(\mathbf{r}', t - R/c)}{R} dv', \tag{I.5}$$

where $R = |\mathbf{r} - \mathbf{r}'|$, c is the speed of light, R/c is the propagation delay time from the source point $\mathbf{r}'$ to the field point $\mathbf{r}$, and the permeability μ_0 and the permittivity ϵ_0 are related by $\mu_0\epsilon_0 = 1/c^2$. It is noticed that these retarded potentials were first introduced by L. V. Lorenz (rather than H. A. Lorentz) in as early as 1867, only two years after the first publication of Maxwell's electromagnetic theory of light [73, 80, 114, 84, 50].

According to the dependences of the force terms in (I.3) on the particle velocity $\mathbf{v}$, one is led to the explicit definitions of the electric and the magnetic field in terms of the potentials. That is,

$$\mathbf{E}(\mathbf{r}, t) = -\nabla\Phi(\mathbf{r}, t) - \frac{\partial}{\partial t}\mathbf{A}(\mathbf{r}, t) \tag{I.6}$$

and

$$\mathbf{B}(\mathbf{r}, t) = \nabla \times \mathbf{A}(\mathbf{r}, t). \tag{I.7}$$

Thereby, the fields $\mathbf{E}$ and $\mathbf{B}$ can be expressed explicitly in terms of the charge and current densities.

It can be shown that the potentials given explicitly in (I.4) and (I.5) satisfy the wave equations (for a derivation, see Appendix A)

$$\nabla^2\Phi(\mathbf{r}, t) - \frac{1}{c^2}\frac{\partial^2}{\partial t^2}\Phi(\mathbf{r}, t) = -\frac{1}{\epsilon_0}\rho(\mathbf{r}, t) \tag{I.8}$$

and

$$\nabla^2\mathbf{A}(\mathbf{r}, t) - \frac{1}{c^2}\frac{\partial^2}{\partial t^2}\mathbf{A}(\mathbf{r}, t) = -\mu_0\mathbf{J}(\mathbf{r}, t). \tag{I.9}$$

As in a fluid, it is known that the density of a convection current is related to the associated charge density by $\mathbf{J} = \rho\mathbf{v}_c$, where $\mathbf{v}_c$ is the velocity of the mobile charged particles forming this current.

By virtue of the conservation of charge, the current and charge densities are also related to each other by the continuity equation

$$\nabla \cdot \mathbf{J}(\mathbf{r},t) = -\frac{\partial}{\partial t}\rho(\mathbf{r},t). \tag{I.10}$$

Then it can be shown that the two potentials are related to each other by (for a derivation, see [114, 107] or Appendix A)

$$\nabla \cdot \mathbf{A}(\mathbf{r},t) = -\frac{1}{c^2}\frac{\partial}{\partial t}\Phi(\mathbf{r},t). \tag{I.11}$$

This important relation for the potentials was first introduced also by Lorenz (rather than Lorentz) in 1867 [73, 114, 84, 50]. In standard textbooks on electromagnetics [49, 95], this Lorenz gauge comes from an assumption before the potentials themselves are given.

Then, based on the definitions of the fields in terms of the potentials, one can derive the divergence and the curl relations for the fields. By applying the curl and the divergence to both sides of the definitions of the fields **E** and **B** in terms of the potentials, respectively, one immediately obtains (I.1b) and (I.1c). Besides, by applying the divergence and the curl to both sides of these two definitions, respectively, one has

$$\nabla \cdot \mathbf{E}(\mathbf{r},t) = -\nabla^2\Phi(\mathbf{r},t) - \frac{\partial}{\partial t}\nabla \cdot \mathbf{A}(\mathbf{r},t) \tag{I.12}$$

and

$$\nabla \times \mathbf{B}(\mathbf{r},t) = -\nabla^2\mathbf{A}(\mathbf{r},t) + \nabla\nabla \cdot \mathbf{A}(\mathbf{r},t). \tag{I.13}$$

Then, by using the Lorenz gauge, the wave equations for the potentials, and the explicit definition of the electric field, it is easy to show that the preceding two equations become (I.1a) and (I.1d), respectively [125]. Thus the derived divergence and curl relations for the fields **E** and **B**, which in turn are defined explicitly in terms of the potentials, are just Maxwell's equations. In other words, Maxwell's equations can be viewed as mathematical consequences derived from the Lorentz force law (I.3) in terms of the potentials.

It is generally expected from intuition that the electromagnetic force exerted on a charged particle should remain unchanged when observed in different reference frames. In classical mechanics the principle of relativity is widely accepted, which states that no reference frames in uniform motion of translation to each other are preferred. Some fundamental formulas, such as Newton's laws of motion and the conservation laws for momentum and kinetic energy, are known to be invariant under Galilean transformations.

However, from a classical viewpoint, the conventional electromagnetics has a fundamental difficulty with reference frames, as many of the preceding formulas involve velocity or time derivative. Obviously, the velocity of a particle is different in different frames. To be invariant, the velocity should be relative or referred to a specific frame. Moreover, based on Galilean transformations, the time derivative of a function of space and time also depends on reference frames, while the spatial derivative remains unchanged in different frames.

Consider two reference frames, where frame 2 is moving at a speed v along the x direction with respect to frame 1. Based on Galilean transformations, the time t of the two frames is identical, while the x coordinates of the two frames are related to each other by

$$x_2 = x_1 - vt, \tag{I.14}$$

where the origins of the two frames are supposed to coincide at the instant $t = 0$.

Accordingly, the time derivative of an arbitrary function f of space and time taken under the condition of x_1 being fixed tends to be different from the one taken under the corresponding condition of x_2 being fixed at a given position. Quantitatively, the two time derivatives are related to each other by

$$\left.\frac{\partial f}{\partial t}\right|_{x_2=const} = \left.\frac{\partial f}{\partial t}\right|_{x_1=const} + v\frac{\partial f}{\partial x}. \tag{I.15}$$

Thus the time derivative $\partial f/\partial t$ observed in a chosen reference frame can be expressed in terms of the derivative $(\partial f/\partial t)_k$ observed in another frame which moves at a velocity $\mathbf{v}_k$ with respect to the chosen frame. Quantitatively, the time derivatives observed in these two frames at a given position are related to each other by

$$\left(\frac{\partial f(\mathbf{r},t)}{\partial t}\right)_k = \frac{\partial f(\mathbf{r},t)}{\partial t} + \mathbf{v}_k \cdot \nabla f(\mathbf{r},t), \tag{I.16}$$

where the time derivatives $\partial f/\partial t$ and $(\partial f/\partial t)_k$ are understood to be taken under constant $\mathbf{r}$ and $(\mathbf{r} - \mathbf{v}_k t)$, respectively, as $\mathbf{r}$ is referred to the chosen frame.

Further, from the preceding relation, the second time derivatives observed in these two frames are related to each other by

$$\left(\frac{\partial^2 f(\mathbf{r},t)}{\partial t^2}\right)_k = \frac{\partial^2 f}{\partial t^2} + 2\left(\mathbf{v}_k \cdot \nabla\right)\frac{\partial f}{\partial t} + \left(\mathbf{v}_k \cdot \nabla\right)\left(\mathbf{v}_k \cdot \nabla\right) f. \tag{I.17}$$

The preceding two Galilean formulas have been given in the literature (see, for example, [108, 10, 49]). It is seen that the difference between two first or second time derivatives in different frames depends on the relative velocity $\mathbf{v}_k$ between the two frames.

Therefore, in order for their values to remain unchanged in different frames, the time derivatives as well as the velocity should be referred to their respective frames. However, the reference frame of the particle velocity in the Lorentz force law and the one of the propagation velocity in the integral formulas for the potentials are not specified. Similarly, the particle velocity associated with the current density given in Ampère's law or in the integral formula or wave equation for the vector potential is ambiguous in reference frames. Moreover, in Ampère's law, Faraday's law, the definition of the electric field, the wave equations for the potentials, the continuity equation, and in the Lorenz gauge, the reference frames of the various time derivatives are also not specified. Thus, with the obscurity in reference frames, it appears that Maxwell's equations and the Lorentz force law are not invariant under Galilean transformations.

I.2 Review of Special Relativity

As well as classical mechanics, the special relativity presumes the principle of relativity as one of its two basic postulates. Meanwhile, in order to account for the invariance of Maxwell's equations with respect to reference frames, Lorentz, Poincaré, and then Einstein introduced the Lorentz transformation of space and time, instead of Galilean transformations [71, 114, 24]. Thereby, it has been found that Maxwell's equations together with the Lorentz force law are invariant in different frames in uniform relative motion of translation and then are in accord with the principle of relativity. A derivation of the invariance under the Lorentz transformation is discussed briefly in what follows.

Suppose that two reference frames are moving with a relative speed v along the x direction and that the origins of the two frames coincide at the instant $t = 0$. The Lorentz transformation of space and time states that the coordinate x and time t in frame 1 are related to those in frame 2 in a symmetric way by

$$\begin{cases} x_2 = \gamma(x_1 - \tau_1 v/c) & \text{(I.18a)} \\ \tau_2 = \gamma(\tau_1 - x_1 v/c), & \text{(I.18b)} \end{cases}$$

where $\tau = ct$ and $\gamma = 1/\sqrt{1 - v^2/c^2}$. Meanwhile, the coordinates y and z are unaltered in the two frames. This transformation is self-consistent, since it is easy to show that the inverse transformation is given by

$$\begin{cases} x_1 = \gamma(x_2 + \tau_2 v/c) & \text{(I.18c)} \\ \tau_1 = \gamma(\tau_2 + x_2 v/c), & \text{(I.18d)} \end{cases}$$

with the sign before v being changed. Conversely, the requirement of self-consistence necessitates the introduction of the famous γ factor.

As space and time are supposed to be coupled to each other, both the spatial and the temporal derivative of a function of space and time tend to change in different frames. Quantitatively, by using the chain rule, it is easy to show that the pair of partial derivatives $(\partial f/\partial x, -\partial f/\partial \tau)$ of a function f of space and time transform in the same way as the pair (x, τ) given in the preceding formula, while the derivatives $\partial f/\partial y$ and $\partial f/\partial z$ are unaltered in the two frames. Further, it can be shown that the difference $\partial^2 f/\partial x^2 - \partial^2 f/\partial \tau^2$ as well as the derivatives $\partial^2 f/\partial y^2$ and $\partial^2 f/\partial z^2$ remains unchanged in different frames. That is, the d'Alembert operator $(\nabla^2 - \partial^2/\partial \tau^2)$ is invariant under the Lorentz transformation.

Due to the transformations of the coordinate x and time t, the density and velocity will transform accordingly. By using the transformations of the density and velocity, it can be derived that the pair of the current and charge densities $(J_x, \rho c)$ transform in the same way as (x, τ), where J_x is the x component of the current density $\mathbf{J} = \rho \mathbf{v}$ and $\mathbf{v}$ is the velocity of the mobile charged particles forming this convection current [74]. Meanwhile, the components J_y and J_z are unaltered. Similarly, from the wave equations for the potentials, it is seen that the pair of the vector and scalar potentials $(A_x, \Phi/c)$ as well as the pair $(J_x, \rho c)$ transform just as (x, τ), while A_y and A_z are unaltered. And it can be shown that the continuity equation together with the Lorenz gauge is Lorentz invariant, by using a derivation similar to that for the d'Alembert operator.

From the definitions of the fields in terms of the potentials, it can be shown, with the use of the transformations of the potentials and the partial derivatives, that the pair of the field components (E_y, cB_z) along with the pair $(E_z, -cB_y)$ also transform just as (x, τ), while the components E_x and B_x are unaltered. Thereafter, by using the transformations of the fields, of the partial derivatives, and of the current and charge densities, it can be shown that Maxwell's equations are invariant under the Lorentz transformation. Besides, it can be shown that the electromagnetic force given in terms of the transformations of the fields and the velocity is exactly identical to the force given in terms of the transformation of the time rate of change of momentum [74]. Thereby, the Lorentz force law together with Maxwell's equations is Lorentz invariant and hence no reference frames are preferred.

A direct consequence of the Lorentz transformation is the time dilation, which has been adopted to account for the east-west directional anisotropy in clock rate observed in the Hafele-Keating experiment with circumnavigation atomic clocks [39]. Another consequence is the second-order Doppler effect, which has been adopted to account for the frequency shift associated with the light emitted from fast-moving hydrogen atoms observed in the Ives-Stilwell experiment [33]. Moreover, the velocity addition encountered in the aforementioned transformation of current and charge densities has also been adopted to account for Fizeau's interference experiment dealing with the speed of light in a flowing water [33].

Further, through a quite indirect way of dealing with the case of an elastic or inelastic collision between two identical particles, the speed-dependent mass m is derived [74, 49, 9, 37]. This gives

$$m = m_0 \frac{1}{\sqrt{1 - v^2/c^2}}, \tag{I.19}$$

where m_0 and v are the rest mass and speed of the particle, respectively. This famous formula was first introduced by Lorentz before the advent of the special relativity [71]. The Lorentz mass-variation law in turn has been adopted in the postulates of de Broglie for the angular frequency and wavelength of matter wave. These speed-dependent properties have been used to account for Bucherer's experiment dealing with the variation of mass of high-energy electrons, and for the Davisson-Germer experiment dealing with the scattering of accelerated electrons from the surface of a metal crystal (see, for example, [3, 26]).

As no reference frames are preferred, the experiments dealing with propagation time, phase variation, frequency, mass, or with matter wavelength are then expected to be independent of the position and orientation of the Earth in space. Hence the experimental results are expected to be independent of the rotational and orbital motions of the Earth. This spatial isotropy has been adopted to account for the stability of phase or frequency with respect to time in numerous experiments, including the Kennedy-Thorndike experiment [54], the one-way fiber-link experiment [60], the Hughes-

Drever experiment [45], the Mössbauer rotor experiment [111], and the ammonia-maser experiment [17]. The famous null effect in the Michelson-Morley experiment can also be ascribed to this isotropy. The various experiments associated with the mass-variation factor, the velocity addition, or the spatial isotropy are commonly cited as evidence supporting the special relativity.

I.3 Review of Quantum Mechanics

We then briefly discuss the relationship between the Lorentz force law and Schrödinger's equation in quantum mechanics. It is well known that in the presence of the scalar potential Φ and the vector potential $\mathbf{A}$, Schrödinger's equation reads

$$i\hbar\frac{\partial}{\partial t}\psi(\mathbf{r},t) = \frac{1}{2m_0}[\mathbf{p} - q\mathbf{A}(\mathbf{r},t)]^2\psi(\mathbf{r},t) + q\Phi(\mathbf{r},t)\psi(\mathbf{r},t), \qquad (\text{I.20})$$

where the momentum operator $\mathbf{p} = -i\hbar\nabla$, and m_0 and q are the rest mass and charge of the particle represented by the wavefunction ψ, respectively. According to this equation, the scalar and the vector potential tend to affect the evolution of the wavefunction with time. As in electromagnetics, the reference frames of the position vector and time derivative are not specified.

It is well known that Schrödinger's equation leads to quantum states of matter waves of electrons bound in atoms or molecules. Each quantum state has a specific energy associated with the angular frequency of the wavefunction ψ. The quantum energies can be modified by interactions of atoms with electromagnetic potentials from an external source. The quantum energy has been demonstrated extensively in atomic spectra, as the frequency of the light emitted from or absorbed by an atom is given by the transition frequency associated with the difference in energy between two quantum states participating in the transition.

Schrödinger's equation is also expected to govern the motion of unbound particles under the influence of the potentials. In quantum mechanics, the position of a particle is given by the expectation value of the position operator $\mathbf{r}$, where the expectation value of an operator O is given by the volume integral as $\langle O\rangle = \int \psi^* O\psi dv$. Then the velocity of the particle is given by the time derivative of the expectation value of the position operator $\mathbf{r}$. That is,

$$\mathbf{v} = \frac{d}{dt}\langle\mathbf{r}\rangle\,. \qquad (\text{I.21})$$

By expanding the preceding derivative according to Schrödinger's equation, one has

$$\mathbf{v} = \frac{1}{m_0} \langle \mathbf{p} - q\mathbf{A} \rangle . \tag{I.22}$$

It is noted that the vector potential takes part in the particle velocity.

Further, by using the law of motion $\mathbf{F} = m_0 d\mathbf{v}/dt$ and by expanding the time derivative of $\langle \mathbf{p} - q\mathbf{A} \rangle$ according to Schrödinger's equation again, it can be shown that the electromagnetic force exerted on the charged particle due to the potentials is given by [99]

$$\mathbf{F} = -q\nabla\Phi - q\frac{\partial \mathbf{A}}{\partial t} + \frac{1}{2m_0} q \left\{ \langle (\mathbf{p} - q\mathbf{A}) \times \mathbf{B} \rangle \; - \; \langle \mathbf{B} \times (\mathbf{p} - q\mathbf{A}) \rangle \right\} , \tag{I.23}$$

where $\mathbf{B} = \nabla \times \mathbf{A}$. This force formula is known as the generalization of Ehrenfest's theorem.

As noted in [99], the operator $\mathbf{p}$ involved in $(\mathbf{p} - q\mathbf{A})$ does not commute with the field $\mathbf{B}$. Thus the force law given by the preceding formula does not agree exactly with the Lorentz force law (I.3). The discrepancy between these two force formulas is expected to be $(i\hbar q/2m_0)\nabla \times \mathbf{B}$. Although this discrepancy may be small in magnitude, it has not yet solved to our knowledge.

I.4 Outline of Quantum Electromagnetics

While Maxwell's equations and the Lorentz force law can be shown to be in accord with the principle of relativity by resorting to the Lorentz transformation, it is noticed that the magnetic force observed in ordinary experiments is actually due to the conduction current rather than the convection current. Unlike the convection current, the conduction current is electrically neutralized, such as the familiar one formed by the mobile electrons embedded in the positive ions in a metal wire. For such a neutralized current, it is the drift speed of the mobile charged particles with respect to the neutralizing matrix that determines the current. Consequently, the current density in Ampère's law complies with the principle of relativity simply based on Galilean transformations. Further, the drift speed is quite low ordinarily. If the magnetic force is associated with the squared velocity difference between the involved particles, then, as well as the drift speed, the particle velocity in the Lorentz force law can be referred specifically to the neutralizing matrix. Thus at least some of the major motivations for introducing the Lorentz transformation can be accounted for from an entirely different approach.

The theory of *Quantum Electromagnetics* presents a local-ether wave equation which in turn leads to numerous consequences in accord with a wide variety of experiments. First of all, the local-ether model of wave propagation is proposed in Chapter 1, from which the unique reference frame of the presented wave equation is determined. Then, in order to comply with Galilean transformations and the local-ether propagation model, we present a new classical force law which leads to modifications of the Lorentz force law and of Maxwell's equations, as discussed in Chapters 2 and 3. Further, it is shown in Chapters 4 and 5 that the local-ether wave equation leads to a unified quantum theory of electromagnetic and gravitational forces together with the identity of inertial and gravitational mass. Moreover, it is shown in Chapters 6–8 that the local-ether wave equation leads to the speed-dependence in the mass of a particle, in the angular frequency and wavelength of a matter wave, and in the quantum energy of the matter wave bound in an atom.

I.4.1 Local-ether model of wave propagation

In Chapter 1 it is proposed that electromagnetic wave can be viewed as propagating via a medium like the ether. However, the ether is not universal. Specifically, it is proposed that in the region under a sufficient influence of the gravitation due to the Earth, the Sun, or another celestial body, there forms a local ether which in turn is stationary with respect to the gravitational potential of the respective body [117]. Thus each local ether together with the gravitational potential moves with the associated celestial body. Each individual local ether is finite in extent and may be wholly immersed in another local ether of larger extent. Thus the local ethers may form a multiple-level hierarchy. For earthbound waves, the medium is the earth local ether which is stationary in an earth-centered inertial frame, while the sun local ether for interplanetary waves is stationary in a heliocentric inertial frame. Consequently, the propagation of earthbound waves can depend on earth's rotation but is entirely independent of earth's orbital motion around the Sun or whatever, while the propagation of interplanetary waves depends on the orbital motion around the Sun as well as on the rotation.

This local-ether model has been adopted to account for the effects of earth's motions in a wide variety of propagation phenomena, particularly the Sagnac pseudorange correction in the global positioning system (GPS), the time comparison via the intercontinental microwave link, and the echo time in the interplanetary radar. As examined within the present precision, the local-ether model is still in accord with the Michelson-Morley experiment which is known to make the classical ether notion obsolete. Moreover, this local-ether model is in accord with the Sagnac effect in loop interferometers; the constancy of the speed of light with binary stars, synchrotron electrons, and with semistable particles; the spatial isotropy in the Kennedy-Thorndike experiment, the cavity heterodyne experiment, and in the one-way fiber-link experiment; the Doppler effect in GPS, radar, Roemer's observations, and in the stellar frequency shift; and with the dipole anisotropy in the cosmic microwave background radiation. Meanwhile, the one-way-link rotor experiment is proposed to test the local-ether propagation model [117, 118].

Further, matter wave associated with particles is supposed to follow the local-ether propagation model and then be governed by a wave equation. Quantitatively, it is postulated that a particle is represented by a matter wave Ψ, which in turn is governed by the nonhomogeneous wave equation proposed to be

$$\left\{\nabla^2 - \frac{1}{c^2}\frac{\partial^2}{\partial t^2}\right\}\Psi(\mathbf{r},t) = \frac{\omega_0^2}{c^2}\Psi(\mathbf{r},t), \tag{I.24}$$

where the position vector $\mathbf{r}$ and the time derivative are referred uniquely to the associated local-ether frame, c is the speed of light, and the natural frequency ω_0 is supposed to be an inherent constant of the particle represented by the wavefunction Ψ.

This wave equation looks like the Klein-Gordan equation for free particles, except the reference frame. If the natural frequency is zero, the equation reduces to the homogeneous wave equation for electromagnetic wave in free space. As a consequence, it implies that the propagation speed of electromagnetic wave is c when referred to the specific frame.

I.4.2 Classical theory of local-ether electromagnetics

Under the influence of the electric scalar potential, the local-ether wave equation given in the following subsection leads to an electromagnetic force law in terms of the augmented potentials $\breve{\Phi}$ and $\breve{\mathbf{A}}$, which in turn are derived from the electric scalar potential by incorporating a velocity difference between the effector and the source particles. That is, the electromagnetic force exerted on an effector particle of charge q is given by $\mathbf{F} = q\{-\nabla\breve{\Phi} - (\partial\breve{\mathbf{A}}/\partial t)_e\}$, where the time derivative is referred specifically to the effector frame in which the effector is stationary.

In Chapter 2 this force law is taken as a postulate. Then it can be shown that under the common low-speed condition, where the source particles forming the conduction current drift very slowly in a neutralizing matrix (such as electrons in a metal wire), the force law reduces to [130]

$$\mathbf{F}(\mathbf{r},t) = q\left\{-\nabla\Phi(\mathbf{r},t) - \left(\frac{\partial}{\partial t}\mathbf{A}(\mathbf{r},t)\right)_m + \mathbf{v}_{em}\times\nabla\times\mathbf{A}(\mathbf{r},t)\right\}, \tag{I.25}$$

where the electric scalar potential Φ is due to the net charge density ρ_n and the magnetic vector potential $\mathbf{A}$ is due to the neutralized current density $\mathbf{J}_n$ which in turn is related to the source charge density by $\mathbf{J}_n = \mathbf{v}_{sm}\rho_v$.

This equation represents modifications of the Lorentz force law. The fundamental modifications are that the source velocity $\mathbf{v}_{sm}$ associated with the current density generating the vector potential, the time derivative of this potential in the electric induction force, and the effector velocity $\mathbf{v}_{em}$ connecting to the curl of this potential in the magnetic force are all referred specifically to the matrix frame in which the matrix is stationary, and that the propagation velocity of the potentials is referred specifically to the local-ether frame. Thus the electromagnetic force remains unchanged in different frames in uniform motion of translation, as expected intuitively. It is pointed out that this new classical model is identical to the Lorentz force law, if the latter is observed in the matrix frame as done tacitly in common practice.

Based on the local-ether model of wave propagation and the corresponding electromagnetic force law, the wave equations for the potentials, the continuity equation, and the Lorenz gauge are reexamined in Chapter 3. Then the divergence and curl relations for the electric and magnetic fields are derived. These relations read [131]

$$\left\{\begin{aligned}
\nabla\cdot\mathbf{E}(\mathbf{r},t) &= \frac{1}{\epsilon_0}\rho_n(\mathbf{r},t) && \text{(I.26a)}\\
\nabla\times\mathbf{E}(\mathbf{r},t) &= -\left(\frac{\partial}{\partial t}\mathbf{B}(\mathbf{r},t)\right)_m && \text{(I.26b)}\\
\nabla\cdot\mathbf{B}(\mathbf{r},t) &= 0 && \text{(I.26c)}\\
\nabla\times\mathbf{B}(\mathbf{r},t) &= \mu_0\mathbf{J}_n(\mathbf{r},t) + \frac{1}{c^2}\left(\frac{\partial}{\partial t}\mathbf{E}(\mathbf{r},t)\right)_m, && \text{(I.26d)}
\end{aligned}\right.$$

apart from some deviation terms which are relatively small. This set of relations represent modifications of Maxwell's equations, which comply with Galilean transformations and the local-ether propagation model. The fundamental modifications are that the time derivatives in the two curl relations and the neutralized current density are all referred specifically to the matrix frame.

Further, from the wave equations for the potentials, the local-ether wave equations for the fields are derived. Then the phase speed of electromagnetic wave in a moving medium is derived. Thereby, it is found that the wave equation for the electric field is in accord with several precision interference experiments, including the one-way-link experiment with a geostationary fiber, the Sagnac rotating-loop experiments with a comoving or a geostationary dielectric medium, and Fizeau's experiment with a moving dielectric medium in a geostationary interferometer [132].

I.4.3 Quantum theory of electromagnetic and gravitational forces

In Chapter 4 the local-ether wave equation is proposed to incorporate the electric scalar potential which in turn connects with the augmentation operator. Quantitatively, it is postulated that the matter wave Ψ of a particle of natural frequency ω_0 and charge q is governed by the nonhomogeneous wave equation proposed to be [120, 134]

$$\left\{\nabla^2 - \frac{1}{c^2}\frac{\partial^2}{\partial t^2}\right\}\Psi(\mathbf{r},t) = \frac{\omega_0^2}{c^2}\left\{1 + 2\frac{q\Phi}{\hbar\omega_0}(1+U)\right\}\Psi(\mathbf{r},t), \qquad \text{(I.27)}$$

where the augmentation operator $U = \frac{1}{2}\{(-ic/\omega_0)\nabla - \mathbf{v}_s/c\}^2$. This operator is derived from the Laplace operator by incorporating the source velocity $\mathbf{v}_s$ in the local-ether frame, and tends to enhance the effects of the electric scalar potential and the Laplace operator.

For a harmonic-like wavefunction, a first-order time evolution equation can be derived from the wave equation. For an effector moving slowly with respect to the local-ether frame, the evolution equation becomes

$$i\hbar\frac{\partial}{\partial t}\psi(\mathbf{r},t) = \frac{1}{2m_0}\mathbf{p}^2\psi(\mathbf{r},t) + q\Phi(\mathbf{r},t)\left\{1 + \frac{(\mathbf{p} - m_0\mathbf{v}_s)^2}{2m_0^2c^2}\right\}\psi(\mathbf{r},t), \qquad \text{(I.28)}$$

where the reduced wavefunction ψ is related to the wavefunction Ψ by $\Psi(\mathbf{r},t) = \psi(\mathbf{r},t)e^{-i\omega_0 t}$ and the rest mass is related to the natural frequency by $m_0 = \hbar\omega_0/c^2$.

This evolution equation represents modifications of Schrödinger's equation. The fundamental modification is that the time derivative is referred specifically to the local-ether frame. Furthermore, the vector potential in Schrödinger's equation does not appear in the evolution equation and its effects are implied in the augmentation operator connected with the electric scalar potential.

By following the procedure in deriving Ehrenfest's theorem in quantum mechanics, this modified equation leads to the local-ether electromagnetic force law based on the augmented potentials proposed earlier. Furthermore, it is found that the inertial mass of a charged particle under the influence of the electromagnetic force originates from the natural frequency and hence from the temporal variation of the wavefunction Ψ.

In the presence of the gravitational potential due to a celestial body, it is supposed that the d'Alembert operator in the wave equation needs a refinement. Quantitatively, it is postulated in Chapter 5 that under the influence of the gravitational potential Φ_g and the electric scalar potential Φ, the local-ether wave equation takes the form

$$\left\{\frac{1}{n_g}\nabla^2 - \frac{n_g}{c^2}\frac{\partial^2}{\partial t^2}\right\}\Psi(\mathbf{r},t) = \frac{\omega_0^2}{c^2}\left\{1 + 2\frac{q\Phi}{\hbar\omega_0}(1+U)\right\}\Psi(\mathbf{r},t), \quad (\text{I.29})$$

where the gravitational index n_g is given in terms of the gravitational potential by $n_g(\mathbf{r}) = 1 + 2\Phi_g(\mathbf{r})/c^2$.

Again, from this wave equation, a time evolution equation similar to Schrödinger's equation can be derived. Then the electrostatic and the gravitational force can be derived in a quantum-mechanical way [121]. That is,

$$\mathbf{F} = -q\nabla\Phi + m_0\nabla\Phi_g, \quad (\text{I.30})$$

where the effects of the augmentation operator are omitted for simplicity. Another important consequence is that the gravitational mass associated with the gravitational force as well as the inertial mass is identical to the natural frequency, aside from a common scaling factor. Thereby, the local-ether wave equation leads to a unified quantum theory of electromagnetic and gravitational forces in conjunction with the origin and the identity of inertial and gravitational mass.

For an electron bound in an atom, it is found that the gravitational potential causes a proportional decrease in the energy of each quantum state of the matter wave. The corresponding gravitation-dependence of the transition frequency between two quantum states (to be given in the following subsection) is in accord with the gravitational redshift demonstrated in the Pound-Rebka experiment. Moreover, for electromagnetic wave with a zero natural frequency, the wave equation leads to the deflection of light by the Sun and the increment of echo time in the interplanetary radar [122]. Thereby, alternative interpretations of the evidence supporting the general theory of relativity are provided. However, a discrepancy is that the derived gravitational redshift originates from a quantum nature of the matter wave bound in the involved atom.

I.4.4 Quantum theory of speed-dependent mass and wave properties

In Chapters 6–8, the speed-dependent properties of matter wave of free and bound particles are explored, with the restriction on the particle speed being removed. By using the dispersion of matter wave and by evaluating the particle velocity from the first-order time evolution equation derived from the wave equation, the speed-dependent angular frequency ω and propagation vector $\mathbf{k}$ of a matter wave are derived in Chapter 6. That is, $\hbar\omega = mc^2$ and $\hbar\mathbf{k} = m\mathbf{v}$, where the speed-dependent mass is given by

$$m = m_0 \frac{1}{\sqrt{1 - v^2/c^2}} \tag{I.31}$$

and the particle velocity $\mathbf{v}$ is referred specifically to the local-ether frame. These formulas are identical to the postulates of de Broglie and the Lorentz mass-variation law (I.19), except the reference frame.

By using this mass and Galilean transformations, the time evolution equation for an electron bound in a moving atom becomes a form similar to Schrödinger's equation with the time derivative being multiplied by the mass-variation factor [123]. That is,

$$i\hbar \frac{m}{m_0} \frac{\partial}{\partial t} \psi(\mathbf{r}, t) = -\frac{\hbar^2}{2m_0} \nabla^2 \psi(\mathbf{r}, t) + q\Phi(\mathbf{r})\psi(\mathbf{r}, t), \tag{I.32}$$

where the position vector $\mathbf{r}$ and hence the time derivative are referred to the atom frame in which the nucleus of the atom is stationary.

Thereby, the energy of each quantum state in a moving atom is lowered by this factor. When the gravitational redshift is also taken into account, the transition frequency between two quantum states decreases as

$$f = f_0(1 - v^2/2c^2 - \Phi_g/c^2), \tag{I.33}$$

where v is the atom speed with respect to the local-ether frame and f_0 is the rest transition frequency of the atom when it is stationary and at a zero gravitational potential. The speed- and the gravitation-induced frequency shift derived from the local-ether wave equation are identical to those based on the special and the general relativity, respectively, except the reference frame of the atom velocity.

As the atomic clock rate is determined by the transition frequency, it is pointed out that the local-ether model is actually in accord with the east-west directional anisotropy and the clock-rate difference observed in the Hafele-Keating experiment with circumnavigation atomic clocks, with the synchronism and the clock-rate adjustment in GPS, and with the spatial isotropy associated with frequency stability in the Hughes-Drever experiment. The frequency shifts in an earthbound and an interplanetary spacecraft microwave link are also discussed. Meanwhile, by virtue of a discrepancy in the reference frame chosen for the clock at the ground station in an interplanetary microwave link, the local-ether wave equation predicts a constant deviation in frequency shift from the calculated result reported in the literature, which provides a means to test its validity [123].

In Chapter 7 we present the resonant-absorption condition between moving atoms, by taking both the Doppler frequency shift for electromagnetic wave and the quantum energy variation of matter wave into account. Several phenomena associated with both electromagnetic and matter waves are accounted for, including the Ives-Stilwell experiment with fast-moving hydrogen atoms, the output frequency from ammonia masers, and the Mössbauer rotor experiment [137].

Finally, based on the speed-dependent matter wavelength, the interference between matter waves of two coherent particle beams is explored in Chapter 8. It is elucidated that the local-ether wave equation is in accord with the Davisson-Germer experiment on the Bragg reflection and with other electron-wave interference experiments on the double-slit diffraction and the Sagnac effect, as examined within the present precision. Moreover, it accounts for the effects of earth's rotation and gravity in the neutron-wave loop interferometry [139, 124]. Meanwhile, the local-ether wave equation predicts an anisotropy in the Bragg angle in neutron diffraction due to earth's rotation, which then provides another means to test its validity.

Chapter 1

Local-Ether Model of Wave Propagation

It is pointed out that the classical propagation model can be in accord with the Sagnac effect due to earth's rotational and orbital motions in the high-precision global positioning system (GPS) and interplanetary radar, if the reference frame of the classical propagation medium is endowed with a switchability according to the location of the wave. Accordingly, it is postulated that, as in an obsolete theory, electromagnetic wave propagates via a medium like the ether. However, the ether is not universal. It is proposed that in the region under a sufficient influence of the gravitation due to the Earth, the Sun, or another celestial body, there forms a local ether, which in turn is stationary with respect to the gravitational potential of the respective body. For earthbound or interplanetary waves, the medium is stationary in a geocentric or a heliocentric inertial frame, respectively. Electromagnetic wave propagates at a constant speed with respect to the associated local ether, independent of the motions of the source and the receiver. Based on this local-ether model, a wide variety of earthbound, interplanetary, and interstellar propagation phenomena of electromagnetic wave are accounted for. Strong evidence for this new classical model is its consistent account of the Sagnac effect due to earth's motions among GPS, the intercontinental microwave link, and the interplanetary radar. Moreover, as examined within the present precision, this model is still in accord with the Michelson-Morley experiment. To test the local-ether propagation model, a one-way-link rotor experiment is proposed.

1.1 Motivation for Local-Ether Model

Light is a ubiquitous phenomenon in everyday life. The exploration of the speed of light and the propagation mechanism began a long time ago. A pioneer investigation by Roemer was associated with observations in interplanetary astronomy in as early as 1675, where the apparent time interval between two successive eclipses of a moon of Jupiter was repeatedly recorded over a long duration of a couple of months [33]. It has been found that the apparent interval is a function of earth's position in its orbit around the Sun and depends on the radial speed of the Earth relative to Jupiter, where the speed is mainly due to earth's orbital motion. This variation of the apparent interval demonstrates that the speed of light is finite. Further, with the astronomical knowledge of planetary motions in the solar system, this interval variation has been used to estimate the speed of light with an accuracy of about 10 percent.

The first terrestrial experiment to determine the speed of light is due to Fizeau in 1849 by sending a focused light beam through a toothed wheel with a variable rotation rate to a mirror a few km away and then back. At a suitable angular speed, the reflected beam will hit the tooth and disappear to an observer behind the rotating wheel. From this angular speed along with the structure of teeth and the separation distance between the wheel and mirror, the round-trip propagation time and hence the speed of light can be determined to higher accuracy.

As to the propagation mechanism, it was generally believed, before the advent of Einstein's special relativity, that light propagates by means of a universal medium called ether. Michelson pioneered the attempt to measure the velocity of the Earth with respect to the supposed universal ether by using an interferometer. Meanwhile, it is believed that the Earth should not happen to be stationary with respect to the universal ether and hence the speed of the Earth with respect to it should at least be the linear speed due to earth's orbital motion around the Sun [26].

In 1887 the Michelson-Morley experiment came up with a zero or uncertainly small shift in the interference fringe, which indicates that the speed of the Earth with respect to the supposed ether is much lower than the linear speed due to the orbital motion [33]. This negative result definitively rules out the effect of earth's orbital motion on the propagation of light. Further, it is commonly extrapolated to rule out the effect of earth's rotation, even though the associated linear speed is much lower and its effect on the fringe shift is difficult to determine. Thus the Michelson-Morley experiment is understood to have a null result. Then this widely accepted interpretation makes the existence of the universal ether unreasonable. After the introduction of the special relativity in 1905, the notion of ether eventually becomes obsolete.

More recently, there have been developed several high-precision experiments which rely in a direct way on the propagation mechanism: the global positioning system, the intercontinental microwave link, and the interplanetary radar. Based on the precise measurement of the propagation time and on the precise knowledge of the terrestrial geography and of the motions of earth's satellites, spacecrafts, or planets, these experiments can provide decisive evidence in the determination of the propagation mechanism of electromagnetic wave. In this Chapter we examine the propagation formulas adopted for the routine practice in these experiments, particularly for the roles of earth's rotational and orbital motions.

Thereafter, the key issue of this Chapter will be presented. That is, to point out the simple fact that these propagation formulas are actually in accord with the classical propagation model, except for the reference frame of propagation. However, the adopted propagation frames vary among these experiments and hence there exist discrepancies in the effects of earth's motions. Further, it will be elucidated that the discrepancy can be solved if the classical propagation model is slightly modified in such a way that the propagation frame is endowed with a switchability according to the location of the wave: earthbound, interplanetary, or interstellar. Thereby, this new classical model can be in excellent accord with the aforementioned high-precision experiments. Moreover, it can account for the Michelson-Morley experiment and a variety of other propagation phenomena. Meanwhile, the proposed model also leads to some predictions which then provide different approaches to test its validity.

1.2 Classical Propagation Model and Sagnac Effect

To begin with, we briefly review the classical model of wave propagation, particularly the associated Sagnac effect. Consider an acoustic or electromagnetic wave propagating from a transmitter to a receiver via a medium. The *transmission path* is understood to be the line connecting the transmitter and the receiver at the instant when a short pulse of wave is emitted. Quantitatively, the transmission-path length R_t is the geometric distance from the transmitter to the receiver at the instant t' of wave emission. That is, $R_t = |\mathbf{R}_t|$ and

$$\mathbf{R}_t = \mathbf{r}_e(t') - \mathbf{r}_s(t'), \tag{1.1}$$

where $\mathbf{r}_e$ and $\mathbf{r}_s$ are the position vectors of the receiver and the transmitter, respectively.

An important quantity closely related to the transmission-path length is the propagation range which represents the actual length of wave propagation over the medium. Quantitatively, the *propagation range* R is the line (and its length) from the transmitter at the instant t' of wave emission to the receiver at the instant t of reception. That is,

$$R = |\mathbf{r}_e(t) - \mathbf{r}_s(t')| = |\mathbf{R}_t + \mathbf{r}_e(t) - \mathbf{r}_e(t')|. \tag{1.2}$$

It is of essence to note that there is a significant discrepancy between R_t and R in their dependences on reference frames. The transmission-path length R_t is associated with two positions at an *identical* instant and hence is invariant in different frames. On the other hand, the propagation range R in general is different when observed in different frames, since it is associated with two positions (or with the receiver position) at two *distinct* instants (see Fig. 1).

According to the classical propagation model, it is known that the propagation speed of electromagnetic wave in free space is c, the speed of light, with respect to the ether. Further, the propagation delay time τ $(= t - t')$ from the source to the receiver can be given in terms of the propagation speed c in the simple form

$$\tau = R/c, \tag{1.3}$$

if and only if the position vectors $\mathbf{r}_e$ and $\mathbf{r}_s$ are referred to the unique frame in which the ether is stationary. Otherwise, the propagation speed as well as the propagation range will change in a complicated way to make the propagation time invariant in a different frame, as it should be. Thus the propagation range R as well as the speed c is understood to be referred to the unique propagation frame.

It can be more convenient to express the propagation time in terms of the frame-invariant path length. However, due to the movement of the receiver, the propagation time τ is not equal to R_t/c, though the difference is slight ordinarily. To make this simple relationship more accurate, a treatment for the path length is needed.

The difference between the propagation range R and the path length R_t corresponds to the *Sagnac effect* which is due to the movement of the receiver during wave propagation with respect to the

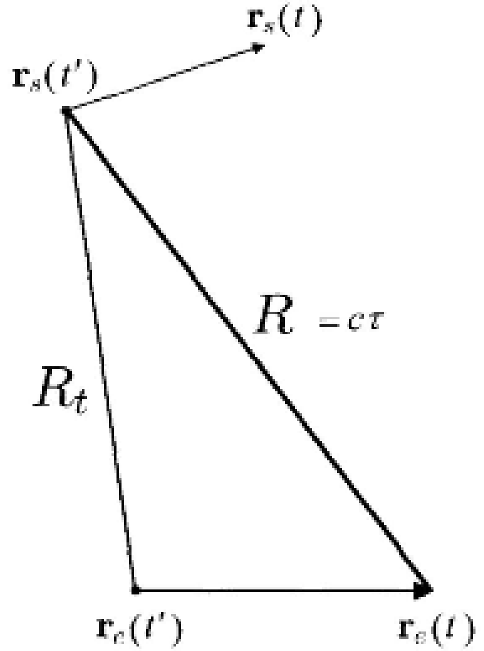

Fig. 1 Propagation range and transmission path. The transmission-path length $R_t = |\mathbf{r}_e(t') - \mathbf{r}_s(t')|$ and the propagation range $R = |\mathbf{r}_e(t) - \mathbf{r}_s(t')| = c\tau$, where $\mathbf{r}_s$ and $\mathbf{r}_e$ are the positions of the transmitter and the receiver, respectively, t' and t are the instants of wave emission and reception, respectively, and the propagation delay time $\tau = t - t'$. For a receiver moving at a fixed velocity $\mathbf{v}_e$ with respect to the propagation frame, $\mathbf{r}_e(t) = \mathbf{r}_e(t') + \mathbf{v}_e\tau$. The difference between R and R_t determines the Sagnac effect.

unique propagation frame. For a receiver moving at a fixed velocity $\mathbf{v}_e$, the propagation range R is given implicitly by

$$R = |\mathbf{R}_t + \mathbf{v}_e R/c|\,, \tag{1.4}$$

where the receiver velocity $\mathbf{v}_e$ as well as the position vector $\mathbf{r}_e$ is referred to the unique propagation frame.

When the receiver is moving radially (namely, in a direction longitudinal to the transmission path) so that $\mathbf{v}_e$ is parallel to $\pm\mathbf{R}_t$, the propagation range R can then be given explicitly in terms of the path length R_t. That is,

$$R = R_t \frac{c}{c \mp v_e}, \tag{1.5}$$

where the receiver speed $v_e = |\mathbf{v}_e|$. This formula for a radial motion immediately leads to $\tau = R_t/(c \mp v_e)$, which in turn is occasionally interpreted in such a way that the propagation speed changes to $c \mp v_e$ while the Sagnac effect is omitted tacitly.

For an arbitrary receiver velocity, the propagation range becomes $R = \left|\mathbf{R}_t + \mathbf{v}_e R/c + \mathbf{a}_e R^2/2c^2\right|$ when given to the second order of $1/c$, where $\mathbf{a}_e$ is the receiver acceleration and the propagation time R/c is assumed to be short. Then, by solving the quadratic polynomial equation in R obtained from a direct expansion of the square of the absolute value, it can be shown that to the second order of normalized speed (with respect to c), the propagation range is given explicitly by

$$R = R_t \left\{ 1 + \frac{u_e}{c} + \frac{1}{2c^2} \left(u_e^2 + v_e^2 + \mathbf{a}_e \cdot \mathbf{R}_t \right) \right\}, \tag{1.6}$$

where the receiver radial speed $u_e = \mathbf{v}_e \cdot \hat{R}_t$ and the unit vector $\hat{R}_t = \mathbf{R}_t/R_t$. To the first order, the propagation range becomes a simpler form

$$R = R_t + \mathbf{R}_t \cdot \mathbf{v}_e/c. \tag{1.7}$$

The last term in the preceding formula represents the first-order Sagnac effect which plays an important role in this Chapter.

We next consider the round-trip propagation where a wave is emitted from a transceiver, reaches and is reflected back from a target, and then is received by the transceiver. Suppose that the target and the transceiver move at velocities $\mathbf{v}_a$ and $\mathbf{v}_b$ with accelerations $\mathbf{a}_a$ and $\mathbf{a}_b$ with respect to the unique propagation medium, respectively. For the forward path from the transceiver to the target, the propagation range can be given by (1.6), where $\mathbf{v}_e$ is replaced by $\mathbf{v}_a$, $\mathbf{a}_e$ by $\mathbf{a}_a$, and R_t is understood to be the geometric distance from the transceiver to the target at the instant of wave emission. The propagation range for the backward path from the target to the transceiver can also be given by (1.6), where $\mathbf{v}_e$ is replaced by $\mathbf{v}_b$, $\mathbf{a}_e$ by $\mathbf{a}_b$, and R_t is understood to be the geometric distance from the target to the transceiver at the instant when the wave strikes the target.

Thereby, it can be shown that to the second order of normalized speed, the round-trip propagation time τ is given by

$$\tau = \frac{2R_t}{c} \left\{ 1 + \frac{u_{ab}}{c} + \frac{1}{2c^2} \left[u_a^2 + v_b^2 + v_{ab}^2 + (\mathbf{a}_{ab} - \mathbf{a}_b) \cdot \mathbf{R}_t \right] \right\}, \tag{1.8}$$

where $\mathbf{v}_{ab}$ $(= \mathbf{v}_a - \mathbf{v}_b)$ is the Newtonian relative velocity between the target and the transceiver, $u_{ab} = u_a - u_b$, $\mathbf{a}_{ab} = \mathbf{a}_a - \mathbf{a}_b$, the radial speed $u = \mathbf{v}\cdot\hat{R}_t$, $\hat{R}_t$ points from the transceiver to the target, and $\mathbf{R}_t$, $\mathbf{v}_a$, $\mathbf{v}_b$, $\mathbf{a}_a$, and $\mathbf{a}_b$ are all referred to the instant of wave emission from the transceiver (for a derivation, see [127] or Appendix B).

It is noted that the first-order one-way Sagnac effect given in (1.7) is associated with the receiver velocity and tends to be different from the one observed in a frame different from the unique propagation frame. However, the first-order round-trip Sagnac effect given in (1.8) is associated with the radial component of a relative velocity and hence remains unchanged in different frames. For the round-trip case, the dependence on reference frames emerges in the second-order Sagnac effect. These frame-dependent terms will be used to explore the existence and feature of the unique propagation frame of electromagnetic wave, which is the key issue of this Chapter.

1.3 Propagation Mechanisms and Sagnac Effects in High-Precision Experiments

In this section, we examine the propagation formulas that have been actually adopted in the global positioning system, the intercontinental microwave link, and the interplanetary radar. These high-precision experiments depend on wave propagation in a quite direct way and can provide crucial tests for a propagation model. Let us note that the transmission-path length is frame-invariant, though some reference frames can be more convenient from a certain viewpoint. On the other hand, the classical propagation range should be referred specifically to the unique propagation frame, when it is understood to be related to the propagation time simply by $R = \tau c$. Conversely, the frame in which the propagation range is related to the propagation time in this familiar form is just the unique propagation frame of the classical model.

1.3.1 Global positioning system

Recently, by virtue of its high accuracy in positioning, the global positioning system (GPS) has been put in everyday practice ubiquitously [69, 53, 8, 2, 34, 89, 115]. The NAVSTAR GPS employs about 24 non-geostationary (half-synchronous) satellites, each of which carries highly precise and synchronized atomic clocks in six nearly circular orbits of a radius of about 26,600 km [69, 34]. Each of the GPS satellites repeatedly broadcasts microwaves carrying a sequence of its own unique codes which can be used to determine the instant of signal emission. At the user site, the receiver generates a synchronous replica of the codes and compares them with the received ones. Then the shift between the two sequences of codes corresponds to the measured propagation delay time which, when multiplied by the speed c, is called the pseudorange which in turn becomes the propagation range in the ideal case.

Quantitatively, the satellite position $\mathbf{r}_s$ at the instant t' of signal emission is determined from the instant t of signal reception and the measured propagation delay time τ, together with the satellite ephemeris constants. Then the satellite position $\mathbf{r}_s$ at the instant of emission is related to the position $\mathbf{r}_e$ of a geostationary receiver at that instant implicitly by the pseudorange formula [8, 2, 89]

$$R = R_\ell + \mathbf{R}_\ell \cdot (\boldsymbol{\omega}_E \times \mathbf{r}_e)/c = R_\ell + 2\mathbf{S} \cdot \boldsymbol{\omega}_E/c, \tag{1.9}$$

where R $(= \tau c)$ represents the pseudorange, $\mathbf{R}_\ell = \mathbf{r}_e - \mathbf{r}_s$, the position vectors $\mathbf{r}_e$ and $\mathbf{r}_s$ are referred to earth's center, $\boldsymbol{\omega}_E$ is the directed rate of earth's rotation, and $\mathbf{S}$ $(= \mathbf{r}_s \times \mathbf{r}_e/2)$ denotes the directed area of the triangle with vertices at the satellite, the receiver, and earth's center. The term associated with earth's rotation rate is known as the GPS Sagnac correction in pseudorange.

After measuring a set of pseudoranges from different satellite transmitters to a given ground receiver even at different instants, the receiver position $\mathbf{r}_e$ (at a given instant, if it is moving in the adopted frame) can be found by solving a set of nonlinear equations processed with coordinates transformation from the preceding pseudorange formula. For a terrestrial receiver, it is convenient to express its position in the earth-centered earth-fixed (ECEF) frame which rotates with the Earth. Then the longitude, latitude, and altitude of the GPS receiver are calculated. This process is practiced numerously everyday around the globe.

For a geostationary receiver, its velocity is zero or $\boldsymbol{\omega}_E \times \mathbf{r}_e$ with respect to the ECEF or an earth-centered inertial (ECI) frame, respectively. Meanwhile, if the receiver velocity is referred to a heliocentric inertial frame or even to a frame beyond the solar system (say, a galaxy frame), earth's orbital motion should be taken into account in addition. It is of essence to note that the GPS pseudorange formula (1.9) is just the classical propagation-range formula (1.7), if $\mathbf{v}_e = \boldsymbol{\omega}_E \times \mathbf{r}_e$ is adopted for geostationary receivers. In doing so, the receiver velocity that determines the pseudorange is then referred uniquely to an ECI frame. Thus earth's rotation influences the Sagnac effect in GPS, while earth's orbital motion does not.

In GPS the actual magnitude of the Sagnac pseudorange correction due to earth's rotation depends on the positions of the satellites and receiver and a typical value is 30 m, as the propagation time is about 0.1 s and the linear speed due to earth's rotation is about 464 m/s on the equator. The GPS provides an accuracy of about 10 m or better in positioning. Thus the precision of GPS will be degraded significantly, if the Sagnac correction due to earth's rotation is not taken into account. On the other hand, the orbital motion of the Earth around the Sun has a linear speed of about 30 km/s which is about 100 times that of earth's rotation. Thus the present high-precision GPS would be impractical if the omitted correction due to the orbital motion is really necessary.

1.3.2 Intercontinental microwave link

In an intercontinental microwave link between Japan and USA via a geostationary satellite as the relay, the influence of earth's rotation is also demonstrated in a high-precision time comparison between the atomic clocks at the two ground stations located far apart [98].

In this transpacific-link experiment, a synchronization error of as large as about 0.3 μs was observed unexpectedly. After a detailed analysis, the synchronization error in this two-way microwave link is found to be proportional to the sum of the projected areas of two triangles (which are similar to that discussed in GPS), and is ascribed to an ignored shift in propagation time. This shift in the two-way link depends on the difference in longitude between the two stations. In another microwave link between the two neighboring countries of Japan and Korea, a similar but smaller shift in propagation time of about 40 ns has also been observed [64]. Evidently, as in GPS, the propagation-time shift in the two-way microwave link is associated with the Sagnac effect due to earth's rotation.

Meanwhile, as in GPS, no effects of earth's orbital motion are reported in these links, though they would be easier to observe if they are in existence. Thereby, it is evident that the wave propagation in GPS and the intercontinental microwave link depends on earth's rotation, but is entirely independent of earth's orbital motion around the Sun or whatever. As a consequence, the propagation mechanism in GPS and the intercontinental link can be viewed as classical in conjunction with the situation that an ECI frame, rather than the ECEF frame or any other, is selected as the unique propagation frame. In other words, **the wave in GPS and in the intercontinental microwave link can be viewed as propagating via a classical medium stationary in a geocentric inertial frame**.

1.3.3 Interplanetary radar

By using a high-power microwave transmitter (typically, 1 MW) and a high-directivity antenna (typically, 50 dB), radar observations of planets in the solar system have been achieved. In the interplanetary radar, a microwave signal is sent out from an earthbound antenna to a target planet or a spacecraft and then the reflected wave is collected by the earthbound antenna. From the literature the targets with which the microwave radar has been demonstrated include Venus [83, 1, 90, 29, 101], Mercury [90, 29, 101], Mars [96], interplanetary spacecrafts [5], and others [86].

By processing the returned signal with a duplicate of the transmitted one, the radar echo delay time can be measured with high precision. For the interplanetary radar, the echo delay time is of the order of 1000 s, while the uncertainty in the echo-time measurement is typically 100 μs [90]. Part of the uncertainty is due to surface roughness of the target planet.

Meanwhile, based on the planetary positions which as functions of time are determined elaborately by solving the coupled equations of planetary motion numerically in conjunction with suitable planetary ephemeris constants, the interplanetary round-trip propagation time is calculated. By comparing the predicted results with the measured data of radar echo time, high agreements are reported. Typically, the discrepancy in the echo-time comparison is a few hundred microseconds [83, 103]. Part of the discrepancy is due to the uncertainty in the adopted ephemeris constants.

An examination of the propagation formulas adopted in the literature shows that the round-trip propagation time is the sum of the propagation ranges of the forward and the backward path divided by the speed of light c, where the forward propagation range is the distance from the position of the transmitting antenna at the instant of wave emission to the one of the reflecting part on the target planet at the instant of reflection, and the backward propagation range is the distance from the reflecting part to the position of the receiving antenna at the instant of reception.

Quantitatively, as described clearly in [83, 1, 86], the formula adopted for the round-trip propagation time is given by

$$\tau = \tau_f + \tau_b = \frac{1}{c}\left|\mathbf{r}_a(t') - \mathbf{r}_b(t'')\right| + \frac{1}{c}\left|\mathbf{r}_b(t) - \mathbf{r}_a(t')\right|, \qquad (1.10)$$

where τ_f and τ_b denote the propagation time for the forward path and for the backward path, respectively, $\mathbf{r}_a$ and $\mathbf{r}_b$ are the position vector of the reflecting part on the target and of the transceiver, respectively, t'', t', and t denote the instants at which the signal is emitted, reflected, and received, respectively, $\tau_f = t' - t''$, and $\tau_b = t - t'$. (When the target position vector $\mathbf{r}_a$ is assigned instead to the center of the planet, an approximate amount of $2R_P/c$ should be subtracted from the echo time, where R_P is the radius of the target planet [1].) Owing to the movement of the target during the forward propagation of duration τ_f and to that of the transceiver during the round-trip one of duration τ, the position vectors $\mathbf{r}_a(t')$ and $\mathbf{r}_b(t)$ depend on τ_f and τ, respectively. Thus the propagation times given in the preceding formula are implicit and are solved iteratively.

It is of essence to note that the preceding echo-time formula is in accord with the classical propagation-range formula (1.2), aside from the reference frame. Besides, as stated explicitly in most of the literature, the position vectors $\mathbf{r}_a$ and $\mathbf{r}_b$ are based on a heliocentric inertial frame. Needless to say, a heliocentric frame is convenient in dealing with the position vectors of the associated planets under the influence of the gravitation due to the Sun. Further, a significant implication is that the wave propagation is referred uniquely to this heliocentric frame. It should be noted that if this is really the case, the unique propagation frame for the interplanetary radar is then different from the one for GPS and the intercontinental microwave link. However, whether or not the unique propagation frame for the interplanetary radar is really a heliocentric inertial frame is yet subject to a careful verification by comparing the measured echo time with the calculated results based on the plausible propagation frames until an appropriate level of agreement is obtained exclusively.

To perform this verification, it is more instructive to express the echo time explicitly. To the second order, the explicit formula for echo time has been given in (1.8). From this formula it is seen that owing to the round-trip path, the first-order Sagnac effect depends on the radial component of a relative velocity and hence remains unchanged in different frames in uniform motion of translation or rotation. In other words, no frame is preferred for this round-trip effect associated with a radial relative speed. Thus, unlike that in GPS, the major term of the Sagnac effect is frame-invariant and hence cannot be used to determine the uniqueness of the propagation frame. The determination of the unique propagation frame then relies on the various second-order Sagnac effects, which are much smaller in magnitude. Hence the required accuracy in the echo-time comparison is much higher.

Then we employ the explicit propagation formula to examine some frames. When observed in the rotating ECEF frame, the speed of a planet target will be extraordinarily high and the supposed Sagnac effect will be unreasonably large. Obviously, the ECEF frame is ruled out. Thus, as in GPS, earth's rotation is expected to be involved in the velocity of an earthbound receiver in the interplanetary propagation. On the other hand, when observed in a galaxy frame, the speeds of the transceiver and target will incorporate the one due to the orbital motion of the Sun, which is a few hundred km per second. Thus the squared normalized speeds are of the order of as large as 10^{-6}. If this motion does affect the interplanetary radar, the corresponding influence on the echo time would be of the order of as large as 1 ms. This is clearly beyond the comparison agreement and hence a galaxy frame is also ruled out.

However, when observed either in a geocentric inertial frame or in a heliocentric one, the squared normalized speeds in an interplanetary radar are at most of the order of 10^{-8}. The potential contributions to an interplanetary echo time are of the order of 10 μs. Therefore, based on these second-order terms, it appears difficult to discriminate between a geocentric and a heliocentric inertial frame, when the comparison agreement remains a few hundred microseconds. In order to determine the uniqueness of the propagation frame from these minor terms, the agreement in the echo-time comparison should be better than 10 μs.

More recently, the interplanetary radar with echo signals being transponded by a spacecraft has been achieved and the resultant precision in the echo-time measurement can be as high as 0.1 μs or better [5, 96]. Meanwhile, by processing a large number of high-precision measured data to fit the theoretical formula with some undetermined parameters by the least-squares algorithm, an agreement in the echo-time comparison of as high as about 1 μs or better has been achieved over a long duration of several months [5, 96]. Thereupon, as the reference frame adopted for the echo-time formula is a heliocentric inertial frame, the unique propagation frame for the interplanetary radar is then attributed to that frame.

Thereby, the calculated echo time is in agreement with the measured one, if the propagation mechanism in the interplanetary radar is viewed as classical in conjunction with the situation that a heliocentric inertial frame, rather than an ECI frame or any other, is selected as the unique propagation frame. In other words, **the wave in the interplanetary radar can be viewed as propagating via a classical medium stationary in a heliocentric inertial frame.**

1.4 Discrepancy in Effects of Earth's Motions

In some of the literature the Sagnac effect is attributed to a relativistic effect [8, 64, 70]. It is known that the special relativity is based on two postulates. The first one is the principle of relativity which states that no reference frames in uniform relative motion of translation are preferred [24]. This principle is in accord with classical mechanics. On the contrary, the classical propagation model presumes a unique propagation frame to which the position vectors, the propagation range, the propagation speed, and the receiver velocity are referred. The second postulate is the principle of constancy of the speed of light which states that the speed of light is independent of the motion of its source. It is noticed that this principle is actually in accord with the classical propagation model. Furthermore, a salient feature of the special relativity is the adoption of the Lorentz transformation of space and time.

It has been determined deliberately in the preceding section that the wave propagation is in accord with the classical propagation model in conjunction with the unique propagation frame being either a geocentric or a heliocentric inertial frame, among GPS, the intercontinental microwave link, and the interplanetary radar. The Sagnac effect is associated with the difference between the propagation range and the path length, which in turn results from the movement of the receiver with respect to the determined propagation frame. As in an acoustic wave, this difference involves no space-time transformation. From this point, the Sagnac effect has nothing to do with the Lorentz transformation of space and time.

Quantitatively, an obvious reason is that the Sagnac effect incorporates the first order of normalized speed, whereas the time dilation or the length contraction is merely of the second order. Consider the situation where a wave propagation is observed in a laboratory frame which is different from the determined propagation frame and is moving at a velocity $\mathbf{v}_0$ with respect to it. Thus the receiver moves at the velocity $(\mathbf{v}_e - \mathbf{v}_0)$ with respect to the laboratory frame, while it moves at $\mathbf{v}_e$ with respect to the propagation frame. Then the apparent propagation range R_l observed in the laboratory frame tends to be different from the actual propagation range R. From the propagation-range formula (1.7), it is seen that to the first order of normalized speed,

$$R_l = R - \mathbf{R}_t \cdot \mathbf{v}_0 / c. \tag{1.11}$$

The difference between the propagation range R and the apparent range R_l represents the deviation in the Sagnac effect, which in turn

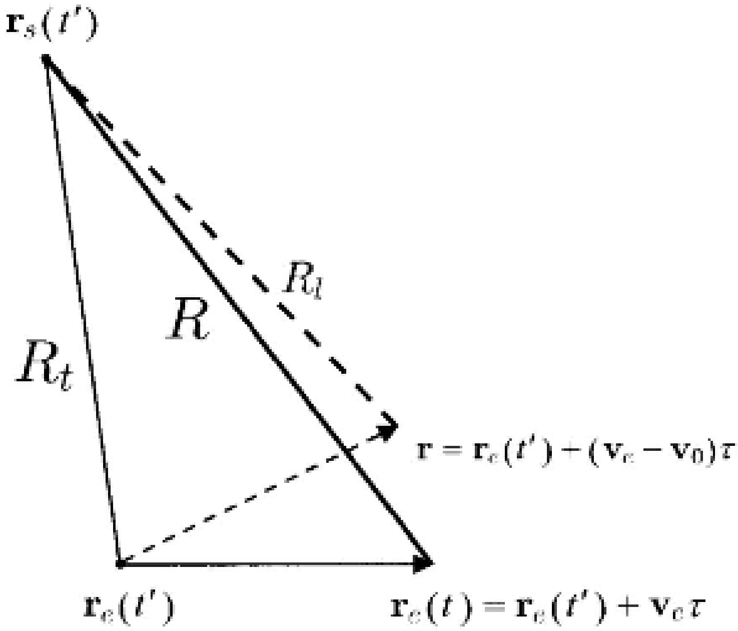
$\mathbf{r}_s(t')$
R_l
R
R_t
$\mathbf{r} = \mathbf{r}_e(t') + (\mathbf{v}_e - \mathbf{v}_0)\tau$
$\mathbf{r}_e(t')$
$\mathbf{r}_e(t) = \mathbf{r}_e(t') + \mathbf{v}_e\tau$

Fig. 2 Sagnac-effect deviation. When viewed from a laboratory frame which is moving at a velocity $\mathbf{v}_0$ with respect to the propagation frame, the apparent range R_l tends to be different from the propagation range R. The difference between R and R_l determines the Sagnac-effect deviation. The propagation delay time $\tau = t - t'$, where t' and t are the instants of wave emission and reception, respectively.

is due to the relative motion between the two frames during wave propagation (see Fig. 2). Thereby, the calculated propagation time will be imposed with an extra first-order deviation term associated with the laboratory velocity $\mathbf{v}_0$, in addition to the Sagnac effect. If no reference frame is preferred, it is puzzling to figure out how this Sagnac-effect deviation term can be compensated for by resorting to the Lorentz transformation when observed in a different frame in uniform relative motion.

In spite of the fact that the principle of relativity has been extensively verified in classical mechanics, such as in the conservation of momentum and of kinetic energy, it is not really tested in the propagation of electromagnetic wave. Although GPS and the intercontinental microwave link are commonly claimed to follow the special relativity, the only reference frame that has been actually adopted is an ECI frame. The ECEF frame is ruled out by reason of the noninertial effects of a rotating frame [8]. Meanwhile, a heliocentric and a galaxy frame are also ruled out by reason of the principle of local Lorentz invariance [8]. No other frames have been really tested in GPS, such as the frame that moves at a fixed velocity with respect to an ECI frame. Perhaps, this frame can also be ruled out by some ignored principle.

However, if these kinds of reasoning are applied consistently to the Michelson-Morley experiment, the famous null result should be reexamined based on an ECI frame. Thus, as in GPS, the effect of earth's rotation has to be considered. Moreover, it is noted that under a space-time transformation in which time is not frame-invariant, the echo-time comparison in the interplanetary radar seems to need a transformation. This is because while the calculation is referred to a heliocentric frame, the measurement of echo time involves only the clocks at ground stations and hence is expected to be associated with the same frame as in the intercontinental link. However, such a transformation has not been adopted, to our knowledge.

These arguments on the special relativity may be disputable. Anyway, the key point is that these high-precision experiments and other related propagation phenomena can be well accounted for by the classical propagation model if the unique propagation frame is suitably selected. The GPS and intercontinental microwave link are in accord with the classical propagation mechanism in conjunction with the unique propagation frame being an ECI frame. Thereby, without invoking any particular space-time transformation, the first-order Sagnac effect based on the classical model is in excellent accord with these experiments. Meanwhile, the interplanetary radar is in accord with the classical mechanism in conjunction with the unique frame being a heliocentric inertial frame.

As the unique propagation frame for the interplanetary radar is a heliocentric inertial frame, then earth's rotation, earth's orbital motion around the Sun, and the orbital motion of the target planet contribute to the Sagnac effect. However, the orbital motion of the Sun has no effects on the interplanetary propagation. On the other hand, as the unique propagation frame for GPS and the intercontinental link is a geocentric inertial frame, the rotational motion of the Earth contributes to the Sagnac effect. However, the orbital motions of the Earth and the Sun have no effects on the earthbound propagation.

By comparing GPS with the interplanetary radar, it is seen that there is a common Sagnac effect due to earth's rotation and a common null effect of orbital motion of the Sun on wave propagation. However, there is a discrepancy in the Sagnac effect due to earth's

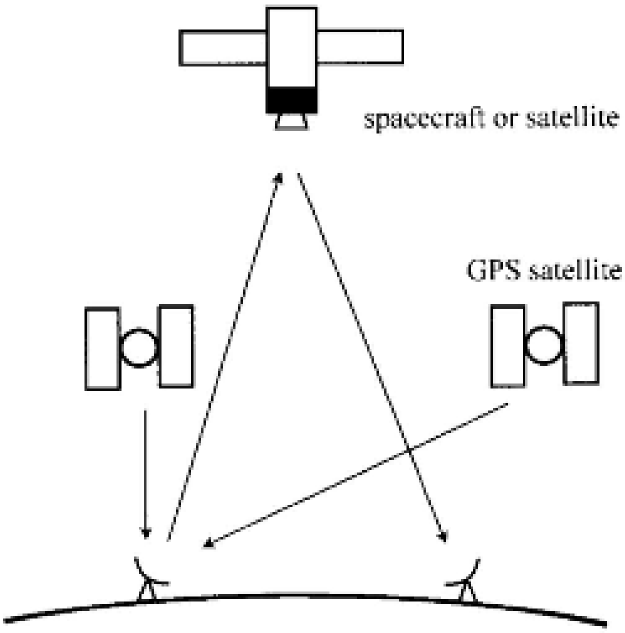

Fig. 3 Uniqueness and switchability of propagation frame. The wave propagation in GPS or in an intercontinental microwave link is referred uniquely to a geocentric inertial frame. Thus the earthbound propagation depends on earth's rotation, but is entirely independent of earth's orbital motion. Meanwhile, when the location of the spacecraft is interplanetary, the propagation frame for the microwave link switches to a heliocentric inertial frame. Thus the interplanetary propagation depends on earth's orbital motion as well as on the rotation.

orbital motion. Meanwhile, by comparing GPS with the widely accepted interpretation of the Michelson-Morley experiment, it is seen that there is a common null effect of the orbital motions on wave propagation, whereas there is a discrepancy in the Sagnac effect due to earth's rotation.

It is noted that the interplanetary radar can be viewed as a microwave link via a planet or a spacecraft as the relay, while the unique propagation frame is different from that for the intercontinental link. Thus, for a spacecraft before or just after its launch, the propagation of the microwave by which the ground station communicates with it is referred to a geocentric inertial frame (see Fig. 3). However, as the spacecraft flies far away on its journey to another planet, the propagation frame then switches to a heliocentric inertial frame. Therefore, it is evident that the propagation mechanism in a microwave link depends on the location of the relay.

Thereby, it is concluded that the examined high-precision experiments are actually in accord with the classical propagation model in conjunction with **a unique propagation frame which is switchable, depending on the location of the wave: earthbound or interplanetary**. Based on this characteristic of uniqueness and switchability of the propagation frame, we propose in the following section the local-ether model of wave propagation to solve the discrepancies in the roles of earth's rotational and orbital motions in the Sagnac effect and to account for a wide variety of propagation phenomena.

1.5 Local-Ether Propagation Model

Imagine that in the universe the ether pervades everywhere. However, the ether does not integrate wholly to form one single universal medium for wave propagation. Instead, there exist numerous local ethers. Each individual local ether is finite in extent and may be wholly immersed in another local ether of larger extent. Thus the local ethers may form a multiple-level hierarchy. Each local ether as a whole may move with respect to another local ether. At a given position, it is the lowest-level local ether that determines the wave propagation locally. For an electromagnetic wave propagating within a single local ether, it is proposed that as in the old ether notion, the propagation speed with respect to the associated local ether is just the speed of light c, independent of the motions of the source and the receiver. This new classical propagation model made its debut in [117, 129].

The physical nature of the local ether is yet to be explored. Like the familiar fact that a volume of air or an elastic membrane which supports the propagation of mechanical wave is composed of numerous interacting molecules or ions, a local ether which supports the propagation of electromagnetic wave could be composed of tiny interacting particles of some undetected kind much smaller than the electron in size. It is expected to be associated with the gravitation of a celestial body. Anyway, some mechanisms tend to integrate the ether surrounding a celestial body. Thus the nearby ether will move with the body. This situation is somewhat like the one that

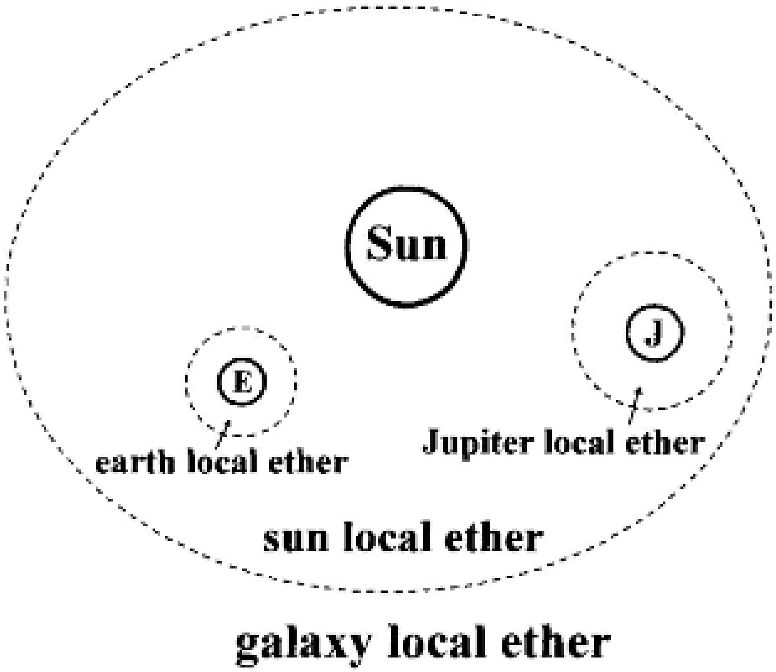

Fig. 4 Hierarchy of local ethers. In the region under a sufficient influence of the gravitation due to the Earth, the Sun, or another celestial body, there forms a local ether, which comoves with the gravitational potential of the associated body. The earth local ether along with the Jupiter local ether is inside the sun local ether, which in turn is inside the galaxy local ether.

a moving balloon tends to drag some air to move with it or like the ether-drag hypothesis proposed a long time ago. Thereby, a local ether associated with that celestial body is formed.

Specifically, it is proposed that **in the region under a sufficient influence of the gravitation due to the Earth, the Sun, or another celestial body, there forms a local ether which in turn is stationary with respect to the gravitational potential of the respective body**. Thereby, each local ether together with the gravitational potential moves with the associated celestial body. According to this model, the earth local ether is inside the sun local ether, which in turn is inside the galaxy local ether, and so on (see Fig. 4). The earth local ether together with earth's gravitational potential moves with earth's orbital motion around the Sun, but not with earth's rotation. Thus the earth local ether is stationary in an ECI frame, but not in the ECEF frame or any other, while the sun local ether is stationary in a heliocentric inertial frame. The earth local ether should be at least so large as to encompass geostationary satellites. Further, it could also encompass the moon, since in the experiment on lunar laser ranging [22], the orbital motions of the Earth and the moon around the Sun are not mentioned in a description of the propagation-time calculation. This situation is identical to that in GPS, but different from that in the interplanetary radar.

Based on the classical propagation model, whether a motion of a receiver contributes to the Sagnac effect depends on whether this motion is incorporated in the movement of the receiver with respect to the propagation medium. In other words, if a receiver and the propagation medium are undergoing a common motion, then the propagation phenomena are entirely independent of this motion. Based on the local-ether model, for the case where both the source and the receiver are bound to the solar system, the interplanetary propagation is entirely independent of the motion of the Sun with respect to upper-level local ethers, such as the orbital motion of the Sun in the galaxy. Further, for the case where both the source and the receiver are bound to the Earth, the propagation medium is stationary in an ECI frame and the earthbound propagation is entirely independent of the orbital motions of the Earth and the Sun.

Consider the Sagnac effect for a geostationary receiver. Based on the local-ether model, the velocity of a geostationary receiver that contributes to the Sagnac effect is then not zero, owing to earth's rotation. Further, the receiver velocity that determines the Sagnac effect depends on the location of the source. If the source is also earthbound, the whole transmission path is then earthbound and the Sagnac effect is due to the rotation alone. However, if the source is located outside the earth local ether, the calculation of the propagation time is complicated. For the interplanetary propagation where the wave is radiated from the Sun, a planet, or a spacecraft, the major part of the transmission path is located in the sun local ether. Thus the calculation can be simplified, if the propagation over the minor part of the path in the earth local ether is approximated by the one in the main sun local ether. Anyway, the interplanetary Sagnac effect is due to earth's orbital motion around the Sun in addition to earth's rotation. Further, for the interstellar propagation where the source is located beyond the solar system, the orbital motion of the Sun contributes to the interstellar Sagnac effect as well.

Evidently, as expected, the proposed local-ether model accounts for the Sagnac effect due to earth's rotation and the null effect of earth's orbital motion in the earthbound propagation in GPS and the intercontinental link. Meanwhile, in the interplanetary radar, it accounts for the Sagnac effect due both to earth's rotation and to earth's orbital motion around the Sun. Moreover, it accounts for the null effect of orbital motion of the Sun in the earthbound and interplanetary propagations. Furthermore, the local-ether model can be used to account for the Michelson-Morley experiment and various other propagation phenomena, as discussed in the following section.

1.6 Reexamination of Various Propagation Phenomena

In this section, we discuss the Sagnac effect in the monostatic radar, the Michelson-Morley experiment, and in the loop interferometer, and examine the constancy of the speed of light and the spatial isotropy in propagation time. Then we discuss the Doppler effect and the spatial anisotropy in Roemer's observations and the cosmic microwave background radiation. Finally, we explore the gravitational effect in the light deflection by the Sun. For the various phenomena to be discussed, the main propagation medium varies from the earth to the sun local ether, and to that beyond the solar system.

In the various propagation formulas to be discussed, the individual velocities of the source, target, and receiver together with the Newtonian relative velocities among them are incorporated. The phenomena associated only with relative velocities comply with the principle of relativity and cannot be used to determine the unique propagation frame unequivocally. On the other hand, those terms incorporating the individual velocity, such as the Sagnac effect in GPS, will in general lead to different predicted results if the chosen reference frame is different from the unique propagation frame. Therefore, an examination of the frame adopted for the individual velocity may provide a test for the propagation model. However, the individual-velocity terms may become the second or a higher order due to some symmetry in propagation. Thus these terms can be difficult to detect or even undetectable. Anyway, the various propagation phenomena at least provide auxiliary evidence for the propagation model.

1.6.1 Round-trip Sagnac effect in monostatic radar

Consider the round-trip propagation in the monostatic radar system composed of a transceiver and a target. For the earthbound radar, the round-trip propagation time τ is quite short and the resolution in echo-time measurement is limited. Thus it normally suffices to use the radar echo time given to the first order. Thus (1.8) immediately leads to

$$\tau = \frac{2R_t}{c}\left(1 + \frac{u_{ab}}{c}\right). \tag{1.12}$$

It is noted that the first-order echo time is with a Newtonian relative velocity and thus complies with the principle of relativity. This first-order formula agrees with the corresponding radar phase shift given in the literature [57, 102]. No second-order echo time in the earthbound radar has been reported before, to our knowledge.

1.6.2 Round-trip Sagnac effect in Michelson-Morley experiment

Then we proceed to consider the Michelson-Morley experiment dealing with the interference between two light beams in two mutually orthogonal transmission paths formed by a beam splitter and mirrors. In each of the two optical arms, light propagates from the beam splitter to a mirror and back. Thus the propagation in each arm is like the one in a monostatic radar with the beam splitter and the mirror serving as the transceiver and the target, respectively. Similarly, the Sagnac effect is of the round-trip nature. Further, since the mirror is stationary with respect to the beam splitter, the propagation formula can be even simpler.

For the case where the target comoves with the transceiver (precisely, $u_{ab} = 0$) and their accelerations can be neglected, the round-trip propagation-time formula (1.8) becomes a simpler form

$$\tau = \frac{2R_t}{c}\left\{1 + \frac{1}{2c^2}\left(u_b^2 + v_b^2 + v_{ab}^2\right)\right\}. \tag{1.13}$$

The first-order Sagnac effect then vanishes.

In the Michelson-Morley experiment, the beam splitter and the mirrors move at a substantially identical velocity **v** with respect to the propagation frame, as far as the second-order terms in the preceding formula are concerned. Thus the round-trip propagation time for each optical arm, when given to the second order of normalized speed, becomes

$$\tau = \frac{2R_t}{c}\left\{1 + \frac{v^2}{2c^2}(1 + \cos^2\theta)\right\}, \tag{1.14}$$

where R_t is the path length between the beam splitter and the mirror, and θ is the angle between $\mathbf{v}$ and $\mathbf{R}_t$.

The difference in round-trip propagation time between the two arms corresponds to a phase difference, which in turn can manifest itself as an interference fringe pattern by suitably arranging the arms. As the turntable on which the interferometer resides is made to change its direction with respect to the ground, the two values of the angle θ and hence the two propagation times will vary. Consequently, a shift of the interference fringe can be observed, if the variation of the phase difference is large enough.

In the original proposal of the experiment, the interferometer velocity $\mathbf{v}$ was supposed to incorporate earth's orbital motion around the Sun. Thus, at least, $v^2/c^2 \simeq 10^{-8}$. Then the amplitude of the corresponding phase-difference variation could be as sufficiently large as $\pi/3$, when the wavelength $\lambda = 0.6\ \mu$m and the path length $R_t = 10$ m. However, it is well known that such a large variation in the fringe pattern is never observed. On the other hand, based on the local-ether model, the propagation in an earthbound experiment is entirely independent of earth's orbital motion around the Sun or whatever. And the velocity $\mathbf{v}$ is referred to an ECI frame and hence is due to earth's rotation alone. Thus the term v^2/c^2 determining the round-trip Sagnac effect is as small as about 10^{-12}.

In order to observe such a predicted second-order Sagnac effect due to earth's rotation, the precision of the Michelson-Morley experiment should be 10^4 times that designed to detect the orbital motion. According to the various measurements surveyed in [100], the interferometry precision has been raised by Joos to a few hundred times the minimum requirement for the orbital motion. Thus, in order to test the effect of earth's rotation, the precision should be further improved by a factor of a few tens. Thereby, based on the local-ether model, **the variations of the round-trip propagation time are not exactly zero, but are too small to cause a currently detectable fringe shift**, when the direction of the turntable is changing with respect to the ground.

On the other hand, in the common understanding, the null effect of orbital motion is extrapolated without direct evidence to rule out the effect of earth's rotation on wave propagation, as in Einstein's original paper on the special relativity where it is assumed clearly that $\tau = 2R_t/c$ [24]. Further, it is expected that the effect of the orbital motion itself is even detectable if the experiment can be conducted on an interplanetary spacecraft. Thereupon, the local-ether interpretation of the Michelson-Morley experiment is fundamentally different from the one based on the special relativity, even though the difference in propagation time may be quite small in magnitude.

From the examined high-precision propagation experiments, it is found that the proposed local-ether model is in accord with all of these experiments, except the undetermined Sagnac effect due to earth's rotation in the Michelson-Morley experiment. Since a correct propagation model should consistently account for the various experiments, we deliberate more on this round-trip Sagnac effect.

From the physical reasoning based on the standpoint of any plausible propagation model, it is expected that the propagation mechanism in the Michelson-Morley experiment in no way can be different from the one in GPS and the earthbound microwave link. The null effect of earth's orbital motion in the Michelson-Morley experiment reflects no Sagnac correction due to this motion in the GPS pseudorange. On the other hand, the Sagnac effect due to earth's rotation in the high-precision GPS and intercontinental microwave link should reflect a nonnull effect of earth's rotation in the Michelson-Morley experiment. The difficulty with the Michelson-Morley experiment is that this effect becomes a term of the second order of normalized speed, owing to the round-trip path and a lack of radial relative motion between the transceiver and target.

The precision of the interferometry may be improved by using a laser heterodyne system, where the transmission path is formed in a resonant cavity. If the resonant frequency of the cavity is shifted due to some mechanisms, the shift will manifest itself as a corresponding one in the beat frequency, as the wave from the cavity is compared with a reference wave. According to the classical propagation model, the resonant frequency of a cylindrical cavity resonator is inversely proportional to the round-trip propagation time over the transmission path that is along the axis and between the end faces of the cylinder. Thus the motion of the cavity with respect to the unique propagation frame tends to affect the round-trip propagation time and hence the resonant frequency, as a consequence of the Sagnac effect.

Based on the local-ether model, the predicted second-order round-trip Sagnac effect due to earth's rotation results in a quadrupole anisotropy in the resonant frequency with respect to the ground, as the axial direction of the cylindrical cavity is changing in a horizontal plane. That is, the resonant frequency is the lowest when the axis is in an east-west direction; while the highest when in a north-south one. The shift in resonant frequency leads to a corresponding one in the beat frequency between the waves from two cylindrical cavities with axes perpendicular to each other [51] or between the wave from a single cavity and a reference wave from a stable source [15, 28].

As the turntable on which the interferometer resides is rotating with respect to the ground, the beat frequency is expected to vary sinusoidally at twice the turntable rotation rate. The sinusoidal variation of the resonant frequency f can be found from the round-trip propagation time given in (1.14). For the case of a single cavity, the peak-to-peak amplitude $\delta f_{\max}$ of this second-harmonic variation is predicted to be

$$\frac{\delta f_{\max}}{f} = \frac{v_E^2}{2c^2}, \tag{1.15}$$

where v_E is the linear speed due to earth's rotation with respect to an ECI frame. As $v_E = \omega_E R_E \cos\theta_l$, then $\delta f_{\max}/f \simeq 1.2\cos^2\theta_l \times 10^{-12}$, where R_E is earth's radius and θ_l is the latitude.

Such a heterodyne system using a stable He-Ne laser at 3.39 μm ($f = 8.8 \times 10^{13}$ Hz) and a stable Fabry-Perot resonator has been developed [15]. According to the local-ether model, the amplitude $\delta f_{\max}$ is expected to be 62 Hz, as the cavity heterodyne experiment is supposed to be conducted at latitude 40°. In the measured data, a term varying at the expected rate has been reported. However, the peak-to-peak amplitude of this second-harmonic term is merely about 17 × 2 Hz and it was attributed to a persistent spurious signal among other larger noises. Similarly, the second-harmonic term is also observed in [28, 51]. However, its amplitudes far exceed the predicted value and the causes were ascribed to an effect of magnetostriction on resonant frequency. It seems too early to make a decisive conclusion from these experiments. A more sophisticated experiment is needed to test the second-order round-trip Sagnac effect supposed due to earth's rotation.

1.6.3 Sagnac effect in loop interferometer

The aforementioned first-order Sagnac effect was actually discovered with a loop interferometer, where two coherent waves propagate in opposite directions along a closed transmission path formed by a beam splitter and a series of mirrors in air (see Fig. 5). Although the paths for the two waves are identical in structure, the propagation ranges can be different owing to the Sagnac effect associated with the movement of the transmission path in the propagation direction. The corresponding phase difference then results in an interference fringe, which was first observed in 1913 by Sagnac with a rotating interferometer. Then in 1925 Michelson and Gale demonstrated the Sagnac effect due to earth's rotation by constructing a geostationary loop interferometer enclosing an area of as large as 0.2 km^2 [6].

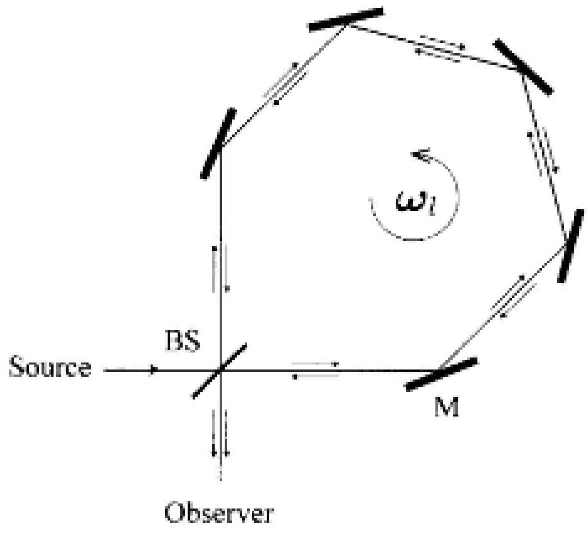

Fig. 5 Sagnac experiment with rotating loop. The Sagnac interferometer is formed by a beam splitter (BS) and a series of mirrors (M), which together rotate at a directed rate $\boldsymbol{\omega}_l$ about an axis. Two waves propagate in opposite directions along each segment of the closed path.

To deal with this Sagnac effect, consider a transmission loop that has a circular shape of radius a and is rotating about the center axis with a rotation rate ω_l. For the moment, the velocity of the axis is omitted for simplicity. Thus, according to the implicit formula (1.4), the actual propagation ranges for the copropagating and the counterpropagating wave traversing the rotating loop once (from entering the loop to exiting from it via the beam splitter) are given by $2\pi a \pm \omega_l a\tau$ rather than $2\pi a$, where τ is the respective propagation time. Thus the difference in propagation time between the waves is

$$\triangle\tau = \frac{2\pi a}{c - \omega_l a} - \frac{2\pi a}{c + \omega_l a} \simeq \frac{4\pi\omega_l a^2}{c^2}, \qquad (1.16)$$

which is proportional to the area enclosed by the loop times the rotation rate.

For the general case, consider a coplanar transmission loop L that has an arbitrary shape and is rotating about an axis at an arbitrary location with a directed rotation rate $\boldsymbol{\omega}_l$. For the two waves copropagating and counterpropagating with the rotating loop, the directed path length $\mathbf{R}_t$ in each linear short segment of the loop is along the longitudinal $\hat{l}$ direction of this path segment, that is,

$\hat{R}_t = \pm\hat{l}$. By using the first-order propagation-range formula (1.7), the propagation-time difference between the two waves traversing the loop once can be given by a path integral (or by a summation for a piecewise connected loop). That is,

$$\triangle\tau = \frac{1}{c}\oint_L \left\{\left(1+\frac{1}{c}\mathbf{v}_l\cdot\hat{l}\right)-\left(1-\frac{1}{c}\mathbf{v}_l\cdot\hat{l}\right)\right\}dl = \frac{2}{c^2}\oint_L \boldsymbol{\omega}_l \times \mathbf{r}\cdot d\mathbf{l}, \tag{1.17}$$

where $\mathbf{v}_l$ $(= \mathbf{v}_0 + \boldsymbol{\omega}_l \times \mathbf{r})$ and $\mathbf{v}_0$ are respectively the velocities of the path segment and (a suitable point on) the axis both with respect to the local-ether frame, $\mathbf{r}$ is the directed distance from the axis to the segment, $d\mathbf{l} = \hat{l}dl$, dl is a differential path length, and we have made use of the result that the integral of a constant vector $\mathbf{v}_0$ over an arbitrary loop is zero.

By using a vector identity and by noting that the directed area $\mathbf{S}$ enclosed by the coplanar path L is

$$\mathbf{S} = \frac{1}{2}\oint_L \mathbf{r}\times d\mathbf{l}, \tag{1.18}$$

then the propagation-time difference, to the first order of normalized speed, takes the form

$$\triangle\tau = \frac{4}{c^2}\boldsymbol{\omega}_l\cdot\mathbf{S}. \tag{1.19}$$

It is seen that the corresponding phase difference is proportional to the rotation rate times the projected loop area.

It is noted that the major terms in the two propagation times in (1.17) cancel each other and only the Sagnac terms survive in the interference. This situation makes it easier to observe the Sagnac effect by using a loop interferometer. The corresponding phase difference has been demonstrated in a rotating interferometer as well as in a geostationary one. In the latter case, namely, the Michelson-Gale experiment, the Sagnac effect is due solely to earth's rotation with $\boldsymbol{\omega}_l = \boldsymbol{\omega}_E$. The rate ω_E is about $2\pi/(86164\ \mathrm{s})$ and the maximum phase difference is as sufficiently large as 2 rad, when the wavelength is 0.6 μm and the loop area $S = 0.2\ \mathrm{km}^2$. Thereby, a loop interferometer can be used as a means to detect earth's rotation rate.

On the other hand, according to the local-ether model, earth's orbital motion around the Sun or others does not contribute to the Sagnac effect in an earthbound transmission loop. In as early as 1904 Michelson supposed that the Sagnac effect due to the orbital motion of the Earth around the Sun might be detectable, even though the angular speed of the orbital motion is much lower than that of the rotation [6]. However, this idea has never been followed up to our knowledge. In [6] the effect of orbital motion is presumed to be null by reason of the principle of local Lorentz invariance.

1.6.4 Constancy of speed of light

According to the classical model, the propagation speed is entirely independent of the source velocity. Thus, without resort to any mathematics, it is obvious that the local-ether model is in accord with the constancy of the speed of light found in the astronomical observation of binary stars, in spite of the fact that they tend to move at considerably different velocities with respect to an observer on the ground [14].

Moreover, the local-ether model is in accord with the constancy of the speed observed in the gamma ray from the synchrotron radiation of high-energy electrons [76] or from the decay of high-energy semistable π^0 mesons [4]. In the practice described in these experiments, the geometric distance between two separated gamma-ray detectors divided by the measured delay time between them is adopted as the propagation speed. This practice implies that the Sagnac effect is omitted tacitly and the path length is taken to be the propagation range. Accordingly, as discussed previously, the propagation speed calculated in such a way involves the velocity of the detectors with respect to the local-ether frame, while it is entirely independent of the velocity of the emitting particles.

In these terrestrial experiments with geostationary detectors, the receiver speed is due to earth's rotation alone. Obviously, this speed is relatively low and hence the calculated speed is substantially identical to c. Nevertheless, by virtue of the Sagnac effect due to earth's rotation, the calculated propagation speed is expected to be slightly different when the propagation direction of the gamma ray is different with respect to the ground. This terrestrial anisotropy in the propagation speed calculated directly in terms of the path length provides a means to test the local-ether model.

1.6.5 Spatial isotropy in geostationary path or cavity

Consider the experiment with a one-way fiber link, where the phase difference between the waves generated from two identical stable hydrogen masers at 100 MHz was measured by using a network analyzer every a few seconds for a couple of days [60]. The two masers are separated by a long distance of about 20 km and linked by a stable optical fiber. One signal was fed directly into the analyzer, while the other was used to modulate a laser carrier to propagate over the fiber to the analyzer. It has been found that the phase difference between the two waves is highly stable, hour by hour and day by day. Thus a spatial isotropy is observed in the link, since the phase difference is stable regardless of earth's rotational and orbital motions and is independent of the orientation and position of the Earth in space.

According to the local-ether model, the propagation time for this terrestrial experiment is obviously independent of earth's orbital motion. Further, the propagation time τ implied in (1.4) can be written implicitly as

$$\tau = \frac{1}{c}\sqrt{R_t^2 + 2\mathbf{R}_t \cdot \mathbf{v}_E\tau + v_E^2\tau^2}, \tag{1.20}$$

where $\mathbf{v}_E$ is the linear velocity due to earth's rotation and represents the velocity of a geostationary path with respect to an ECI frame. As the transmission path is in a fiber rather than in free space, the propagation speed c in the preceding formula has to be modified, as to be discussed in Chapter 3. And, as the link is not straight, the propagation time has to be evaluated by summing up the terms given by the preceding formula over the link, with $\mathbf{R}_t$ representing the directed length of each linear short segment of the fiber link.

Anyway, as long as the fiber link is geostationary, the dot product $\mathbf{R}_t \cdot \mathbf{v}_E$ as well as the speed v_E is invariant during earth's rotation for each individual segment, since the direction of $\mathbf{R}_t$ and the one of $\mathbf{v}_E$ change in a coordinated way with this rotation. Consequently, the Sagnac effect due to earth's rotation and hence the propagation time are invariant under the rotation. Thereby, the proposed local-ether model is in accord with the spatial isotropy associated with the phase stability observed in the one-way-link experiment.

A similar spatial isotropy has been demonstrated in the Kennedy-Thorndike experiment which deals with the interference between two waves propagating along paths different in length and shape [54]. Since the interferometer is geostationary, it can be expected that as in the one-way fiber link, the propagation time for either path is invariant under earth's rotation. Therefore, the phase difference between the two paths is also invariant under earth's motions.

The spatial isotropy has also been demonstrated in the laser heterodyne experiment with a geostationary cavity with high precision [44]. As in the one-way fiber link, the round-trip propagation time for a geostationary cavity is invariant under earth's rotation. Therefore, the resonant frequency of this cavity and hence the beat frequency are invariant under earth's rotational and orbital motions.

However, as discussed previously, the terrestrial anisotropy due to earth's rotation can be expected when the orientation of the path or the cavity is changing with respect to the ground. Thus the phase variation over the one-way fiber link tends to be different when the propagation direction of the wave is different with respect to the ground. For a given link, this terrestrial anisotropy could be observed by using two network analyzers.

The signal from either of the masers is fed directly into an analyzer and at the same time is made to propagate over the link to the other analyzer. And the phase variations detected respectively at the two analyzers are recorded and compared. Suppose that the masers and analyzers can be arranged in a symmetric way with precision and the phase difference between the two masers can be determined *a priori*. Then, based on the propagation-range formula, it is seen that for an east-west-oriented link, the difference in phase variation between the two reciprocal cases with waves propagating in opposite directions is proportional to the path length and to the normalized speed v_E/c. Meanwhile, for a north-south link, the first-order difference between the reciprocal phase variations vanishes. This predicted terrestrial anisotropy in the phase variation over a one-way link then provides a means to test the local-ether model.

1.6.6 Doppler effect and Roemer's observations

Consider the Doppler effect for the case where the source is periodically emitting waves and is moving with respect to the receiver. Due to the relative motion between the transmitter and the receiver, the rate of reception tends to be different from the one of emission. For two waves transmitted with a time difference $\triangle t'$, the received time difference $\triangle t$ is given by

$$\triangle t = \triangle t' + \frac{R(t' + \triangle t')}{c} - \frac{R(t')}{c}, \tag{1.21}$$

where $R(t)$ denotes the propagation range for the wave emitted at an arbitrary instant t. It is seen that the variation in the propagation range determines the shift between $\triangle t$ and $\triangle t'$.

As the wave is emitted continuously, the transmitted time difference $\triangle t'$ can be differentially small. Thus $\triangle t$ and $\triangle t'$ and hence the received frequency f_r and the transmitted frequency f_t are related by

$$\frac{f_t}{f_r} = \frac{\triangle t}{\triangle t'} = 1 + \frac{dR}{cdt}, \tag{1.22}$$

where the time derivative is evaluated at the instant of emission and is supposed to be substantially constant over a few or more periods of the wave as its frequency is normally high. It is seen that the Doppler frequency shift is due to the time rate of change in the propagation range and hence the reference frame of the Doppler effect is identical to the one of the Sagnac effect associated with the propagation range.

Based on the first-order propagation-range formula (1.7), the second-order Doppler frequency relation can be derived, as to be discussed in Chapter 7. Ordinarily, the first-order Doppler effect suffices. For this case $dR/dt \simeq dR_t/dt = u_{es}$, where the radial speed $u_{es} = \mathbf{v}_{es}\cdot\hat{R}_t$ and $\mathbf{v}_{es}$ $(= \mathbf{v}_e - \mathbf{v}_s)$ is the Newtonian relative velocity between the receiver and the source which move at velocities $\mathbf{v}_e$ and $\mathbf{v}_s$, respectively, at the instant of emission. Thus the first-order Doppler formula becomes the familiar form

$$f_t/f_r = 1 + u_{es}/c. \tag{1.23}$$

It is noted that in this approximation the Sagnac effect is wholly ignored and the involved radial speed is relative. Thus the first-order Doppler effect as well as the first-order radar echo time complies with the principle of relativity and hence with Galilean relativity. This Doppler formula has been adopted in GPS for the measurement of the receiver velocity [53] and in the stellar frequency shift.

In Roemer's observations, the apparent time interval $\triangle t$ between two successive eclipses of a moon of Jupiter is expected to vary fractionally as $1 + u_{es}/c$, where u_{es} is the radial speed of the earthbound observer relative to Jupiter and is due mainly to the orbital motion of the Earth. Thus the apparent eclipse interval is expected to exhibit a seasonal variation. With the astronomical knowledge of planetary motions in the solar system, the dependence of the apparent interval $\triangle t$ on the normalized speed u_{es}/c has been used as a pioneer approach to determine the speed of light.

1.6.7 Spatial anisotropy in CMBR

Consider the Doppler effect in the cosmic microwave background radiation (CMBR). It has been found that the measured spectrum of CMBR matches the one of a blackbody radiation at about 2.73 K [88]. Further, it has been found that the blackbody temperature of the spectrum or simply the antenna temperature (namely, the received power per unit bandwidth) at a particular frequency depends slightly on the direction of reception [88, 104, 31, 75]. The shift in the temperatures exhibits an anisotropy with a small dipole distribution with respect to a particular symmetry axis in a frame beyond the solar system. The cosmic microwave is known to be radiated from numerous sources outside the solar system, which in turn are distributed around the Earth. Further, the various sources are expected to be stationary with respect to each other; otherwise, the directional variation in the temperatures should be more complicated than a dipole one.

Based on the local-ether model, these sources may form an immense local ether which encloses the sun local ether. As the sources are stationary with respect to their local ether, the relative velocity $\mathbf{v}$ between the receiver and the source then becomes the receiver velocity with respect to this supposed CMBR local ether. For an earthbound receiver, the velocity $\mathbf{v}$ incorporates the linear velocity due to the orbital motion of the Sun as well as those due to earth's rotational and orbital motions.

According to (1.23), the first-order Doppler frequency shift is given by

$$\frac{\triangle f}{f_t} = -\frac{v}{c}\cos\theta, \tag{1.24}$$

where $\triangle f = f_r - f_t$ and θ is the angle from $\mathbf{v}$ to $\mathbf{R}_t$. As the receiver velocity $\mathbf{v}$ remains substantially constant over a short measurement interval during which the direction of the receiving antenna (represented by $-\hat{R}_t$) is scanning, the Doppler shift then exhibits a dipole anisotropy of $\cos\theta$. The frequency shift becomes the maximum and the minimum when the reception direction is parallel and antiparallel to the receiver velocity $\mathbf{v}$, respectively.

The frequency shift in turn results in a proportional shift in the antenna temperature (and, similarly, in the blackbody temperature), as the radiation power depends on frequency. The amplitude of the fractional variation in these temperatures is then given by v/c, which is about 10^{-3} according to the measurement data reported in the literature. Thereby, the receiver speed v with respect to the CMBR local ether is expected to be about 300 km/s, which apparently incorporates the orbital motion of the Sun, in addition to earth's orbital and rotational motions.

Further, as well as the eclipse interval in Roemer's observations, the receiver speed v and hence the magnitude of the dipole anisotropy are expected to exhibit a seasonal variation, along with a minute diurnal variation. Earth's orbital motion is expected to affect the dipole amplitude by 10 percent. This seasonal variation has been demonstrated quantitatively by comparing two observations separated by an interval of six months [31, 75]. As the effect of earth's motions has been demonstrated, CMBR together with Roemer's observations then possesses the spatial anisotropy. Compared with the aforementioned spatial isotropy in the earthbound experiments, this anisotropy lies in the situation that the sources are located outside the earth local ether.

As the first-order Doppler effect is associated with a relative velocity, it cannot provide decisive evidence for a proposed propagation model. The derived first-order Doppler shift based on wave propagation in the CMBR local ether will be identical to that in another frame or even to that in the universal ether adopted in a theory associated with the "new aether drift" [104]. From (1.22) a second-order Doppler effect can be derived, which provides a test for the local-ether model if the temperature anisotropy can be measured to that order. Anyway, the dipole anisotropy observed in CMBR is not in conflict with the statement that a cosmic wave can be viewed as propagating mainly via a classical medium stationary in a frame beyond the solar system.

1.6.8 Gravitational effects on wave propagation

To make the local-ether model more complete, we consider the deflection of light by the Sun and the increment of echo time in the interplanetary radar which are commonly known as important evidence supporting the general theory of relativity. Based on the local-ether model, alternative interpretations of these phenomena can be given in a classical way without invoking the space-time curvature.

It is postulated that in the gravitational potential of a celestial body, the speed of light decreases slightly from c to c/n_g with respect to this potential and hence to the local ether of this body, where the *gravitational index* n_g in turn is proposed to be associated with the gravitational potential Φ_g $(= GM/r)$ by $n_g = 1 + 2\Phi_g/c^2$, G is the gravitational constant, and r is the radial distance from the center of the celestial body of mass M.

Then the increment of propagation time per unit propagation range is given by $(n_g - 1)/c$. By integrating this term along the path from the source at the instant of wave emission to the receiver at the instant of reception with respect to a heliocentric inertial frame and to a geocentric one, it will be shown quantitatively in Chapter 5 that this propagation model is in accord with the increment of the interplanetary radar echo time for a microwave passing by the Sun [101, 96, 5] and with the increment of the earthbound GPS propagation time [89, 8], respectively.

Furthermore, it will be shown quantitatively in Chapter 5 that the spatial variation of the gravitational index tends to cause a deflection of a light beam passing by a celestial body. This situation is similar to the total internal reflection of a short wave from the ionosphere of which the refractive index is varying with altitude. Thus the local-ether model is in accord with these gravitational effects commonly ascribed to the general relativity.

1.7 Unsolved and Predicted Propagation Phenomena

Lastly, we discuss the stellar aberration, a propagation phenomenon not yet solved with the local-ether model. Meanwhile, we present some proposed propagation experiments. These predicted propagation phenomena together with the predicted second-order round-trip Sagnac effect due to earth's rotation in the Michelson-Morley-type experiments then provide different approaches to test the proposed local-ether model.

1.7.1 Stellar aberration

Consider Bradley's stellar aberration observed in as early as 1725. In this experiment, the axis of a telescope has to be tilted by a small angle α in order for the light beam from a star to form an image at the center of the focal plane [33]. Like the eclipse interval in Roemer's observations and the antenna temperature of CMBR, this tilt angle exhibits a seasonal variation, along with a diurnal variation. Actually, the stellar aberration is detected just by its variations.

Based on the proposed model, no matter how far the star is, the light observable on the ground eventually enters the sun local ether and then the earth local ether. If the latter can be ignored, then it is the motion of the telescope with respect to the sun local ether that determines the aberration. Further, only the motion transverse to the transmission path contributes to the aberration. The tilting is toward this transverse direction. Thereby, a classical derivation immediately leads to the aberration angle

$$\alpha = \tan^{-1}(v_\perp / c), \tag{1.25}$$

where $v_\perp$ is the transverse component of the velocity of a telescope with respect to a heliocentric inertial frame. As this velocity incorporates earth's rotational and orbital motions, the diurnal and the annual stellar aberration can be expected, respectively.

Further, the preceding formula shows that the aberration depends on the position of a star but not at all on the star velocity. This is in accord with the observations that the aberration is identical between binary stars and that the amplitude of the aberration variation is identical among all the stars, in spite of the fact that the velocities of the stars can be quite different with respect to a geostationary telescope [48, 27, 79].

However, when the earth local ether is taken into consideration as it should be, the explanation for the annual aberration is then far from satisfactory. To tackle this problem, the wave behaviors (especially, the propagation direction) across the interface separating the two local ethers in relative motion have to be identified. This interface problem deserves further study. Anyway, the local-ether model is in accord with the diurnal aberration, since this one is associated with the motion of a telescope with respect to the earth local ether and does not involve the interface.

1.7.2 One-way-link rotor experiment

In order to test the Sagnac effect due to earth's rotation with a more feasible approach, we propose the rotor experiment by putting the setup of the aforementioned one-way-link experiment with a shortened link on a rotor or a turntable in a horizontal plane, just as in the Michelson-Morley experiment. However, unlike the situation in that experiment, the Sagnac effect on the one-way propagation time is of the first order and hence the measurement could be easier. To simplify the wave propagation, the fiber had better be replaced simply with free space as the link. The role of a dielectric medium will be discussed in Chapter 3.

As the rotor is made to change its direction with respect to the ground, the direction of $\mathbf{R}_t$ and hence the dot product $\mathbf{R}_t \cdot \mathbf{v}_E$ in the propagation-time formula (1.20) will change, where $\mathbf{R}_t$ is the directed separation distance from the source to the receiver. Accordingly, to the first order of normalized speed, the fractional variation of the one-way propagation time is given by

$$\frac{\delta\tau}{\tau} = \frac{v_E}{c} \cos\theta_t, \tag{1.26}$$

where θ_t is the angle from $\mathbf{v}_E$ to $\mathbf{R}_t$ and corresponds to the rotation of the rotor. Since the velocity $\mathbf{v}_E$ due to earth's rotation is eastward, $\theta_t = 0$ and π when the direction of $\mathbf{R}_t$ points to the east and the west, respectively.

For a signal of frequency f, the corresponding phase variation over the link is then expected to exhibit a sinusoidal change given by

$$\delta\phi = 2\pi f R_t \frac{v_E}{c^2} \cos\theta_t. \tag{1.27}$$

Thus, at a latitude of θ_l, $\delta\phi \simeq 1.86 f R_t \cos\theta_l \cos\theta_t \times 10^{-3}$, where $\delta\phi$ is in deg, f in GHz, and R_t in meters. This change reaches the maximum or the minimum when the rotor comes to such a position that $\mathbf{R}_t$ points to the east or the west, respectively. Consequently, the terrestrial isotropy with respect to the ground is not expected and a dipole anisotropy could be observed, as the rotor is rotating even smoothly. Thereby, the proposed one-way-link rotor experiment can provide a rather direct means to test the propagation model with a strong effect of the first order of normalized speed.

1.7.3 Second-order radar Doppler shift

Then we consider the Doppler frequency shift in the monostatic radar system, where the received frequency f_r after reflection from the target tends to differ from the transmitted frequency f_t. It is seen that the first-order round-trip propagation range implied in (1.12) is given by $R = 2R_t(1 + u/c)$, where the radial speed $u = \mathbf{v}\cdot\hat{R}_t$ and $\mathbf{v}$ is the velocity of the target relative to the transceiver.

By substituting this propagation range into the Doppler formula (1.22), the transmitted and the received frequency for the round-trip propagation are related by

$$\frac{f_t}{f_r} = 1 + 2\frac{dR_t}{cdt} + 2\frac{d\,(\mathbf{v}\cdot\mathbf{R}_t)}{c^2 dt}. \tag{1.28}$$

As given in [128], to the second order the radar Doppler formula becomes

$$\frac{f_t}{f_r} = 1 + \frac{2u}{c} + \frac{2v^2}{c^2} + \frac{2\mathbf{a}\cdot\mathbf{R}_t}{c^2}, \tag{1.29}$$

where the acceleration $\mathbf{a} = d\mathbf{v}/dt$ and we have made use of $d\mathbf{R}_t/dt = \mathbf{v}$. The inverse frequency ratio, when given to the second order, is

$$\frac{f_r}{f_t} = 1 - \frac{2u}{c} - \frac{2v^2}{c^2} - \frac{2\mathbf{a}\cdot\mathbf{R}_t}{c^2} + \frac{4u^2}{c^2}. \tag{1.30}$$

It is noted that the effect of earth's rotation could be detectable from the second-order terms with v or $\mathbf{a}$.

For the case of radial relative motion without acceleration ($u = \pm v$ and $\mathbf{a} = 0$), the preceding radar Doppler formula becomes a simpler form

$$\frac{f_r}{f_t} = 1 - \frac{2u}{c} + \frac{2u^2}{c^2} = \frac{1 - u/c}{1 + u/c}. \tag{1.31}$$

This formula agrees with that derived from various approaches, including the Lorentz transformation [109, 36], the moving boundary conditions on plane wave reflection [57], and the variation in radar range [36].

However, for the general case, the formula based on the local-ether propagation model disagrees with the preceding formula in the second-order terms. It has been pointed out that for the case of radar tracking where the target is a low-earth-orbit satellite, the discrepancy between the preceding two formulas can be a few Hz when the transmitted frequency is 10 GHz [128]. For the case of transverse relative motion where $u = 0$, the local-ether model leads to a nonzero frequency shift of $\triangle f / f_t = -2v^2/c^2$, in addition to that due to the acceleration. Thus the second-order radar Doppler shift also provides a means to test the propagation model.

1.8 Summary

It is supposed that electromagnetic wave propagates via a medium like the ether. However, the ether is not universal. It is proposed that in the region under a sufficient influence of the gravitation due to the Earth, the Sun, or another celestial body, there forms a local ether which in turn is stationary with respect to the gravitational potential of the respective body. Thereupon, each local ether together with the gravitational potential comoves with the associated celestial body. Thus the earth and the sun local ether are stationary in a geocentric and a heliocentric inertial frame, respectively. Consequently, the propagation of an earthbound electromagnetic wave is referred to this geocentric frame and is entirely independent of earth's orbital motion around the Sun or whatever. Meanwhile, for the interplanetary propagation, the major part of the transmission path is located in the sun local ether and the propagation is entirely independent of the orbital motion of the Sun. The speed of light is referred to the associated local ether and is independent of the motions of the source and the receiver. However, by virtue of the Sagnac effect due to the movement of the receiver with respect to the local ether during wave propagation, the propagation range over the associated medium tends to be different from the frame-invariant path length.

Based on the propagation-range formula, the local-ether model has been used to solve the discrepancies in the effects of earth's rotational and orbital motions. By referring the earthbound propagation range to an ECI frame, the local-ether model accounts for the first-order Sagnac effect due to earth's rotation in GPS, the intercontinental microwave link, and in the loop interferometer. Meanwhile, it immediately accounts for the null effect of earth's orbital motion on the earthbound propagation in these experiments as well as in the one-way fiber-link experiment, the Kennedy-Thorndike experiment, the cavity heterodyne experiment, and in the Michelson-Morley experiment. By referring the interplanetary propagation range to a heliocentric inertial frame, both the rotational and the orbital motion of the Earth are expected to contribute to the Sagnac effect. Thereby, the local-ether model accounts for the discrepancy in the Sagnac effect due to earth's orbital motion between the interplanetary radar and the earthbound GPS and microwave link. When the source and hence the main transmission path are outside the solar system, the orbital motion of the Sun as well as earth's motions is expected to contribute to the Doppler effect. This is in accord with the dipole anisotropy found in the antenna and the blackbody temperature of CMBR and with the seasonal variation of the dipole amplitude.

Moreover, the local-ether model is in accord with the earthbound radar echo time, with the constancy of the speed of light with binary stars, synchrotron electrons, and with semistable particles, and with the Doppler effect in GPS, the stellar frequency shift, Roemer's observations, and in the earthbound radar. Further, by modifying the speed of light under a gravitational potential, the local-ether model is in accord with the deflection of light by the Sun and the increment of echo time in the interplanetary radar, which are commonly cited as evidence supporting the general theory of relativity.

While earth's rotation contributes to the Sagnac effect, the contribution for a geostationary transmission path is invariant under this rotation. This invariance accounts for the hourly and daily stability of phase difference in the one-way fiber-link experiment and in the Kennedy-Thorndike experiment, and accounts for the one of beat frequency in the cavity heterodyne experiment. Thus it is the invariance in the Sagnac effect that corresponds to the spatial isotropy observed in these geostationary interference experiments. However, if the interferometer is put on a turntable as in the Michelson-Morley experiment, the terrestrial isotropy can no longer hold and hence an anisotropy can be observed as the turntable is rotating. Based on the round-trip Sagnac effect due to earth's rotation, we predict a quadrupole anisotropy in phase difference in the Michelson-Morley experiment and a like one in beat frequency in the cavity heterodyne experiment. Further, based on the one-way Sagnac effect due to earth's rotation, we propose the one-way-link rotor experiment, in which a terrestrial dipole anisotropy in phase variation is predicted. Unlike the situation in the Michelson-Morley-type experiments, the one-way Sagnac effect is of the first order of normalized speed and hence the measurement could be easier.

Although the proposed local-ether model is just a simple modification of the classical propagation model with the switchability of the unique propagation frame, it does account for a wide variety of earthbound, interplanetary, and interstellar propagation phenomena, except for the annual stellar aberration. The strong evidence for this model is its consistent account of the Sagnac effect due to earth's motions among GPS, the intercontinental microwave link, the interplanetary radar, the Michelson-Gale experiment, and the Michelson-Morley experiment. Moreover, it leads to the predictions associated with the one-way or round-trip Sagnac effect due to earth's rotation, which then provide different approaches to test the local-ether model. Further, the proposed propagation model provides the groundwork for the local-ether wave equation which will be shown to lead to a unified quantum theory of gravitational and electromagnetic forces and to the speed-dependence in mass, quantum energy, transition frequency, and in matter wavelength.

Chapter 2

Modifications of Lorentz Force Law

It is generally expected from intuition that the electromagnetic force exerted on a charged particle should remain unchanged when observed in different reference frames in uniform motion of translation. In the special relativity, this invariance is achieved by invoking the Lorentz transformation of space and time. However, it is noticed that the electric current generating the magnetic force is commonly the conduction current rather than the convection current. The mobile charged particles forming a conduction current are embedded in a neutralizing matrix. Thus an entirely different interpretation of the invariance of force is possible. In this Chapter we present a new model of the electromagnetic force given in terms of the augmented potentials, which in turn are derived from the electric scalar potential by incorporating a velocity difference between the involved particles. The propagation of the potentials is supposed to follow the local-ether model presented in Chapter 1. All of the position vectors, time derivatives, and velocities involved in the proposed potentials and force law are referred specifically to their respective frames. By virtue of this feature, the electromagnetic force is frame-invariant simply based on Galilean transformations. The proposed model looks quite different from the Lorentz force law, except the electrostatic force. However, under the common low-speed condition where the mobile charged particles drift very slowly with respect to the matrix, it is shown that the proposed model reduces to the Lorentz force law, if the latter is observed in the matrix frame as done tacitly in common practice.

2.1 Frame-Invariance of Electromagnetic Force

It is widely accepted that the electromagnetic force exerted on a particle of charge q and velocity $\mathbf{v}$ is governed by the Lorentz force law which, in terms of electric and magnetic fields, is given in the form $\mathbf{F} = q(\mathbf{E} + \mathbf{v} \times \mathbf{B})$. According to this famous law, the force consists of the electric and the magnetic force. The magnetic force is associated with the magnetic field and depends on the velocity $\mathbf{v}$ of the affected particle, while the electric force is with the electric field and is independent of the motion of this particle. Moreover, the current density, which generates the magnetic field, is commonly given by the product of the charge density and the velocity of the mobile charged particles and hence corresponds to the convection current, as the one adopted in the formulations presented by Maxwell [80], Heaviside [43], Lorentz [72], and by Einstein [24].

It is generally expected from intuition that a force exerted on a particle should remain unchanged when observed in different reference frames in uniform motion of translation to each other. That is, the observed force is frame-invariant. Thus it was widely presumed that the velocities of the affected and the source particles associated with the magnetic force should have a preferred reference frame. Otherwise, the Lorentz force law is obviously not invariant under Galilean transformations, while Galilean invariance is common in classical mechanics, such as in Newton's laws of motion and in the conservation laws for momentum and kinetic energy.

Historically, there was disagreement over the reference frame of the particle velocity among Maxwell, Thomson, Lorentz, and Einstein who pioneered in the development of electromagnetics. In Maxwell's treatise on electricity and magnetism, the velocity seems to mean the relative velocity, since it had been noticed that it is the relative motion between one coil and another that determines the induction in Faraday's experiments [80]. And the electric current had been attributed to a motion associated with "the velocity with which the electricity passes through the body". In the analysis of the experiments on magnetic deflection with cathode rays, which eventually led to the discovery of the electron, Thomson supposed that the electromagnetic force depends both on the relative velocities and on the *actual* velocities of the involved particles, where the actual velocity is referred to the magnetic medium through which the particle is moving [110]. In Lorentz's theory of electrons, the velocity seems to be referred to the ether, since it was supposed that the charges move through the ether, which occupies all space between particles and pervades the particles [72].

However, in the past century, an almost unanimously accepted explanation is provided by Einstein's special relativity, whereby the velocity is referred to an arbitrary inertial frame. When observed in another frame, as discussed in the Introduction, the relevant electromagnetic quantities of the charge density, current density, potentials, and fields will change with the relative velocity between the two frames according to the Lorentz transformation of space and time. Meanwhile, the kinematical quantities of the velocity, momentum, and force will also change under this transformation. It can be shown that the transformation of the time rate of change of momentum of a charged particle is exactly identical to the Lorentz force given in terms of the transformed fields and velocity [74]. In other words, the Lorentz force law is invariant under the Lorentz transformation.

While the Lorentz transformation solves the problem associated with the changes of the particle velocities and current density with reference frames, it is noticed that the electric current generating the magnetic force in the magnetic deflection or in motors is commonly electrically neutralized. Precisely, it is the conduction current rather than the convection current. That is, the mobile source particles that form this current are actually embedded in a matrix, and the ions that constitute the matrix tend to electrically neutralize the mobile particles drifting through it, such as electrons in a metal wire. Without doubt, the ions also form a current if the matrix is moving, as well as the mobile source particles. Therefore, by superposition, the velocity that determines the neutralized current density is the drift velocity of the mobile particles with respect to the neutralizing matrix, regardless of the motions of the matrix and the observer. Thus the neutralized current density and hence the conduction current remain unchanged when observed in different frames.

Further, it is noticed that the mobile source particles commonly drift very slowly in the matrix. For conduction electrons in a metal, the drift speed is normally lower than 1 mm/s. Thereby, if the magnetic force is associated with the squared velocity difference between the affected and the source particles, then, by virtue of the compensation due to the neutralizing matrix, the magnetic force can be linearly proportional to the velocities of the affected and the source particles both with respect to the matrix. This situation is somewhat similar to the relation $(\mathbf{v}-\mathbf{v}_s)^2-(\mathbf{v}-\mathbf{v}_m)^2 \simeq -2(\mathbf{v}-\mathbf{v}_m)\cdot(\mathbf{v}_s-\mathbf{v}_m)$ if $\mathbf{v}_s \simeq \mathbf{v}_m$. Thus the magnetic force as well as the neutralized current density can be frame-invariant simply based on Galilean transformations.

Another quantity pertinent to the issue of the reference frame is the propagation velocity of the potentials and fields. In Chapter 1 we have presented a local-ether model of wave propagation, whereby electromagnetic wave is supposed to propagate via a medium like the ether. However, the ether is not universal. Specifically, it is proposed that in the region under a sufficient influence of the gravitation due to the Earth, the Sun, or another celestial body, there forms a local ether which in turn moves with the gravitational potential of the respective body. Thus, as well as earth's gravitational potential, the earth local ether for earthbound propagation is stationary in an earth-centered inertial (ECI) frame. Consequently, earthbound wave phenomena can depend on earth's rotation but are entirely independent of earth's orbital motion around the Sun or whatever. Meanwhile, the sun local ether for interplanetary propagation is stationary in a heliocentric inertial frame. This local-ether model has been adopted to account for the effects of earth's motions in a wide variety of propagation phenomena, particularly the Sagnac correction in the global positioning system, the time comparison via the intercontinental microwave link, and the echo time in the interplanetary radar. Moreover, as examined within the present precision, the local-ether model is still in accord with the Michelson-Morley experiment which is known to make the classical ether notion obsolete.

As a consequence, the propagation mechanism of the potentials associated with the electromagnetic fields and force is expected to follow the local-ether model. Thus the potentials propagate away from the location of the source at the speed of light c with respect to an ECI frame for earthbound phenomena. This propagation model also implies that the position vectors of the affected and the source particles involved in the potentials should be referred specifically to the associated local-ether frame in calculating the propagation delay time in terms of the isotropic propagation speed c. A further consequence is that this restriction on reference frames necessitates the construction of a new model of electromagnetic force which complies with the frame-invariance of magnetic force, with Galilean transformations, and with the local-ether propagation model, and is still in accord quantitatively with the well-studied phenomena known to follow the Lorentz force law.

Accordingly, we propose in this Chapter the augmented potential, which is derived from the electric scalar potential by additionally incorporating a squared velocity difference between the affected and the source particles. Then, in terms of the spatial and temporal derivatives of the augmented potential, we propose a new model of electromagnetic force. Each of the position vectors, time derivatives, propagation velocity, particle velocities, and current density involved in the proposed model will be imposed with a deliberately selected reference frame. By virtue of this simple feature, the augmented potential and the electromagnetic force are frame-invariant, as expected intuitively. Thereby, an entirely different explanation of the invariance of electromagnetic force is presented. The proposed force law looks quite different from the Lorentz force law given in terms of the potentials. However, it will be shown elaborately that in spite of the dissimilarity and the restriction on reference frames, this new classical model can reduce to a form quite similar to the famous Lorentz force law under some ordinary conditions.

2.2 Augmented Potentials and Electromagnetic Force Law

In this section we present the new electromagnetic force law given in terms of the potential $\breve{\Phi}$, which is a modification of the electric scalar potential by additionally incorporating a squared velocity difference and hence is called the augmented scalar potential. Consider an ensemble of mobile source particles of volume charge density ρ_v. The various source particles contribute collectively to the potential which in turn will propagate to and then affect another charged particle under consideration called the *effector*.

It is proposed that the *augmented scalar potential* $\breve{\Phi}$ experienced by an effector particle is given explicitly by the integral over a volume containing all the source particles

$$\breve{\Phi}(\mathbf{r}, t) = \frac{1}{4\pi\epsilon_0} \int \left(1 + \frac{v_{es}^2}{2c^2}\right) \frac{\rho_v(\mathbf{r}', t - R/c)}{R} dv', \qquad (2.1)$$

where $v_{es} = |\mathbf{v}_{es}|$, the velocity difference $\mathbf{v}_{es} = \mathbf{v}_e - \mathbf{v}_s$, $\mathbf{v}_e$ is the velocity of the effector particle located at position $\mathbf{r}$ at instant t, $\mathbf{v}_s$ is that of the source particles distributed at position $\mathbf{r}'$ at an earlier instant t' $(= t - R/c)$, the propagation range R $(= |\mathbf{r} - \mathbf{r}'|)$ is the distance from the source point $\mathbf{r}'$ to the field point $\mathbf{r}$, R/c denotes the propagation delay time from the source to the effector at the respective positions and instants, and ϵ_0 is the permittivity.

It is noted that $\mathbf{v}_{es}$ denotes the difference between the velocities of the effector and the source at two distinct instants. For quasi-static cases where the propagation delay time R/c can be neglected or for the case where the velocity $\mathbf{v}_s$ is fixed, the non-simultaneous velocity difference $\mathbf{v}_{es}$ then becomes the Newtonian relative velocity between the effector and the source. It is supposed that the effector speed v_e, the source speed v_s, and hence v_{es} are much lower than c, as they are ordinarily. Thus the augmentation with the scalar potential is of the second order of normalized speed (with respect to c) and is actually quite small in magnitude.

Now we address ourselves to the issue of the reference frames of the position vectors, the particle velocities, and the propagation velocity. According to the evidence supporting the local-ether model, the propagation range R for an earthbound electromagnetic wave is referred specifically to an ECI frame; otherwise, the propagation delay time tends to differ from R/c. Accordingly, the position vectors $\mathbf{r}$ and $\mathbf{r}'$, which determine the propagation range, are also referred specifically to that frame. Thus, when observed in the associated local-ether frame, the potential propagates at the isotropic speed c away from the emission position, regardless of the motions of the source and effector. Moreover, in order to comply with the reference frame of the corresponding position vectors, the effector velocity $\mathbf{v}_e$ and the source velocity $\mathbf{v}_s$ are also referred specifically to the local-ether frame. Thereby, all the position vectors and velocities involved in the proposed augmented potential are referred uniquely to the local-ether frame.

In addition to the augmented scalar potential $\breve{\Phi}$, we define the *augmented vector potential* $\breve{\mathbf{A}}$ also in terms of the velocity difference $\mathbf{v}_{es}$ and the charge density ρ_v. That is,

$$\breve{\mathbf{A}}(\mathbf{r}, t) = \frac{-1}{4\pi\epsilon_0 c^2} \int \frac{\mathbf{v}_{es}\rho_v(\mathbf{r}', t - R/c)}{R} dv'. \tag{2.2}$$

It is noted that both of the augmented potentials depend on the effector velocity and hence tend to be different for different effectors.

Under the influence of the augmented potentials originating from an ensemble of mobile source particles, the electromagnetic force exerted on an effector particle of charge q and located at position $\mathbf{r}$ at instant t is hereby postulated to be

$$\mathbf{F}(\mathbf{r}, t) = q \left\{ -\nabla\breve{\Phi}(\mathbf{r}, t) - \left(\frac{\partial}{\partial t} \breve{\mathbf{A}}(\mathbf{r}, t) \right)_e \right\}, \tag{2.3}$$

where the time derivative $(\partial\breve{\mathbf{A}}/\partial t)_e$ is referred specifically to the effector frame with respect to which the effector of velocity $\mathbf{v}_e$ is stationary. Physically, an effector-frame time derivative represents the time rate of change in some quantity experienced by the effector.

As all of the position vectors, the particle velocities, the propagation velocity, and the time derivative are referred specifically to their respective frames, the values of the augmented potentials and their derivatives at a given position are indeed frame-invariant. And the corresponding electromagnetic force remains unchanged in different frames in uniform motion of translation, as expected intuitively.

It is noted that the augmented vector potential $\breve{\mathbf{A}}$ is related to the negative of the derivative of $\breve{\Phi}$ with respect to the effector speed v_e. Thus the proposed electromagnetic force law can be rewritten in terms of the augmented scalar potential alone. That is,

$$\mathbf{F}(\mathbf{r},t) = q\left\{-\nabla\breve{\Phi}(\mathbf{r},t) + \left(\frac{\partial}{\partial t}\sum_i \hat{i}\frac{\partial}{\partial v_{ei}}\breve{\Phi}(\mathbf{r},t)\right)_e\right\}, \tag{2.4}$$

where $v_{ei} = \mathbf{v}_e \cdot \hat{i}$, $\hat{i}$ is a unit vector, and the index $i = x, y, z$. It is noticed that this formula resembles Lagrange's equations in classical mechanics adopted by Thomson in exploring magnetic force [110].

In Chapter 4, based on the local-ether propagation model, we will present a wave equation which incorporates the electric scalar potential and an operator corresponding to the squared velocity difference. From this local-ether wave equation, the proposed force law, together with the augmented potentials and the inertial mass of the effector, can be derived from a quantum-mechanical approach. Anyway, in this Chapter, formulas (2.1)–(2.3) (or, equivalently, (2.1) and (2.4)) serve as our fundamental postulates for the electromagnetic force law complying with Galilean transformations and the local-ether model of wave propagation. This local-ether electromagnetic force law made its debut in [130].

It is noted that in the proposed model the force term associated with the major part of $\nabla\breve{\Phi}$ is independent of the particle velocities, while the other terms depend on them. The velocity-dependent force terms are expected to be much weaker than the velocity-independent one by nature, since they incorporate the common factor $1/c^2$. The velocity-independent term is identical to the conventional electrostatic force when the propagation delay of the potentials is not considered. However, the velocity-dependent force terms look quite different from their counterparts in the Lorentz force law given by (I.3). The similarity will emerge under the common low-speed condition where the source particles drift very slowly in a neutralizing matrix, as discussed in the following sections.

2.3 Augmented Potentials under Neutralization

Consider the common case where the conduction current is involved. Thus the ensemble of mobile charged particles forming the current is actually embedded in a matrix. There are various types of the matrix, such as metal in antennas, semiconductor in light-emitting diodes, dielectric in optical fibers, and magnet in motors. The ions that constitute the matrix tend to electrically neutralize the mobile particles. Without the neutralizing matrix, the electrostatic force will be overwhelmingly dominant over the others.

Anyway, the charge density ρ_m of the matrix is supposed to be arbitrary for generality. The neutralizing matrix can be not really in existence, for which case $\rho_m = 0$ and all the charged particles, positive or negative, are taken as the sources. Ordinarily, the matrix is fixed in shape and moves as a whole at a substantially uniform velocity $\mathbf{v}_m$, which for convenience is also referred to the local-ether frame identical to the one of the source and effector velocities. Thus the various ions forming the matrix also move at this velocity.

Then, due to the ensemble of mobile source particles and the matrix, the total electromagnetic force exerted on an effector is given by superposition. A little algebra yields that the augmented potentials under neutralization take the forms

$$\breve{\Phi}(\mathbf{r},t) = \Phi(\mathbf{r},t)\left(1 + \frac{v_{em}^2}{2c^2}\right) - \mathbf{v}_{em}\cdot\mathbf{A}(\mathbf{r},t) + \frac{1}{2\epsilon_0 c^2}\int \frac{v_{sm}^2 \rho_v}{4\pi R}dv' \quad (2.5)$$

and

$$\breve{\mathbf{A}}(\mathbf{r},t) = \mathbf{A}(\mathbf{r},t) - \frac{1}{c^2}\mathbf{v}_{em}\Phi(\mathbf{r},t), \quad (2.6)$$

where $v_{em} = |\mathbf{v}_{em}|$, $\mathbf{v}_{em} = \mathbf{v}_e - \mathbf{v}_m$, $v_{sm} = |\mathbf{v}_{sm}|$, $\mathbf{v}_{sm} = \mathbf{v}_s - \mathbf{v}_m$, and ρ_v stands for $\rho_v(\mathbf{r}', t - R/c)$. The electric scalar potential Φ and the magnetic vector potential $\mathbf{A}$ in turn are defined respectively as

$$\Phi(\mathbf{r},t) = \frac{1}{\epsilon_0}\int \frac{\rho_n(\mathbf{r}', t - R/c)}{4\pi R}dv' \quad (2.7)$$

and

$$\mathbf{A}(\mathbf{r},t) = \frac{1}{\epsilon_0 c^2}\int \frac{\mathbf{J}_n(\mathbf{r}', t - R/c)}{4\pi R}dv', \quad (2.8)$$

where the potential Φ is due to the net charge density $\rho_n = \rho_v + \rho_m$ and the potential $\mathbf{A}$ is due to the *neutralized current density* $\mathbf{J}_n$ which in turn is related to the source charge density ρ_v by

$$\mathbf{J}_n(\mathbf{r},t) = \mathbf{v}_{sm}\rho_v(\mathbf{r},t). \quad (2.9)$$

2.3 Augmented Potentials under Neutralization

Consider the common case where the conduction current is involved. Thus the ensemble of mobile charged particles forming the current is actually embedded in a matrix. There are various types of the matrix, such as metal in antennas, semiconductor in light-emitting diodes, dielectric in optical fibers, and magnet in motors. The ions that constitute the matrix tend to electrically neutralize the mobile particles. Without the neutralizing matrix, the electrostatic force will be overwhelmingly dominant over the others.

Anyway, the charge density ρ_m of the matrix is supposed to be arbitrary for generality. The neutralizing matrix can be not really in existence, for which case $\rho_m = 0$ and all the charged particles, positive or negative, are taken as the sources. Ordinarily, the matrix is fixed in shape and moves as a whole at a substantially uniform velocity $\mathbf{v}_m$, which for convenience is also referred to the local-ether frame identical to the one of the source and effector velocities. Thus the various ions forming the matrix also move at this velocity.

Then, due to the ensemble of mobile source particles and the matrix, the total electromagnetic force exerted on an effector is given by superposition. A little algebra yields that the augmented potentials under neutralization take the forms

$$\breve{\Phi}(\mathbf{r}, t) = \Phi(\mathbf{r}, t)\left(1 + \frac{v_{em}^2}{2c^2}\right) - \mathbf{v}_{em} \cdot \mathbf{A}(\mathbf{r}, t) + \frac{1}{2\epsilon_0 c^2}\int \frac{v_{sm}^2 \rho_v}{4\pi R} dv' \quad (2.5)$$

and

$$\breve{\mathbf{A}}(\mathbf{r}, t) = \mathbf{A}(\mathbf{r}, t) - \frac{1}{c^2}\mathbf{v}_{em}\Phi(\mathbf{r}, t), \quad (2.6)$$

where $v_{em} = |\mathbf{v}_{em}|$, $\mathbf{v}_{em} = \mathbf{v}_e - \mathbf{v}_m$, $v_{sm} = |\mathbf{v}_{sm}|$, $\mathbf{v}_{sm} = \mathbf{v}_s - \mathbf{v}_m$, and ρ_v stands for $\rho_v(\mathbf{r}', t - R/c)$. The electric scalar potential Φ and the magnetic vector potential $\mathbf{A}$ in turn are defined respectively as

$$\Phi(\mathbf{r}, t) = \frac{1}{\epsilon_0}\int \frac{\rho_n(\mathbf{r}', t - R/c)}{4\pi R} dv' \quad (2.7)$$

and

$$\mathbf{A}(\mathbf{r}, t) = \frac{1}{\epsilon_0 c^2}\int \frac{\mathbf{J}_n(\mathbf{r}', t - R/c)}{4\pi R} dv', \quad (2.8)$$

where the potential Φ is due to the net charge density $\rho_n = \rho_v + \rho_m$ and the potential $\mathbf{A}$ is due to the *neutralized current density* $\mathbf{J}_n$ which in turn is related to the source charge density ρ_v by

$$\mathbf{J}_n(\mathbf{r}, t) = \mathbf{v}_{sm}\rho_v(\mathbf{r}, t). \quad (2.9)$$

It is noted that the velocity $\mathbf{v}_{sm}$ of the mobile source particles forming the neutralized current density is referred specifically to the matrix. This velocity is a Newtonian relative velocity representing the drift velocity of the source particles in the matrix. Thus the neutralized current density and hence the conduction current are frame-invariant and comply with Galilean relativity. Moreover, the values of the local-ether potentials Φ and $\mathbf{A}$ defined in the preceding formulas are also frame-invariant. It is noted that unlike the augmented potentials, the potentials Φ and $\mathbf{A}$ do not depend on the effector velocity and hence their distributions apply to different effectors. Thus it can be more convenient to express an electromagnetic force in terms of Φ and $\mathbf{A}$ when possible.

2.4 Force Law under Low-Speed Condition

Ordinarily, the mobile source particles forming a conduction current drift very slowly with respect to the matrix. Besides, the speeds of terrestrial particles with respect to an ECI frame are normally of the order of the linear speed due to earth's rotation, which in turn is much lower than c. Thus the particle speeds and the matrix speed are supposed to satisfy the *low-speed condition* given by

$$v_{sm} \lll c \quad \text{and} \quad v_{em}, v_m \ll c. \tag{2.10}$$

In words, this ordinary condition states that the effector, sources, and matrix move somewhat slowly with respect to the local-ether frame and the sources drift very slowly with respect to the matrix frame in which the matrix is stationary.

Thereby, the augmented scalar potential becomes a simpler form

$$\breve{\Phi}(\mathbf{r}, t) = \Phi(\mathbf{r}, t) - \mathbf{v}_{em} \cdot \mathbf{A}(\mathbf{r}, t). \tag{2.11}$$

It is noted that under the low-speed condition, the augmented scalar potential as well as the augmented vector potential can be determined from Φ, $\mathbf{A}$, and $\mathbf{v}_{em}$. As the drift speed is very low with respect to the matrix frame and thus the quadratic term v_{sm}^2 can be neglected, the matrix frame then becomes the most convenient reference frame in dealing with the electromagnetic force, where the matrix is supposed to move at a substantially fixed velocity.

The forces due to the velocity-dependent parts of the potentials are much weaker than the electrostatic force by nature and hence they are substantially observable only under sufficient neutralization. That is, $\rho_m \simeq -\rho_v$ and hence $|\rho_n| \ll |\rho_v|$. Under complete neutralization $\rho_n = 0$, $\breve{\mathbf{A}}$ becomes identical to $\mathbf{A}$. Suppose for the moment that the density ρ_n incorporated in $\breve{\mathbf{A}}$ can be neglected. Then the augmented vector potential reduces to the magnetic vector potential. That is,

$$\breve{\mathbf{A}}(\mathbf{r}, t) = \mathbf{A}(\mathbf{r}, t). \tag{2.12}$$

The roles of the omitted parts in the preceding two relations for the potentials will be discussed in a later section.

And, from the Galilean transformation (I.16), the time derivative $(\partial \mathbf{A}/\partial t)_e$ referred to the effector frame can be given in terms of the time derivative $(\partial \mathbf{A}/\partial t)_m$ referred to the matrix frame. That is,

$$\left(\frac{\partial}{\partial t}\mathbf{A}(\mathbf{r}, t)\right)_e = \left(\frac{\partial}{\partial t}\mathbf{A}(\mathbf{r}, t)\right)_m + (\mathbf{v}_{em} \cdot \nabla)\mathbf{A}(\mathbf{r}, t). \tag{2.13}$$

Thereby, the proposed electromagnetic force law (2.3) based on the augmented potentials can then be given in terms of the local-ether potentials Φ and $\mathbf{A}$ by

$$\begin{aligned}\mathbf{F}(\mathbf{r}, t) = & -q\nabla\Phi(\mathbf{r}, t) + q\nabla\left[\mathbf{v}_{em} \cdot \mathbf{A}(\mathbf{r}, t)\right] \\ & -q\left(\frac{\partial}{\partial t}\mathbf{A}(\mathbf{r}, t)\right)_m - q\left(\mathbf{v}_{em} \cdot \nabla\right)\mathbf{A}(\mathbf{r}, t). \end{aligned} \tag{2.14}$$

The terms $-q\nabla\Phi$ and $-q(\partial \mathbf{A}/\partial t)_m$ represent the electrostatic force and the electric induction force, respectively; meanwhile, the terms $q\nabla(\mathbf{v}_{em} \cdot \mathbf{A})$ and $-q(\mathbf{v}_{em} \cdot \nabla)\mathbf{A}$ represent the magnetostatic force and the magnetic induction force, respectively.

By using a vector identity, the two force terms associated with the effector velocity $\mathbf{v}_{em}$ can be combined into the magnetic force. Thus the electromagnetic force law becomes a more familiar form

$$\mathbf{F}(\mathbf{r}, t) = q\left\{-\nabla\Phi(\mathbf{r}, t) - \left(\frac{\partial}{\partial t}\mathbf{A}(\mathbf{r}, t)\right)_m + \mathbf{v}_{em} \times \nabla \times \mathbf{A}(\mathbf{r}, t)\right\}. \tag{2.15}$$

According to the dependences of the force terms on $\mathbf{v}_{em}$, one is led to express the force law in terms of the fields $\mathbf{E}$ and $\mathbf{B}$ in the form

$$\mathbf{F}(\mathbf{r}, t) = q\left\{\mathbf{E}(\mathbf{r}, t) + \mathbf{v}_{em} \times \mathbf{B}(\mathbf{r}, t)\right\}, \tag{2.16}$$

where the electric field **E** and the magnetic field **B** are then defined explicitly in terms of the local-ether potentials Φ and **A** as

$$\mathbf{E}(\mathbf{r},t) = -\nabla\Phi(\mathbf{r},t) - \left(\frac{\partial}{\partial t}\mathbf{A}(\mathbf{r},t)\right)_m \tag{2.17}$$

and

$$\mathbf{B}(\mathbf{r},t) = \nabla \times \mathbf{A}(\mathbf{r},t). \tag{2.18}$$

The electromagnetic force law (2.15) or (2.16) under the ordinary low-speed condition represents modifications of the Lorentz force law, which comply with Galilean transformations and the local-ether propagation model.

The fundamental modifications are that the current density generating the potential **A**, the time derivative of **A** in the electric induction force, and the effector velocity connecting to $\nabla \times \mathbf{A}$ in the magnetic force are all referred specifically to the matrix frame, and that the propagation velocity of the potentials is referred specifically to the local-ether frame. Thereupon, the values of the current density, the potentials, the fields, and the force are frame-invariant. The divergence and the curl relations for the electric and magnetic fields together with the local-ether wave equations for the potentials and fields will be discussed in Chapter 3.

2.5 Sagnac-Effect Deviation and Galilean Relativity

In many cases it can be more convenient to deal with the propagation of the potentials in a laboratory frame (such as the matrix frame), instead of the local-ether frame. We then go on to consider the consequence due to the motion of the laboratory frame.

According to the local-ether model, the propagation range R in the definitions of the potentials is the distance between the source point $\mathbf{r}'$ at which the potentials are emitted and the field point $\mathbf{r}$ at which the potentials propagate to the effector, where both $\mathbf{r}'$ and $\mathbf{r}$ are referred uniquely to the local-ether frame. As discussed in Chapter 1, a quantity closely related to the propagation range R is the transmission-path length R_t, which is the geometric distance from the source to the effector right at the instant of wave emission. The difference between the propagation range R and the path length R_t is known to represent the Sagnac effect, which is due to the movement of the effector with respect to the local-ether frame during wave propagation. To the first order of normalized speed, it is known that $R = R_t(1+\hat{R}_t\cdot\mathbf{v}_e/c)$, where the unit vector $\hat{R}_t$ points from the source to the effector at the instant of emission.

Consider the wave propagation observed in a laboratory frame which is moving at a velocity $\mathbf{v}_0$ with respect to the local-ether frame. Thus the apparent propagation range R_l observed in the laboratory frame tends to be different from the actual propagation range R. As discussed in Chapter 1, the difference between the propagation range R and the apparent range R_l represents the deviation in the Sagnac effect, which in turn is due to the motion of the laboratory frame with respect to the local-ether frame during wave propagation. To the first order of normalized speed, it is known that $R - R_l = R_l\hat{R}_t\cdot\mathbf{v}_0/c$.

Ordinarily, a terrestrial laboratory frame is stationary or moving slowly with respect to the ground. The Sagnac-effect deviation is at most of the order of the normalized speed v_0/c which is then as small as about 10^{-6}. If this small term of the normalized laboratory speed can be neglected, then the apparent range is substantially identical to the propagation range. And the corresponding deviation in the propagation time is negligible.

Consequently, when formulated in a laboratory frame with the corresponding Sagnac-effect deviation being omitted, the propagation range R, the propagation time R/c, and the velocity differences $\mathbf{v}_{es}$ and $\mathbf{v}_{em}$ (which in general depend on the propagation time) then become independent of the laboratory velocity. Therefore, the augmented potentials $\breve{\Phi}$ and $\breve{\mathbf{A}}$, the local-ether potentials Φ and $\mathbf{A}$, the local-ether fields $\mathbf{E}$ and $\mathbf{B}$, and then the corresponding electromagnetic force law formulated in a laboratory frame also become independent of the laboratory velocity and hence comply with Galilean relativity, when the Sagnac-effect deviation due to the motion of the laboratory frame is omitted.

As an example, consider the familiar case of the cathode-ray tube (CRT), where an electron beam is accelerated electrostatically by applying a voltage to a pair of electrode plates, and then the beam direction is adjusted by using the magnetic deflection yokes to form an image on a screen. The yoke is a current-carrying winding which results in a magnetic field and hence a magnetic force exerted on the electron beam. Obviously, the yokes form the matrix of this case. According to the local-ether electromagnetic force law, the magnetic force is associated with the velocity of electrons with respect to the laboratory frame in which the matrix together with other components of the CRT is stationary.

Since the Sagnac-effect deviation associated with the laboratory velocity can be neglected, the magnetic field and the magnetic force in a geostationary CRT are independent of earth's rotation and the latitude of the device, let alone earth's orbital motion. Further, when the device is put on a vehicle moving smoothly with respect to the ground, the field and the force are also independent of the ground velocity of the vehicle. This invariance of magnetic deflection keeps the image on a moving CRT unaffected, which is in accord with common experience with this device. Therefore, the operation of the CRT is substantially independent of the laboratory velocity and thus complies with Galilean relativity. Moreover, it is independent of the orientation of the device with respect to the ground and thus exhibits the terrestrial isotropy. A similar argument of the invariance of magnetic force can be applied to a motor, where the current in the stator winding or in the stator magnet, which forms the matrix, results in a magnetic force exerted on the current-carrying rotor.

On the other hand, we examine the laboratory frame adopted in the conventional analysis of the magnetic deflection based on the Lorentz force law. From standard textbooks, it is noticed that the electron speed associated with the magnetic force is commonly given by the square root of the accelerating voltage, aside from a scaling factor incorporating the charge-mass ratio. In doing so, the adopted reference frame is actually the one with respect to which the electrode plates are stationary. In practical designs, the plates are commonly stationary with respect to the deflection yokes, though this restriction is not necessary in principle. By virtue of this seemingly trivial coincidence, the matrix frame has been adopted tacitly in the conventional practice dealing with the effector speed. On the contrary, the magnetic deflection with the yokes being made purposely to move relative to the electrode plates provides a means to test the proposed force law. Besides, as the current in the yoke is neutralized, the source speed associated with this conduction current is also referred to the matrix frame tacitly in common practice.

Therefore, based on the local-ether electromagnetic force law (2.15) or (2.16) with the Sagnac-effect deviation being omitted, **the modified force law is identical to the Lorentz force law, if the latter is observed in the matrix frame** as done tacitly in common practice. In other words, the Lorentz force law is valid only under hidden restrictions. That is, the effector and matrix speeds are low, the drift speed is very low, the laboratory frame is actually the matrix frame, and the corresponding Sagnac-effect deviation is omitted. However, these conditions are so common and seem so trivial as to be ignored easily.

Further, if the propagation delay time R/c and then the Sagnac effect due to the movement of the effector can be neglected, the velocity difference $\mathbf{v}_{es}$ becomes Newtonian relative and the term $1/R$ in the augmented potentials reduces to $1/R_t$. Thus both $\mathbf{v}_{es}$ and R possess symmetry between a pair of charged particles. Consequently, as seen directly from (2.3), the electromagnetic force between two charged particles complies with Newton's third law of motion which states that action is equal to reaction in magnitude.

2.6 Extra Force Terms

To complete the proposed force law, we proceed to estimate the magnitudes of the extra forces which are omitted under the low-speed condition. From the general forms of the augmented potentials (2.5) and (2.6), the electromagnetic force law is given by

$$\mathbf{F} = q\left\{-\nabla\Phi - \left(\frac{\partial}{\partial t}\mathbf{A}\right)_m + \mathbf{v}_{em} \times \nabla \times \mathbf{A}\right\} + \mathbf{F}_1 + \mathbf{F}_2 + \mathbf{F}_3, \quad (2.19)$$

where the extra force terms

$$\mathbf{F}_1 = -\frac{q}{c^2}\frac{1}{2}v_{em}^2\nabla\Phi, \quad (2.20)$$

$$\mathbf{F}_2 = -\frac{q}{c^2}\frac{1}{2\epsilon_0}\nabla\int\frac{v_{sm}^2\rho_v}{4\pi R}dv', \quad (2.21)$$

and

$$\mathbf{F}_3 = \frac{q}{c^2}\left(\frac{\partial}{\partial t}\mathbf{v}_{em}\Phi\right)_e. \quad (2.22)$$

All of these extra terms are velocity-dependent and incorporate the common factor $1/c^2$.

The extra force terms $\mathbf{F}_1$ and $\mathbf{F}_3$ are associated both with the effector velocity $\mathbf{v}_{em}$ and with the scalar potential Φ. These two terms will vanish either if $\Phi = 0$ or if $v_{em} = 0$. In the cases where only the magnetic force is involved, such as the situation with the aforementioned deflection yoke or stator magnet, $\Phi = 0$ for the complete neutralization holds. Meanwhile, in the cases where the effector is bound to the matrix, such as the conduction electron or the polarization charge in antennas, waveguides, optical fibers, or in the scattering, $v_{em} = 0$ for a stationary effector holds substantially.

Anyway, whenever the extra force term $\mathbf{F}_1$ does not vanish, it will be much weaker in magnitude than the accompanying electrostatic force $\mathbf{F}_{es}$ by a factor of as small as $v_{em}^2/2c^2$, which in turn is much less than unity ordinarily. That is,

$$\frac{|\mathbf{F}_1|}{|\mathbf{F}_{es}|} = \frac{v_{em}^2}{2c^2} \ll 1. \tag{2.23}$$

In other words, even when the neutralization is not sufficient, the extra force $\mathbf{F}_1$ will be relatively too weak to be observed.

Even in the situation where the neutralization is not complete and the effector is not stationary, the extra force term $\mathbf{F}_3$ can vanish in a static potential. Consider the worst case where $\Phi \neq 0$, $\mathbf{v}_{em} \neq 0$, and their time derivatives also do not vanish, such as in the communication between mobile antennas. It is noted that for a potential even rapidly varying with time (say, of the form of a plane wave $\Phi(x - ct)$ or a spherical wave $\Phi(r - ct)/r$), the order of magnitude of its time derivative divided by c is not expected to exceed the one of its gradient. Physically, this is owing to wave motion whereby a temporal variation in a potential tends to cause a spatial variation in it. Thus $|(\partial\Phi/c\partial t)_e| \lesssim |\nabla\Phi|$. (Besides, $|(q\Phi/c^2)d\mathbf{v}_{em}/dt| \ll |\mathbf{F}|$, since the potential is weak ordinarily and hence $|q\Phi|/m_0c^2 \ll 1$, where m_0 is the mass of the effector.)

Therefore, whenever the extra force $\mathbf{F}_3$ does not vanish, it will be much weaker than the accompanying electrostatic force by a factor of v_{em}/c or less. That is,

$$\frac{|\mathbf{F}_3|}{|\mathbf{F}_{es}|} \lesssim \frac{v_{em}}{c} \ll 1. \tag{2.24}$$

Thus, even when the neutralization is not sufficient and the term $\mathbf{v}_{em}\Phi/c^2$ in the augmented vector potential is not negligible, the extra force $\mathbf{F}_3$ will be relatively too weak to be observed. Again, this is because the accompanying electrostatic force will overwhelmingly dominate, so long as the low-speed condition holds. Thereby, the sufficient neutralization which leads to the approximation (2.12) is not necessary and the validity of the force law (2.16) does not depend on the extent of neutralization.

The extra force $\mathbf{F}_2$ is due to a term similar to the conduction current and emerges even in the situation with complete neutralization, a stationary effector, and a static potential. Thus an effector stationary with respect to a loop carrying a direct current will experience this extra force. However, it may be difficult to observe. Like the electrostatic force, this extra force is conservative. Thus, for an effector bound in a conducting wire, the induced electromotive force along a closed wire is zero. On the other hand, an unbound effector tends to have a speed $v_{em} \gg v_{sm}$, due to thermal fluctuation or whatever. It is noticed that the drift speed v_{sm} of the mobile source particles with respect to the matrix is very low ordinarily. Even for a copper wire carrying a current of density as high as 10 amp/mm^2, the drift speed of the conduction electrons is merely as low as 7.4×10^{-4} m/s. Thus the situation of very low drift speed ($v_{sm} \lll c$) holds ordinarily.

Therefore, the extra force $\mathbf{F}_2$ is ordinarily much weaker than the accompanying magnetic force $\mathbf{F}_m$ by a factor of the order of v_{sm}/v_{em}. That is,

$$\frac{|\mathbf{F}_2|}{|\mathbf{F}_m|} \sim \frac{v_{sm}}{v_{em}} \ll 1. \tag{2.25}$$

Even in the case where the effector speed v_{em} happens to be quite low and hence the preceding relation does not hold, the extra force $\mathbf{F}_2$ as well as $\mathbf{F}_m$ will be too weak to be observed. In the worst case where the drift speed v_{sm} is no longer very low (such as in a plasma), the neutralization could be difficult to sustain and then the electrostatic force would dominate again.

Consequently, under the ordinary low-speed condition, all the three extra forces exerted on an effector can be neglected as compared to the accompanying electrostatic or magnetic force, and hence the force law (2.15) or (2.16) is valid. For those complicated situations where the roles of the extra force terms are difficult to determine, the force law (2.19) should be invoked. Let us note that the adoption of the matrix frame is for convenience of analysis when possible. Otherwise, a direct approach is to use the force law (2.3) or (2.4) where the matrix frame can then be abandoned.

2.7 Summary

In order to comply with Galilean transformations and the local-ether model of wave propagation, a new classical model of electromagnetic force is presented in terms of the augmented potentials, which in turn are derived from the electric scalar potential by incorporating the velocity difference between the effector and the source. The propagation of the potentials is proposed to follow the local-ether model and hence the propagation range is referred uniquely to an

ECI frame for earthbound phenomena. Thus the position vectors and velocities of the effector and sources are referred to that frame. As a consequence, the values of the augmented potentials at a given position remain unchanged as observed in different frames. Furthermore, in the proposed force law, the time derivative of the augmented vector potential is associated with the change in the potential experienced by the effector and hence is referred specifically to the effector frame. Consequently, the electromagnetic force exerted on an effector is frame-invariant, as expected intuitively.

The dominant part of the force based on the augmented potentials does not depend on the particle velocities and is identical to the conventional electrostatic force, as the Sagnac-effect deviation is not considered. On the other hand, the velocity-dependent force terms look quite different from their counterparts in the Lorentz force law. However, a situation commonly encountered in the magnetic force is that the magnetic field is due to the conduction current. Thus the mobile source particles forming the current are embedded in a neutralizing matrix. Then the augmented potentials are expressed in terms of the local-ether potentials which in turn are associated with the net charge density and the neutralized current density.

Further, under the ordinary low-speed condition where the effector, sources, and matrix move slowly with respect to the local-ether frame and the sources drift very slowly in the matrix, the proposed force law reduces to a form similar to the Lorentz force law, apart from three extra force terms. This represents modifications of the Lorentz force law which comply with the frame-invariance of force, Galilean transformations, and with the local-ether propagation model. The fundamental modifications are that the current density generating the vector potential, the time derivative of this potential in the electric induction force, and the effector velocity connecting to the curl of this potential in the magnetic force are all referred to the matrix frame, and that the propagation velocity of the potentials is referred to the local-ether frame.

It is shown quantitatively that all the extra force terms are much weaker than the accompanying electrostatic or magnetic force under the low-speed condition. Then the proposed Galilean model is in accord with the Lorentz force law, if the latter is observed in the matrix frame and the Sagnac-effect deviation due to the motion of this frame is neglected. Thereby, hidden restrictions for the Lorentz force law imposed tacitly on particle speeds and reference frames are unveiled.

Chapter 3

Modifications of Maxwell's Equations

In Chapter 1 we have presented the local-ether model, whereby the propagation of earthbound waves is supposed to be referred uniquely to a geocentric inertial frame. Further, in Chapter 2, in compliance with Galilean transformations and the local-ether propagation model, the modified Lorentz force law is developed, which is formulated in terms of the potentials originating from the net charge density and the neutralized current density. The relationships between the potentials and the electromagnetic fields are also derived. In this Chapter, the corresponding wave equations for the potentials and the fields along with the corresponding continuity equation and Lorenz gauge are derived. Then the phase speed of electromagnetic wave in a moving dielectric or magnetic medium is derived. After the Sagnac effect due to the movement of the transmission path is taken into consideration, it is shown that the local-ether wave equation for the electric field can account for various precision interference experiments in a consistent way, including the one-way-link experiment with a geostationary fiber, the Sagnac rotating-loop experiments with a comoving or a geostationary dielectric medium, and Fizeau's experiment with a moving dielectric medium in a geostationary interferometer. These experiments together then provide support for the local-ether wave equation. Meanwhile, some other phenomena are predicted, which provide a means to test its validity. Thereafter, we derive the divergence and the curl relations for the electric and magnetic fields, which represent modifications of Maxwell's equations complying with Galilean transformations.

3.1 Issue of Reference Frame in Electromagnetics

It is known that Maxwell's equations and the Lorentz force law form the foundations of electromagnetics. Maxwell's equations relate the spatial variations of electric and magnetic fields with their temporal variations and with the charge and current densities generating these fields. And the Lorentz force law relates electric and magnetic fields with the electromagnetic force exerted on a charged particle moving in these fields.

In the formulations of Ampère's law and the continuity equation presented by Maxwell [80], Heaviside [43], Lorentz [72], and by Einstein [24] who pioneered in the development of electromagnetics, the adopted current density corresponds to the convection current as it is given by the product of the density and the velocity of the charged particles. Besides, according to the Lorentz force law, the magnetic force is proportional to the velocity of the affected particle. It is known that the velocity of a particle and the temporal rate of change of a function of space and time tend to be different when observed in different reference frames. Consequently, Maxwell's equations and the Lorentz force law are not invariant under Galilean transformations, if the involved velocities and time derivatives do not have their preferred reference frames.

In order to make Maxwell's equations invariant in different reference frames, Lorentz, Poincaré, and then Einstein introduced the Lorentz transformation of space and time, instead of Galilean transformations [71, 114, 24]. It can be shown that the wave equations for the potentials, the continuity equation, and the Lorenz gauge, which are fundamental equations of electromagnetics, are invariant under the Lorentz transformation, as discussed in the Introduction. Further, Maxwell's equations can be shown to be Lorentz invariant. Besides, by resorting to the Lorentz transformation, it can be shown that electric and magnetic fields together with the particle velocity transform in such a way that the Lorentz force is exactly identical to the transformation of the time rate of change of momentum [74]. That is, the Lorentz force law is also Lorentz invariant.

While the Lorentz transformation solves the problem associated with the changes of the particle velocities and current density with reference frames, it has been noticed that the electric current generating the magnetic field is commonly the conduction current. The mobile charged particles that form this kind of current are actually drifting in a neutralizing matrix, such as electrons in a metal wire. Thus, by superposition, the velocity that determines the conduction current or the neutralized current density is the drift velocity of the mobile particles with respect to the matrix. Then the neutralized current density itself and, further, the magnetic force can remain unchanged in different frames simply based on Galilean transformations.

Motivated by this seemingly trivial finding, we have developed in Chapter 2 an electromagnetic force law which complies with Galilean transformations. In this new classical model all of the involved position vectors, time derivatives, and velocities are referred specifically to their respective frames. Owing to this simple feature, the associated potentials, fields, and electromagnetic force remain unchanged when observed in different frames in uniform motion of translation. Under the common low-speed condition where the source particles drift very slowly with respect to the matrix, the proposed force law can be formulated in terms of the potentials originating from the net charge density and the neutralized current density. Further, it is found that the proposed model can reduce to the Lorentz force law.

Moreover, the propagation of the associated potentials is supposed to follow the local-ether model presented in Chapter 1, whereby the propagation of earthbound or interplanetary waves is referred specifically to a geocentric or a heliocentric inertial frame, respectively. Consequently, earthbound wave phenomena can depend on earth's rotation, but are entirely independent of earth's orbital motion around the Sun. This local-ether model has been adopted to account for a wide variety of propagation phenomena, particularly the Sagnac effect due to earth's motions in the global positioning system, the rotating-loop interferometer, the intercontinental microwave link, the interplanetary radar, and in the Michelson-Morley experiment.

In this Chapter, based on the local-ether propagation model, the wave equations for the potentials are derived. Further, based on the modified Lorentz force law and the corresponding definitions of the electric and magnetic fields in terms of the potentials, the local-ether wave equations for the fields are derived. Thereby, the propagation constant and phase speed of the electromagnetic wave propagating in a moving dielectric or magnetic medium are explored. Then, after the Sagnac effect due to the movement of the transmission path is taken into account, we present reinterpretations for several precision interference experiments in a consistent way, including the fiber-link experiment with a geostationary setup and a geostationary optical fiber, the Sagnac rotating-loop experiments with a comoving or a geostationary dielectric medium, and Fizeau's experiment with a geostationary interferometer and a moving dielectric medium. Thereafter, by using the continuity equation and the consequent Lorenz gauge, the divergence and the curl relations for the local-ether fields are discussed and then their relationship with Maxwell's equations is explored.

3.2 Modified Lorentz Force Law

Based on Galilean transformations, we have presented in Chapter 2 an electromagnetic force law given in terms of the augmented potentials which in turn are derived from the electric scalar potential by incorporating the velocity difference between the effector and the source particles. Consider the electromagnetic force exerted on an effector particle of charge q due to an ensemble of source particles of charge density ρ_v and drifting in a matrix of charge density ρ_m. The drift velocity of the source particles with respect to the matrix is given by the difference $\mathbf{v}_{sm} = \mathbf{v}_s - \mathbf{v}_m$, where $\mathbf{v}_s$ and $\mathbf{v}_m$ are the velocities of the source particles and the matrix, respectively, both with respect to a particular frame. The matrix can be a metal wire, a dielectric medium, or a magnet, and tends to electrically neutralize the mobile source particles to some extent.

Under the common low-speed condition where the source particles drift very slowly with respect to the matrix, it has been shown in Chapter 2 that the electromagnetic force law proposed in terms of the augmented potentials reduces to the modified Lorentz force law

$$\mathbf{F}(\mathbf{r},t) = q\left\{\mathbf{E}(\mathbf{r},t) + \mathbf{v}_{em} \times \mathbf{B}(\mathbf{r},t)\right\}, \tag{3.1}$$

where the velocity difference $\mathbf{v}_{em} = \mathbf{v}_e - \mathbf{v}_m$ and $\mathbf{v}_e$ is the effector velocity at instant t with respect to the particular frame adopted for $\mathbf{v}_s$ and $\mathbf{v}_m$. The matrix velocity $\mathbf{v}_m$ is supposed to be substantially fixed and then $\mathbf{v}_{em}$ represents the effector velocity with respect to the matrix frame in which the matrix is stationary.

The electric field $\mathbf{E}$ and the magnetic field $\mathbf{B}$ in turn are defined explicitly in terms of the potentials Φ and $\mathbf{A}$ as

$$\mathbf{E}(\mathbf{r},t) = -\nabla\Phi(\mathbf{r},t) - \left(\frac{\partial}{\partial t}\mathbf{A}(\mathbf{r},t)\right)_m \tag{3.2}$$

and

$$\mathbf{B}(\mathbf{r},t) = \nabla \times \mathbf{A}(\mathbf{r},t), \tag{3.3}$$

where the time derivative $(\partial\mathbf{A}/\partial t)_m$ is referred specifically to the matrix frame. The electric scalar potential Φ and the magnetic vector potential $\mathbf{A}$ are associated with the augmented potentials and are given explicitly by

$$\Phi(\mathbf{r}, t) = \frac{1}{\epsilon_0} \int \frac{\rho_n(\mathbf{r}', t - R/c)}{4\pi R} dv' \tag{3.4}$$

and

$$\mathbf{A}(\mathbf{r}, t) = \mu_0 \int \frac{\mathbf{J}_n(\mathbf{r}', t - R/c)}{4\pi R} dv', \tag{3.5}$$

where the net charge density $\rho_n = \rho_v + \rho_m$, the neutralized current density $\mathbf{J}_n = \mathbf{v}_{sm}\rho_v$, the propagation range $R = |\mathbf{r} - \mathbf{r}'|$, the position vectors $\mathbf{r}$ and $\mathbf{r}'$ are referred to the particular frame adopted for the associated particle velocities, and $\mu_0\epsilon_0 = 1/c^2$.

Obviously, the value of the neutralized current density and those of the potentials remain unchanged when observed in different frames. Moreover, since both the time derivative in the definition of $\mathbf{E}$ and the effector velocity in the force law are referred specifically to the matrix frame, the values of the fields and then the electromagnetic force exerted on a charged particle also remain unchanged in different frames in uniform motion of translation. That is, based on the preceding formulas complying with Galilean transformations, the values of the potentials, fields, and electromagnetic force are frame-invariant. Further, it is noted that the drift velocity $\mathbf{v}_{sm}$ involved in the neutralized current density is Newtonian relative and hence this current density complies with Galilean relativity. For quasi-static cases where the propagation delay of the potentials can be neglected, the potentials Φ and $\mathbf{A}$ then comove with the matrix.

It is seen that the force law (3.1) looks like the Lorentz force law. However, the fundamental modification is that the current density generating the magnetic vector potential, the time derivative of this potential in the electric induction force, and the effector velocity connecting to the curl of this potential in the magnetic force are all referred specifically to the matrix frame. Meanwhile, it is elucidated in Chapter 2 that in the conventional practice where the Lorentz force law is applied to the analysis of the magnetic deflection and of a motor, the adopted reference frame is actually the one with respect to which the magnet or the corresponding current-carrying winding is stationary. Thus the matrix frame has been adopted tacitly as the laboratory frame. Therefore, the modified equation is identical to the Lorentz force law, if the latter is observed in the matrix frame as done tacitly in common practice.

3.3 Local-Ether Wave Equations for Potentials

Based on the local-ether model of wave propagation, it is supposed that each individual source particle continuously excites the electric scalar potential, which in turn propagates radially outward from the source position at the isotropic speed c with respect to the associated local-ether frame, regardless of the motions of the source and effector. All the potentials involved in the modified force law are derived from the electric scalar potential and hence they share the same propagation features. In the potentials Φ and $\mathbf{A}$ defined in (3.4) and (3.5), the ratio R/c represents the propagation delay time from the position $\mathbf{r}'$ of emission of the potentials to the position $\mathbf{r}$ of reception. Thus the position vectors $\mathbf{r}$ and $\mathbf{r}'$ as well as the propagation range R are referred uniquely to the local-ether frame. To comply with the frame of the corresponding position vectors, the velocities $\mathbf{v}_e$, $\mathbf{v}_s$, and $\mathbf{v}_m$ are also referred to the local-ether frame, which is an earth-centered inertial (ECI) frame for earthbound phenomena.

By applying the Laplace operator to both sides of the integral formulas (3.4) and (3.5) for the potentials and then by expanding the Laplacians of the time-dependent charge and current densities divided by R, it can be shown that (for a derivation, see Appendix A)

$$\nabla^2\Phi(\mathbf{r},t) - \frac{1}{c^2}\frac{\partial^2}{\partial t^2}\Phi(\mathbf{r},t) = -\frac{1}{\epsilon_0}\rho_n(\mathbf{r},t) \tag{3.6}$$

and

$$\nabla^2\mathbf{A}(\mathbf{r},t) - \frac{1}{c^2}\frac{\partial^2}{\partial t^2}\mathbf{A}(\mathbf{r},t) = -\mu_0\mathbf{J}_n(\mathbf{r},t), \tag{3.7}$$

where the time derivative $\partial/\partial t$ as well as the position vector $\mathbf{r}$ is referred to the local-ether frame, identical to the frame of the wave propagation. The Laplace operator and the second time derivative form the d'Alembert (wave) operator. Thus the preceding equations represent the local-ether wave equations for the potentials.

It is of essence to note that in the neutralized current density $\mathbf{J}_n$, the drift velocity $\mathbf{v}_{sm}$ of the mobile source particles of charge density ρ_v is referred to the matrix frame. Consequently, the conservation of charge leads to another relationship between $\mathbf{J}_n$ and ρ_v. That is,

$$\nabla\cdot\mathbf{J}_n(\mathbf{r},t) = -\left(\frac{\partial}{\partial t}\rho_v(\mathbf{r},t)\right)_m . \tag{3.8}$$

It is noted that as in a fluid, the time derivative of the source charge density is referred specifically to the matrix frame, identical to the frame of the drift velocity. (Thus, for the trivial case with $\mathbf{v}_{sm}=0$, the matrix-frame time derivative of ρ_v of arbitrary spatial distribution is always zero, as it should be.) The preceding relation is just the continuity equation, except the reference frame. Further, this matrix-frame continuity equation can be given in terms of the net charge density by

$$\nabla \cdot \mathbf{J}_n(\mathbf{r},t) = -\left(\frac{\partial}{\partial t}\rho_n(\mathbf{r},t)\right)_m . \tag{3.9}$$

This is a consequence of the fact that the matrix charge density ρ_m is time-independent in the matrix frame, regardless of the motion of the matrix.

By applying the divergence and the matrix-frame time derivative to both sides of the wave equations (3.7) and (3.6), respectively, and then by using (3.9) and an argument associated with initial condition given in Appendix A, it can be shown that the two potentials are related to each other in a form similar to the continuity equation. That is,

$$\nabla \cdot \mathbf{A}(\mathbf{r},t) = -\frac{1}{c^2}\left(\frac{\partial}{\partial t}\Phi(\mathbf{r},t)\right)_m . \tag{3.10}$$

This matrix-frame continuity equation for the potentials looks like the Lorenz gauge discussed in the Introduction. However, the fundamental difference is that the time derivative of the scalar potential is referred specifically to the matrix frame.

3.4 Local-Ether Wave Equations for Fields

Then, by manipulating the wave equations for the potentials according to the definitions of the fields, we have the local-ether wave equation for the magnetic field

$$\nabla^2\mathbf{B}(\mathbf{r},t) - \frac{1}{c^2}\frac{\partial^2}{\partial t^2}\mathbf{B}(\mathbf{r},t) = -\mu_0\nabla \times \mathbf{J}_n(\mathbf{r},t) \tag{3.11}$$

and the local-ether wave equation for the electric field

$$\nabla^2\mathbf{E}(\mathbf{r},t) - \frac{1}{c^2}\frac{\partial^2}{\partial t^2}\mathbf{E}(\mathbf{r},t) = \frac{1}{\epsilon_0}\nabla\rho_n(\mathbf{r},t) + \mu_0\left(\frac{\partial}{\partial t}\mathbf{J}_n(\mathbf{r},t)\right)_m , \tag{3.12}$$

where, again, the position vector $\mathbf{r}$ together with the time derivative $\partial/\partial t$ is referred to the local-ether frame. It is noted that in the preceding equation the time derivative of the neutralized current density is referred to the matrix frame and the velocity of the mobile source particles forming this current density is also referred to this frame. These local-ether wave equations made their debut in [131, 132, 119].

In free space having no sources and matrix, the local-ether wave equations take a simpler form

$$\nabla^2 \Psi(\mathbf{r}, t) - \frac{1}{c^2} \frac{\partial^2}{\partial t^2} \Psi(\mathbf{r}, t) = 0, \tag{3.13}$$

where Ψ denotes the scalar potential Φ or any Cartesian component of the vector potential $\mathbf{A}$, the electric field $\mathbf{E}$, or the magnetic field $\mathbf{B}$. It is seen that both electric and magnetic fields as well as the potentials propagate at the speed c with respect to the local-ether frame. The presence of the charge or current induced in a dielectric or magnetic material tends to adjust the spatial or temporal variation in the wave equations and hence to change the propagation speed.

Consider the case of wave propagation in a uniform magnetic material of permeability μ, where $\mathbf{J}_n = \nabla \times \mathbf{M}$ for the magnetization current and the magnetization vector $\mathbf{M} = (1/\mu_0 - 1/\mu)\mathbf{B}$. Thereby, the wave equation for the magnetic field becomes

$$\frac{\mu_0}{\mu} \nabla^2 \mathbf{B}(\mathbf{r}, t) - \frac{1}{c^2} \frac{\partial^2}{\partial t^2} \mathbf{B}(\mathbf{r}, t) = 0, \tag{3.14}$$

where we have made use of the relation $\nabla \cdot \mathbf{B} = 0$ which in turn is a consequence of (3.3). It is seen that in a uniform magnetic medium of μ, the field propagates at the speed $c\sqrt{\mu_0/\mu}$ with respect to the local-ether frame. In the preceding derivation, no information about the motion of the medium is involved. Thus the derived propagation speed is independent of the motion of the magnetic medium.

Consider the analogous case of wave propagation in a dielectric material of permittivity ϵ, where $\mathbf{J}_n = (\partial \mathbf{P}/\partial t)_m$ for the polarization current and the polarization vector $\mathbf{P} = (\epsilon - \epsilon_0)\mathbf{E}$. The polarization vector is due to the displacement of the polarization charge relative to the ions of the matrix under the influence of the electric field. The polarization current is thus associated with the time derivative of the polarization vector with respect to the matrix frame, just as the drift velocity $\mathbf{v}_{sm}$ of the mobile source particles forming a conduction current is referred to this frame. Moreover, due to the matrix-frame continuity equation (3.9), the polarization charge density is related to the polarization vector by $\rho_n = -\nabla \cdot \mathbf{P}$, where we have made use of the initial condition that a uniform polarization ($\nabla \cdot \mathbf{P} = 0$) corresponds to the complete neutralization ($\rho_n = 0$).

Thereby, by using the electric field to express the net charge density and the neutralized current density induced in a dielectric medium, the wave equation for the electric field becomes

$$\nabla^2 \mathbf{E}(\mathbf{r},t) - \frac{1}{c^2}\frac{\partial^2}{\partial t^2}\mathbf{E}(\mathbf{r},t) = -\frac{1}{\epsilon_0}\nabla\nabla\cdot[(\epsilon-\epsilon_0)\mathbf{E}(\mathbf{r},t)] + \frac{\epsilon-\epsilon_0}{\epsilon_0}\frac{1}{c^2}\left(\frac{\partial^2}{\partial t^2}\mathbf{E}(\mathbf{r},t)\right)_m, \quad (3.15)$$

where the dielectric material is supposed to be temporally invariant, as it is commonly, and hence the permittivity ϵ is time-independent in the matrix frame. It is noted that this wave equation involves two time derivatives of the electric field referred to different frames.

Based on the Galilean transformation (1.17), the time derivative $(\partial^2\mathbf{E}/\partial t^2)_m$ referred to the matrix frame can be given in terms of the derivative $\partial^2\mathbf{E}/\partial t^2$ referred to the local-ether frame. That is,

$$\left(\frac{\partial^2\mathbf{E}}{\partial t^2}\right)_m = \frac{\partial^2\mathbf{E}}{\partial t^2} + 2\left(\mathbf{v}_m\cdot\nabla\right)\frac{\partial\mathbf{E}}{\partial t} + \left(\mathbf{v}_m\cdot\nabla\right)\left(\mathbf{v}_m\cdot\nabla\right)\mathbf{E}. \quad (3.16)$$

Thus the local-ether wave equation for the electric field becomes

$$\nabla^2\mathbf{E} - \frac{\epsilon}{\epsilon_0}\frac{1}{c^2}\frac{\partial^2\mathbf{E}}{\partial t^2} = -\frac{1}{\epsilon_0}\nabla\nabla\cdot[(\epsilon-\epsilon_0)\mathbf{E}] + \frac{\epsilon-\epsilon_0}{\epsilon_0}\frac{1}{c^2}\left[2\left(\mathbf{v}_m\cdot\nabla\right)\frac{\partial\mathbf{E}}{\partial t} + \left(\mathbf{v}_m\cdot\nabla\right)\left(\mathbf{v}_m\cdot\nabla\right)\mathbf{E}\right]. \quad (3.17)$$

It is noted that this wave equation involves the matrix velocity with respect to the local-ether frame. This feature is quite different from that in the wave equation for the magnetic field (3.14). Physically, this difference is related to the situation that the polarization current is associated with the matrix-frame time derivative of the field, while the magnetization current is with a spatial derivative.

In terms of the matrix-frame time derivatives, the wave equation for the electric field can be rewritten as

$$\nabla^2\mathbf{E} - \frac{\epsilon}{\epsilon_0}\frac{1}{c^2}\left(\frac{\partial^2\mathbf{E}}{\partial t^2}\right)_m = -\frac{1}{\epsilon_0}\nabla\nabla\cdot[(\epsilon-\epsilon_0)\mathbf{E}] - \frac{2}{c^2}\left(\mathbf{v}_m\cdot\nabla\right)\left(\frac{\partial\mathbf{E}}{\partial t}\right)_m, \quad (3.18)$$

where the second-order term of the normalized speed v_m/c is ignored. In the preceding equation it is seen that the last term is associated with the matrix velocity and thus tends to be smaller in magnitude than the other terms by a factor of the order of v_m/c. It is noticed that the preceding matrix-frame wave equation is dissimilar to the corresponding one adopted in [66], while the Galilean transformation of the former in the local-ether frame, namely, (3.17) happens to be similar to the Lorentz transformation of the latter in a laboratory frame, when the divergence term along with the second-order term of the matrix velocity is ignored.

Consider the simpler case where a z-polarized uniform plane wave propagates along the x direction in a uniform dielectric medium. The medium is moving at a velocity $\mathbf{v}_f$ with respect to a laboratory frame which in turn is moving at a velocity $\mathbf{v}_0$ with respect to the local-ether frame. Based on Galilean transformations, the matrix velocity with respect to the local-ether frame is simply $\mathbf{v}_m = \mathbf{v}_f + \mathbf{v}_0$. Then, to the first order of normalized speed, the local-ether wave equation (3.17) can be simplified to a form

$$\frac{\partial^2}{\partial x^2}E_z(x,t) - \frac{\epsilon}{\epsilon_0}\frac{1}{c^2}\frac{\partial^2}{\partial t^2}E_z(x,t) = 2v_{mx}\frac{\epsilon-\epsilon_0}{\epsilon_0}\frac{1}{c^2}\frac{\partial^2}{\partial x\partial t}E_z(x,t), \tag{3.19}$$

where the coordinate x and the time derivatives are referred to the local-ether frame and the component $v_{mx} = \mathbf{v}_m\cdot\hat{x}$. It is noted that the term $\nabla\cdot(\epsilon-\epsilon_0)\mathbf{E}$ associated with the polarization charge vanishes, since both the permittivity ϵ and the field $\mathbf{E}$ have been supposed to have no variations along the z direction of the polarization.

Suppose further that the solution of this wave equation is of a harmonic form like $E_z = E_0 e^{ikx}e^{-i\omega t}$, where x is still referred to the local-ether frame and E_0 is an arbitrary constant. For such a wave, the preceding wave equation reduces to an algebraic equation

$$k^2 - \frac{\epsilon}{\epsilon_0}\frac{\omega^2}{c^2} = -2v_{mx}\frac{\epsilon-\epsilon_0}{\epsilon_0}\frac{1}{c^2}k\omega. \tag{3.20}$$

It is easy to show that to the first order of normalized speed, the propagation constant k can be given in terms of the angular frequency ω by

$$k = \frac{\omega}{c}\left\{n - \frac{v_{mx}}{c}\left(n^2-1\right)\right\}, \tag{3.21}$$

where the refractive index $n = \sqrt{\epsilon/\epsilon_0}$.

It is noted that this propagation constant depends on the speed v_{mx}, in addition to the familiar dependence on n. Consequently, this relation represents a modification of the propagation constant due to the motion of the dielectric medium with respect to the local ether along the wave propagation direction. Physically, the dependence on the matrix velocity originates from the situation that the polarization current and its time derivative which contribute to an electric field are referred to the matrix frame rather than to the local-ether one.

The phase speed c_m $(= \omega/k)$ of the electromagnetic wave propagating in the moving dielectric medium is then given by

$$c_m = \frac{c}{n} + v_{mx}\left(1 - \frac{1}{n^2}\right), \tag{3.22}$$

where the phase speed and the frequency ω as well as the coordinate x in the harmonic are referred specifically to the local-ether frame. It is seen that the component of the matrix velocity parallel to the propagation direction of the plane wave affects the phase speed, while the transverse ones do not. It is noted that the matrix-velocity modification of the phase speed vanishes for the trivial case with $n = 1$, as expected intuitively for free space.

The local-ether wave equation (3.19) can also be written in the matrix frame. To the first order of normalized speed, the matrix-frame wave equation reads

$$\frac{\partial^2}{\partial x^2}E_z(x,t) - \frac{\epsilon}{\epsilon_0}\frac{1}{c^2}\left(\frac{\partial^2}{\partial t^2}E_z(x,t)\right)_m = -2v_{mx}\frac{1}{c^2}\left(\frac{\partial^2}{\partial x \partial t}E_z(x,t)\right)_m . \tag{3.23}$$

The corresponding algebraic equation leads to $kc = \omega'(n + v_{mx}/c)$ and then $c'_m = c/n - v_{mx}/n^2$, where ω' and c'_m $(= \omega'/k)$ are respectively the angular frequency and the phase speed of the wave when observed in the matrix frame instead of the local-ether one. It is seen that

$$c'_m = c_m - v_{mx}, \tag{3.24}$$

which states that the difference in the observed phase speed between the two reference frames is just the relative speed between the frames along the propagation direction. In other words, the derived phase speeds of a plane wave in the two frames comply with Galilean transformations.

It is seen that the phase speed given in (3.22) is similar to the speed obtained from the velocity transformation in the special relativity [24, 74, 49] or to the one derived from the aforementioned wave equation in a laboratory frame based on the Lorentz transformation [66]. However, the fundamental difference is that the phase speed c_m and the matrix velocity $\mathbf{v}_m$ are referred specifically to the local-ether frame. Thus the matrix velocity $\mathbf{v}_m$ incorporates the laboratory velocity $\mathbf{v}_0$ with respect to the local-ether frame. However, it will be elucidated later that the laboratory velocity can cancel out in some situation and hence it is difficult to determine the discrepancy in reference frames with the results of the famous Fizeau's interference experiment with flowing water, which is known as important evidence demonstrating the phase speed in a moving medium.

An old interpretation of the dependence of the phase speed on the medium velocity given in a form like (3.22) is known as the Fresnel drag effect [49, 66, 77], whereby the ether is dragged partially by the moving medium to an extent depending on the refractive index n. If n is large enough, $c_m \simeq c/n + v_{mx}$ and $c'_m \simeq c/n$. Thus the phase speed with respect to the moving medium becomes independent of the medium velocity and then it seems that the ether is completely dragged by the medium. However, according to the wave equation (3.15), the earth local ether is still stationary in an ECI frame, regardless of the permittivity and the velocity of a terrestrial medium. The change in the phase speed of a wave propagating in a dielectric medium, stationary or moving, is due to the interaction of the polarization with the electric field, whereby the field induces the polarization which in turn tends to change the field.

Further, it is noted that the presented phase speed, though similar to the one from other approaches, is derived only for a uniform plane wave propagating in a uniform dielectric medium and only to the first order. In other words, according to the local-ether wave equation, the phase-speed formula (3.22) does not hold for a magnetic medium and can no longer be valid for a nonuniform dielectric medium where the polarization charge emerges. Thus the applicability of the phase-speed formula has some hidden restrictions. This represents a viewpoint different from the ether-dragging notion and another discrepancy from the special relativity.

3.5 Reexamination of Various Interference Experiments

In this section, we reexamine some precision interference experiments reported in the literature to test the local-ether wave equation for the electric field. The experiments to be examined include the fiber-link experiment with a geostationary setup and a geostationary optical fiber, the Sagnac loop interferometry with a rotating path and a comoving or a geostationary dielectric medium, and Fizeau's experiment with a geostationary interferometer and a moving dielectric medium. For these earthbound experiments, the local ether is stationary in an ECI frame and hence earth's rotation should be taken into consideration, even for a geostationary medium or path. On the other hand, these experiments are entirely independent of earth's orbital motion around the Sun or others.

3.5.1 Phase variation with moving medium and path

First of all, consider an interferometer of which each segment of the transmission path has a fixed shape and is implemented with a pair of mirrors in air, with a pipe filled with a flowing dielectric liquid, or with a solid dielectric fiber. For a plane wave propagating in the $\hat{l}$ direction along an arbitrary path filled with a moving dielectric medium, the propagation constant can be written as

$$k = k_0 \left\{ n + \left(1 - n^2\right) \hat{l} \cdot \mathbf{v}_m / c \right\}, \tag{3.25}$$

where $k_0 = \omega/c$, n is the refractive index of the uniform medium, and $\mathbf{v}_m$ is its velocity with respect to the local-ether frame.

Further, consider a transmission path segment of length l, such as a linear section of the pipe or fiber. Owing to the movement of the segment during the wave propagation through it, the propagation range which represents the actual propagation length tends to be different from the path length. As in the classical propagation model, the propagation range depends on the velocity of the path segment with respect to the local ether. The influence on wave propagation due to the difference between the propagation range l_p and the path length l is known as the Sagnac effect.

By following the derivation of the Sagnac effect for an electromagnetic wave propagating in free space discussed in Chapter 1, the propagation range l_p for a wave propagating in a dielectric medium of index n in the $\hat{l}$ direction along a moving segment can be given. To the first order of normalized speed, we have

$$l_p = l \left\{ 1 + n \hat{l} \cdot \mathbf{v}_l / c \right\}, \tag{3.26}$$

where $\mathbf{v}_l$ is the velocity of the path segment with respect to the local-ether frame.

The phase variation of electromagnetic wave over this propagation range is given by $\phi = k l_p$, since the propagation time is l_p / c_m.

Thus the phase variation over a moving path filled with a moving dielectric medium can be given from the preceding two formulas. To the first order of normalized speed, the velocity-dependent phase variation is given by

$$\phi = k_0 l \left\{ n + (1 - n^2)\hat{l} \cdot \mathbf{v}_m / c + n^2 \hat{l} \cdot \mathbf{v}_l / c \right\}. \tag{3.27}$$

It is seen that the phase variation depends on the longitudinal (to the transmission path) $\hat{l}$ components of the matrix velocity and the path velocity both with respect to the local-ether frame. Furthermore, these longitudinal speeds connect to the refractive index. Thus, in addition to the familiar effect on the propagation constant, the refractive index also has effects on the matrix-velocity modification of the propagation constant and on the path-velocity modification of the propagation length.

The preceding phase-variation formula can be rewritten as

$$\phi = k_0 l \left\{ n + n^2 \hat{l} \cdot \mathbf{v}_{lm} / c + \hat{l} \cdot \mathbf{v}_m / c \right\}, \tag{3.28}$$

where $\mathbf{v}_{lm} = \mathbf{v}_l - \mathbf{v}_m$ denotes the Newtonian relative velocity of the moving path with respect to the moving dielectric medium. It is seen that one of the velocity-dependent terms depends on the refractive index and is associated with the relative velocity, while the other velocity-dependent term is independent of the index and is associated with the individual velocity of the dielectric medium. For the case where the medium comoves with the transmission path ($\mathbf{v}_{lm} = 0$), the velocity-induced phase variation is no longer dependent on the index.

3.5.2 Geostationary fiber-link experiment

Then we reconsider the experiment with a one-way fiber link by Krisher *et al.* discussed in Chapter 1, where the phase difference between two waves generated from two identical stable hydrogen masers separated by a long distance and linked by a stable optical fiber was measured by using a network analyzer [60]. One signal was fed directly into the analyzer, while the other was used to modulate a laser carrier to propagate over the fiber to the analyzer.

For a geostationary fiber, $\mathbf{v}_m = \mathbf{v}_l = \mathbf{v}_E$, where $\mathbf{v}_E$ is the linear velocity due to earth's rotation. Then formula (3.28) immediately yields that the phase variation $d\phi$ over a geostationary fiber segment of differential length dl is given by

$$d\phi = k_0 \left(n + \hat{l} \cdot \mathbf{v}_E / c \right) dl. \tag{3.29}$$

Thus the phase variation over a transmission path L of length l is given by the path integral

$$\phi = k_0 \left(nl + \frac{1}{c} \int_L \mathbf{v}_E \cdot d\mathbf{l} \right), \tag{3.30}$$

where the directed differential length $d\mathbf{l} = \hat{l} dl$.

It is noted that the velocity-induced phase variation is independent of the refractive index, since the velocity difference $\mathbf{v}_{lm} = 0$. Furthermore, while this phase variation is due to earth's rotation, its value is invariant under this rotation. This is because the directions of $\mathbf{v}_E$ and $d\mathbf{l}$ change in a coordinated way and thus their dot product remains unchanged during earth's rotation. This invariance is in accord with the spatial isotropy demonstrated in the one-way fiber-link experiment, where it has been observed that the phase variation over the link is highly stable (as determined from the phase difference between the two waves measured every a few seconds for a couple of days), regardless of earth's rotational and orbital motions and of the orientation and position of the Earth in space [60].

If the fiber link can be placed in a geographically small region so that the velocity $\mathbf{v}_E$ due to earth's rotation is substantially uniform, the phase variation over the link becomes a simpler form

$$\phi = k_0 \left(nl + \frac{1}{c} \mathbf{v}_E \cdot \mathbf{d} \right), \tag{3.31}$$

where $\mathbf{d}$ is the directed separation distance from the end through which the light enters the fiber to the other end. It is noted that the phase variation can be independent of the actual wiring, but depends on the orientation of the distance $\mathbf{d}$ with respect to the ground. If the fiber-link experimental setup is put on a turntable or a rotor, it is expected that the phase variation will change as the turntable is rotating even smoothly. Consequently, the terrestrial isotropy with respect to the ground does not hold.

From the minor term in the preceding formula, the dependence of the phase variation on the orientation of the rotor is given by

$$\delta\phi = \frac{\omega}{c^2} \omega_E R_E |\mathbf{d}| \cos\theta_l \cos\theta_t, \tag{3.32}$$

where ω_E is earth's rotation rate, R_E earth's radius, θ_l the latitude, θ_t the angle of the distance $\mathbf{d}$ from the east, and the turntable is suitably positioned in a horizontal plane. The phase variation associated with earth's rotation is independent of the refractive index of the fiber and hence is identical to the one in the case with a free-space link discussed in Chapter 1. It is noted that the phase variation becomes the maximum and the minimum, as the distance **d** points to the east and the west, respectively. Furthermore, the phase variation changes sinusoidally with the angle θ_t. This terrestrial dipole anisotropy in phase variation predicted in the proposed one-way-link rotor experiment then provides a means to test the local-ether wave equation with a first-order effect.

3.5.3 Sagnac rotating-loop experiments

Moreover, reconsider the Sagnac effect in a rotating-loop interferometer, which results in an interference between two coherent waves corotating and counterrotating with respect to the transmission loop, respectively. In Chapter 1 the transmission path is composed of a beam splitter and a series of mirrors in air. Then the phase difference between the two waves results from the asymmetry that the modification of propagation length due to a rotation of the loop is different between these waves propagating in opposite directions along the loop. Here we deal with a path filled with a general dielectric medium rather than a path in free space.

Suppose that the transmission loop is rotating about an axis as observed in a geostationary laboratory, which in turn is rotating with the Earth. Thus the velocities of the various path segments with respect to an ECI frame can be given by $\mathbf{v}_l = \mathbf{v}_I + \mathbf{v}_{E0} + \mathbf{v}_0$, where $\mathbf{v}_0$ is the laboratory velocity with respect to an ECI frame referred to a suitable point $\mathbf{r}_0$ on the rotation axis of the interferometer, $\mathbf{v}_I = \boldsymbol{\omega}_I \times (\mathbf{r} - \mathbf{r}_0)$ and $\mathbf{v}_{E0} = \boldsymbol{\omega}_E \times (\mathbf{r} - \mathbf{r}_0)$ denote the contributions to the path velocity due to the rotations of the loop and the Earth at the directed rotation rates $\boldsymbol{\omega}_I$ and $\boldsymbol{\omega}_E$, respectively, and the position vectors $\mathbf{r}$ of the path segments are referred to the frame adopted for the reference point $\mathbf{r}_0$.

Consider the case where the dielectric medium is comoving with the rotating loop. Thus the velocity difference $\mathbf{v}_{lm} = 0$ and hence formula (3.28) yields that the phase variation $d\phi$ over a transmission path of differential length dl is given by

$$d\phi = k_0 \left(n + \hat{l} \cdot \mathbf{v}_l / c \right) dl. \tag{3.33}$$

The unit vectors $\hat{l}$ for the two waves in interference are antiparallel to each other in each path segment of the loop. Thus the difference in the phase variation over the loop L between the two waves is given by the path integral

$$\triangle\phi = \frac{2k_0}{c}\oint_L (\mathbf{v}_I + \mathbf{v}_{E0}) \cdot d\mathbf{l}, \tag{3.34}$$

where we have made use of the facts that the major term $k_0 n dl$ in (3.33) is identical for the two waves and hence its contributions to the phase difference cancel out, and that the contributions of a virtually constant vector $\mathbf{v}_0$ to the phase variation over a closed path cancel out collectively, regardless of the actual structure of the loop.

Suppose the loop is coplanar. Then, by using a vector identity, the phase difference can be given by

$$\triangle\phi = \frac{4k_0}{c}(\boldsymbol{\omega}_I + \boldsymbol{\omega}_E) \cdot \mathbf{S}, \tag{3.35}$$

where $\mathbf{S}$ $(= \frac{1}{2}\oint_L (\mathbf{r} - \mathbf{r}_0) \times d\mathbf{l})$ denotes the directed area enclosed by the loop L. It is noted that the phase difference is independent of the index n and hence is identical to the one in the case with a free-space path discussed in Chapter 1. Again, this independence is owing to the coincidence that the effect of the index-dependent modification of the propagation constant happens to cancel the one of the propagation length.

This null effect of the refractive index on the phase difference in the Sagnac loop interferometry was demonstrated experimentally by Harzer in as early as 1914 [91]. Further, the preceding phase-difference formula has been put in practical use in fiber gyroscopes [7, 30, 21]. Alternative derivations of the formula with $\boldsymbol{\omega}_I$ alone by taking the Sagnac effect and one of various approaches to the phase speed into account can be found in the literature [91, 7, 30]. Anyway, in spite of the restriction on reference frames, the local-ether wave equation for the electric field is in accord with the detection of earth's rotation and of a loop rotation by using the Sagnac interferometer with a comoving dielectric medium. On the other hand, the local-ether wave equation precludes the possibility of detecting earth's orbital motion by using earthbound fiber gyroscopes.

Next, consider the case where the medium is geostationary while the transmission loop is rotating with respect to the laboratory. Thus $\mathbf{v}_m = \mathbf{v}_{E0} + \mathbf{v}_0$, $\mathbf{v}_{lm} = \mathbf{v}_I$, and hence formula (3.28) yields that the phase variation $d\phi$ over a path of differential length dl is given by

$$d\phi = k_0 dl \left(n + n^2 \hat{l} \cdot \mathbf{v}_I/c + \hat{l} \cdot \mathbf{v}_{E0}/c + \hat{l} \cdot \mathbf{v}_0/c \right). \tag{3.36}$$

The corresponding phase difference over the loop between the waves becomes

$$\triangle\phi = \frac{4k_0}{c}(n^2\boldsymbol{\omega}_I + \boldsymbol{\omega}_E) \cdot \mathbf{S}. \tag{3.37}$$

It is seen that the phase difference then depends on the index n which in turn connects to the loop rotation rate $\boldsymbol{\omega}_I$. Again, the phase difference is independent of the laboratory velocity $\mathbf{v}_0$ and the difference associated with earth's rotation is independent of the index.

Ordinarily, $\omega_E \ll \omega_I$ and hence the phase difference is substantially proportional to n^2. This index-dependence of the phase difference is identical to that given in [91], though the approach is quite different. The increase of the phase difference in the presence of a geostationary dielectric medium was demonstrated experimentally by Dufour and Prunier in 1942 [91]. The various index-dependences among the phase-difference terms associated with the rate $\boldsymbol{\omega}_I$ or $\boldsymbol{\omega}_E$ in (3.35) and (3.37) then provide another means to test the local-ether wave equation.

3.5.4 Fizeau's experiment with moving medium

Then we discuss the last case where the interferometer is geostationary while the medium is moving. Consider Fizeau's experiment dealing with the interference between two coherent optical waves, one propagating parallel to a flowing water along a stationary pipe, and the other antiparallel to it. As in the Sagnac interferometer, the transmission path in Fizeau's experiment actually forms a closed shape, of which each path segment is filled with flowing water, with a stationary dielectric, or merely with air (see Fig. 6 or a similar one in [33]). For clarity, suppose that the pipe together with the beam splitter, mirrors, and other components of the interferometer is stationary in a laboratory.

As the interferometer is geographically small, the path velocity is then substantially uniform over the setup with respect to an ECI frame. Thus the path velocity is identical to the laboratory velocity, that is, $\mathbf{v}_l = \mathbf{v}_0$. Besides, suppose that the dielectric medium is flowing at a velocity $\mathbf{v}_f$ with respect to the pipe. Thus the matrix velocity $\mathbf{v}_m = \mathbf{v}_f + \mathbf{v}_0$ and the velocity difference $\mathbf{v}_{lm} = -\mathbf{v}_f$. Then formula (3.28) yields that the phase variation $d\phi$ over a path of differential length dl is given by

$$d\phi = k_0 dl \left\{ n + (1-n^2)\hat{l} \cdot \mathbf{v}_f/c + \hat{l} \cdot \mathbf{v}_0/c \right\}, \tag{3.38}$$

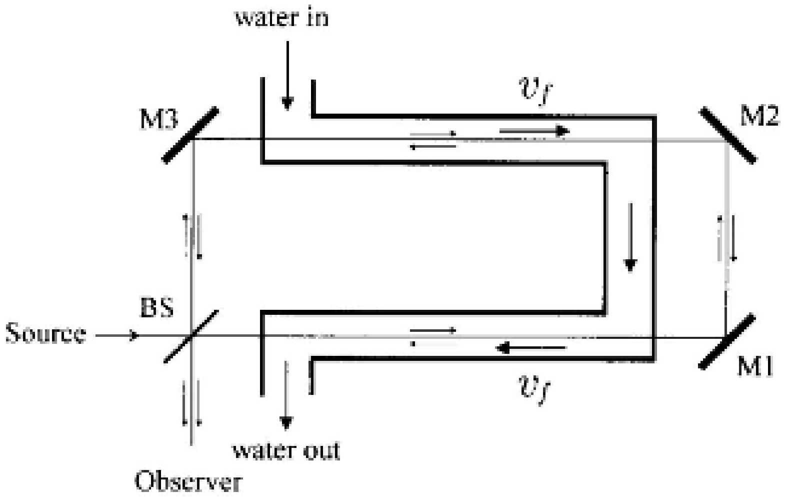

Fig. 6 Fizeau's experiment with flowing water. The Fizeau interferometer is formed by a beam splitter (BS), mirrors (M1, M2, and M3), and a transparent pipe filled with flowing water. Two waves propagate in opposite directions along each segment of the closed path. This structure is similar to the Sagnac loop interferometer, except the flowing water.

where $\hat{l}\cdot\mathbf{v}_f = \pm v_f$ for the two waves in interference as they propagate in opposite directions along each segment of the closed path.

Again, the contributions of the major term $k_0 n dl$ in (3.38) to the phase difference between the waves cancel out. Moreover, it is noted that the velocity $\mathbf{v}_0$ in this formula does not connect to the index n and hence its contributions to the phase variation over a loop cancel out collectively, as in the Sagnac loop interferometry. Further, it is seen from the preceding formula that the path segments filled with air or a stationary dielectric do not contribute to the phase difference. The contributions come from the path segments filled with flowing water.

Suppose that the water speed v_f is uniform along the pipe and the total length of the water-flowing path is l. Then the difference in the phase variation over the loop between the two waves is given by

$$\triangle\phi = 2k_0 l(n^2 - 1)v_f/c, \tag{3.39}$$

where n is the index of the water. It is noted that the phase difference is proportional to $(n^2 - 1)$ and to the water speed v_f with respect to the pipe. The preceding phase-difference formula agrees with the one determined from the interference fringe observed in Fizeau's experiment with various speeds v_f and indices n, as the reference frame of v_f is assumed to be the pipe tacitly in common practice.

More precisely, owing to earth's rotation and the minute differences in geocentric position, the path velocity $\mathbf{v}_l$ is not actually a constant value $\mathbf{v}_0$ over the closed path. That is, $\mathbf{v}_l = \mathbf{v}_{E0} + \mathbf{v}_0$ and $\mathbf{v}_m = \mathbf{v}_f + \mathbf{v}_{E0} + \mathbf{v}_0$, where $\mathbf{v}_0$ is then referred to a suitable point in the setup. Thus the Sagnac effect due to earth's rotation in a loop interferometer should also appear in Fizeau's experiment. However, as earth's rotation rate is low, its effect in Fizeau's experiment is ordinarily much smaller than that due to a motion of the dielectric medium, just as its effect in the rotating-loop experiment is ordinarily much smaller than that due to a rotation of the loop. Thereby, the phase difference is substantially independent of earth's rotation.

Furthermore, as the phase differences given by (3.35), (3.37), and (3.39) in the Sagnac rotating-loop experiments and Fizeau's experiment are independent of the laboratory velocity $\mathbf{v}_0$, at least to the first order of normalized speed, these interference experiments then comply with Galilean relativity, in spite of the restriction on the reference frame of the matrix velocity $\mathbf{v}_m$ and the path velocity $\mathbf{v}_l$. Conversely, the actual reference frame of $\mathbf{v}_m$ and $\mathbf{v}_l$ then cannot be determined unequivocally from these experiments.

3.6 Derivation of Modifications of Maxwell's Equations

In addition to wave equations which involve second derivatives, the relations that involve first spatial and temporal derivatives of the fields can be given. Based on the explicit definitions of the fields in terms of the potentials, we derive the divergence and the curl relations for the local-ether electric and magnetic fields. Then these relations are compared with Maxwell's equations which have played the fundamental role in electromagnetics for more than one hundred years.

By applying the curl and the divergence to both sides of (3.2) and (3.3), namely, the definitions of the fields in terms of the potentials, respectively, one immediately has

$$\nabla \times \mathbf{E}(\mathbf{r}, t) = -\left(\frac{\partial}{\partial t}\mathbf{B}(\mathbf{r}, t)\right)_m \tag{3.40}$$

and

$$\nabla \cdot \mathbf{B}(\mathbf{r}, t) = 0. \tag{3.41}$$

Besides, by applying the divergence and the curl to both sides of these definitions of the fields, respectively, one has

$$\nabla \cdot \mathbf{E}(\mathbf{r},t) = -\nabla^2\Phi(\mathbf{r},t) - \left(\frac{\partial}{\partial t}\nabla \cdot \mathbf{A}(\mathbf{r},t)\right)_m \tag{3.42}$$

and

$$\nabla \times \mathbf{B}(\mathbf{r},t) = -\nabla^2\mathbf{A}(\mathbf{r},t) + \nabla\nabla \cdot \mathbf{A}(\mathbf{r},t). \tag{3.43}$$

It is seen that either of these relations involves the Laplacian of a potential and the divergence $\nabla \cdot \mathbf{A}$.

Then, by using the local-ether wave equations and the matrix-frame continuity equation for the potentials, the preceding divergence and curl relations become

$$\nabla \cdot \mathbf{E}(\mathbf{r},t) = \frac{1}{\epsilon_0}\rho_n(\mathbf{r},t) + \frac{1}{c^2}\left\{\left(\frac{\partial^2\Phi}{\partial t^2}\right)_m - \frac{\partial^2\Phi}{\partial t^2}\right\} \tag{3.44}$$

and

$$\nabla \times \mathbf{B}(\mathbf{r},t) = \mu_0\mathbf{J}_n(\mathbf{r},t) + \frac{1}{c^2}\left(\frac{\partial}{\partial t}\mathbf{E}(\mathbf{r},t)\right)_m + \frac{1}{c^2}\left\{\left(\frac{\partial^2\mathbf{A}}{\partial t^2}\right)_m - \frac{\partial^2\mathbf{A}}{\partial t^2}\right\}, \tag{3.45}$$

where we have also made use of the definition of the electric field in terms of the potentials. It is seen that either of these relations involves the difference between the second time derivative of a potential referred to the matrix frame and to the local-ether frame. These differences represent the effects of the deviation in the wave operator due to the change of the reference frame.

From the two curl relations (3.40) and (3.45) together with the divergence relation for and the definition of the magnetic field, the local-ether wave equation for the magnetic field (3.11) can be derived alternatively, where the time derivative of **B** with respect to the matrix frame cancels out. The wave equation for the electric field can also be derived from the two curl relations. Thus one has

$$\nabla \times \nabla \times \mathbf{E} + \frac{1}{c^2}\left(\frac{\partial^2\mathbf{E}}{\partial t^2}\right)_m = -\frac{1}{c^2}\left(\frac{\partial}{\partial t}\left\{\frac{1}{\epsilon_0}\mathbf{J}_n + \left(\frac{\partial^2\mathbf{A}}{\partial t^2}\right)_m - \frac{\partial^2\mathbf{A}}{\partial t^2}\right\}\right)_m. \tag{3.46}$$

It is noted that this equation also incorporates the wave-operator deviation and thus becomes quite complicated. However, by using the divergence relation for and the definition of the electric field, it is easy to show that the preceding equation reduces to the local-ether wave equation for the electric field (3.12).

For quasi-static cases or for the case where the matrix happens to be stationary in the local-ether frame, the wave-operator deviation terms vanish. As a consequence, we arrive at

$$\begin{cases} \nabla \cdot \mathbf{E}(\mathbf{r},t) = \dfrac{1}{\epsilon_0}\rho_n(\mathbf{r},t) & (3.47\text{a}) \\ \nabla \times \mathbf{E}(\mathbf{r},t) = -\left(\dfrac{\partial}{\partial t}\mathbf{B}(\mathbf{r},t)\right)_m & (3.47\text{b}) \\ \nabla \cdot \mathbf{B}(\mathbf{r},t) = 0 & (3.47\text{c}) \\ \nabla \times \mathbf{B}(\mathbf{r},t) = \mu_0\mathbf{J}_n(\mathbf{r},t) + \dfrac{1}{c^2}\left(\dfrac{\partial}{\partial t}\mathbf{E}(\mathbf{r},t)\right)_m . & (3.47\text{d}) \end{cases}$$

This set of the divergence and curl relations represent modifications of Maxwell's equations, which comply with Galilean transformations and the local-ether model of wave propagation, apart from the wave-operator deviation terms associated with the differences between time derivatives of the potentials for general cases. The fundamental modification is that the time derivatives in the two curl relations and the particle velocity in the neutralized current density are all referred specifically to the matrix frame. The modifications made their debut in [131, 132].

The wave-operator deviation terms are associated with the motion of the matrix in the local-ether frame and will be shown later to be negligible for ordinary terrestrial cases. Besides, the modifications associated with the reference frame could have been assumed tacitly in common practice. As an example, consider the familiar case of the transformer which is composed of a primary winding connected to an alternating-current source, of a secondary winding connected to a load, and of a ferromagnetic core. A time-varying input current flowing through the primary winding generates a time-varying magnetic field and induces an electric field around the secondary winding. For simplicity, let the secondary winding be open-circuit. Thus the electric force induced along this winding tends to develop an open-circuit voltage between the two ends of the winding, where charges of opposite polarities accumulate respectively.

Ordinarily, the primary winding and the core have no relative motion between them and thus they together form the matrix of this case. Based on the modified Ampère law (3.47d), the magnetic field is associated with the current density in the laboratory frame with respect to which the matrix together with other components of the transformer is stationary. Besides, based on the modified Faraday law (3.47b), the induced electric field and the corresponding open-circuit voltage are associated with the time rate of change of the magnetic field also in this laboratory frame.

If the wave-operator deviation terms can be omitted, the matrix velocity and hence the laboratory velocity with respect to an ECI frame are then not involved in the modified Maxwell equations. Consequently, the input current, the magnetization current, the magnetic field, the induced electric field, and then the induced voltage in a geostationary transformer are all independent of earth's rotation and the latitude of the device, let alone earth's orbital motion. Further, when the transformer is put on a vehicle moving smoothly with respect to the ground, the currents, the fields, and the voltage are also independent of the ground velocity of the vehicle.

This invariance of electric induction keeps the open-circuit voltage of a moving transformer unaffected, which is in accord with common experience with this device. Therefore, the operation of the transformer, as well as that of the cathode-ray tube discussed in Chapter 2, is substantially independent of the laboratory velocity and thus complies with Galilean relativity. Moreover, these familiar operations are independent of the orientation of the device with respect to the ground and thus possess the terrestrial isotropy. A similar argument of the invariance of electric induction can be applied to an inductor, where a time-varying current in a coil results in an electric induction on itself.

On the other hand, we examine the laboratory frame actually adopted in the conventional analysis of transformers and of inductors based on Maxwell's equations. Commonly, the induced voltage is given by the time derivative of the input current, aside from a scaling factor associated with the inductance. As the input current is neutralized in the primary winding, the drift speed associated with this conduction current is then referred to the matrix frame tacitly in common practice. This frame also applies to the magnetization current.

Besides, suppose that the transformer is operated at a low frequency, as it is ordinarily. Thus the propagation delay of the potentials and hence the corresponding Sagnac effect can be neglected. Then the potential **A** and hence the magnetic field **B** due to the input current in the primary winding and to the magnetization current in the core tend to comove with the matrix. Thus an input current of a fixed amount leads to a magnetic field of a fixed spatial distribution which is at rest with respect to the matrix frame. Meanwhile, a change in the input current leads to a proportional change in the field distribution when observed also in the matrix frame. That is, the time derivative of the input current actually corresponds to the time rate of change of the magnetic field referred specifically to the matrix frame. Thus the matrix frame has been adopted tacitly in the conventional practice dealing with the transformer based on Faraday's law. A similar argument of the reference frame can be applied to an inductor.

In practical designs, the secondary winding is commonly stationary with respect to the primary winding and to the ferromagnetic core, though this restriction is not necessary in principle. As the secondary winding is stationary in the matrix frame, the time derivative of the magnetic field in this frame just stands for the time rate of change in the field experienced by this winding. By virtue of this seemingly trivial coincidence, the conventional practice, where the matrix frame is adopted tacitly with the use of the derivative of the input current, happens to work well. On the contrary, for the unusual case of the mutual induction between two coils in relative motion, the induction then cannot be solved merely either by Maxwell's equations or by their modifications. For such a case, the electromagnetic force law has to be called for.

Therefore, with the wave-operator deviation terms being omitted, **the modified equations are identical to Maxwell's equations, if the latter set are observed in the matrix frame** as done tacitly in common practice. In other words, Maxwell's equations are valid only under some hidden restrictions, in addition to the low-speed condition which makes the force law (3.1) itself valid. That is, the effector and matrix speeds are low, the drift speed is very low, the laboratory frame is actually the matrix frame, and the corresponding wave-operator deviation terms are omitted. However, these conditions are so common as to be ignored easily.

Lastly, we estimate the magnitudes of the wave-operator deviation terms which are omitted in the simplified modifications of Maxwell's equations. From the Galilean formula (I.17) or (3.16), it is seen that these terms are associated with the matrix velocity in the local-ether frame. Further, as noted in Chapter 2, owing to wave motion, a temporal variation in a potential tends to cause a spatial variation in it. For a potential even rapidly varying with time, the order of magnitude of its time derivative divided by c is not expected to exceed the one of its gradient. That is, $|\partial\Phi/c\partial t| \lesssim |\nabla\Phi|$. Thus the wave-operator deviation is estimated to be

$$\frac{1}{c^2}\left|\left(\frac{\partial^2\Phi}{\partial t^2}\right)_m - \frac{\partial^2\Phi}{\partial t^2}\right| \simeq \frac{2}{c}\left|\mathbf{v}_m\cdot\nabla\frac{\partial\Phi}{c\partial t}\right| \lesssim \frac{2}{c}\left|(\mathbf{v}_m\cdot\nabla)\nabla\Phi\right| \sim \frac{2v_m}{c}\frac{1}{\epsilon_0}\left|\rho_n\right|, \tag{3.48}$$

where it is assumed that the terms $(\mathbf{v}_m\cdot\nabla)\nabla\Phi$, $\mathbf{v}_m\nabla^2\Phi$, and $\mathbf{v}_m\rho_n/\epsilon_0$ are of the same order in magnitude and the charge distribution is smooth. Similarly,

$$\frac{1}{c^2}\left|\left(\frac{\partial^2\mathbf{A}}{\partial t^2}\right)_m - \frac{\partial^2\mathbf{A}}{\partial t^2}\right| \lesssim \frac{2v_m}{c}\mu_0\left|\mathbf{J}_n\right|. \tag{3.49}$$

Thereby, the wave-operator deviation term in (3.44), or in (3.45), tends to be weaker than the other terms by a factor of the normalized matrix speed v_m/c or less. For terrestrial phenomena, the matrix velocity incorporates the linear velocity due to earth's rotation. Ordinarily, the matrix is stationary or moving at a low speed with respect to the ground. Thus the normalized speed $v_m/c \sim 10^{-6}$ and hence the wave-operator deviation terms are negligibly small. Consequently, the simplified modifications of Maxwell's equations (3.47) hold under the ordinary low-speed condition.

Physically, the wave-operator deviation terms are due to the motion of the matrix and hence are associated with the matrix velocity with respect to the local-ether frame. It is noted that the wave-operator deviation corresponds to the Sagnac-effect deviation discussed in Chapters 1 and 2, which in turn is associated with the propagation of the potentials and is also due to the motion of the matrix frame.

When the deviation terms cannot be neglected in some high-precision experiments, the divergence relation for the electric field and the curl relation for the magnetic field become rather complicated. Anyway, these terms have been taken into account in the local-ether wave equations for the fields and are in accord with the aforementioned precision interference experiments. These experiments together then provide evidence for the wave-operator deviation and for the modified Maxwell equations.

3.7 Summary

Based on the local-ether model of wave propagation, the potentials propagate at the isotropic speed c with respect to an ECI frame in earthbound experiments, regardless of the motions of the source and effector. Thereby, the corresponding local-ether wave equations and the matrix-frame continuity equation for the potentials are derived. Under the ordinary low-speed condition where the source particles drift very slowly in a neutralizing matrix which in turn moves slowly in the local-ether frame, the electromagnetic force can be given in terms of the electric and magnetic fields which in turn are given explicitly in terms of the local-ether potentials. The position vectors, time derivatives, particle velocities, and propagation velocity involved are all referred specifically to their respective frames. Consequently, the values of the current density, potentials, fields, and force remain unchanged in different frames in uniform motion of translation.

Further, based on the definitions of the fields in terms of the potentials, the local-ether wave equations for the fields are derived. From the wave equation for the magnetic field, the propagation speed of electromagnetic wave in a uniform magnetic medium is found to depend on the permeability, but not on the motion of the medium. However, from the wave equation for the electric field, the phase speed of a uniform plane wave propagating in a moving uniform dielectric medium is found to depend on the medium velocity and incorporate the familiar Fresnel drag coefficient. This phase speed looks like the speed obtained from the velocity transformation in the special relativity. However, the fundamental discrepancy is that both the phase speed and the medium speed are referred specifically to the local-ether frame. Moreover, this phase-speed formula is not expected to hold for a magnetic or a nonuniform dielectric medium.

Then the phase difference in various interference experiments are analyzed, where both the matrix-velocity modification of the propagation constant and the Sagnac path-velocity modification of the propagation length are taken into account in a consistent way. It is found that the consequent phase-variation formula is in accord with the spatial isotropy in the one-way fiber-link experiment, with the null effect of the refractive index in the Harzer experiment with a dielectric medium comoving with a rotating Sagnac interferometer, with the increase of the phase difference in the Dufour-Prunier experiment with a geostationary dielectric medium instead, and with the dependence of the phase difference on the speed and index of the flowing water in Fizeau's experiment. These together provide support for the local-ether wave equation.

Moreover, it is predicted that when the fiber-link experimental setup is put on a turntable, the phase variation over the link will change sinusoidally as the orientation of the turntable is changing smoothly with respect to the ground. The predicted terrestrial anisotropy in the proposed one-way-link rotor experiment, the predicted null effect of earth's orbital motion in the earthbound interferometry, the various index-dependences among the phase-difference terms associated with the rotation rates in the Sagnac interferometry, and the aforementioned discrepancy in the phase-speed formula for a moving medium and the restrictions on the use of this formula then provide different approaches to test the local-ether wave equation.

Thereafter, the divergence and the curl relations for the electric and magnetic fields are derived from the definitions of the fields in terms of the potentials, by using the local-ether wave equations and the continuity equation for the potentials. It is found that for quasi-static cases or the case where the matrix is stationary in the local-ether frame, these divergence and curl relations for the fields look like Maxwell's equations. However, the fundamental modification is that the neutralized current density and the time derivatives in the curl relations are all referred specifically to the matrix frame. For general cases, the divergence relation for the electric field and the curl relation for the magnetic field are found to additionally incorporate the wave-operator deviation terms due to the motion of the matrix with respect to the local-ether frame. These represent modifications of Maxwell's equations, which comply with Galilean transformations and the local-ether propagation model. The wave-operator deviation terms are estimated to be of the first order of the normalized matrix speed. For ordinary terrestrial phenomena, the matrix speed is merely or mainly due to earth's rotation and is only about a millionth of the speed of light. Thus the simplified modifications of Maxwell's equations hold under the low-speed condition. Then these equations are identical to Maxwell's equations, if the latter set are observed in the matrix frame as done tacitly in common practice. Thereby, hidden restrictions for Maxwell's equations imposed tacitly on particle speeds and reference frames are unveiled.

Chapter 4

Modifications of Schrödinger's Equation

A wave equation incorporating a natural frequency and the electric scalar potential is presented, which is supposed to govern the matter wave of a charged particle, which in turn is supposed to follow the local-ether propagation model. From the local-ether wave equation, the electrostatic force together with the inertial mass is derived. As a consequence, it is found that the inertial mass of a charged particle originates from the temporal variation of the associated matter wave. Further, the wave equation is refined by connecting the scalar potential with the augmentation operator which is associated with the momentum operator and the velocity of the source particles. From this local-ether wave equation, a first-order time evolution equation is derived, which in turn leads to the electromagnetic force law based on the augmented potentials proposed in Chapter 2. Under some ordinary conditions, this law reduces to the modified Lorentz force law. The evolution equation then represents modifications of Schrödinger's equation complying with Galilean transformations and the local-ether propagation model. The fundamental modification is that the position vector and the time derivative are referred specifically to the local-ether frame. Furthermore, the role of the vector potential in Schrödinger's equation is replaced by the augmentation operator connected with the scalar potential. The evolution equation looks quite different from Schrödinger's equation. However, under some ordinary conditions, it is shown that these two equations become substantially identical.

4.1 Force Law and Wave Equation

It is generally expected from intuition that the electromagnetic force exerted on a charged particle should remain unchanged when observed in different reference frames in uniform motion of translation to each other. However, it is well known that the famous Lorentz force law $\mathbf{F} = q(\mathbf{E} + \mathbf{v} \times \mathbf{B})$ for a particle of charge q and velocity $\mathbf{v}$ under the influence of electric and magnetic fields is not invariant under Galilean transformations. To make the electromagnetic force invariant, the Lorentz transformation of space and time seems the only successful approach known in the past century.

In Chapter 2, based on the augmented potentials which are derived from the electric scalar potential by incorporating a velocity difference between the involved particles, an electromagnetic force law complying with Galilean transformations has been proposed. In this new classical model all of the involved position vectors, time derivatives, and velocities are referred to their respective frames. Owing to this simple feature, the electromagnetic force exerted on a charged particle remains unchanged in different frames in uniform motion of translation, as expected intuitively.

Further, it is noticed that the magnetic force is commonly due to a conduction current and the mobile source particles forming this current drift very slowly with respect to a neutralizing matrix, such as electrons in a metal wire. Under this low-speed condition, it has been found in Chapter 2 that the proposed force law reduces to a form similar to the Lorentz force law. However, the fundamental modification is that the current density generating the magnetic vector potential, the time derivative of this potential in the electric induction force, and the particle velocity connecting to the curl of this potential in the magnetic force are all referred specifically to the matrix frame in which the matrix is stationary.

Moreover, based on the modified force law, the divergence and the curl relations for the electric and magnetic fields are derived in Chapter 3, which represent modifications of Maxwell's equations. The fundamental modification is that the current density and the time derivatives in the curl relations are all referred specifically to the matrix frame, too. It has been elucidated that these modifications have been actually adopted tacitly in common practice. Thereby, we have presented a reinterpretation of this century-old issue of the invariance of the electromagnetic force law and Maxwell's equations from an entirely different approach.

The propagation of the potentials is supposed to follow the local-ether model presented in Chapter 1, whereby electromagnetic wave can be viewed as propagating via a medium like the ether. However, the ether is not universal. It is supposed that in the region under a sufficient influence of the gravitation due to the Earth, the Sun, or another celestial body, there forms a local ether which in turn moves with the gravitational potential of the respective body. For earthbound waves the medium is the earth local ether which is stationary in an earth-centered inertial (ECI) frame, while the sun local ether for interplanetary waves is stationary in a heliocentric inertial frame. Consequently, earthbound experiments can depend on earth's rotation but are entirely independent of earth's orbital motion around the Sun or whatever.

In order to provide a quantum origin of the modified electromagnetic force law, we present a wave equation in this Chapter, which incorporates a natural frequency and the electric scalar potential and is proposed to govern the matter wave associated with charged particles. As well as electromagnetic wave, matter wave is supposed to follow the local-ether propagation model. Accordingly, the position vector and time derivative involved in this wave equation are referred specifically to an ECI frame for earthbound phenomena. Based on this local-ether wave equation, we derive the velocity and then the acceleration of a charged particle under the influence of the electric scalar potential. Then the electrostatic force exerted on the particle and the associated inertial mass are explored.

Further, the local-ether wave equation is refined in such a way that the electric scalar potential is made to connect with an augmentation operator which in turn will be proposed to preserve the local-ether feature and to correspond to the velocity difference incorporated in the augmented potentials. Then we explore the relationships of the local-ether wave equation with the electromagnetic force law, the augmented potentials, and Schrödinger's equation.

4.2 Local-Ether Wave Equation and Evolution Equation

It is supposed that a charged particle contributes to the electric scalar potential Φ which in turn will be experienced by and then will affect another charged particle under consideration called the effector. Moreover, it is supposed that a particle is associated with a matter wave which as well as electromagnetic wave follows the local-ether propagation model. Accordingly, it is postulated that under the influence of the electric scalar potential Φ, the matter wave Ψ of the effector particle is governed by the nonhomogeneous wave equation proposed hereby to be

$$\left\{\nabla^2 - \frac{1}{c^2}\frac{\partial^2}{\partial t^2}\right\}\Psi(\mathbf{r},t) = \frac{\omega_0^2}{c^2}\left\{1 + \frac{2}{\hbar\omega_0}q\Phi(\mathbf{r},t)\right\}\Psi(\mathbf{r},t), \tag{4.1}$$

where c is the speed of light, $\hbar$ is Planck's constant divided by 2π, the *natural frequency* ω_0 as well as the charge q is an inherent constant of the effector particle, and the position vector $\mathbf{r}$ and the time derivative are referred to the associated local-ether frame. This uniqueness feature of the reference frame is simply analogous to the fact that the position vector and time derivative in the wave equation governing the mechanical wave on a violin string are referred specifically to the frame in which the violin is stationary.

In the absence of the potential, the local-ether wave equation reduces to a form which looks like the Klein-Gordan equation for free particles [58], aside from the difference in reference frames. Further, if the natural frequency is zero, the equation reduces to a homogeneous wave equation which in turn implies that the wave propagates at the speed c with respect to the local-ether frame. Obviously, this wave equation provides the basis for the local-ether propagation model of electromagnetic wave discussed in Chapter 1. By replacing c with another speed, the homogeneous equation then reduces to a form like the wave equation governing mechanical waves.

The incorporation of the factor $\hbar/2$ in the potential term of the wave equation may be not so obvious at first sight. However, this factor is indispensable if the proposed wave equation is expected to lead to the well-studied electrostatic force in terms of the potential Φ. Anyway, it makes the potential term $2q\Phi/\hbar\omega_0$ dimensionless, as this term should be. The physical meaning and the actual value of the natural frequency of the effector particle are yet to be explored from the consequences derived from the wave equation. For the case with a zero natural frequency, the matter wave reduces to electromagnetic wave. Thus both matter wave and electromagnetic wave are governed by the proposed local-ether wave equation.

Quantitatively, the electric scalar potential Φ due to a single source particle of charge q and located at $\mathbf{r}'$ at instant t' is given by

$$\Phi(\mathbf{r},t) = \frac{1}{4\pi\epsilon_0}\frac{q}{R}, \tag{4.2}$$

where $t = t' + R/c$, R/c is the propagation delay time from the source point $\mathbf{r}'$ to the field point $\mathbf{r}$, the propagation range $R = |\mathbf{r} - \mathbf{r}'|$, and

ϵ_0 is a constant known as the permittivity. The potential due to an ensemble of source particles can be given by superposition. This potential is identical to that given in the conventional electromagnetics, aside from the reference frame.

Based on the local-ether model which has been shown to be in accord with various experiments dealing with the propagation or interference of electromagnetic wave, it is expected that the electric scalar potential Φ propagates away from the emission position at the isotropic speed c with respect to the local-ether frame, regardless of the motions of the source and the effector. Thereby, in order for the propagation time to be given simply by R/c, the position vectors $\mathbf{r}'$ and $\mathbf{r}$ and hence the propagation range R in the preceding formula are referred specifically to the local-ether frame. It is noted that in the scalar potential and further in the wave equation, all of the involved position vectors, time derivative, and velocity are referred to the local-ether frame.

Consider the ordinary case where the scalar potential Φ and the spatial rate of variation of Ψ are weak. Thus the temporal variation of Ψ is close to the one of the harmonic $e^{-i\omega_0 t}$ and then the wavefunction can be given by $\Psi(\mathbf{r},t) = \psi(\mathbf{r},t)e^{-i\omega_0 t}$, where ψ is a weak function of time. Then, by an expansion, its second time derivative becomes

$$\frac{\partial^2}{\partial t^2}\Psi(\mathbf{r},t) = e^{-i\omega_0 t}\left\{\frac{\partial^2}{\partial t^2}\psi(\mathbf{r},t) - i2\omega_0\frac{\partial}{\partial t}\psi(\mathbf{r},t) - \omega_0^2\psi(\mathbf{r},t)\right\}. \tag{4.3}$$

As the temporal variation of ψ is relatively weak, the second time derivative $\partial^2\psi/\partial t^2$ can be neglected.

Thereby, the proposed local-ether wave equation can be approximated by the first-order time evolution equation in terms of the *reduced wavefunction* ψ. That is,

$$\frac{\partial}{\partial t}\psi(\mathbf{r},t) = i\frac{c^2}{2\omega_0}\nabla^2\psi(\mathbf{r},t) - i\frac{1}{\hbar}q\Phi(\mathbf{r},t)\psi(\mathbf{r},t), \tag{4.4}$$

where the time derivative is referred to the local-ether frame. It is of essence to note that the major term $(\omega_0/c)^2\Psi$ in the wave equation has been cancelled out in the preceding equation. This evolution equation states that the temporal variation of the wavefunction ψ is determined by its spatial distribution and the potential. Given the wavefunction ψ at a particular instant, the space-time behavior of the wavefunction after that instant is governed by the evolution equation. If the potential is static, the space-time wavefunction is then determined from its starting spatial distribution.

4.3 Derivation of Electrostatic Force and Mass

As in quantum mechanics, it is supposed that the velocity $\mathbf{v}_e$ of the effector particle is given by the time derivative of the expectation value of the operator associated with the position vector $\mathbf{r}$. Thereby,

$$\mathbf{v}_e = \frac{d\langle \mathbf{r} \rangle}{dt}, \tag{4.5}$$

where the position vector represented by the position operator $\mathbf{r}$ and hence the velocity $\mathbf{v}_e$ are referred to the local-ether frame, and the expectation value of an operator O is given by the familiar volume integral as $\langle O \rangle = \int \psi^* O \psi dv$ which is evaluated in terms of the reduced wavefunction ψ. It is seen that as the velocity $\mathbf{v}_e$ represents the Newtonian relative velocity between the effector and the local-ether frame, it is Galilean invariant.

It is noted that the operators ∇^2 and Φ involved in the evolution equation are self-adjoint whereby $\int \psi_a^*(O\psi_b)dv = \int (O\psi_a)^*\psi_b dv$ for any such operator O and for two arbitrary wavefunctions ψ_a and ψ_b. Thus it is seen that

$$\int (\tilde{H}\psi_a)^*\psi_b dv = -\int \psi_a^* \tilde{H}\psi_b dv, \tag{4.6}$$

where $\tilde{H}$ represents the sum of the operators on the right-hand side of the evolution equation (4.4), that is, $\tilde{H}\psi = \partial\psi/\partial t$.

Then, by a direct expansion, the time derivative of the expectation value of a time-independent operator O can be given by

$$\frac{d\langle O \rangle}{dt} = \left\langle [O, \tilde{H}] \right\rangle, \tag{4.7}$$

where the commutator $[O, \tilde{H}] = O\tilde{H} - \tilde{H}O$ and the time derivative is chosen to be referred to the local-ether frame, identical to the frame of the time derivative in the evolution equation.

It is straightforward to show the two useful commutator relations

$$[\mathbf{r}, f(\nabla - \mathbf{s})^2] = f[\mathbf{r}, (\nabla - \mathbf{s})^2] = -2f(\nabla - \mathbf{s}) \tag{4.8}$$

and

$$[\nabla, f(\nabla - \mathbf{s})^2] = (\nabla f)(\nabla - \mathbf{s})^2, \tag{4.9}$$

where f is an arbitrary scalar function of space and $\mathbf{s}$ is an arbitrary constant vector.

Based on the evolution equation (4.4), the use of the commutator relation (4.8) immediately leads to the effector velocity

$$\mathbf{v}_e = \left\langle [\mathbf{r}, \tilde{H}] \right\rangle = -i\frac{c^2}{\omega_0} \langle \nabla \rangle . \tag{4.10}$$

It is seen that the effector velocity is proportional to the expectation value of the del operator and thus is associated with the spatial variation of ψ. Thereby, a zero or weak spatial rate of variation of the wavefunction corresponds to the particle being stationary or moving at a low speed with respect to the local-ether frame. Consequently, the evolution equation (4.4) is valid only for a low-speed effector under a weak potential.

Further, the acceleration of the effector particle can be given in terms of the time derivative of expectation value of the del operator. That is,

$$\mathbf{a} = -i\frac{c^2}{\omega_0}\frac{d}{dt} \langle \nabla \rangle = -i\frac{c^2}{\omega_0} \left\langle [\nabla, \tilde{H}] \right\rangle . \tag{4.11}$$

It is straightforward to show that the acceleration is given by

$$\mathbf{a} = -\frac{c^2}{\hbar\omega_0} q\nabla\Phi. \tag{4.12}$$

It is noted that the acceleration is proportional to the gradient of the potential Φ. Physically, this relation states that the spatial variation of the potential Φ tends to cause a change in the spatial variation of the wavefunction ψ and then a change in the effector velocity. It is also noted that the acceleration is inversely proportional to the natural frequency. Consequently, the natural frequency just plays the important role of inertial mass.

Based on the electrostatic force $\mathbf{F} = -q\nabla\Phi$ and on Newton's second law of motion in classical mechanics, it is well known that the acceleration of a charged particle under the influence of the electric scalar potential is

$$\mathbf{a} = -\frac{1}{m_0} q\nabla\Phi, \tag{4.13}$$

where m_0 is the rest mass of the accelerated particle.

By comparing the preceding two formulas for acceleration, the local-ether wave equation can be in accord with classical mechanics and electrostatics, if the rest mass m_0 and the natural frequency ω_0 are related to each other in the familiar form

$$m_0 = \frac{\hbar}{c^2}\omega_0. \tag{4.14}$$

This frequency-mass relation links the inertial mass of a particle to the natural frequency of the associated matter wave, and unveils that **the physical origin of inertial mass is wave motion**. In other words, the inertial mass of the effector particle originates from the temporal variation of the wavefunction Ψ (rather than the one of the reduced wavefunction ψ).

Precisely, the natural frequency ω_0 multiplied by the constant $(\hbar/c^2)$ is just the inertial mass m_0 of the particle under the influence of the electric scalar potential Φ, where it is supposed that the potential is weak and the particle is stationary or moving slowly with respect to the local-ether frame. Planck's constant $\hbar$ foresightedly incorporated in the potential term in the local-ether wave equation (4.1), when divided by c^2, serves to adapt the natural frequency ω_0 in the acceleration formula (4.12) to the rest mass m_0 which has been measured in kilogram or the like long before the introduction of the charge q and the potential Φ.

It is of interest to note that the acceleration of an electron due to the potential (4.2) from another electron can be written as

$$\mathbf{a} = -\frac{\alpha c^3}{\omega_0}\nabla\left(\frac{1}{R}\right), \tag{4.15}$$

where the dimensionless factor α $(= e^2/4\pi\epsilon_0\hbar c)$ is just the fine-structure constant in atomic spectra [3, 81]. The permittivity in this constant or in the potential (4.2) is defined as $\epsilon_0 = 1/\mu_0 c^2$ and the permeability in turn is defined as $\mu_0 = 4\pi \times 10^{-7}$ (kg·m·C^{-2}).

Suppose the charge of the electron $e = 1.602 \times 10^{-19}$ (C) and Planck's constant $2\pi\hbar = 6.626 \times 10^{-34}$ (kg·m^2·s^{-1}). Thus $\alpha \simeq 1/137$. Alternatively, as the ratio $e^2/\hbar$ incorporated in α also appears in the energies of quantum states, at least, in a hydrogen-like atom [26, 81], the ratio $e^2/\hbar$ or the constant α can be determined experimentally from spectroscopy. Then a measurement of the electrostatic acceleration would lead to the natural frequency $\omega_0 = 7.8 \times 10^{20}$ s^{-1} for electrons, which corresponds to the rest mass $m_0 = 9.1 \times 10^{-31}$ kg.

In terms of the rest mass m_0, the first-order time evolution equation (4.4) can be rewritten in a more familiar form

$$i\hbar\frac{\partial}{\partial t}\psi(\mathbf{r},t) = -\frac{\hbar^2}{2m_0}\nabla^2\psi(\mathbf{r},t) + q\Phi(\mathbf{r},t)\psi(\mathbf{r},t). \tag{4.16}$$

This evolution equation looks like the famous Schrödinger's equation with the potential energy $q\Phi$, except the difference that the position vector **r** and the time derivative are referred specifically to the local-ether frame. The foresighted incorporation of Planck's constant $\hbar$ in the potential term makes the time derivative and the Laplacian in the evolution equation connect with the factors $\hbar$ and $\hbar^2$, respectively, just as in Schrödinger's equation.

4.4 Local-Ether Wave Equation with Augmentation Operator

In order to derive the whole electromagnetic force, it is proposed that the wave equation is refined by connecting the potential Φ with a dimensionless operator U. In the presence of the electric scalar potential Φ due to source particles which move at a given velocity $\mathbf{v}_s$ with respect to the local-ether frame at the emission, it is postulated that the local-ether wave equation is refined to be

$$\left\{\nabla^2 - \frac{1}{c^2}\frac{\partial^2}{\partial t^2}\right\}\Psi(\mathbf{r},t) = \frac{\omega_0^2}{c^2}\left\{1 + \frac{2}{\hbar\omega_0}q\Phi(\mathbf{r},t)(1+U)\right\}\Psi(\mathbf{r},t), \tag{4.17}$$

where the operator U is derived from the Laplace operator and is defined as

$$U \triangleq -\frac{c^2}{2\omega_0^2}\left(\nabla - i\frac{\omega_0}{c^2}\mathbf{v}_s\right)^2. \tag{4.18}$$

The operator U is introduced deliberately to enhance the effect of the electric scalar potential and then the one of the Laplace operator. Hence it is named the *augmentation operator*. For source particles of various velocities, the whole potential term should be given by superposition. As the source velocity is referred to a specific frame, the incorporation of U does not spoil the local-ether feature. The local-ether wave equation made its debut in [120, 133, 136].

In terms of the rest mass m_0, the augmentation operator U takes the form

$$U = \frac{1}{2c^2}\left(\frac{\mathbf{p}}{m_0} - \mathbf{v}_s\right)^2, \tag{4.19}$$

where the operator $\mathbf{p} = -i\hbar\nabla$. From (4.10) one has $\langle\mathbf{p}\rangle = m_0\mathbf{v}_e$. As the operator $\mathbf{p}$ is associated with the momentum of the effector, the augmentation operator U then corresponds to the squared velocity difference between the effector and the source normalized with respect to c. The speeds of these particles are supposed to be much lower than that of light, as they are ordinarily. Thus the modification with the augmentation operator is of the second order of normalized speed and is actually quite slight in magnitude.

Suppose again that both the electric scalar potential Φ and the spatial variation of the wavefunction Ψ are weak. Hence the effector speed v_e is indeed much lower than c. Moreover, the temporal variation of Ψ is still close to the one of the time harmonic $e^{-i\omega_0 t}$ and then $\partial^2\psi/\partial t^2$ can be neglected, where $\Psi(\mathbf{r},t) = \psi(\mathbf{r},t)e^{-i\omega_0 t}$. Thereby, the local-ether wave equation can be approximated by the time evolution equation in terms of the reduced wavefunction ψ. That is,

$$i2\omega_0 \frac{1}{c^2}\frac{\partial}{\partial t}\psi(\mathbf{r},t) = -\nabla^2\psi(\mathbf{r},t) + \frac{2\omega_0}{\hbar c^2} q\Phi(1+U)\psi(\mathbf{r},t), \qquad (4.20)$$

where the position vector $\mathbf{r}$ and the time derivative are referred to the local-ether frame.

In terms of the rest mass m_0, the first-order time evolution equation for an effector in the presence of the potential Φ due to source particles moving at a given velocity $\mathbf{v}_s$ becomes

$$i\hbar\frac{\partial}{\partial t}\psi(\mathbf{r},t) = \frac{1}{2m_0}\mathbf{p}^2\psi(\mathbf{r},t) + q\Phi(\mathbf{r},t)\left\{1 + \frac{(\mathbf{p} - m_0\mathbf{v}_s)^2}{2m_0^2c^2}\right\}\psi(\mathbf{r},t). \qquad (4.21)$$

This evolution equation represents modifications of Schrödinger's equation, which comply with Galilean transformations and the local-ether propagation model.

The fundamental modification is that the position vectors, the time derivative, the propagation velocity of the potential, and the source velocity are all referred specifically to the local-ether frame. Furthermore, the electric scalar potential connects with the augmentation operator. This augmentation with the scalar potential will be shown to correspond to the magnetic vector potential. The preceding equation looks quite different from Schrödinger's equation (I.20) or (4.41) reproduced later which incorporates both the scalar and the vector potential. However, the similarity will come out under some common conditions discussed later.

4.5 Derivation of Local-Ether Electromagnetic Force

Then, based on the evolution equation just developed from the proposed local-ether wave equation, we go on to derive the consequent electromagnetic force law in a way similar to that in deriving the generalization of Ehrenfest's theorem in quantum mechanics. Again, the effector velocity $\mathbf{v}_e$ is given by the time derivative of expectation value of the position operator $\mathbf{r}$ and hence by the commutator between $\mathbf{r}$ and the self-adjoint operator H. That is,

$$\mathbf{v}_e = \frac{d}{dt}\langle \mathbf{r}\rangle = \frac{1}{i\hbar}\langle [\mathbf{r}, H]\rangle , \tag{4.22}$$

where the involved position vector $\mathbf{r}$, the time derivative, and hence the effector velocity $\mathbf{v}_e$ are referred to the local-ether frame, the expectation value is evaluated in terms of ψ, and the Hamiltonian H represents the sum of all the operators on the right-hand side of the evolution equation (4.21), that is, $H\psi = i\hbar\partial\psi/\partial t$.

The use of the commutator relation (4.8) immediately leads to

$$\mathbf{v}_e = \frac{1}{m_0}\left\{\langle \mathbf{p}\rangle + \frac{1}{m_0c^2}\langle q\Phi\left(\mathbf{p} - m_0\mathbf{v}_s\right)\rangle\right\} . \tag{4.23}$$

It is noted that by virtue of the momentum operator $\mathbf{p}$ incorporated in the augmentation operator U, the scalar potential Φ and the source velocity $\mathbf{v}_s$ connected to it tend to affect the effector velocity $\mathbf{v}_e$. For a localized particle over which the spatial variation of the potential Φ can be neglected, the effector velocity then becomes

$$\mathbf{v}_e = \frac{1}{m_0}\left\{\langle \mathbf{p}\rangle + q\Phi_e\frac{1}{m_0c^2}\left(\langle \mathbf{p}\rangle - m_0\mathbf{v}_s\right)\right\} , \tag{4.24}$$

where Φ_e denotes the potential experienced by the effector and hence is equal to the functional value of the potential Φ at the instantaneous location of the effector particle.

According to the preceding formula for the effector velocity, define the *augmented vector potential* $\breve{\mathbf{A}}$ originating from source particles moving at a velocity $\mathbf{v}_s$ in terms of the corresponding potential Φ as

$$\breve{\mathbf{A}}(\mathbf{r}, t) \overset{\triangle}{=} -\Phi(\mathbf{r}, t)\frac{1}{m_0c^2}\left(\langle \mathbf{p}\rangle - m_0\mathbf{v}_s\right) . \tag{4.25}$$

Then the effector velocity can be given by

$$\mathbf{v}_e = \frac{1}{m_0}\left\{\langle \mathbf{p}\rangle - q\breve{\mathbf{A}}_e\right\} , \tag{4.26}$$

where $\breve{\mathbf{A}}_e$ denotes the augmented potential experienced by the effector and hence is equal to the functional value of the potential $\breve{\mathbf{A}}$

at the instantaneous location of the effector. It is noted that the effector velocity is $\langle \mathbf{p} \rangle / m_0$ modified by a quantity of $q\breve{\mathbf{A}}_e/m_0$. It is seen that the effector velocity is associated with the augmented vector potential, which in turn is associated with the effector velocity itself. The fact that the expectation value $\langle \mathbf{p} \rangle$ and the experienced potential $\breve{\mathbf{A}}_e$ remain unchanged in different frames is consistent with the Galilean invariance of the effector velocity $\mathbf{v}_e$.

Further, the acceleration $\mathbf{a}$ of the effector or the second time derivative of expectation value of the position operator $\mathbf{r}$ is then given by

$$\mathbf{a} = \frac{1}{m_0} \left\{ \frac{d}{dt} \langle \mathbf{p} \rangle - q \frac{d}{dt} \breve{\mathbf{A}}_e \right\}, \tag{4.27}$$

where the time derivative $d\breve{\mathbf{A}}_e/dt$ represents the time rate of change of the augmented potential experienced by the effector.

It is noted that $\breve{\mathbf{A}}_e$ is not a function of space and thus its time derivative as well as its value remains unchanged in different frames. Further, for the effector located at position $\mathbf{r}$ at instant t, it is noted that $d\breve{\mathbf{A}}_e/dt$ is equal to $(\partial \breve{\mathbf{A}}(\mathbf{r}, t)/\partial t)_e$ which in turn denotes the time rate of change of the augmented potential with respect to the effector frame (in which the effector is stationary) at the location of the effector. This time derivative is due partly to a variation of the source velocity and partly to a relative displacement between the source and effector particles which affects the actually experienced potential Φ_e.

Besides, the time derivative of expectation value of the momentum operator $\mathbf{p}$ can be given by

$$\frac{d}{dt} \langle \mathbf{p} \rangle = \frac{1}{i\hbar} \langle [\mathbf{p}, H] \rangle = -q(\nabla \Phi) \{1 + \langle U \rangle\}, \tag{4.28}$$

where the commutator relation (4.9) has been made use of. According to the preceding formula, define the *augmented scalar potential* $\breve{\Phi}$ originating from source particles moving at a velocity $\mathbf{v}_s$ in terms of the corresponding potential Φ as

$$\breve{\Phi}(\mathbf{r}, t) \overset{\triangle}{=} \Phi(\mathbf{r}, t) \{1 + \langle U \rangle\}. \tag{4.29}$$

It is seen that the augmented scalar potential is the electric scalar potential with a fractional increment given by the expectation value of the augmentation operator.

Then the time derivative of expectation value of the momentum operator $\mathbf{p}$ can be given in terms of the augmented scalar potential by

$$\frac{d}{dt}\langle \mathbf{p} \rangle = -q\nabla\breve{\Phi}. \tag{4.30}$$

This relation shows that the effect of the spatial variation of the potential Φ on the change in the spatial variation of the wavefunction ψ is enhanced slightly by the augmentation operator.

Thus the acceleration of the effector can be given in terms of the augmented scalar potential $\breve{\Phi}$ and the augmented vector potential $\breve{\mathbf{A}}$. Based on Newton's second law of motion with the inertial mass of the effector being the rest mass m_0, the electromagnetic force exerted on the effector can be given in terms of the augmented potentials. That is,

$$\mathbf{F}(\mathbf{r},t) = q\left\{-\nabla\breve{\Phi}(\mathbf{r},t) - \left(\frac{\partial}{\partial t}\breve{\mathbf{A}}(\mathbf{r},t)\right)_e\right\}. \tag{4.31}$$

In this force law all of the involved position vectors, time derivatives, and velocities are referred specifically to their respective frames. Consequently, the force exerted on an effector remains unchanged when observed in different frames in uniform motion of translation, as expected intuitively.

It is noted that the augmented potentials incorporate the expectation value of the momentum operator and hence tend to be different for different effectors. It is also noted that both of the augmented potentials originate from the electric scalar potential and hence they propagate together at exactly the same velocity.

4.6 Augmented Potentials under Weak-Potential and Low-Speed Conditions

Let us note that the time evolution equation and hence its consequences concerning the effector velocity, acceleration, and force are derived under the ordinary conditions of weak potential and low particle speed, whereby the reduced wavefunction has a weak temporal variation. These conditions also imply that the modification term $q\breve{\mathbf{A}}_e/m_0$ in the effector velocity $\mathbf{v}_e$ is weaker than the major term by a factor of about $|q\Phi|/m_0c^2$, which is then much less than unity. Thereby, the effector velocity with respect to the local-ether frame can be approximated as $\mathbf{v}_e = \langle \mathbf{p} \rangle / m_0$.

Consequently, the augmented scalar potential and the augmented vector potential, due to source particles moving at a given velocity $\mathbf{v}_s$ at the emission, defined in (4.29) and (4.25) in terms of the electric scalar potential Φ can be approximated as

$$\breve{\Phi}(\mathbf{r}, t) = \left(1 + \frac{v_{es}^2}{2c^2}\right) \Phi(\mathbf{r}, t) \tag{4.32}$$

and

$$\breve{\mathbf{A}}(\mathbf{r}, t) = -\frac{\mathbf{v}_{es}}{c^2} \Phi(\mathbf{r}, t), \tag{4.33}$$

where $v_{es} = |\mathbf{v}_{es}|$ and the velocity difference $\mathbf{v}_{es} = \mathbf{v}_e - \mathbf{v}_s$.

The augmented potentials originating from an ensemble of mobile source particles of various velocities, together with the corresponding electromagnetic force, can be given simply by superposition. Thus, due to the sources of charge density ρ_v, the augmented potentials experienced by an effector located at position $\mathbf{r}$ at instant t are given by the integrals over a volume containing all the sources

$$\breve{\Phi}(\mathbf{r}, t) = \frac{1}{4\pi\epsilon_0} \int \left(1 + \frac{v_{es}^2}{2c^2}\right) \frac{\rho_v(\mathbf{r}', t - R/c)}{R} dv' \tag{4.34}$$

and

$$\breve{\mathbf{A}}(\mathbf{r}, t) = \frac{-1}{4\pi\epsilon_0 c^2} \int \frac{\mathbf{v}_{es} \rho_v(\mathbf{r}', t - R/c)}{R} dv', \tag{4.35}$$

where the involved $\mathbf{v}_e$ is the effector velocity at instant t, $\mathbf{v}_s$ is the velocity of the source particles located at $\mathbf{r}'$ at an earlier instant $t' = t - R/c$, and the position vectors $\mathbf{r}$ and $\mathbf{r}'$ are referred to the local-ether frame.

The derived electromagnetic force law (4.31) together with the augmented potentials (4.34) and (4.35) has been treated in Chapter 2 as the fundamental postulate to derive the modified Lorentz force law complying with Galilean transformations. It is seen that both of the augmented potentials depend on the velocity difference $\mathbf{v}_{es}$ and the source charge density ρ_v. For quasi-static cases where the propagation time R/c can be neglected or for the case with a fixed $\mathbf{v}_s$, the velocity difference $\mathbf{v}_{es}$ then becomes the Newtonian relative velocity between the effector and the source. It is also seen that the augmented vector potential is related to the negative of the derivative of the augmented scalar potential with respect to the effector speed v_e. This connection results from the commutator relation (4.8) employed in deriving the effector velocity (4.23).

The augmented potentials given in (4.34) and (4.35) can be further simplified. As discussed in Chapter 2, consider the ordinary case where the source particles are moving in a matrix which tends to neutralize them, such as the case with a conduction current formed by mobile electrons in a metal wire. Suppose the neutralizing matrix has an arbitrary charge density ρ_m and moves as a whole at a velocity $\mathbf{v}_m$ with respect to the local-ether frame. Under the ordinary low-speed condition where all the involved particles move slowly in the local-ether frame and the sources drift very slowly in the matrix frame ($v_{sm} \lll c$ and $v_{em}, v_m \ll c$), it has been shown that the augmented potentials can be simplified to

$$\breve{\Phi}(\mathbf{r}, t) = \Phi(\mathbf{r}, t) - \mathbf{v}_{em} \cdot \mathbf{A}(\mathbf{r}, t) \tag{4.36}$$

and

$$\breve{\mathbf{A}}(\mathbf{r}, t) = \mathbf{A}(\mathbf{r}, t), \tag{4.37}$$

where the velocity differences $\mathbf{v}_{em} = \mathbf{v}_e - \mathbf{v}_m$ and $\mathbf{v}_{sm} = \mathbf{v}_s - \mathbf{v}_m$. The electric scalar potential Φ and the magnetic vector potential $\mathbf{A}$ in turn are given by

$$\Phi(\mathbf{r}, t) = \frac{1}{\epsilon_0} \int \frac{\rho_n(\mathbf{r}', t - R/c)}{4\pi R} dv' \tag{4.38}$$

and

$$\mathbf{A}(\mathbf{r}, t) = \frac{1}{\epsilon_0 c^2} \int \frac{\mathbf{J}_n(\mathbf{r}', t - R/c)}{4\pi R} dv', \tag{4.39}$$

where the potential Φ is due to the net charge density $\rho_n = \rho_v + \rho_m$ and the potential $\mathbf{A}$ to the neutralized current density which in turn is related to the source charge density by $\mathbf{J}_n = \mathbf{v}_{sm}\rho_v$.

Thereby, under the ordinary weak-potential and low-speed conditions, the electromagnetic force law (4.31) can be given in terms of the local-ether potentials Φ and $\mathbf{A}$. That is,

$$\mathbf{F}(\mathbf{r}, t) = q \left\{ -\nabla\Phi(\mathbf{r}, t) - \left(\frac{\partial}{\partial t} \mathbf{A}(\mathbf{r}, t) \right)_m + \mathbf{v}_{em} \times \nabla \times \mathbf{A}(\mathbf{r}, t) \right\}, \tag{4.40}$$

where we have made use of the Galilean transformation (2.13). That is, $(\partial \mathbf{A}/\partial t)_e = (\partial \mathbf{A}/\partial t)_m + (\mathbf{v}_{em} \cdot \nabla)\mathbf{A}$, where the two time derivatives are referred to the effector and the matrix frame, respectively.

As discussed in Chapter 2, the preceding equation represents modifications of the Lorentz force law. The fundamental modifications are that the current density generating the potential $\mathbf{A}$, the time derivative of $\mathbf{A}$, and the effector velocity before $\nabla \times \mathbf{A}$ are all referred specifically to the matrix frame, and that the propagation velocity of the potentials Φ and $\mathbf{A}$ is referred specifically to the local-ether frame. It has been elucidated that the modified force law is actually identical to the Lorentz force law, if the latter is observed in the matrix frame as done tacitly in common practice. In other words, the Lorentz force law has a hidden restriction to a weak potential, in addition to those on particle speeds and reference frames found in Chapter 2.

4.7 Comparison with Schrödinger's Equation

Lastly, we compare the local-ether evolution equation (4.21) with the famous Schrödinger's equation. It is well known that in the presence of the scalar potential Φ and the vector potential $\mathbf{A}$, Schrödinger's equation reads

$$i\hbar\frac{\partial}{\partial t}\psi(\mathbf{r},t) = \frac{1}{2m_0}[\mathbf{p} - q\mathbf{A}(\mathbf{r},t)]^2\psi(\mathbf{r},t) + q\Phi(\mathbf{r},t)\psi(\mathbf{r},t). \quad (4.41)$$

As discussed in the Introduction, the Lorentz force law can be derived from the preceding equation, apart from a minute discrepancy.

Further, for the interaction of a hydrogen-like atom or ion with electromagnetic radiation from an external source, the complicated treatment starts from Schrödinger's equation given by [99, 81]

$$i\hbar\frac{\partial}{\partial t}\psi(\mathbf{r},t) = \frac{1}{2m_0}\mathbf{p}^2\psi + q\Phi_a\psi - \frac{1}{m_0}q\mathbf{A}\cdot\mathbf{p}\psi + \frac{1}{2m_0}(q\mathbf{A})^2\psi, \quad (4.42)$$

where Φ_a is the scalar potential due to the nucleus of the atom and $\mathbf{A}$ is the vector potential due to the external source of radiation. In our understanding, the reference frame of the position vector in the wavefunction and potentials and the one of the time derivative are not specified in Schrödinger's equation.

As in the literature, in writing the preceding equation we have made use of $\mathbf{p}\cdot(\mathbf{A}\psi) = \mathbf{A}\cdot\mathbf{p}\psi$ since $\mathbf{p}\cdot\mathbf{A}$ is taken to be zero. Physically, the Coulomb gauge $\nabla\cdot\mathbf{A} = 0$ implies that the source generating the vector potential is electrically neutralized, as it is ordinarily. If the term $\mathbf{p}\cdot\mathbf{A}$ does not vanish, one has $\mathbf{p}\cdot\mathbf{A}/m_0 = (i/\omega_0)\partial\Phi_s/\partial t$ as determined from the Lorenz gauge, where the potential Φ_s is due to the charge associated with the non-neutralized current generating the potential $\mathbf{A}$. For this case, the scalar potential Φ_s has to be included in Schrödinger's equation, in addition to Φ_a. The corresponding time rate of change of Φ_s divided by ω_0 should be much less than the potential Φ_s itself in magnitude, as the natural frequency ω_0 is so high. Therefore, the term $\mathbf{p}\cdot\mathbf{A}/m_0$ is not expected to have an appreciable physical consequence even if it does not vanish.

In what follows, we derive the corresponding evolution equation for the interaction from the local-ether wave equation. Consider a hydrogen-like atom which is moving at a low velocity $\mathbf{v}_a$ in the local-ether frame. It is expected that the electric scalar potential Φ_a due to the nucleus will comove with the atom, as the propagation within the atom can be neglected. Accordingly, the potential is stationary in the atom frame with respect to which the nucleus of the atom is stationary, while it is moving in the local-ether frame. That is, based on Galilean transformations, while the potential is given simply by $\Phi(\mathbf{r})$ with $\mathbf{r}$ being referred to the atom frame, it is given by $\Phi(\mathbf{r}-\mathbf{v}_a t)$ with $\mathbf{r}$ being referred to the local-ether frame.

The average value of the velocity of the electron bound in the moving atom should be identical to the atom velocity $\mathbf{v}_a$; otherwise, the electron tends to escape the atom. Thus, as seen from (4.10), the spatial distribution of Ψ of the electron bound in the moving atom is expected to additionally incorporate the space harmonic $e^{i\mathbf{k}\cdot\mathbf{r}}$, where the propagation vector $\mathbf{k}$ is related to the atom velocity by $\hbar\mathbf{k} = m_0\mathbf{v}_a$ and the position vector $\mathbf{r}$ is referred to the local-ether frame (for a proof, see Chapter 6). Then the Laplacian becomes

$$\nabla^2\Psi(\mathbf{r},t) = e^{i\mathbf{k}\cdot\mathbf{r}}\left\{\nabla^2\tilde{\psi}(\mathbf{r},t) + i2\mathbf{k}\cdot\nabla\tilde{\psi}(\mathbf{r},t) - k^2\tilde{\psi}(\mathbf{r},t)\right\}, \quad (4.43)$$

where $\Psi(\mathbf{r},t) = \tilde{\psi}(\mathbf{r},t)e^{i\mathbf{k}\cdot\mathbf{r}}$. The term associated with k^2 can be neglected, as the atom speed v_a is supposed to be low.

For such a wave, the local-ether wave equation (4.17) becomes

$$\left\{\nabla^2 - \frac{1}{c^2}\frac{\partial^2}{\partial t^2}\right\}\tilde{\psi}(\mathbf{r},t) = \frac{\omega_0^2}{c^2}\tilde{\psi} + \frac{2\omega_0}{\hbar c^2}q\Phi(1+U_k)\tilde{\psi} - i2\mathbf{k}\cdot\nabla\tilde{\psi}, \quad (4.44)$$

where the augmentation operator U_k for the wavefunction $\tilde{\psi}$ associated with the factored-out space harmonic $e^{i\mathbf{k}\cdot\mathbf{r}}$ is defined as

$$U_k = \frac{1}{2c^2}\left(\frac{\mathbf{p}}{m_0} + \frac{\hbar\mathbf{k}}{m_0} - \mathbf{v}_s\right)^2. \quad (4.45)$$

Then, by introducing the reduced wavefunction ψ which is now related to $\tilde{\psi}$ as $\tilde{\psi}(\mathbf{r},t) = \psi(\mathbf{r},t)e^{-i\omega_0 t}$, the local-ether wave equation can be approximated by the first-order time evolution equation

$$\frac{\partial}{\partial t}\psi(\mathbf{r},t) = i\frac{c^2}{2\omega_0}\nabla^2\psi - i\frac{1}{\hbar}q\Phi(\mathbf{r}-\mathbf{v}_a t)(1+U_k)\psi - \frac{c^2}{\omega_0}\mathbf{k}\cdot\nabla\psi. \quad (4.46)$$

We then go on to rearrange the evolution equation to express it in the atom frame.

It is noted that the last term in the preceding equation can be written as $-\mathbf{v}_a\cdot\nabla\psi$, since the propagation vector is related to the atom velocity. Further, by using the Galilean transformation again, we have $\partial\psi/\partial t + \mathbf{v}_a\cdot\nabla\psi = (\partial\psi/\partial t)_a$, where the two time derivatives are referred to the local-ether and the atom frame, and hence are taken under constant $\mathbf{r}$ and $(\mathbf{r}-\mathbf{v}_a t)$, respectively, as $\mathbf{r}$ is referred to the local-ether frame.

Thereby, the time evolution equation for the electron bound in the moving atom becomes a more compact form when observed in the atom frame. That is,

$$i\hbar\frac{\partial}{\partial t}\psi(\mathbf{r},t) = -\frac{\hbar^2}{2m_0}\nabla^2\psi(\mathbf{r},t) + q\Phi(\mathbf{r})(1+U_k)\psi(\mathbf{r},t), \quad (4.47)$$

where the position vector $\mathbf{r}$ and hence the time derivative are referred to the atom frame, instead of the local-ether frame.

For the interaction case, the electric scalar potential experienced by the electron can be expected to be $\Phi = \Phi_a + \Phi_s + \Phi_m$, where Φ_a is due to the nucleus of the atom, Φ_s to the mobile charged particles forming the current in the external source of radiation, and Φ_m to the matrix in this source which is supposed to be neutralized. Further, suppose that the source is stationary with respect to the atom ($\mathbf{v}_m = \mathbf{v}_a$). Thus the Doppler frequency shift is not involved. As the mobile charged particles drift at a given velocity $\mathbf{v}_{sm}$ with respect to the matrix and hence to the atom, the augmentation operator U_k then becomes $(\mathbf{p}/m_0 - \mathbf{v}_{sm})^2/2c^2$ for Φ_s. Meanwhile, it becomes $(\mathbf{p}/m_0)^2/2c^2$ for Φ_m.

Thus, even under the complete neutralization $\Phi_s = -\Phi_m$, the action term due to the external source does not vanish and is given by

$$(\Phi_s + \Phi_m)(1+U_k) = -\frac{1}{m_0}\mathbf{A}\cdot\mathbf{p} + \frac{1}{2}\mathbf{A}\cdot\mathbf{v}_{sm}, \quad (4.48)$$

where

$$\mathbf{A} = \frac{1}{c^2}\mathbf{v}_{sm}\Phi_s. \quad (4.49)$$

As seen from (4.39), this vector potential in turn just represents the one due to the neutralized source of radiation, in which the mobile particles drift at a given velocity $\mathbf{v}_{sm}$.

Thereby, for the interaction with the radiation from a neutralized and stationary source, the atom-frame evolution equation becomes

$$i\hbar\frac{\partial}{\partial t}\psi(\mathbf{r},t) = \frac{1}{2m_0}\mathbf{p}^2\psi(\mathbf{r},t) + q\Phi_a(\mathbf{r})\psi(\mathbf{r},t) - \frac{q}{m_0}\mathbf{A}\cdot\mathbf{p}\psi + \frac{q}{2}\mathbf{A}\cdot\mathbf{v}_{sm}\psi, \tag{4.50}$$

where the augmentation operator connected to the potential Φ_a is omitted as its influence on the quantum states has negligible effect in dealing with the interaction. It is noted that the evolution equation as well as the potentials is independent of the motion of the atom, whenever the equation is observed in the atom frame and the corresponding Sagnac-effect deviation associated with the propagation of the potentials is omitted.

The preceding atom-frame evolution equation then looks like Schrödinger's equation (4.42), except the last term and the reference frame. The last term in the preceding equation is of the second order of v_{sm}/c and is very weak as the drift speed v_{sm} is very low, while its counterpart in Schrödinger's equation is of the second order of $q\mathbf{A}$. Based on (4.49) it is seen that the latter is even smaller in magnitude than the former by a factor of $|q\Phi_s|/m_0c^2$ which in turn is much less than unity. This quadratic term is commonly ignored in analysis [99, 81] and no quantitative measurements are reported, to our knowledge. Anyway, the second-order interaction may provide a means to test the local-ether wave equation, especially when the drift speed can be high.

Besides, one fundamental difference is that the position vector, the time derivative, the potential Φ_a, and the drift velocity are referred specifically to the atom frame. In the perturbation treatment of interaction, the wavefunctions of the unperturbed system with the interaction term being dropped out can be used to evaluate the effect of a small interaction, as to be discussed in Chapter 5. In common practice, the unperturbed wavefunctions are usually taken from the solutions of Schrödinger's equation with a *stationary* potential Φ_a. In doing so, one has actually adopted the atom frame tacitly. The calculation based on the unperturbed wavefunctions in another frame could yield the same result, but is expected to be more difficult.

Therefore, based on the atom-frame evolution equation (4.50), **the modified equation is substantially identical to Schrödinger's equation, if the latter is observed in the atom frame** as done tacitly in common practice. In other words, Schrödinger's equation for the interaction has some hidden restrictions. That is, the potentials are weak, the atom speed is low, the drift speed is very low, the source generating the acting potential is electrically neutralized and is stationary with respect to the atom, and the reference frame is actually the atom frame. However, these conditions are so common as to be ignored easily.

It is noted that while the evolution equation (4.50) is referred to the atom frame, the atom velocity is not involved individually in it. Suppose the atom together with the external source is stationary in a laboratory frame. Then the quantum effects of interaction derived from the local-ether wave equation can be independent of the laboratory velocity and hence comply with Galilean relativity, in spite of the various restrictions on reference frames encountered. However, this is owing to the approximation that the Sagnac-effect deviation and the k^2 term in (4.43) are omitted. When this second-order term is retained and the restriction to low atom speed is removed, it will be shown in Chapter 6 that the local-ether wave equation leads to the speed-dependent angular frequency and wavelength of a matter wave and to the speed-dependent mass of the associated particle. Further, as a consequence of the mass variation, it leads to the speed-dependence of quantum energies in an atom. The associated formulas are identical to the postulates of de Broglie and the Lorentz mass-variation law, except that the particle speed is referred specifically to the local-ether frame. Thus Galilean relativity breaks down.

4.8 Summary

Based on the local-ether wave equation incorporating a natural frequency and the electric scalar potential, the electrostatic force in conjunction with the inertial mass of the effector particle is derived from a quantum-mechanical approach by evaluating the acceleration. It is found that the inertial mass of a low-speed particle is just the natural frequency of the associated matter wave, aside from a scaling factor. This frequency-mass relation unveils that the physical origin of inertial mass is a temporal variation of matter wave.

Further, the local-ether wave equation is refined by connecting the electric scalar potential with the augmentation operator which in turn is associated with the momentum operator and the source velocity. The position vectors, the time derivative, the source velocity, and the propagation velocity of the potential are referred specifically to the local-ether frame. As a consequence, the derived electromagnetic force remains unchanged when observed in different frames in uniform motion of translation, as expected intuitively.

Under the ordinary conditions of weak potential and low particle speed, the local-ether wave equation leads to a first-order time evolution equation. It is shown from the evolution equation that the electromagnetic force exerted on an effector can be given in terms of the augmented potentials which in turn originate from the electric scalar potential and incorporate the velocity difference between the effector and source particles. Thereby, the local-ether wave equation provides a quantum foundation for the electromagnetic force law based on the augmented potentials, which in turn leads to the modifications of the Lorentz force law under the common low-speed condition where the source particles drift very slowly with respect to the matrix.

The evolution equation then represents modifications of Schrödinger's equation complying with Galilean transformations and the local-ether propagation model. The fundamental modification is that the position vector and the time derivative are referred specifically to the local-ether frame. Moreover, the role of the vector potential in Schrödinger's equation is replaced by the augmentation operator connected with the electric scalar potential. This makes the evolution equation look quite different from Schrödinger's equation. Nevertheless, for the interaction of atoms with electromagnetic radiation, these two equations become identical, except a very small term of second-order interaction. Precisely, this identity holds under some hidden restrictions, in addition to the weak-potential and low-speed conditions. That is, the source of radiation is neutralized and stationary with respect to the atom and the adopted reference frame is actually the atom frame. Commonly, these conditions have been assumed tacitly. The discrepancy in the second-order interaction provides a means to test the local-ether wave equation.

Chapter 5

Unified Quantum Theory of Electromagnetic and Gravitational Forces

In Chapter 4, based on the local-ether wave equation incorporating a natural frequency and the electric scalar potential, the electromagnetic force together with the inertial mass has been derived. In this Chapter, by incorporating the gravitational potential into the local-ether wave equation, the gravitational force together with the gravitational mass is also derived. Thereby, a unified quantum theory of electromagnetic and gravitational forces in conjunction with the origin and the identity of inertial and gravitational mass is presented. Meanwhile, for a particle bound in an atom, the gravitational potential is found to cause a decrease in the energy of each quantum state of the associated matter wave. The corresponding gravitation-dependence of the transition frequency is in accord with the experiments demonstrating the gravitational redshift. The local-ether wave equation also leads to the gravitation-dependence of the propagation speed of electromagnetic wave, which in turn leads to the deflection of light by the Sun and the increment of echo time in the interplanetary radar. Thereby, based on the wave equation complying with Galilean transformations, alternative interpretations of the evidence supporting the general theory of relativity are provided. However, the derived gravitational redshift originates from a quantum nature of the involved atoms and the gravitation-dependence can be different for different transitions. This discrepancy then provides a means to test the local-ether wave equation.

5.1 Gravitational Effects

The action of gravity is ubiquitous in everyday life. Gravitation also governs the motions of celestial bodies. It has been well known for a long time that a celestial body contributes to gravitation. More recently, it is known from astronomical observations that a huge celestial body like the Sun affects the propagation direction and the propagation speed of electromagnetic wave. It has been found that a light beam from a remote star tends to deflect toward the Sun as the beam passes by it. Moreover, by sending a microwave radar signal to a planet and back, it has been found that the echo delay time tends to increase as the transmission path is close to the Sun.

A celestial body also affects the frequency of electromagnetic wave. When a wave is radiated from a source located closer to such a body, the observed frequency tends to shift to a lower value, as demonstrated in the experiments cited to test the gravitational redshift. The deflection of light by the Sun, the increment of echo time in the interplanetary radar, and the gravitational redshift are commonly attributed to consequences of the general theory of relativity [3, 55]. It is known that the general relativity invokes the space-time curvature associated with the length contraction and the time dilation supposed to be caused by a gravitational field [3, 55].

We have presented in Chapter 1 the local-ether model of propagation of electromagnetic wave. It is supposed that electromagnetic wave propagates via a medium like the ether. However, the ether is not universal. Specifically, it is supposed that in the region under a sufficient influence of the gravitation due to the Earth, the Sun, or another celestial body, there forms a local ether which as well as the associated gravitational potential moves with the respective body. Thereby, for earthbound or interplanetary waves, the propagation is referred specifically to a geocentric or a heliocentric inertial frame, respectively. This local-ether model has been adopted to account for the effects of earth's motions in a wide variety of propagation phenomena, particularly the Sagnac pseudorange correction in the global positioning system and the echo time in the interplanetary radar.

Further, as discussed in Chapter 4, the matter wave associated with charged particles has been supposed to follow the local-ether propagation model and be governed by a wave equation incorporating a natural frequency and the electric scalar potential. From the local-ether wave equation, a first-order time evolution equation similar to Schrödinger's equation is derived. From the electrostatic force derived from this evolution equation, it has been found that the rest mass of a particle is just the natural frequency, aside from a scaling factor. That is, the inertial mass of a particle under the influence of the electric scalar potential originates from the natural frequency and hence from the temporal variation of the associated matter wave. Furthermore, the local-ether wave equation is refined by connecting the electric scalar potential with the augmentation operator which in turn is derived from the Laplace operator. Thereby, the corresponding evolution equation leads to the electromagnetic force law based on the augmented potentials, which in turn reduces to the Lorentz force law under some ordinary conditions.

In this Chapter the local-ether wave equation is refined by connecting the d'Alembert operator with the gravitational potential. The corresponding first-order time evolution equation will be derived. By following the procedure in deriving Ehrenfest's theorem in quantum mechanics, the velocity and then the acceleration of a particle under the influence of the gravitational and the electric scalar potential will be derived. Then we explore the quantum origins of the gravitational force and the gravitational mass, along with those of the electromagnetic force and the inertial mass. Thereby, based on the local-ether wave equation incorporating the gravitational and the electric scalar potential, a unified quantum theory of gravitational and electromagnetic forces is presented.

Moreover, the local-ether wave equation indicates that the gravitational potential tends to affect the energies of quantum states of the matter wave bound in an atom. The gravitational potential and its spatial variation also tend to affect the speed and direction of electromagnetic wave propagating in space. Thus we explore the gravitational effects concerning the frequency shift, light deflection, and echo-time increment. Thereby, we present entirely different interpretations of the evidence supporting the general relativity without invoking any particular space-time transformation. Meanwhile, based on the gravitation-dependent quantum effect, we point out the differences between the local-ether theory and the general relativity.

5.2 Local-Ether Wave Equation with Gravitational Potential

In Chapter 4, based on the local-ether model of wave propagation, we have presented a wave equation incorporating the natural frequency ω_0 and the electric scalar potential Φ. Quantitatively, it is postulated that the matter wave Ψ associated with a particle of charge q is governed by the nonhomogeneous wave equation proposed to be

$$\left\{\nabla^2 - \frac{1}{c^2}\frac{\partial^2}{\partial t^2}\right\}\Psi(\mathbf{r},t) = \frac{\omega_0^2}{c^2}\left\{1 + \frac{2}{\hbar\omega_0}q\Phi(\mathbf{r},t)\right\}\Psi(\mathbf{r},t), \qquad (5.1)$$

where the natural frequency ω_0 as well as the charge q is an inherent constant of the effector particle, $\hbar$ is Planck's constant divided by 2π, and the position vector $\mathbf{r}$ and the time derivative are referred to the associated local-ether frame.

If the scalar potential Φ and the spatial rate of variation of Ψ are weak, the temporal variation of Ψ is close to the one of the time harmonic $e^{-i\omega_0 t}$ and thus $\Psi(\mathbf{r},t) = \psi(\mathbf{r},t)e^{-i\omega_0 t}$, where ψ has a weak temporal variation. Then it has been shown that the wave equation reduces to the first-order time evolution equation in terms of the reduced wavefunction ψ

$$i\hbar\frac{\partial}{\partial t}\psi(\mathbf{r},t) = -\frac{\hbar^2}{2m_0}\nabla^2\psi(\mathbf{r},t) + q\Phi\psi(\mathbf{r},t), \qquad (5.2)$$

where the rest mass m_0 is related to the natural frequency ω_0 in the familiar form

$$m_0 = \frac{\hbar}{c^2}\omega_0. \qquad (5.3)$$

This evolution equation looks like the famous Schrödinger's equation with the potential energy $q\Phi$, aside from the reference frame.

Then, for a particle moving slowly in the local-ether frame, it has been shown from this evolution equation that its acceleration is given by

$$\mathbf{a} = -\frac{1}{m_0}q\nabla\Phi. \qquad (5.4)$$

This acceleration formula is in accord with the electrostatic force in conjunction with Newton's second law of motion with the inertial mass being the rest mass of the effector. The frequency-mass relation (5.3) then connects the physical origin of the inertial mass to the temporal variation of the wavefunction Ψ. Further, in Chapter 4, the whole electromagnetic force has been derived from the local-ether wave equation with a refinement whereby the electric scalar potential is made to connect with the augmentation operator which in turn is derived from the Laplace operator.

In the presence of a gravitational potential, it is supposed that the d'Alembert operator in the local-ether wave equation (5.1) also needs a refinement, so that more phenomena can be accounted for. As in classical gravitation, it is supposed that each celestial body is associated with a gravitational potential Φ_g. In a positive definite form, it is given by

$$\Phi_g(\mathbf{r}) = \frac{GM}{r}, \tag{5.5}$$

where G is the gravitational constant and r $(= |\mathbf{r}|)$ is the radial distance from the center of the celestial body of mass M. The position vector $\mathbf{r}$ here as well as that in the local-ether wave equation is supposed to be referred to the local-ether frame associated with the body. Thus the gravitational potential along with the associated local ether moves with the celestial body. The gravitational potential associated with the Earth or the Sun is then stationary in a geocentric or a heliocentric inertial frame, respectively.

Under the influence of the gravitational potential due to a celestial body, it is postulated that the local-ether wave equation is refined in such a way that the d'Alembert operator is connected with the gravitational potential Φ_g. That is,

$$\left\{\frac{1}{n_g}\nabla^2 - \frac{n_g}{c^2}\frac{\partial^2}{\partial t^2}\right\}\Psi(\mathbf{r},t) = \frac{\omega_0^2}{c^2}\left\{1 + \frac{2}{\hbar\omega_0}q\Phi(\mathbf{r},t)\right\}\Psi(\mathbf{r},t), \tag{5.6}$$

where the *gravitational index* n_g is defined as

$$n_g(\mathbf{r}) \overset{\triangle}{=} 1 + \frac{2}{c^2}\Phi_g(\mathbf{r}) \tag{5.7}$$

and the aforementioned augmentation operator is neglected for simplicity. Again, the time derivative as well as the position vector $\mathbf{r}$ is referred specifically to the local-ether frame. The gravitational potential is supposed to be weak so that its value divided by c^2 is much less than unity. Thus the gravitational index is just slightly greater than unity and the gravitational modifications in the wave equation are quite small in magnitude. This local-ether wave equation incorporating the gravitational potential made its debut in [123, 121, 135].

From the preceding wave equation, it is seen that the gravitational potential tends to affect the spatial and temporal variations of matter wave and to modify the influence of the electric scalar potential. For electromagnetic wave with a zero natural frequency, it is seen immediately that the gravitational potential tends to affect the wave propagation by slightly decreasing the propagation speed from c to c/n_g.

5.3 Derivation of Unified Quantum Theory

Based on the local-ether wave equation in the presence of both the gravitational and the electric scalar potential, a unified quantum theory of gravitational and electromagnetic forces can be presented. The local-ether wave equation for an effector particle of natural frequency ω_0 and charge q can be written as

$$\left\{\left(1-\frac{2\Phi_g}{c^2}\right)^2\nabla^2-\frac{1}{c^2}\frac{\partial^2}{\partial t^2}\right\}\Psi(\mathbf{r},t)=\frac{\omega_0^2}{c^2}\left(1+\frac{2q\Phi}{\hbar\omega_0}\right)\left(1-\frac{2\Phi_g}{c^2}\right)\Psi(\mathbf{r},t), \tag{5.8}$$

as the gravitational potential is supposed to be weak. When the electric scalar potential and the spatial rate of variation of the wavefunction are weak as well, the temporal variation of Ψ is close to that of the harmonic $e^{-i\omega_0 t}$. Again, one has $\Psi(\mathbf{r},t)=\psi(\mathbf{r},t)e^{-i\omega_0 t}$, where ψ still has a weak temporal variation.

By expanding the second derivative $\partial^2\Psi/\partial t^2$ and then omitting the second derivative $\partial^2\psi/\partial t^2$ as done in Chapter 4, the local-ether wave equation can be approximated by the first-order time evolution equation in terms of the reduced wavefunction ψ. That is,

$$i2\omega_0\frac{\partial}{\partial t}\psi(\mathbf{r},t)=-c^2\nabla^2\psi(\mathbf{r},t)+2\frac{\omega_0}{\hbar}q\Phi\psi(\mathbf{r},t)-2\frac{\omega_0^2}{c^2}\Phi_g\psi(\mathbf{r},t), \tag{5.9}$$

where the two major terms with $\omega_0^2\psi$ cancel out and the higher-order terms with the gravitational potential connected to the Laplace operator or to the electric scalar potential are also omitted, since Φ_g, Φ, and $\nabla^2\psi$ are supposed to be weak.

In terms of the rest mass m_0 defined from the natural frequency ω_0, the time evolution equation takes the form

$$i\hbar\frac{\partial}{\partial t}\psi(\mathbf{r},t)=-\frac{\hbar^2}{2m_0}\nabla^2\psi(\mathbf{r},t)+q\Phi\psi(\mathbf{r},t)-m_0\Phi_g\psi(\mathbf{r},t), \tag{5.10}$$

where the position vector $\mathbf{r}$ and the time derivative are referred to the local-ether frame. This evolution equation looks like Schrödinger's equation with the potential energy being given by $(q\Phi-m_0\Phi_g)$, aside from the difference in reference frames. It is noticed that in dealing with the gravitation-induced matter-wave interference, a Hamiltonian that incorporates a similar gravitational energy has been assumed in the literature [106].

As in deriving Ehrenfest's theorem in quantum mechanics, the velocity $\mathbf{v}$ of an effector particle is supposed to be given by the time derivative of the expectation value of the position operator $\mathbf{r}$. That is, $\mathbf{v} = d\langle \mathbf{r} \rangle /dt$, where the position vector represented by the operator $\mathbf{r}$ and hence the velocity $\mathbf{v}$ are referred to the local-ether frame, and the expectation value of an operator O is evaluated in terms of the reduced wavefunction ψ as $\langle O \rangle = \int \psi^* O \psi dv$.

By expanding the just-mentioned time derivative in the local-ether frame according to the evolution equation (5.10) as done in Chapter 4, it is straightforward to show that the effector velocity is given in a familiar form

$$\mathbf{v} = -\frac{i\hbar}{m_0} \langle \nabla \rangle . \tag{5.11}$$

It is seen that the effector velocity with respect to the local-ether frame is proportional to the expectation value of the momentum operator $-i\hbar\nabla$ and hence is associated with the spatial rate of variation of the wavefunction. Thus the evolution equation (5.10) is valid only for a low-speed particle of which the matter wave has a weak spatial variation as assumed earlier.

Further, the acceleration of the effector particle can be given in terms of the time derivative of expectation value of the momentum operator. That is, $\mathbf{a} = (-i\hbar/m_0)d\langle \nabla \rangle /dt$. By expanding this time derivative in the local-ether frame according to the evolution equation (5.10) again, the acceleration is then given by

$$\mathbf{a} = -\frac{q}{m_0}\nabla\Phi + \nabla\Phi_g. \tag{5.12}$$

Physically, this relation implies that the spatial variations of the potentials Φ and Φ_g contribute to the change in the spatial variation of the wavefunction ψ and then to the change in the effector velocity. The contribution due to the potential Φ is inversely proportional to m_0, while the one due to the potential Φ_g is independent of m_0. The acceleration of gravity due to the gravitational potential is then given by $\mathbf{g} = \nabla\Phi_g$. Since $\mathbf{g}$ is independent of the rest mass, different kinds of particles then tend to have an identical gravitational acceleration at a given position.

Based on Newton's second law of motion with the inertial mass m_0, the force exerted on the particle moving slowly under the electric scalar and the gravitational potential is then given by

$$\mathbf{F} = -q\nabla\Phi + m_0\nabla\Phi_g. \tag{5.13}$$

It is noted that due to the gradient and the similar spatial distributions of the potentials, both the electrostatic and the gravitational force follow the inverse square law.

Further, it is noted that as the acceleration of gravity is independent of mass, the gravitational force is then linearly proportional to the inertial mass. As a consequence, the gravitational mass associated with this gravitational force is just equal to the inertial mass associated with the influence of the electric scalar potential. Thus the gravitational mass as well as the inertial mass of an effector particle stationary or moving slowly in the local-ether frame is just the natural frequency of the associated matter wave, aside from the common scaling factor $(\hbar/c^2)$. That is, the gravitational and inertial mass of a particle originates from the natural frequency and hence is a consequence of wave motion of the associated matter wave.

It has been shown in Chapter 4 that the rest mass m_0 is also the inertial mass of a low-speed effector under the electric induction force and the magnetic force, which together with the electrostatic force form the whole electromagnetic force. Thereby, the local-ether wave equation incorporating the natural frequency, the gravitational potential, the electric scalar potential, and the augmentation operator leads to **a unified quantum theory of electromagnetic and gravitational forces in conjunction with the origin and the identity of inertial and gravitational mass.**

It is known that based on the general relativity, the gravitation should be modified slightly by a factor of $(1 + 3v^2/c^2)$, where v is the linear speed due to the orbital motion of an object under the gravitation [55]. This slight modification leads to the precession of the perihelion which in turn has been demonstrated in Mercury and other planets. It is noted that in planetary motions the squared normalized speed v^2/c^2 is of the order of Φ_g/c^2. Thus the precession could be accounted for, if the wave equation is refined to the second order of Φ_g/c^2.

5.4 Reexamination of Evidence for General Relativity

The gravitation considered in the preceding section demonstrates the gravitational effect on the matter wave of an unbound effector. In this section, we discuss the gravitational effect on the matter wave of an effector bound in an atom or a molecule. Moreover, we discuss the gravitational effects on electromagnetic wave of which the natural frequency is zero. Thereby, based on the local-ether wave equation complying with Galilean transformations, we present alternative interpretations of the gravitational redshift, the gravitational deflection of light, and the increments of propagation time and radar echo time, which are commonly cited as supporting evidence for the general theory of relativity. The cases with electromagnetic wave are simpler and are discussed first.

5.4.1 Increments of propagation time and radar echo time

The case with a zero natural frequency corresponds to the propagation of electromagnetic wave, for which the local-ether wave equation becomes a simpler form

$$\left\{ \nabla^2 - \frac{n_g^2}{c^2} \frac{\partial^2}{\partial t^2} \right\} \Psi(\mathbf{r}, t) = 0. \tag{5.14}$$

As a consequence, under the influence of the gravitational potential Φ_g, electromagnetic wave propagates at a speed c/n_g with respect to the associated local ether. The stronger the gravitational potential is, the slower the propagation speed becomes. The region with a gravitational potential can be treated as a dielectric medium of which the refractive index is given by n_g, and hence the speed of light decreases from c to c/n_g in this region.

An obvious consequence of the gravitation-dependent propagation speed is the increment of propagation time for an electromagnetic wave passing by a celestial body. The increment of propagation time per unit propagation length is given by $(n_g - 1)/c$. The total increment of the one-way propagation time is then given by the path integral of the term $(n_g - 1)/c$ along the propagation range from the source at the instant of wave emission to the receiver at the instant of reception, with respect to the local-ether frame associated with the body. As in the classical propagation model, the reference frame and the reference instants for the source and the receiver are particularly specified. Otherwise, the analysis of wave propagation is not unequivocal.

Consider the earthbound propagation from a transmitter (say, aboard an earth's satellite) to a receiver (say, on or near the ground). Arrange the geocentric inertial frame so that the wave propagates along the x direction. Thus the increment of the one-way propagation time due to the gravitational potential of the Earth is given by the path integral

$$\triangle\tau_g = \frac{-1}{c} \int_{x_s}^{x_e} (n_g - 1)\, dx = \frac{2GM}{c^3} \int_{x_e}^{x_s} \frac{dx}{\sqrt{b^2 + x^2}}, \tag{5.15}$$

where x_s is the x coordinate of the transmitter at the instant of wave emission, x_e is that of the receiver at the instant of reception ($0 < x_e < x_s$), b ($= \sqrt{r^2 - x^2}$) is the vertical distance from earth's center to the propagation range in the geocentric frame, and M is the mass of the Earth.

A direct integration yields

$$\triangle\tau_g = \frac{2GM}{c^3} \ln \frac{r_s + x_s}{r_e + x_e}, \tag{5.16}$$

where r_s ($= \sqrt{b^2 + x_s^2}$) and r_e ($= \sqrt{b^2 + x_e^2}$) are the geocentric distance of the transmitter at the instant of emission and of the receiver at the instant of reception, respectively. The increment can be rewritten as

$$\triangle\tau_g = \frac{2GM}{c^3} \ln \frac{r_e - x_e}{r_s - x_s} = \frac{2GM}{c^3} \ln \frac{r_s + r_e + R}{r_s + r_e - R}, \tag{5.17}$$

where the propagation range $R = x_s - x_e$.

This propagation-time increment is exactly identical to the one given in [89] for the global positioning system (GPS), including the reference frame and the reference instants, which in turn is derived based on the general relativity. The increment $\triangle\tau_g$ depends on the positions of the GPS satellite and the receiver and a typical value is 50 ps [122]. This one-way increment has been proposed as a subtle GPS pseudorange correction due to earth's gravitational potential, in addition to the correction due to the Sagnac effect [89].

Next, reconsider the interplanetary radar discussed in Chapter 1, where a high-power microwave is transmitted from an earth-based antenna, passes by the Sun, reaches and is reflected back from the target planet, passes the Sun again, and then is received by the earth-based antenna. For the interplanetary propagation, the main local-ether frame switches to a heliocentric inertial frame. Based on the preceding one-way formula, one immediately obtains that the increment of the round-trip propagation time in the interplanetary radar due to the gravitational potential of the Sun is given by the sum

$$\triangle\tau_g = \frac{2GM}{c^3} \left\{ \ln \frac{r_{Ef} + r_P + R_f}{r_{Ef} + r_P - R_f} + \ln \frac{r_{Eb} + r_P + R_b}{r_{Eb} + r_P - R_b} \right\}, \tag{5.18}$$

where r_{Ef} and r_{Eb} are the heliocentric distances of the earth-based transceiver at the instants of emission and reception, respectively, r_P

is that of the target planet-based reflector at the instant of reflection, R_f and R_b are respectively the forward and the backward propagation range with respect to a heliocentric frame, and M is the mass of the Sun.

The difference between r_{Ef} and r_{Eb} and the one between R_f and R_b are small and thus can be neglected in calculating this small gravitational effect. If the positions of the transceiver and the reflector are referred to an appropriate common instant (say, the instant of emission or reception), then the increment of the interplanetary radar echo time becomes

$$\triangle\tau_g = \frac{4GM}{c^3} \ln \frac{r_E + r_P + R_{EP}}{r_E + r_P - R_{EP}}, \tag{5.19}$$

where r_E and r_P are the heliocentric distance of the transceiver and of the reflector, respectively, and R_{EP} is the separation distance between the transceiver and reflector, all at the reference instant.

The preceding echo-time increment $\triangle\tau_g$ is identical to the one reported in the literature [101, 96, 5] without clearly specifying the reference instants, which in turn has been demonstrated by sending microwaves to Venus, Mercury, Mars, and to spacecrafts when the Sun is near the transmission path. For the earth-Venus radar, the increment $\triangle\tau_g$ can be larger than 200 μs.

5.4.2 Gravitational deflection of light

Another consequence of the gravitation-dependent propagation speed is the beam deflection. Based on the simple propagation model with the gravitational index n_g, the deflection of a light beam passing by a celestial body can be ascribed to the spatial variation of the index n_g. It is noticed that in a region closer to the surface of a body, the index becomes larger. The gravitational deflection of light is somewhat similar to the total internal reflection of a short wave from the ionosphere of which the refractive index is decreasing with increasing altitude. As the index of the medium is slowly varying and is close to unity, it is known that the deflection over a differential propagation range dl is equal to dl times the partial derivative of the index in a transverse direction (for a derivation, see Appendix C). The total deflection angle α is then given by the integral of the derivative of the index over the entire propagation range.

Consider the deflection of a light beam passing by a celestial body of radius R_S. In a slowly-varying medium, the deflection is quite small and hence the beam propagates substantially along a straight line. Arrange the associated local-ether frame so that the beam propagates in the x direction along the line at $y = 0$ and $z = b$, where the parameter b ($\geq R_S$) is the vertical distance from the center of the celestial body to the propagation range. Thus the index n_g varies transversely in the z direction along the line and the deflection $d\alpha$ toward the $-z$ direction over a differential propagation range dx is related to the directional derivative of the index by

$$\frac{d\alpha}{dx} = -\frac{\partial n_g}{\partial z}, \tag{5.20}$$

where we have made use of the gravitational index n_g being quite close to unity.

For simplicity, the straight propagation range is further supposed to extend to infinity. Thus the total deflection angle α over the entire propagation range can be given by the path integral of the derivative of the index

$$\alpha = -\int_{-\infty}^{\infty} \frac{\partial n_g(x,z)}{\partial z} dx = \frac{2GM}{c^2} \int_{-\infty}^{\infty} \frac{b}{(b^2 + x^2)^{3/2}} dx, \tag{5.21}$$

where the propagation range and the geometry of calculation are referred specifically to the associated local-ether frame. A direct integration yields

$$\alpha = \frac{4GM}{c^2 b}. \tag{5.22}$$

This result is identical to that derived from the general relativity [55], even though no space-time curvature is invoked here.

It is noticed that the preceding path integral is like the one of a directional derivative of a spatially-varying speed, which was pioneered by Einstein in exploring his general theory of relativity [25], aside from a quantitative discrepancy in the gravitation-dependence of the speed of light. Without specifying the reference frame explicitly, a similar approach with the spatially-varying speed has been treated as a pedagogic aid in the literature [3].

It is seen that the deflection depends on the parameter b. The minimum value of b is the radius, which occurs for a ray grazing the celestial body. The corresponding maximum deflection is then given by

$$\alpha_{\max} = \frac{4GM}{c^2 R_S}. \tag{5.23}$$

For a ray grazing the Sun, $\alpha_{\max} = 4.9 \times 10^{-4}$ deg. It is well known that the deflection of optical waves passing by the Sun was first confirmed in 1919, shortly after the introduction of the general theory of relativity. Moreover, the deflection of microwaves passing by the Sun has been demonstrated with high precision by using an interferometer with a baseline of as long as 35 km [32].

5.4.3 Gravitational redshift

Then we go on to consider another gravitational effect on matter wave. For a particle of natural frequency ω_0 and charge q under the influence of the gravitational potential Φ_g and the electric scalar potential Φ, the local-ether wave equation (5.6) can be rewritten as

$$-\frac{\partial^2}{\partial t^2}\Psi(\mathbf{r},t) = \frac{1}{n_g}\omega_0^2\Psi(\mathbf{r},t) + 2\frac{1}{n_g}\frac{\omega_0}{\hbar}q\Phi\Psi(\mathbf{r},t) - \frac{c^2}{n_g^2}\nabla^2\Psi(\mathbf{r},t). \quad (5.24)$$

Consider the matter wave bound in an atom or a molecule. It is known that the wave then exists in one of some particular quantum states in which the temporal variation of Ψ can follow the one of a pure time harmonic $e^{-i\omega t}$, as a consequence of resonance. That is, $\Psi(\mathbf{r},t) = \psi(\mathbf{r})e^{-i\omega t}$, where ψ is independent of time when observed in the local-ether frame. This independence holds for atoms stationary in the local-ether frame and is a useful approximation for slowly-moving atoms as to be discussed in Chapter 6.

For such a wave, a manipulation associated with the expectation value renders the preceding wave equation into the algebraic relation

$$\omega^2 = \frac{1}{n_g}\omega_0^2\left\{1 + \frac{2}{\hbar\omega_0}\langle q\Phi\rangle - \frac{1}{n_g}\frac{c^2}{\omega_0^2}\left\langle\nabla^2\right\rangle\right\}, \qquad (5.25)$$

where the wavefunction is supposed to be normalized so that $\int \psi^*\psi dv = 1$. As seen from the preceding relation, the angular frequency ω of a bound matter wave depends on the gravitational potential and can be easily determined if the reduced wavefunction is known.

However, it is noted that the reduced wavefunction ψ itself as well as the angular frequency ω generally depends on the gravitational potential. On the other hand, it is also noted as in Chapter 4 that the operators ∇^2 and Φ involved in the wave equation are self-adjoint whereby $\int \psi_a^*(O\psi_b)dv = \int (O\psi_a)^*\psi_b dv$ for any such operator O. Thus the perturbation method can be applied and then the angular frequency can be evaluated correctly by using an approximate reduced wavefunction.

Treat the gravitational potential as a perturbation and let the solution of the case where the gravitational potential is absent be the unperturbed wavefunction. By virtue of the self-adjoint property, it can be shown that all the terms associated with the correction of the wavefunction cancel out collectively to the first order of the perturbation, where the correction denotes the difference between the true reduced wavefunction and the unperturbed one. Thereby, the angular frequency evaluated by substituting the unperturbed wavefunction into the expectation values in (5.25) is correct to the first order of the gravitational potential, which in turn has been supposed to be weak in all the cases discussed.

It is noted that the major component of the angular frequency ω is the natural frequency ω_0. Moreover, ω depends on the spatial distribution and variation of the wavefunction, on the electric scalar potential, and on the gravitational potential. If the scalar potential Φ and the spatial variation of Ψ are omitted, then $\omega = \omega_0/\sqrt{n_g}$. Thereby, we have

$$\hbar\omega = m_0 c^2 - m_0 \Phi_g, \tag{5.26}$$

where $\hbar\omega$ is known as the quantum energy of the matter wave, $m_0 c^2$ the rest energy of the particle, and $-m_0\Phi_g$ the gravitational energy (for a positive definite Φ_g). It is seen that when a matter wave is placed in a gravitational potential, its quantum energy decreases by an amount of $m_0\Phi_g$ or by a fractional amount of Φ_g/c^2.

The presence of the electric scalar potential or of a spatial variation of the wavefunction tends to introduce a change in the temporal variation of the wavefunction Ψ and thus modify the quantum energy. Consider the ordinary case where the scalar potential Φ and the spatial variation of Ψ are weak. Thus, by evaluating the square root of the right-hand side of the frequency formula (5.25) with the binomial expansion to the first order, the quantum energy $\hbar\omega$ of the matter wave bound in an atom can be given by

$$\hbar\omega = \frac{1}{\sqrt{n_g}}\hbar\omega_0 + \frac{1}{\sqrt{n_g}}\langle q\Phi\rangle - \frac{1}{n_g^{3/2}}\frac{\hbar^2}{2m_0}\left\langle\nabla^2\right\rangle. \tag{5.27}$$

It is noted that the dependence of the last term on the gravitational index is different from the one of the other terms, as a consequence of the gravitational refinement connected to the Laplace operator. An expansion to the second order and the consequence will be discussed in Chapter 6.

As in quantum mechanics, the frequency of the light emitted from or absorbed by an atom or a molecule is supposed to be given by the transition frequency which in turn is associated with the difference in energy between the two quantum states participating in the transition. It is noted that the major term of the quantum energy, namely, the first term on the right-hand side of the preceding energy formula is identical in different states and hence its effect on the transition frequency cancels out. Thus the state transition frequency is due to the minor energy terms.

Consider the case where the term associated with the Laplacian can be omitted. Thus under the influence of a gravitational potential, the transition frequency f decreases as

$$f = f_0 \left(1 - \frac{\Phi_g}{c^2}\right), \tag{5.28}$$

where f_0 is the transition frequency of the atom in the absence of the gravitational potential. It is seen that when the atom is placed in a gravitational potential, the transition frequency decreases by a fractional amount of Φ_g/c^2.

Quantitatively, the frequency f_0 is given by

$$f_0 = \frac{1}{2\pi\hbar} \int (\psi_a^* q\Phi\psi_a - \psi_b^* q\Phi\psi_b) dv, \tag{5.29}$$

where ψ_a and ψ_b are associated with the two quantum states participating in the transition in the absence of the gravitational potential. The wavefunctions of these states can be determined from the evolution equation (5.2) or from the Helmholtz equation to be given in Chapter 6.

In the gravitational redshift experiments discussed later, the spatial distributions of the wavefunctions involved in the state transition are identical and the transition is associated with the wavefunctions of different spin states. Thus the Laplacian term indeed does not contribute to the transition frequency. Although the spin cannot be treated by the local-ether wave equation, it is expected that the spin-spin interaction will lead to an energy formula similar to (5.27), except for a suitable modification in the energy term $\hbar\omega_0$ or $\langle q\Phi \rangle$. Thus the gravitation-dependence of the transition frequency is identical to the one given in (5.28). Moreover, a similar formula can be given for the case where the augmentation operator is taken into account by suitably refining the potential Φ.

Thereby, between two positions of different radial distances r_H and r_L from the center of the celestial body, the difference in the gravitation-dependent transition frequency is given by

$$\triangle f = -f_0 \frac{MG}{c^2} \left(\frac{1}{r_H} - \frac{1}{r_L} \right) = f_0 \frac{g}{c^2} (r_H - r_L), \qquad (5.30)$$

where the acceleration of gravity $g = MG/r_H r_L$. It is seen that the fractional shift of the transition frequency is then given by the acceleration times the difference in altitude, aside from a factor of c^{-2}. This gravitation-induced frequency shift apparently agrees with the gravitational redshift (or blueshift) based on the general relativity, which in turn has been tested in the Pound-Rebka experiment and some others discussed later.

However, there is one fundamental difference in the physical origin of the gravitation-induced frequency shift. In the famous Pound-Rebka experiment, a gamma ray is radiated from a source and then received by an absorber of the identical kind of atom but placed at a different altitude [93]. In the ideal case where the minor effects are absent, the radiation will be resonantly absorbed, as the transition frequencies of the source and absorber atoms are identical. However, the gravitational effect tends to incur a frequency shift from the resonant absorption. This shift can manifest itself as an increase in the scattering of gamma rays from the absorber, which in turn can be measured by using a counter. To restore the resonant absorption, a subtle relative motion between the source and the absorber is purposely introduced. Thereby, the resultant Doppler frequency shift can be used to compensate for the gravitation-induced frequency shift and thus to measure it.

Based on the local-ether wave equation, the frequency of electromagnetic wave propagating in space remains unchanged during the entire propagation, regardless of the spatial variation of the gravitational potential. This argument applies to the Pound-Rebka experiment, the gravitational deflection, and the interplanetary radar. The gravitational redshift given by (5.30) is a consequence of the quantum effect that the state transition frequency of an atom tends to shift downward as it is placed in a gravitational potential. This downshift in turn is due to the gravitational effect with which the energy of each quantum state of the matter wave bound in an atom is lowered proportionally. In other words, the frequency downshift due to the gravitational effect (as well as the one due to the effect dependent on the speed of the atom to be discussed in Chapter 6) originates from an intrinsic quantum property of the matter wave bound in the emitting or absorbing atom, rather than from a kinematical feature of electromagnetic wave propagating in space.

The frequency formula (5.28) also implies that the frequency of the light emitted from atoms of a certain kind placed on a star depends on the gravitational potential and hence on the mass of the star. In other words, the gravitation-induced frequency shift leads to the consequence that the atomic spectrum from a heavy star tends to shift downward. However, the stellar frequency shift tends to incorporate the Doppler frequency shift due to the relative motion between the star and the Earth, as discussed in Chapter 1. If the Doppler effect can be determined separately, the gravitation-induced downshift of the stellar spectrum then provides a means to test the local-ether wave equation.

5.4.4 Spatial distributions of wavefunctions in gravitational redshift experiments

The earthbound experiments that provide high-precision measurement data supporting the gravitational redshift quantitatively include the Pound-Rebka experiment [93], GPS [69, 8], the Hafele-Keating experiment [39], and the spacecraft microwave link by Vessot *et al.* [113, 112, 56].

In the Pound-Rebka experiment, the gamma ray involved in the resonant absorption is due to a recoilless transition known as the Mössbauer effect and hence has a quite narrow linewidth. According to the local-ether wave equation, the gravitational redshift is ascribed to the dependence of the Mössbauer transition on the gravitational potential. In the other experiments, the tick rates of cesium atomic clocks or hydrogen masers placed at different altitudes are compared. These rates are due to state transition and the associated gravitational redshift can also be ascribed to the gravitation-dependence of transition frequency, which together with the accompanying dependence on the atom speed will be investigated in Chapter 6.

In these various experiments, the emitting and the absorbing atoms are expected to have a common feature in the spatial distributions of the involved wavefunctions. The state transition in the atomic clock is known to be associated with the hyperfine splitting which in turn is due to the spin-spin interaction between the electron and nucleon [69]. Thus the wavefunctions participating in the transition between different spin states are identical in their spatial distribution.

As to the Mössbauer effect, the 14.4-keV gamma ray from iron atoms employed in the Pound-Rebka experiment has been suggested to be associated with the hyperfine transition between the nuclear excited and ground states of different spins [92]. Anyway, since the nuclear space is quite small, a change of the spatial distribution of the accommodated matter wave is unlikely. Otherwise, the transition frequency should be much higher than the frequency of this gamma ray.

Thus the local-ether wave equation is actually in accord with these gravitational redshift experiments which provide evidence supporting the general relativity. However, the derived gravitational redshift originates from quantum properties of the matter wave bound in an atom and its dependence on gravity can be more complicated when some other kind of state transition is involved. The simple relationship between the frequency shift and the acceleration of gravity given by (5.30) is expected to hold only for the transition between states of different spins. For the transition where the involved wavefunctions have different spatial distributions, it is predicted that the transition frequency can have two components with different dependences on the gravitational potential. Thus the ratio of the fractional shift in transition frequency to the difference in altitude times g/c^2 can differ from unity. This transition-dependence of the gravitational redshift then provides another means to test the local-ether wave equation.

5.5 Summary

The local-ether wave equation incorporating a natural frequency and the electric scalar potential is refined by connecting the d'Alembert operator with the gravitational potential. Then the wave equation leads to a first-order time evolution equation which is similar to Schrödinger's equation with the potential energy being given by the electric scalar and the gravitational potential, aside from the difference that the position vector and the time derivative are referred specifically to the local-ether frame. Then, by following the quantum-mechanical procedure in deriving Ehrenfest's theorem, the evolution equation leads to the well-known fact that the gravitational and the electrostatic force are proportional to the gradients of the gravitational and the electric scalar potential, respectively. Besides, as the effector particle moves slowly with respect to the local-ether frame, it is found that the gravitational mass associated with the gravitational force as well as the inertial mass with the electromagnetic force is equal to the natural frequency of the associated matter wave, aside from a common scaling factor. Thereby, the local-ether wave equation leads to a unified quantum theory of electromagnetic and gravitational forces in conjunction with the identity and the wave-motion origin of inertial and gravitational mass.

For the matter wave bound in an atom or a molecule, the gravitational potential incorporated in the local-ether wave equation leads to a decrease in the energy of each quantum state. For the state transition where the spatial distributions of the wavefunctions of the two involved quantum states are identical, the fractional shift of the transition frequency is simply proportional to the acceleration of gravity times the difference in altitude. For this transition, the gravitation-induced frequency downshift based on the local-ether wave equation can agree with the gravitational redshift based on the general relativity. Meanwhile, for electromagnetic wave with a zero natural frequency, the gravitational potential leads to the consequence that the wave propagates at a slightly reduced speed with respect to the local-ether frame. Thus the propagation time or the radar echo time tends to increase as the wave passes by a celestial body. Besides, owing to the spatial variation of the propagation speed, the wave tends to deflect toward the region where the gravitational potential is stronger. Thereby, the local-ether wave equation accounts for the gravitational redshift, the increment of echo time in the interplanetary radar, and the deflection of light by the Sun, which are commonly cited as important evidence supporting the general theory of relativity.

The other phenomenon that supports the general relativity is the precession of the perihelion, which is associated with a small modification term of gravitation. This term is of the second order and could be accounted for if the gravitational refinement of the wave equation is extended from the present first order to the second order of the gravitational potential. However, a fundamental difference between the local-ether theory and the general relativity is that the gravitational redshift is ascribed to a quantum origin of the matter wave bound in the emitting or absorbing atom. For the state transition where the wavefunctions of the two involved quantum states have different spatial distributions, the dependence of the frequency shift on gravity is expected to be of a more complicated form. Another consequence is that the frequency of the light emitted from atoms placed on a star depends on the gravitational potential and hence on the mass of the star. The quantum origin and the transition-dependence of the gravitation-induced frequency shift together with the gravitation-dependence of the stellar spectrum then provide a means to test the local-ether wave equation.

Chapter 6

Speed-Dependent Mass and Quantum Energy

The east-west directional anisotropy in clock rate observed in the Hafele-Keating experiment with circumnavigation atomic clocks is commonly ascribed to the special relativity. In this Chapter, based on the local-ether wave equation, an entirely different interpretation of this anisotropy is presented by showing that the clock-rate variation can originate from intrinsic quantum properties of atoms. For a particle in a moving atom, the local-ether wave equation leads to a first-order time evolution equation similar to Schrödinger's equation. However, the time derivative connects with a speed-dependent factor similar to that in the Lorentz mass-variation law. Consequently, the quantum energy, the transition frequency, and hence the atomic clock rate decrease with the atom speed by this speed-dependent mass-variation factor. According to the local-ether model, the speed in this factor is referred specifically to a geocentric or heliocentric inertial frame for earthbound or interplanetary atoms, respectively. It is shown that this restriction on the reference frame is actually in accord with the various experimental results, namely, the anisotropy and the clock-rate difference in the Hafele-Keating experiment, the synchronism and the clock-rate adjustment in the global positioning system, and the spatial isotropy in the Hughes-Drever experiment. And the switching of the unique reference frame is in accord with the frequency-shift formulas adopted individually in an earthbound and an interplanetary spacecraft microwave link. Meanwhile, the local-ether model predicts a constant deviation in frequency shift from the calculated result reported in an interplanetary link. This discrepancy then provides a means to test the local-ether wave equation.

6.1 Speed-Dependence of Atomic Clock Rate

From the experiment with circumnavigation atomic clocks by Hafele and Keating in 1971, it has been verified that the tick rate of an atomic clock depends on its speed. In this experiment, cesium atomic clocks were flown around the Earth, first east- and then westward. After each trip, the circumnavigation clocks were compared with another clock stationary on the ground. It was found that the atomic clocks flying westward tick at a faster rate than the geostationary one, while the ones flying eastward tick at a slower rate [39, 49].

Further, it has been inferred that when the atomic clock is moving at a speed v, its tick rate slows down with a factor of $\sqrt{1 - v^2/c^2}$, where c is the speed of light. This factor is just the inverse of the Lorentz mass-variation factor which in turn has been demonstrated in the charge-mass ratio of high-energy electrons in the famous Bucherer's experiment [26]. This speed-dependent variation of clock rate is commonly attributed to a consequence of the special relativity, namely, the time dilation between two frames in uniform relative motion of translation.

However, it is noticed that in the numerical calculation which agrees with the experiment, both the linear speed due to earth's rotation and the ground speed of the clock are taken into account [39, 49]. On the other hand, the linear speed due to earth's orbital motion around the Sun is not. Thus the speed that determines the clock rate is actually referred specifically to an earth-centered inertial (ECI) frame. And it is just this unique frame that can unequivocally account for the asymmetry in clock rate between the east- and the west-flying atomic clocks. This frame is also adopted in analyzing the speed-dependent clock rate for the atomic clocks in the global positioning system (GPS) [8] and for the hydrogen masers in an earthbound spacecraft microwave link [113]. Meanwhile, in an interplanetary spacecraft microwave link, a heliocentric inertial frame is adopted instead [61].

This feature of uniqueness and switchability of the reference frame is a reminiscence of the local-ether model of wave propagation presented in Chapter 1. That is, electromagnetic wave can be viewed as propagating via a medium like the ether. However, the ether is not universal. It is supposed that in the region under a sufficient influence of the gravitation due to the Earth, the Sun, or another celestial body, there forms a local ether which in turn moves with the gravitational potential of the respective body. Each individual local ether is finite in extent and may be wholly immersed in another local ether of larger extent. For earthbound waves, the medium is the earth local ether which is stationary in an ECI frame, while the sun local ether for interplanetary waves is stationary in a heliocentric inertial frame. Consequently, the phenomena associated only with earthbound waves can depend on earth's rotation but are entirely independent of earth's orbital motion around the Sun or whatever, while those with interplanetary waves depend on the orbital motion around the Sun as well as on the rotation. This local-ether model has been adopted to account for a wide variety of propagation phenomena, particularly the GPS Sagnac correction, the time comparison via an intercontinental microwave link, and the interplanetary radar echo time.

Further, in Chapters 4 and 5, matter wave is supposed to follow the local-ether model and then be governed by a wave equation. Under the condition of low particle speed, the local-ether wave equation leads to a first-order time evolution equation which is similar to the famous Schrödinger's equation. From the evolution equation, the velocity and the acceleration of a particle can be derived in a quantum-mechanical approach. Under the influence of the electric scalar and the gravitational potential, a unified quantum theory of electromagnetic and gravitational forces in conjunction with the identity of inertial and gravitational mass has been derived.

In this Chapter, the restriction imposed on particle speed is removed. Then the particle velocity is derived from the corresponding evolution equation. Further, from the dispersion of matter wave, the speed-dependent mass is derived without invoking any particular space-time transformation. Thereafter, we explore the effects of the speed-dependent mass and of the gravitational potential on the energies of quantum states of the matter wave in a moving atom. Then the speed- and gravitation-dependent transition frequency is used to account for the clock rates in the Hafele-Keating experiment, GPS, an earthbound and an interplanetary spacecraft microwave link, and in the Hughes-Drever experiment in a consistent way.

6.2 Evolution Equation beyond Low-Speed Condition

It is supposed that matter wave associated with particles follows the local-ether propagation model. In the presence of the electrical scalar potential Φ due to charged particles and of the gravitational potential Φ_g due to a celestial body, the matter wave Ψ associated with a particle of charge q and natural frequency ω_0 is supposed to be governed, as in Chapter 5, by the local-ether wave equation

$$\left\{\frac{1}{n_g}\nabla^2 - \frac{n_g}{c^2}\frac{\partial^2}{\partial t^2}\right\}\Psi(\mathbf{r},t) = \frac{\omega_0^2}{c^2}\left\{1 + \frac{2}{\hbar\omega_0}q\Phi(\mathbf{r},t)\right\}\Psi(\mathbf{r},t), \quad (6.1)$$

where the gravitational index $n_g = 1 + 2\Phi_g/c^2$, $\Phi_g(\mathbf{r}) = GM/r$, G is the gravitational constant, and r $(= |\mathbf{r}|)$ is the radial distance from the center of the celestial body of mass M. The position vector $\mathbf{r}$ and the time derivative in this wave equation are referred specifically to the local-ether frame associated with the celestial body, which is a geocentric or a heliocentric inertial frame for an earthbound or an interplanetary particle, respectively.

From the wave equation it is seen that if the potentials and the spatial variation of the wavefunction are weak, the wavefunction tends to oscillate at the natural frequency ω_0. Under the influence of the potentials, which are functions of space, the spatial variation of the wavefunction tends to change. Then its temporal variation will increase accordingly.

Consider the case where the spatial distribution of Ψ incorporates a space harmonic $e^{i\mathbf{k}\cdot\mathbf{r}}$, where $\mathbf{k}$ is known as the propagation vector and $\mathbf{r}$ is still referred to the local-ether frame. Thus the wavefunction can be given by $\Psi(\mathbf{r},t) = \tilde{\psi}(\mathbf{r},t)e^{i\mathbf{k}\cdot\mathbf{r}}$ and then its Laplacian becomes

$$\nabla^2\Psi(\mathbf{r},t) = e^{i\mathbf{k}\cdot\mathbf{r}}\left\{\nabla^2\tilde{\psi}(\mathbf{r},t) + i2\mathbf{k}\cdot\nabla\tilde{\psi}(\mathbf{r},t) - k^2\tilde{\psi}(\mathbf{r},t)\right\}. \quad (6.2)$$

If k is small, the term associated with k^2 can be neglected, as done in Chapter 4. However, this restriction on k is removed here.

For such a wave, the local-ether wave equation becomes

$$\left\{\nabla^2 - \frac{1}{c^2}\frac{\partial^2}{\partial t^2}\right\}\tilde{\psi}(\mathbf{r},t) = \frac{\omega^2}{c^2}\tilde{\psi}(\mathbf{r},t) + \frac{2\omega_0}{\hbar c^2}q\Phi\tilde{\psi}(\mathbf{r},t) - i2\mathbf{k}\cdot\nabla\tilde{\psi}(\mathbf{r},t), \quad (6.3)$$

where the gravitational potential is omitted for simplicity and its effect will be considered later. It is of essence to note that the angular frequency ω in the preceding wave equation combines the natural frequency ω_0 and the propagation constant k as

$$\omega^2 = \omega_0^2 + c^2k^2. \quad (6.4)$$

By virtue of the natural frequency, the relationship between ω and k becomes nonlinear and hence the preceding formula represents a dispersion relation for the matter wave.

The spatial variation of $\tilde{\psi}$ can be weak, if the spatial distribution of Ψ is close to the space harmonic $e^{i\mathbf{k}\cdot\mathbf{r}}$. Further, if the potential Φ is weak as well, the temporal variation of $\tilde{\psi}$ or Ψ can be expected to be close to the one of the time harmonic $e^{-i\omega t}$. Thus the wavefunction can be given by $\tilde{\psi}(\mathbf{r},t) = \psi(\mathbf{r},t)e^{-i\omega t}$ and then its second time derivative becomes

$$\frac{\partial^2}{\partial t^2}\tilde{\psi}(\mathbf{r},t) = e^{-i\omega t}\left\{\frac{\partial^2}{\partial t^2}\psi(\mathbf{r},t) - i2\omega\frac{\partial}{\partial t}\psi(\mathbf{r},t) - \omega^2\psi(\mathbf{r},t)\right\}. \quad (6.5)$$

As the temporal variation of ψ is relatively weak, the second time derivative $\partial^2\psi/\partial t^2$ can be neglected as done in Chapters 4 and 5.

Thereby, the local-ether wave equation can be approximated by the first-order time evolution equation in terms of ψ. That is,

$$\frac{\partial}{\partial t}\psi(\mathbf{r},t) = i\frac{c^2}{2\omega}\nabla^2\psi(\mathbf{r},t) - i\frac{\omega_0}{\hbar\omega}q\Phi\psi(\mathbf{r},t) - \frac{c^2}{\omega}\mathbf{k}\cdot\nabla\psi(\mathbf{r},t), \quad (6.6)$$

where the major term $(\omega/c)^2\tilde{\psi}$ in the wave equation has been cancelled out. If k is zero, the preceding evolution equation reduces to (4.4) or (6.11) reproduced later. This restriction on k has been shown in Chapter 4 to correspond to the situation that the particle speed is low. By allowing the propagation vector $\mathbf{k}$ to be arbitrary, the low-speed condition is then removed. Thus the preceding evolution equation remains valid beyond this condition.

The wavefunctions Ψ and ψ are related to each other by

$$\Psi(\mathbf{r},t) = \psi(\mathbf{r},t)e^{i\mathbf{k}\cdot\mathbf{r}}e^{-i\omega t}. \quad (6.7)$$

The wavefunction ψ can have a greatly reduced variation in space and time, as the wavefunction Ψ is close to the space-time harmonic $e^{i\mathbf{k}\cdot\mathbf{r}}e^{-i\omega t}$. For such a harmonic-like wavefunction, its space-time behavior is close to the one of the factored-out harmonic. Thus the associated matter wave is dispersive as represented by (6.4).

According to the wave equation or the evolution equation in conjunction with the associated initial conditions, the wavefunction Ψ or the reduced wavefunction ψ as a function of space and time can be determined. The evolution equation is simpler as the involved time derivative is only of the first order. Further, some important formulas representing physical quantities, such as velocity and acceleration, of the associated particle can be derived from the evolution equation, as in the treatment based on Schrödinger's equation. However, the applicability of the evolution equation is more restricted, since the propagation vector **k** together with the angular frequency ω of the factored-out harmonic should be suitably chosen, if possible, to keep the omitted derivative $\partial^2\psi/\partial t^2$ negligibly small and thus to maintain the accuracy.

6.3 Particle Velocity and Speed-Dependent Mass

As in quantum mechanics, the physical quantity represented by an operator O is supposed to be given by the expectation value of the operator evaluated in terms of the reduced wavefunction ψ as $\langle O\rangle = \int \psi^* O\psi dv$. Thus the velocity of a particle is given by the time derivative of the expectation value of the position operator, that is, $\mathbf{v} = d\langle \mathbf{r}\rangle/dt$, where the position vector represented by the operator $\mathbf{r}$ and hence the velocity $\mathbf{v}$ are referred to the local-ether frame.

By expanding the just-mentioned time derivative in the local-ether frame according to the evolution equation (6.6), it can be shown that the particle velocity is given by

$$\mathbf{v} = -i\frac{c^2}{\omega}\langle\nabla\rangle + \frac{c^2}{\omega}\mathbf{k}, \tag{6.8}$$

where the wavefunction is supposed to be normalized.

Introduce the expectation value $\langle O\rangle_\Psi$ $(= \int \Psi^* O\Psi dv)$ which is evaluated in terms of the wavefunction Ψ, instead of the reduced wavefunction ψ. It is easy to see that the expectation value $\langle\nabla\rangle_\Psi$ in Ψ is related to the expectation value $\langle\nabla\rangle$ in ψ by

$$\langle\nabla\rangle_\Psi = \langle\nabla\rangle + i\mathbf{k}. \tag{6.9}$$

Thereby, the velocity can be given alternatively by

$$\mathbf{v} = -i\frac{c^2}{\omega}\langle\nabla\rangle_\Psi. \tag{6.10}$$

It is noted that for a harmonic-like matter wave, the particle velocity with respect to the local-ether frame is proportional to the spatial rate of change of the wavefunction Ψ (rather than of the reduced wavefunction ψ) and to the inverse of its temporal rate of change.

When the particle speed is low enough, the propagation vector **k** of the factored-out harmonic can be chosen to be zero and hence the angular frequency ω becomes the natural frequency ω_0. Thereby, the evolution equation for a slowly-moving particle reduces to

$$\frac{\partial}{\partial t}\psi(\mathbf{r},t) = i\frac{c^2}{2\omega_0}\nabla^2\psi(\mathbf{r},t) - i\frac{1}{\hbar}q\Phi\psi(\mathbf{r},t). \tag{6.11}$$

From this evolution equation, it has been shown in Chapter 4 that the acceleration of a low-speed particle under the influence of the electric scalar potential is given by

$$\mathbf{a} = -\frac{c^2}{\hbar\omega_0}q\nabla\Phi. \tag{6.12}$$

It is noted that the acceleration is inversely proportional to ω_0.

Then, from Newton's second law of motion and the electrostatic force $\mathbf{F} = -q\nabla\Phi$, it has been pointed out that the natural frequency ω_0 multiplied by the constant $(\hbar/c^2)$ is just the inertial mass of the effector particle under the low-speed condition. That is, the natural frequency ω_0 is related to the rest mass m_0 of the particle by

$$m_0 = \hbar\omega_0/c^2. \tag{6.13}$$

This simple frequency-mass relation then connects the physical origin of mass to wave motion.

When the spatial distribution of the wavefunction Ψ is quite close to the harmonic $e^{i\mathbf{k}\cdot\mathbf{r}}$, the expectation value $\langle\nabla\rangle$ approaches zero. On the other hand, for a bound particle with a real ψ, it is known $\langle\nabla\rangle = 0$. In either case, the velocity formula (6.8) reduces to a simpler form

$$\mathbf{k} = \frac{\omega}{c^2}\mathbf{v}. \tag{6.14}$$

This propagation vector-velocity relation is derived from the evolution equation with the low-speed condition being removed and hence is valid even when the particle speed is high. It is noted that the propagation vector $\mathbf{k}$ is linearly proportional to the velocity $\mathbf{v}$ with the angular frequency ω divided by c^2 as the proportionality.

Further, on substituting the preceding relation back into the dispersion relation (6.4), the angular frequency can be expressed in terms of the particle speed v as

$$\omega = \omega_0\frac{1}{\sqrt{1 - v^2/c^2}}, \tag{6.15}$$

where the speed v is referred to the local-ether frame. It is seen that the angular frequency is given by the natural frequency times the speed-dependent factor.

Based on this speed-dependent frequency and the frequency-mass relation (6.13), one is led to define the *speed-dependent mass* m in terms of the rest mass m_0 in the familiar form

$$m = m_0 \frac{1}{\sqrt{1 - v^2/c^2}}. \tag{6.16}$$

Then, in terms of the speed-dependent mass m, the angular frequency and the propagation vector associated with the wavefunction Ψ can be rewritten in the familiar forms

$$\hbar\omega = mc^2 \tag{6.17}$$

and

$$\hbar\mathbf{k} = m\mathbf{v}. \tag{6.18}$$

It is noted that the speed-dependence in the angular frequency and mass is a consequence of the dispersion of matter wave, and is derived without invoking any particular space-time transformation. Thus, based on the local-ether wave equation, the mass variation as well as the mass itself originates from wave motion.

It is noticed that the preceding three formulas for the speed-dependent mass, angular frequency, and propagation vector are just the Lorentz mass-variation law and the postulates of de Broglie for matter wave, if the reference frame of the particle velocity $\mathbf{v}$ is ignored. The speed-dependent mass was pioneered by Lorentz [71] and then by Einstein (in a somewhat different form) [24] by employing the Lorentz transformation of space and time. The corresponding speed-dependent wavelength has been demonstrated in the Davisson-Germer experiment and the Sagnac effect for matter wave. The issue of the reference frame and the effects of earth's motions associated with these earthbound experiments will be discussed in Chapter 8.

6.4 Speed-Dependent Quantum Energy

In terms of the speed-dependent mass m, the time evolution equation (6.6) governing the reduced wavefunction ψ can be rewritten as

$$i\hbar\frac{\partial}{\partial t}\psi(\mathbf{r},t) = -\frac{\hbar^2}{2m}\nabla^2\psi(\mathbf{r},t) + \frac{m_0}{m}q\Phi\psi(\mathbf{r},t) - i\frac{\hbar^2}{m}\mathbf{k}\cdot\nabla\psi(\mathbf{r},t), \tag{6.19}$$

where the position vector $\mathbf{r}$ and the time derivative are referred to the local-ether frame. It is noted that the whole term with Φ decreases with increasing mass as $(m_0/m)q\Phi$.

Consider a hydrogen-like atom which is moving at a velocity $\mathbf{v}_a$ with respect to the local-ether frame. The electric scalar potential Φ due to the nucleus tends to comove with the atom, as the propagation within the atom can be neglected. Accordingly, the potential can be stationary in the atom frame in which the nucleus of the atom is stationary, while it is moving in the local-ether frame. Under Galilean transformations, the potential moving with the atom can be written as $\Phi(\mathbf{r})$ or as $\Phi(\mathbf{r} - \mathbf{v}_a t)$, where the position vector $\mathbf{r}$ is referred to the atom or to the local-ether frame, respectively.

The average value of the velocity of a particle (electron or nucleon) bound in the moving atom should be identical to the atom velocity $\mathbf{v}_a$; otherwise, the particle tends to escape the atom. As seen from (6.8), it is assumed for the moment that the wavefunction Ψ of the particle bound in the moving atom additionally incorporates the space harmonic $e^{i\mathbf{k}_a\cdot\mathbf{r}}$ and hence the time harmonic $e^{-i\omega_a t}$, where $\mathbf{k}_a = m\mathbf{v}_a/\hbar$, $\omega_a = mc^2/\hbar$, $m = m_0/\sqrt{1 - v_a^2/c^2}$, and the position vector $\mathbf{r}$ is referred to the local-ether frame. If the reduced wavefunction has a weak second time derivative, it is then governed by the preceding evolution equation with $\mathbf{k}$ being replaced by $\mathbf{k}_a$. Moreover, the potential is given by $\Phi(\mathbf{r} - \mathbf{v}_a t)$.

We next go on to rearrange the evolution equation to express it in the atom frame, instead of the local-ether frame. Similar to the situation in Chapter 4, it is noted that the last term in (6.19) can be rewritten as $-i\hbar\mathbf{v}_a\cdot\nabla\psi$. From the Galilean transformation (I.16), one has $\partial\psi/\partial t + \mathbf{v}_a\cdot\nabla\psi = (\partial\psi/\partial t)_a$, where the two time derivatives are referred to the local-ether and the atom frame, and are understood to be taken under constant $\mathbf{r}$ and $(\mathbf{r} - \mathbf{v}_a t)$, respectively, as $\mathbf{r}$ is referred to the local-ether frame.

Thereby, for a particle bound in a moving atom, the time evolution equation in the atom frame becomes

$$i\hbar\frac{\partial}{\partial t}\psi(\mathbf{r},t) = -\frac{\hbar^2}{2m}\nabla^2\psi(\mathbf{r},t) + \frac{m_0}{m}q\Phi(\mathbf{r})\psi(\mathbf{r},t), \tag{6.20}$$

where the position vector $\mathbf{r}$ and hence the time derivative are referred to the atom frame, instead of the local-ether frame. It is seen that the mass connecting to the Laplacian is the speed-dependent mass, instead of the rest mass. Besides, the term with Φ incorporates an extra factor of m_0/m, inverse to the mass-variation factor.

It is noted that the preceding evolution equation as well as the potential is independent of the motion of the atom if the equation is observed in the atom frame and the mass variation is neglected. Thus the quantum effects derived from the evolution equation can comply with Galilean relativity, in spite of the restriction on reference frames. In common practice where Schrödinger's equation with a *stationary* potential is employed to deal with quantum effects in an atom, one has tacitly adopted the atom frame. Thus the preceding equation can be substantially identical to Schrödinger's equation.

As the matter wave is bound in an atom, the temporal variation of ψ can be purely time-harmonic when observed in the atom frame, as a consequence of resonance. That is, $\psi(\mathbf{r}, t) = \psi(\mathbf{r})e^{-i\omega_q t}$, where ω_q corresponds to the resonant frequency and the position vector $\mathbf{r}$ is referred to the atom frame. Then the sum $\hbar(\omega_a + \omega_q)$ represents the quantum energy of the matter wave bound in the atom. In order for the evolution equation itself to remain valid, it is required that $\omega_q \ll \omega_a$. For such a wave, the preceding atom-frame evolution equation becomes the time-independent Helmholtz equation

$$-\frac{\hbar^2}{2m_0}\nabla^2\psi(\mathbf{r}) + q\Phi(\mathbf{r})\psi(\mathbf{r}) = \frac{m}{m_0}\hbar\omega_q\psi(\mathbf{r}). \qquad (6.21)$$

This equation looks like the time-independent equation derived from (6.11) for an atom stationary in the local-ether frame, aside from the differences that the position vector $\mathbf{r}$ here is referred specifically to the atom frame and that the energy $\hbar\omega_q$ connects with the mass-variation factor m/m_0. It is seen that ψ is real for a real Φ.

It is of essence to note that the solutions for the eigenfunction ψ and the eigenvalue $\hbar\omega_q(m/m_0)$ of the preceding equation are independent of the atom speed v_a when observed in the atom frame. Accordingly, the wavefunction of a particle bound in the moving atom is given by $\Psi(\mathbf{r}, t) = \psi(\mathbf{r} - \mathbf{v}_a t)e^{i\mathbf{k}_a\cdot\mathbf{r}}e^{-i\omega_a t}e^{-i\omega_q t}$, where $\mathbf{r}$ is referred to the local-ether frame. Just as the earlier assumption, Ψ indeed incorporates the space harmonic $e^{i\mathbf{k}_a\cdot\mathbf{r}}$. And the velocity of the bound particle is indeed $\mathbf{v}_a$, as determined from (6.14) for a real ψ. Besides, as compared to those in a stationary atom, the minor energy $\hbar\omega_q$ of each quantum state in the moving atom decreases by the mass-variation factor, whereas the major energy $\hbar\omega_a$ increases by this factor.

It is known that the transition frequency is associated with the difference in energy between two involved quantum states. As the major energy $\hbar\omega_a$ is identical among all the states, its effect on this frequency cancels out. Thus the transition frequency f is determined by the quantum-state energy $\hbar\omega_q$ and then is inversely proportional to the speed-dependent mass m. Precisely, the transition frequency decreases with increasing atom speed by the mass-variation factor as

$$f = f_0\sqrt{1 - v_a^2/c^2}, \tag{6.22}$$

where the atom speed v_a is referred specifically to the local-ether frame, f_0 is the *rest transition frequency* of the atom when it is stationary in the local-ether frame, and the frequency is observed in the atom frame so that the Doppler effect due to the relative motion between the source and receiver is not involved.

Aside from the physical meaning and reference frame, a speed-dependent frequency of this form was first introduced by Fitzgerald, Lorentz, and Larmor before the advent of the special relativity [46], and was later derived by assuming the length contraction [54] or the time dilation [33]. According to the local-ether wave equation, the speed that determines the transition frequency of an earthbound atom is the atom speed with respect to a geocentric inertial frame. Meanwhile, for an atom on board an interplanetary spacecraft, the reference frame then switches to a heliocentric one.

6.5 Reexamination of Experiments with Atomic Clock Rate

The atomic clock rate is determined by the transition frequency between two quantum states in the atom. In the cesium atomic clock, vaporized atoms floating in a cavity are exposed to a microwave from a crystal oscillator. The output frequency of the oscillator is adjusted through a feedback loop until the resonant absorption by the atoms is achieved [69]. The state transition in the atomic clock is associated with a hyperfine interaction due to the spin which cannot be treated by the local-ether wave equation. However, it is expected that this interaction leads to an equation similar to (6.1) or (6.21), except for a suitable modification in the term $q\Phi$. Thus the transition frequency and the clock rate still decrease by the mass-variation factor. As in the ammonia maser to be discussed in Chapter 7, the motion of the cesium atoms with respect to the cavity leads to a second-order Doppler effect and a shift in the output frequency. This shift cancels out in the clock-rate comparison discussed here and thus this part of the atom motion is omitted.

Meanwhile, as the precision of the experiments to detect the speed-dependent effect is high, the accompanying gravitational effect often becomes significant and is also taken into account. Thereafter, the derived formula for the gravitation- and speed-dependent transition frequency is used in a consistent way to account for the phenomena associated with atomic clocks in the Hafele-Keating experiment, GPS, an earthbound and an interplanetary spacecraft microwave link, and in the Hughes-Drever experiment, which are commonly attributed to consequences of the general and the special relativity.

6.5.1 Gravitation- and speed-dependent transition frequency

To deal with the gravitational effect, we consider the wave equation, instead of the time evolution equation. Since the matter wave bound in a moving atom incorporates the local-ether space harmonic $e^{i\mathbf{k}_a\cdot\mathbf{r}}$, it can be given by $\Psi(\mathbf{r},t) = \psi(\mathbf{r}-\mathbf{v}_at)e^{i\mathbf{k}_a\cdot\mathbf{r}}e^{-i\omega t}$. Thus $\hbar\omega$ represents the quantum energy of the bound matter wave. A manipulation associated with the expectation value with a normalized ψ renders the local-ether wave equation (6.1) into the algebraic relation

$$\omega^2 = \frac{1}{n_g}\omega_0^2\left\{1 + \frac{2}{\hbar\omega_0}\langle q\Phi\rangle - \frac{1}{n_g}\frac{c^2}{\omega_0^2}\left\langle\nabla^2\right\rangle_\Psi\right\} + \left\langle(\mathbf{v}_a\cdot\nabla)^2\right\rangle, \quad (6.23)$$

where in expanding the second time derivative we have made use of the Galilean transformations (I.16) and (I.17), of $(\partial\psi/\partial t)_a = 0$, and of $\langle\nabla\rangle = 0$, as ψ is time-independent in the atom frame and is real. If $\mathbf{k}_a = 0$, this formula reduces to (5.25).

It can be shown that $\hbar\omega$ is identical to the aforementioned energy $\hbar(\omega_a + \omega_q)$, when the gravitational potential and the terms due to $\partial^2\psi/\partial t^2$ in (6.5) are omitted as in deriving (6.6). When the gravitational potential is weak, the perturbation method can be applied. Thereby, the angular frequency can be evaluated in terms of the unperturbed wavefunction in the absence of the gravitational potential, as discussed in Chapter 5. For this, ψ is determined from (6.21).

For the experiments to be discussed, it suffices to suppose that both the potential Φ and the spatial rate of change of Ψ as well as the potential Φ_g are weak. Then, by evaluating the square root of the right-hand side of the preceding frequency formula with the binomial expansion to the second order, the quantum energy $\hbar\omega$ of a matter wave bound in a moving atom can be given. That is,

$$\hbar\omega = \frac{1}{\sqrt{n_g}}\hbar\omega_0 + \frac{1}{\sqrt{n_g}}\langle q\Phi\rangle - \frac{1}{n_g^{3/2}}\frac{\hbar^2}{2m_0}\left\langle\nabla^2\right\rangle_\Psi + \frac{\hbar^2}{2m_0c^2}\left\langle(\mathbf{v}_a\cdot\nabla)^2\right\rangle$$

$$+\frac{\hbar^2}{2m_0^2c^2}\langle q\Phi\rangle\left\langle\nabla^2\right\rangle_\Psi - \frac{1}{2\hbar\omega_0}\langle q\Phi\rangle^2 - \frac{\hbar^4}{8m_0^3c^2}\left\langle\nabla^2\right\rangle_\Psi^2, \quad (6.24)$$

where the gravitational index involved in the last four minor terms is simply taken to be unity as the corresponding gravitational effects are relatively small. It is noted that $\langle \nabla^2 \rangle_\Psi = \langle \nabla^2 \rangle - k_a^2$, where we have made use of an expansion like (6.2) and of $\langle \nabla \rangle = 0$.

Consider the case of atomic clocks which are associated with the spin-spin interaction between wavefunctions of identical spatial distribution but of different spin states, as discussed in Chapter 5. Thus the state transition does not involve the del or the Laplace operator unless it connects to $q\Phi$. Then, by retaining only those terms associated with $q\Phi$, it is easy to show that for an atom moving slowly in a gravitational potential, the transition frequency f decreases as

$$f = f_0 \left(1 - \frac{v_a^2}{2c^2} - \frac{\Phi_g}{c^2} \right) + f_{ex}, \tag{6.25}$$

where f_0 is the transition frequency of the atom due to $\langle q\Phi \rangle$, and f_{ex} denotes the extra minor term of the order of c^{-2} which is due to $\langle q\Phi \rangle \langle \nabla^2 \rangle$ and $\langle q\Phi \rangle^2$ and is independent of the atom speed and of the gravitational potential.

As the atom speed v_a has been supposed to be much lower than c in deriving (6.24) with the binomial expansion, it is seen that the speed-dependence in the preceding frequency formula is in accord with (6.22) which incorporates the mass-variation factor. It is noted that according to the local-ether wave equation, the gravitation- and the atom speed-induced variation of transition frequency originate from a quantum nature of the bound matter wave.

Based on the perturbation method, the wavefunctions ψ involved in the calculation of the f_0 in the preceding formula can be those of the f_0 in (6.22), which in turn are solutions of the Helmholtz equation (6.21) where the gravitational potential is omitted. As these solutions ψ are found to be independent of the atom speed, f_0 then represents the rest transition frequency of the atom stationary with respect to the local-ether frame and in the absence of the gravitational potential. And the formula for f_0 is then identical to (5.29), where the effect of atom speed is omitted.

6.5.2 Clock-rate difference in Hafele-Keating experiment

Consider the clock rate of the cesium atomic clocks on board a circumnavigating aircraft in the Hafele-Keating experiment. According to the local-ether model, the speed in the mass-variation factor for earthbound atomic clocks is the speed of the clock referred specifically to an ECI frame, rather than to the ground or to an observer.

Thus this speed depends on earth's rotation and latitude, but is entirely independent of the orbital motion of the Earth around the Sun or whatever. When the aircraft is flying westward, the clock tends to have a lower speed with respect to an ECI frame than a geostationary one. Consequently, the atomic clock flying westward ticks at a faster rate than a geostationary one, whereas the one flying eastward ticks at a slower rate. Thereby, earth's rotation leads to an east-west directional anisotropy in the atomic clock rate.

Quantitatively, for the atomic clocks on board an aircraft flying at a ground speed v_f east- or westward, the speed of the clock that determines the tick rate is given by the sum $v_E + u_f$, where v_E is the speed of the ground due to earth's rotation and $u_f = v_f$ or $-v_f$ for the clocks flying east- or westward, respectively. Then, by taking both the speed- and the gravitation-dependent effect into account, the frequency formula (6.25) yields that the fractional difference in transition frequency between the flying and the geostationary atomic clock at an identical latitude is given by

$$\frac{\triangle f}{f_0} = -\frac{2v_E u_f + v_f^2}{2c^2} + \frac{GM}{c^2 R_E^2} h_a, \tag{6.26}$$

where M and R_E are the mass and the radius of the Earth, respectively, and h_a is the altitude of the aircraft from the ground.

In the Hafele-Keating experiment, based on the recorded flight data of aircraft ground speed, latitude, altitude, and of clock time, the difference in clock time between the flying and the geostationary clock was calculated by numerical integration for each circumnavigation trip in either direction. The formula adopted for calculation in [39] is identical to (6.26), even though it is based on the special and the general relativity. Thereby, the calculated clock-time difference for each circumnavigation trip east- or westbound is −40 or 275 ns, respectively, which in turn have been found to agree with the experimental results [39]. Thus, just with its restriction on the reference frame, the local-ether wave equation is actually in accord with the east-west directional anisotropy in atomic clock rate demonstrated in the Hafele-Keating experiment.

6.5.3 Clock-rate adjustment in GPS

As discussed in Chapter 1, GPS employs 24 half-synchronous satellites carrying highly precise and synchronized cesium and rubidium atomic clocks in nearly circular orbits [69]. It is known that the various GPS atomic clocks keep a high synchronism within a few ns among themselves over a long duration before daily routine clock correction [69]. As the orbits are nearly circular, the various GPS clocks move at nearly identical speeds with respect to an ECI frame. Therefore, the local-ether model is in accord with the high synchronism among the GPS atomic clocks. Further, to keep the GPS clocks synchronous with the clocks on the ground, the differences in the speed-dependent mass-variation and gravitational effects have been treated by purposely adjusting the GPS clock rate before the launch of satellites [69, 67].

According to classical mechanics, the various clocks in circular orbits of radius r_H move at an identical speed of $v_a = \sqrt{GM/r_H}$ with respect to an ECI frame, where M is the mass of the Earth. Meanwhile, the clock stationary on the ground has the speed v_E due to earth's rotation. This speed is much lower than that of the orbiting satellites. Thus the mass-variation effect tends to slow down the atomic clock rate after the launch. On the contrary, as the satellite is launched to an orbit with a weaker gravitational potential, the gravitational effect tends to speed up the clock rate. By taking both the speed- and the gravitation-induced variation into account, the frequency formula (6.25) yields that the fractional shift in transition frequency after the launch from the ground to the orbit is given by

$$\frac{\triangle f}{f_0} = \frac{1}{2c^2}\left(v_E^2 - v_a^2\right) + \frac{GM}{c^2}\left(\frac{1}{r_L} - \frac{1}{r_H}\right), \tag{6.27}$$

where r_L and r_H denote the geocentric distances of GPS satellites before and after the launch, respectively.

Quantitatively, by taking $r_H = 26,600$ km for the half-synchronous orbit and $GM/c^2 = 4.43$ mm, one has $v_a = 3870$ m/s. Then, by taking $r_L = 6380$ km for the ground and $v_E = 350$ m/s, the preceding formula yields that the fractional shift is 4.45×10^{-10}, to which the mass-variation and the gravitational effect contribute -8.3×10^{-11} and 5.28×10^{-10}, respectively. The speed v_E has a much smaller influence on the mass-variation effect and hence the given shift is substantially independent of the latitude. The given shift for the gravitational effect is also substantially independent of the altitude of the ground within a few km.

The GPS microwave L1 carrier is operated at a frequency of 1575.42 MHz, which is generated by multiplying the output frequency of the atomic clock at 10.23 MHz by a factor of 154 [34]. This carrier is then modulated by a series of digital data at a rate of 10.23 Mbit/s, which contain the codes for positioning discussed in

Chapter 1. Suppose that the received GPS data rate is designed to be 10.23 Mbit/s with respect to a reference clock (say, another atomic clock at sea level on the equator). Thus, according to the calculated fractional shift, the GPS clock rate has to be adjusted on the ground a little lower to 10.22999999545 ($= 10.23 \times (1 - 4.45 \times 10^{-10})$) MHz with respect to the reference clock. This calculated downshift agrees excellently with the practice of clock-rate adjustment in GPS [67]. If the clock-rate shift is not offset, it tends to incur a synchronism error of as large as 38 μs in one day.

It is noticed that the speed- and gravitation-induced frequency shifts derived from the local-ether wave equation are identical to those presented in [8] based on the special and the general relativity, respectively. However, the mechanism of frequency shift and its consequence are different. According to the local-ether wave equation, the frequency shifts due to the gravitational and mass-variation effects originate from an intrinsic quantum property of the matter wave bound in an atom, rather than from a kinematical feature of electromagnetic wave propagating in space.

Thus, after the launch to the orbit, the atomic clock rate increases slightly to 10.23 MHz. Thereafter, during the entire propagation from the satellite to the ground, the carrier frequency and the data rate remain fixed at 1575.42 MHz and 10.23 Mbit/s, respectively, where the Doppler effect due to the relative motion between the transmitter and receiver is omitted for simplicity (just as in the case with a geostationary satellite). Thus, over an interval of time, the total number of bits of data received on the ground or elsewhere tends to be identical to that transmitted from the satellite, as expected intuitively. On the other hand, an alternative interpretation of the clock-rate adjustment may be that the frequency of the microwave increases slightly to the designed one as it propagates from the satellite to the ground. However, this interpretation violates the causality, since it implies that the received number of bits tends to be greater than the transmitted one.

6.5.4 Frequency shifts in earthbound and interplanetary spacecraft microwave links

Consider the frequency-shift experiment employing a spacecraft microwave link, where a microwave is generated from a stable source on board a spacecraft, received by a ground station, and then compared to a reference signal from another stable source at the station. As the spacecraft moves at a high speed in a vast domain, the Doppler, the mass-variation, and the gravitational effect are incorporated in the frequency shift between the received and the reference signal.

Suppose the two microwave sources at the spacecraft and the ground station are of identical rest transition frequency f_0. According to the local-ether wave equation, the frequency shift due to the speed-dependent mass-variation effect alone is given by the corresponding difference between the two transition frequencies. That is,

$$\triangle f = f_0 \left(v_E^2 - v_{sc}^2 \right) / 2c^2, \tag{6.28}$$

where v_{sc} and v_E are respectively the speeds of the spacecraft and the ground station referred specifically to their respective local-ether frames. The speed v_{sc} is referred to a geocentric or a heliocentric inertial frame, depending on the location of the spacecraft being earthbound or interplanetary, respectively. Further, if the spacecraft comes close to or lands on a planet, the reference frame of the speed v_{sc} should switch to the local-ether frame associated with that planet. On the other hand, the speed v_E has nothing to do with the location of the spacecraft and is referred uniquely to an ECI frame both for the earthbound and for the extraterrestrial case.

Consider the spacecraft microwave link by Vessot *et al.*, where a microwave was generated from a stable hydrogen maser at 1.420 GHz on board a spacecraft and then was received and compared with another identical maser at a ground station [113, 112, 56]. By using microwave mixers, the frequency shift between the waves can be measured with high precision. The spacecraft was launched nearly vertically to the apogee at an altitude of 10,000 km, then fell down, and finally impacted upon ocean. It is noticed that the frequency shift given by the preceding formula with both v_{sc} and v_E being referred to an ECI frame actually agrees with the one presented in this earthbound spacecraft experiment [56], laying aside the frequency shifts due to the Doppler and gravitational effects.

On the other hand, for the interplanetary case, the local-ether model leads to the prediction that the speeds v_{sc} and v_E in (6.28) are referred to a heliocentric and a geocentric inertial frame, respectively. Consider the spacecraft microwave link by Krisher *et al.*, where the spacecraft ventured along an extraterrestrial trajectory with a flyby of Saturn [59] or of Venus [61]. A microwave was transmitted at about 2.3 GHz from the spacecraft and then was received and compared at an earth-based station, with a stable quartz oscillator on board and a hydrogen maser on the ground.

It is noticed that the frequency-shift formula presented in this interplanetary spacecraft experiment (laying aside the frequency shifts due to the Doppler and gravitational effects) looks like (6.28), except that both v_{sc} and v_E are in a heliocentric inertial frame [59, 61]. Thus there is a discrepancy in the role of earth's orbital motion for the speed v_E of the ground station. The linear speed due to earth's orbital motion around the Sun is about 30 km/s, which is much higher than the one due to earth's rotation. Thus the frequency shift predicted from the local-ether model deviates from the calculated result made in [59, 61] by a constant amount of about $\delta f = -11.5$ Hz as f_0 is close to 2.3 GHz. Meanwhile, it is reported that the frequency of the onboard quartz oscillator tends to shift due to aging. This frequency shift also contains a constant term with a coefficient determined empirically by the least-squares algorithm [61]. Thus it seems not appropriate to test the predicted constant deviation with the results of this experiment.

Anyway, according to the frequency shift of the form given by (6.28), the reference frame for the onboard clock has been shown from the earthbound and the interplanetary experiment to depend on the location of the spacecraft. In other words, the uniqueness and switchability of the reference frame, which is the fundamental feature of the local-ether model proposed in Chapter 1, is in accord with the frequency-shift formulas adopted individually in the earthbound and the interplanetary spacecraft microwave link. On the other hand, the determination of the reference frame for the ground clock in an interplanetary microwave link provides a means to test the local-ether wave equation.

6.5.5 Spatial isotropy in Hughes-Drever experiment

In the Hughes-Drever experiment, it has been found that the transition frequency of an atom or an ion is quite stable hour by hour and day by day, in spite of earth's rotational and orbital motions [41]. Similarly, the stability of the phase over a transmission path is also found in the fiber-link experiment [60] and in the Kennedy-Thorndike experiment [54] discussed in Chapter 1. This hourly and daily stability of frequency or phase is known as the spatial isotropy as the orientation and position of the Earth are changing in space.

According to the local-ether model, earth's orbital motion around the Sun is not involved in the speed v of an earthbound particle with respect to an ECI frame. Thus the quantum energy associated with an earthbound atom is entirely independent of the orbital motion. Further, the quantum energy can even be invariant under earth's rotation, if the speed v remains constant during the rotation. Such a *constant-speed condition* is met by a geostationary atom, by an atom moving at a fixed velocity with respect to the ground at a substantially fixed latitude, and by an atom moving in a circular orbit of earth's satellite.

For an atom satisfying the constant-speed condition, the energies of quantum states and hence the transition frequency between two states are invariant under earth's rotation, whatever the dependence of quantum energy on the speed. This leads to the spatial isotropy in frequency. Obviously, the synchronism among the various GPS clocks can be ascribed to this isotropy. A similar argument with a constancy under earth's rotation has been applied in Chapter 1 to the explanation of the aforementioned spatial isotropy in phase.

The transition frequency in the Hughes-Drever experiment is associated with the Zeeman splitting due to the interaction of nuclear spin with external magnetic fields [41]. In these experiments, the atoms or ions are in a gaseous or liquid state and their ground velocities are constant under earth's rotation in statistics. Therefore, the local-ether model is in accord with the Hughes-Drever experiment, whatever the dependence of nuclear magnetic interaction on the mass and speed. A variety of atoms or ions have been shown to exhibit this isotropy, including lithium [45], beryllium [94], mercury [62], and neon [20]. It is noticed that in some of the literature this isotropy is ascribed to the local Lorentz invariance [94, 62, 20].

6.6 Summary

Based on the local-ether wave equation, a harmonic-like wavefunction is dispersive, as the angular frequency and the propagation constant are related nonlinearly to each other owing to the presence of the natural frequency. From the first-order time evolution equation derived from the wave equation, it is found that the velocity of the associated particle with respect to the local-ether frame is proportional to the propagation vector and to the inverse of the angular frequency. Further, due to the dispersion of matter wave, the angular frequency is equal to the natural frequency times a speed-dependent factor, which is just the famous Lorentz mass-variation factor, except the reference frame of particle speed. As the natural frequency corresponds to the rest mass of a particle, the angular frequency is then the speed-dependent mass, aside from a common scaling factor. These speed-dependent angular frequency, propagation vector, and mass derived from the local-ether wave equation are in accord with the postulates of de Broglie in conjunction with the Lorentz mass-variation law, except the reference frame.

Based on Galilean transformations, the time evolution equation for a particle bound in a moving atom reduces to a form which looks like Schrödinger's equation. However, the position vector and hence the time derivative are referred to the atom frame. Moreover, the time derivative connects with an additional term of the mass-variation factor. Thereby, the energies of quantum states and hence the transition frequency decrease by this factor. The atomic clock rate is then expected to decrease with the speed of the clock by the mass-variation factor, where the speed is referred specifically to the local-ether frame. When the gravitational effect is taken into account by the perturbation method, it is seen that the transition frequency and hence the atomic clock rate also decrease under the gravitational potential. Quantitatively, it has been shown that the atom speed- and gravitation-induced frequency shift is actually in accord with the clock-rate difference in the Hafele-Keating experiment and with the clock-rate adjustment in GPS. However, according to the local-ether wave equation, the frequency shifts due to the gravitational and mass-variation effects originate from an intrinsic quantum property of the matter wave bound in an atom, rather than from a kinematical feature of electromagnetic wave propagating in space.

According to the local-ether model, the speed that determines the mass-variation factor is the atom speed referred to an ECI frame for earthbound atoms. Obviously, this is in accord with the east-west directional anisotropy in the Hafele-Keating experiment, the synchronism in GPS, and with the spatial isotropy in the Hughes-Drever experiment. Further, for the atomic clock on board the spacecraft in the earthbound or the interplanetary microwave link, the local-ether model leads to the prediction that the speed determining the mass-variation factor is referred specifically to a geocentric or a heliocentric inertial frame, respectively. This switching in the unique reference frame is in accord with the frequency-shift formulas adopted individually in the earthbound and the interplanetary experiment. However, for the atomic clocks at ground stations in both links, the local-ether model predicts that the speeds are referred uniquely to an ECI frame. For the interplanetary link, this prediction leads to a constant deviation from the calculated result of frequency shift reported in the literature. This constant deviation in frequency shift is yet to be verified and then provides a means to test the local-ether wave equation.

Chapter 7

Resonant Absorption between Moving Atoms

In Chapter 1, the Doppler effect due to the relative motion between the source and receiver of electromagnetic wave is investigated. Meanwhile, by exploring quantum properties of the matter wave bound in a moving atom based on the local-ether wave equation, it has been found in Chapter 6 that the energies of quantum states and hence the transition frequency of the atom decrease with its speed by the famous mass-variation factor, where the atom speed is referred uniquely to the local-ether frame. In this Chapter, by taking the Doppler frequency shift for electromagnetic wave in conjunction with the quantum energy variation of matter wave into account, a resonant-absorption condition is presented. Thereby, some phenomena associated with both electromagnetic and matter waves can be accounted for consistently, including the Ives-Stilwell experiment with fast-moving hydrogen atoms, the output frequency from ammonia masers, and the Mössbauer rotor experiment. In the resonant-absorption condition, the major term associated with the laboratory velocity is a dot product of this velocity and the velocity of the emitting or the absorbing atom. It is found that this term appears both in the Doppler frequency shift and in the transition-frequency variation, and then cancels out. Therefore, the consequences can be independent of the laboratory velocity and hence comply with Galilean relativity, in spite of the restriction on the reference frame of the involved velocities. However, by examining the resonant-absorption condition in the Mössbauer rotor experiment to a higher order, it is found that Galilean relativity breaks down.

7.1 Frequency Shifts

It is well known that the Doppler effect due to the relative motion between a transmitter and a receiver causes a shift in the received frequency of the electromagnetic or acoustic wave. The Doppler effect has been employed by Ives and Stilwell to analyze the frequency shift associated with the light that is emitted from fast-moving hydrogen atoms and then is absorbed by a spectrograph [47]. It has been found that the frequency shift observed with a precision spectrograph agrees with the Doppler effect only to the first order of the atom speed normalized to the speed of light c.

In order to account for the observed shift correctly to the second order, a hypothesis of Larmor and Lorentz was adopted, which states that the frequency of a wave radiated from a moving source of speed v is altered by a factor of $\sqrt{1 - v^2/c^2}$ [47]. This speed-dependent factor is identical to the one in the famous Lorentz mass-variation law. At present, a widely accepted explanation of this additional frequency shift is to attribute it to the second-order Doppler effect [33], which has been derived in Einstein's original paper on the special relativity based on the Lorentz transformation of space and time [24].

However, the just-mentioned explanation seems to imply that the frequency shift to the second order between a transmitter and a receiver in relative motion is purely a kinematical feature of wave propagation and has nothing to do with the intrinsic properties of the transmitter and receiver themselves. Specifically, it seems to imply that the transition frequency of the emitting or the absorbing atom or molecule remains unaltered when it is moving. Meanwhile, it is well known in standard textbooks on quantum mechanics that at least for hydrogen-like atoms, the energies of quantum states depend on the mass of the electron. Further, the mass is known to depend on the particle speed. Thus the quantum energies and hence the transition frequency are expected to depend on the particle speed.

Besides, in the common understanding the speed v that determines the second-order Doppler frequency shift by the mass-variation factor is the relative speed between the transmitter and the receiver. However, as discussed in Chapter 6, in the Hafele-Keating experiment with circumnavigating atomic clocks and in the global positioning system (GPS) with atomic clocks on board the orbiting satellites, it has been observed with high precision that the clock rate also depends on the mass-variation factor and the speed determining this factor is the speed of the clock referred specifically to an earth-centered inertial (ECI) frame. Thus there seems to exist a discrepancy in the frame for the speed in the mass-variation factor.

In Chapter 1 we have presented the local-ether model of wave propagation, whereby electromagnetic wave is supposed to propagate via a medium like the ether. However, the ether is not universal. Specifically, it is supposed that for earthbound experiments electromagnetic wave propagates at the speed of light c with respect to an ECI frame, regardless of the motions of the source and receiver. Meanwhile, the propagation is referred to a heliocentric inertial frame for interplanetary waves. This model has been adopted to account for a wide variety of propagation phenomena, including the first-order Doppler effect in GPS, radar, the stellar spectrum, Roemer's observations, and in the cosmic microwave background radiation.

Further, in Chapters 4-6, the matter wave associated with charged particles is supposed to follow the local-ether propagation model and be governed by a wave equation incorporating a natural frequency and the electric scalar potential. From the local-ether wave equation, a first-order time evolution equation similar to Schrödinger's equation is derived. From the electrostatic force derived from this evolution equation, it has been found that the inertial mass of a particle originates from the natural frequency and hence from the temporal variation of the associated matter wave. Further, due to the dispersion of matter wave, it has been derived that the angular frequency of a matter wave and the mass of the particle increase with the particle speed by the Lorentz mass-variation factor, except that the speed is referred specifically to the local-ether frame. Moreover, a feature different from Schrödinger's equation is that the time derivative in the evolution equation connects with an extra multiplying term of the mass-variation factor. Consequently, the energies of quantum states and hence the transition frequency of an atom decrease with the atom speed by this factor. In addition, the gravitational redshift has been derived as an effect of the gravitational potential on the quantum energy and transition frequency.

The atomic clock rate is based on the transition frequency of the involved atom. Therefore, the aforementioned observations of the speed-dependent clock rate demonstrate that the transition frequency decreases with speed by the mass-variation factor as an intrinsic quantum property of the matter wave bound in the moving atom. According to the local-ether model, the speed that determines this factor is the atom speed referred uniquely to an ECI frame for earthbound atoms. Thus the quantum energy, the transition frequency, and hence the atomic clock rate tend to depend on earth's rotation, but are entirely independent of earth's orbital motion around the

Sun or others. This consequence has been used in Chapter 6 to account for the east-west directional anisotropy in the Hafele-Keating experiment, for the synchronism among GPS atomic clocks, and for the spatial isotropy in the Hughes-Drever experiment.

In this Chapter, based on the local-ether model of wave propagation, a higher-order Doppler frequency shift for electromagnetic wave is derived. Further, by taking the speed-dependent variation of quantum energy of matter wave into account, we present a resonant-absorption condition between the emitting and the absorbing atom in motion. Then this frequency relation is used to deal with various experiments consistently, including the Ives-Stilwell experiment, the ammonia-maser experiment, and the Mössbauer rotor experiment. Thereafter, we examine the spatial isotropy, the terrestrial isotropy, Galilean relativity, and their breakdowns in the relevant experiments.

7.2 Higher-Order Doppler Frequency Shift

Based on the local-ether model of wave propagation, we have derived the Doppler effect in Chapter 1. In this section, we derive the Doppler frequency shift to higher orders. Suppose the source and the receiver are moving at velocities $\mathbf{v}_s$ and $\mathbf{v}_e$ with respect to the associated local-ether frame, respectively. According to the classical propagation model, the propagation time τ is the propagation range R divided by the isotropic speed c as $\tau = R/c$.

Let us recall that the propagation range represents the line (and its length) from the position of the source at the instant of wave emission to the one of the receiver at the instant of reception, as viewed in the local-ether frame. A quantity closely related to the propagation range is the transmission path which represents the line from the source to the receiver both at the instant of emission. The difference between the propagation range R and the transmission-path length R_t determines the Sagnac effect which is due to the movement of the receiver with respect to the local ether during wave propagation. Thus the propagation range and hence the propagation time depend on the velocity $\mathbf{v}_e$ and the acceleration $\mathbf{a}_e$ of the receiver with respect to the local-ether frame.

Quantitatively, when τ is short, the propagation range is given implicitly by

$$R = \left|\mathbf{R}_t + \mathbf{v}_e R/c + \mathbf{a}_e R^2/2c^2\right|, \tag{7.1}$$

where $\mathbf{R}_t$ denotes the directed length of the transmission path. As discussed in Chapter 1, the propagation range can be given explicitly in terms of the path length R_t. To the second order of normalized speed, the formula reads

$$R = R_t \left\{ 1 + \frac{1}{c} u_e + \frac{1}{2c^2} \left(u_e^2 + v_e^2 + \mathbf{a}_e \cdot \mathbf{R}_t \right) \right\}, \qquad (7.2)$$

where the radial speed u $(= \mathbf{v} \cdot \hat{R}_t)$ is the component of a velocity $\mathbf{v}$ along $\mathbf{R}_t$, and the unit vector $\hat{R}_t = \mathbf{R}_t / R_t$.

Consider the Doppler effect for the case where the source is periodically emitting waves and is moving with respect to the receiver. Due to the motions of the transmitter and receiver, the rate of reception tends to be different from the one of emission. The received time difference $\triangle t$ between two waves transmitted with a time difference $\triangle t'$ can be given by the variation in the propagation range as $\triangle t = \triangle t' + [R(t' + \triangle t') - R(t')]/c$, where $R(t)$ denotes the propagation range for the wave emitted at an arbitrary instant t. Thus, as discussed in Chapter 1, the received frequency f_r and the transmitted frequency f_t are related to each other by

$$\frac{f_t}{f_r} = 1 + \frac{dR}{cdt}, \qquad (7.3)$$

where the time derivative of the propagation range is evaluated at the instant of wave emission.

The second-order Doppler effect can be given if the first-order formula for the propagation range is used. In this way, the Doppler frequency relation becomes

$$\frac{f_t}{f_r} = 1 + \frac{dR_t}{cdt} + \frac{d}{c^2 dt} (\mathbf{v}_e \cdot \mathbf{R}_t). \qquad (7.4)$$

Due to the relative motion between the source and receiver, one has $d\mathbf{R}_t/dt = \mathbf{v}_{es}$ and hence $dR_t/dt = u_{es}$, where $\mathbf{v}_{es}$ $(= \mathbf{v}_e - \mathbf{v}_s)$ is the Newtonian relative velocity between the receiver and source at the instant of emission and u_{es} $(= u_e - u_s)$ is the corresponding radial relative speed.

Thus, to the second order of normalized speed, the Doppler frequency relation becomes

$$\frac{f_t}{f_r} = 1 + \frac{u_{es}}{c} + \frac{\mathbf{v}_e \cdot \mathbf{v}_{es}}{c^2} + \frac{\mathbf{a}_e \cdot \mathbf{R}_t}{c^2}. \qquad (7.5)$$

It is noted that the transverse components of velocities are also involved in the second-order Doppler shift. To the second order, the inverse frequency ratio reads

$$\frac{f_r}{f_t} = 1 - \frac{u_{es}}{c} - \frac{\mathbf{v}_e \cdot \mathbf{v}_{es}}{c^2} - \frac{\mathbf{a}_e \cdot \mathbf{R}_t}{c^2} + \frac{u_{es}^2}{c^2}. \qquad (7.6)$$

For the cases where the third-order Doppler effect is investigated, the second-order formula for the propagation range should be used, as discussed later.

When the acceleration $\mathbf{a}_e$ is zero, the preceding frequency relation agrees with the one derived in [82], aside from the difference in the interpretation of $\hat{R}_t$ and in the reference frame of velocities. For the case of radial relative motion without acceleration, where the relative velocity $\mathbf{v}_{es}$ is parallel to $\pm\mathbf{R}_t$ and hence $\mathbf{v}_e \cdot \mathbf{v}_{es} = u_e u_{es}$, the frequency relation becomes the familiar form

$$\frac{f_r}{f_t} = \frac{1 - u_e/c}{1 - u_s/c}. \qquad (7.7)$$

This agrees with the classical Doppler formula derived in an alternative way [3].

7.3 Quantum Energy Variation and Resonant-Absorption Condition

It is known that the frequency of the light emitted from or absorbed by an atom is equal to the transition frequency, which in turn corresponds to the difference in energy between two involved quantum states. Based on the local-ether wave equation, it has been found in Chapter 6 that the state transition frequency f of a moving atom decreases with its speed by the speed-dependent mass-variation factor as

$$f = f_0 \sqrt{1 - v^2/c^2}, \qquad (7.8)$$

where v is the atom speed referred to the local-ether frame which is an ECI frame for earthbound atoms, f_0 is the rest transition frequency of an identical atom stationary in the local-ether frame, and the frequency is observed in the atom frame which moves with the atom so that the Doppler shift is not involved.

The atomic clock rate depends on the transition frequency and hence decreases with speed by the mass-variation factor. The preceding speed-dependent frequency-variation formula has been adopted in Chapter 6 to account for the east-west directional anisotropy in clock rate demonstrated in the Hafele-Keating experiment with cesium atomic clocks on board an aircraft undergoing circumnavigation. In this experiment the observed clock rate is determined from the number of the atomic clock ticks which in turn are detected and counted by a device comoving with the clock without relative motion. Thus the observed variation of clock rate with the flight originates from a variation of the quantum-state energy and not from the Doppler frequency shift.

A speed-dependent frequency of the form given by (7.8) was first introduced before the advent of the special relativity [46] and was later derived by assuming the length contraction [54] or the time dilation [33]. Based on the local-ether wave equation, the preceding frequency-variation formula is due to a quantum effect and is not expected to hold for all state transitions in all atoms, and other forms of the speed-dependence are not precluded. This is viewed from the complication that the interactions that affect the energies of quantum states are versatile, such as electronic or nuclear, spin or orbital, electric or magnetic, and internal or external. In Chapter 6 this formula is derived only for electronic states under the influence of the electric scalar potential in a hydrogen-like atom, and a minor term given in (6.25) is omitted. Nevertheless, it is assumed that this frequency-variation formula holds in the experiments discussed in this Chapter.

Then we proceed to consider the emission and absorption between a source atom s and a receiver atom e, which are moving at velocities $\mathbf{v}_s$ and $\mathbf{v}_e$ with respect to the common local-ether frame, respectively. Suppose f_{0s} and f_{0e} are the rest transition frequencies of atoms s and e, respectively. The transmitted frequency f_t of the wave emitted from the moving atom s is related to the rest transition frequency f_{0s} by

$$f_t = f_{0s}\sqrt{1 - v_s^2/c^2}. \tag{7.9}$$

Due to the motions of the source and receiver, the Doppler effect also causes a frequency shift. Thus, in order for the electromagnetic wave to be resonantly absorbed by the moving atom e, the rest transition frequency f_{0e} should be related to the received frequency f_r by

$$f_r = f_{0e}\sqrt{1 - v_e^2/c^2}. \tag{7.10}$$

The received frequency f_r and the transmitted frequency f_t in turn are related to each other by the Doppler effect given in (7.5) or (7.6).

Thus, by taking both the Doppler frequency shift for electromagnetic wave and the quantum energy variation of matter wave into account, we arrive at the *resonant-absorption condition* in terms of the rest transition frequencies f_{0s} and f_{0e}, which, to the second order of normalized speed, is given by

$$f_{0e}\sqrt{1-\frac{v_e^2}{c^2}} = f_{0s}\sqrt{1-\frac{v_s^2}{c^2}}\left\{1-\frac{u_{es}}{c}-\frac{\mathbf{v}_e\cdot\mathbf{v}_{es}+\mathbf{a}_e\cdot\mathbf{R}_t-u_{es}^2}{c^2}\right\}. \tag{7.11}$$

It is seen that this condition depends on the velocities of the receiver and source atoms in a complicated way. However, for the case where the receiver moves with the source ($\mathbf{v}_e = \mathbf{v}_s$) without acceleration, the preceding formula becomes a trivial form $f_{0e} = f_{0s}$. The resonant-absorption condition made its debut in [137].

When this condition is not perfectly met, the off-resonance absorption tends to be much weaker. The deviation in frequency from the resonant-absorption condition is given by the difference between the received frequency and the transition frequency of the absorbing atom in motion. That is,

$$\delta f = f_r - f_{0e}\sqrt{1 - v_e^2/c^2}. \tag{7.12}$$

This deviation then determines the off-resonance absorption.

By using (7.9) which relates f_t and f_{0s}, the frequency deviation can be written as

$$\delta f = \triangle f_D - \triangle f_Q, \tag{7.13}$$

where $\triangle f_D$ and $\triangle f_Q$ denote the frequency shifts due to the Doppler and the quantum effect, respectively, and are given by

$$\triangle f_D = f_r - f_t \tag{7.14}$$

and

$$\triangle f_Q = f_{0e}\sqrt{1 - v_e^2/c^2} - f_{0s}\sqrt{1 - v_s^2/c^2}. \tag{7.15}$$

In words, $\triangle f_Q$ is the difference in the speed-dependent transition frequency between the receiver and source atoms in motion. From (7.3) it is seen that the fractional Doppler frequency shift is given by

$$\frac{\triangle f_D}{f_r} = -\frac{dR}{cdt}. \tag{7.16}$$

The resonant-absorption condition then corresponds to the situation with a zero deviation, which means that the frequency shift due to the Doppler effect for the electromagnetic wave propagating in free space exactly cancels the one due to the quantum effect of the matter waves bound in the atoms.

7.4 Reexamination of Resonant-Absorption Experiments

According to the derived resonant-absorption condition, we reexamine some related terrestrial experiments reported in the literature. Thereby, we present reinterpretations of the Ives-Stilwell experiment, the output frequency from ammonia masers, and of the Mössbauer rotor experiment in a consistent way. Then we explore the spatial isotropy, the terrestrial isotropy, Galilean relativity, and their breakdowns. The first experiment is associated with a radial relative motion ($u_{es} \simeq \pm v_{es}$) and the last two are with a transverse relative motion ($u_{es} = 0$).

7.4.1 Ives-Stilwell experiment

Consider the case where the source is moving at a velocity $\mathbf{v}_s$ and the receiver is stationary, both with respect to an ECI frame. Thus $a_e = 0$, $v_e = 0$, and $u_{es} = -u_s$. Then, to the second order, the resonant-absorption condition becomes a simpler form

$$f_{0e} = f_{0s} \frac{\sqrt{1 - v_s^2/c^2}}{1 - u_s/c}. \tag{7.17}$$

For this case $f_r = f_{0e}$ and thus this formula is identical to that derived in different ways based on the transformation of four-vectors [63] or on the time dilation [33], except the difference in the reference frame of the velocity $\mathbf{v}_s$. According to the local-ether wave equation, the term $1/(1 - u_s/c)$ in the preceding formula is due to the Doppler frequency shift to the second order, while the square-root term is due to the quantum energy variation.

A similar frequency shift has been demonstrated in the Ives-Stilwell experiment, where light is emitted from fast-moving hydrogen atoms in an excited state and is absorbed by a spectrograph [47, 78]. The radiation from the moving atoms is reflected from two mirrors and then the two reflected light beams are focused and guided to a photographic plate where the frequencies of the absorbed waves are recorded for measurement and comparison. The two mirrors are arranged in such a way that the atomic beam is moving toward one of

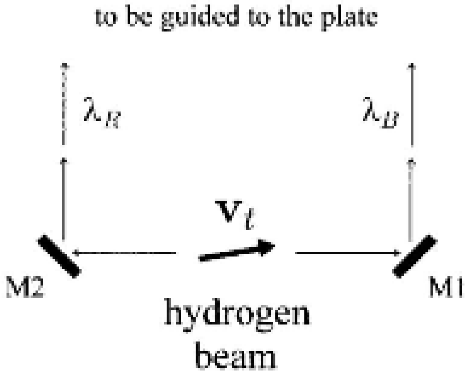

Fig. 7 Ives-Stilwell experiment. Two light beams to be focused and guided to the photographic plate are emitted from a fast-moving hydrogen atomic beam of velocity $\mathbf{v}_t$, which approaches the mirror M1 and recedes from the mirror M2.

them and away from the other [78] (see Fig. 7). Due to the Doppler effect associated with the relative motions between the emitting atoms and the mirrors, the light beams reflected from the mirrors tend to shift in frequency and wavelength. On the other hand, by virtue of no relative motions among the mirrors, the spectrograph, and other components of the experimental setup, no further Doppler effect is introduced after the reflection.

More precisely, owing to earth's rotation, the receiver tends to be nonstationary with respect to an ECI frame even in a geostationary experimental setup. Consider the laboratory frame in which the setup together with the receiver is stationary. Suppose that the emitting atoms are moving at a velocity $\mathbf{v}_t$ with respect to the laboratory frame, which in turn moves at a velocity $\mathbf{v}_0$ with respect to an ECI frame. Thus $\mathbf{v}_e = \mathbf{v}_0$, $\mathbf{v}_s = \mathbf{v}_t + \mathbf{v}_0$, and $\mathbf{v}_{es} = -\mathbf{v}_t$. And, as earth's rotation rate is low, the acceleration a_e is still taken as zero.

In the experiment the atoms move quite parallel to the optical path which connects the reflecting point on one mirror and that on the other. The light beams that will be reflected and guided to the spectrograph are radiated in such two directions that the transmission path is parallel to the optical path, where the transmission path connects the emitting atom and the reflecting point on either mirror. Thus $u_{es} = \mp v_t \cos\theta$, where θ denotes the small angle between the direction of the atomic beam represented by $\mathbf{v}_t$ and that of the optical path, and the upper or the lower sign applies to the light beam reflected from the mirror which the atomic beam approaches or recedes from, respectively.

Then the resonant-absorption condition (7.11) yields that the received frequencies associated with the two reflected light beams are

$$f_{r\pm} = f_{0s}\sqrt{1 - \frac{(\mathbf{v}_t + \mathbf{v}_0)^2}{c^2}} \left\{1 \pm \frac{v_t \cos\theta}{c} + \frac{\mathbf{v}_0 \cdot \mathbf{v}_t + v_t^2 \cos^2\theta}{c^2}\right\}. \tag{7.18}$$

It is noted that the first-order term is independent of the laboratory velocity $\mathbf{v}_0$. Both the Doppler and the quantum effect contribute to the second-order terms. If $\mathbf{v}_0$ is neglected, the preceding formula reduces to (7.17). To the second order of normalized speed, the received frequencies can be written as

$$f_{r\pm} = f_{0s}\left\{1 \mp \frac{v_t}{c}\cos\theta + \frac{v_t^2 + v_0^2}{2c^2}\right\}^{-1}. \tag{7.19}$$

It is of essence to note the coincidence that the dot-product term $\mathbf{v}_0 \cdot \mathbf{v}_t$ appears both in the Doppler and in the quantum effect and then cancels out.

In the Ives-Stilwell experiment the speed v_t of hydrogen atoms is of the order of 10^6 m/s, which is achieved by electrostatically accelerating hydrogen ions with a voltage of tens of kV. Thus the particle speed v_t is much higher than the laboratory speed v_0 which is due to earth's rotation and, perhaps, to the motion of a vehicle carrying the experimental setup. Then the preceding frequency formula can be substantially independent of the laboratory velocity $\mathbf{v}_0$, as the quadratic term v_0^2/c^2 can be neglected.

The first- and the second-order frequency shift are associated with the difference between the two received frequencies and with the sum of them, respectively. Thus, in terms of the wavelengths, the normalized particle speed and its square can be given by

$$\frac{v_t}{c} = \frac{\lambda_R - \lambda_B}{\lambda_0}\frac{1}{2\cos\theta} \tag{7.20}$$

and

$$\frac{v_t^2}{c^2} = \frac{\lambda_R + \lambda_B}{\lambda_0} - 2 - \frac{v_0^2}{c^2}, \tag{7.21}$$

where $\lambda_B = c/f_{r+}$, $\lambda_R = c/f_{r-}$, and $\lambda_0 = c/f_{0s}$.

By measuring λ_R and λ_B, the first- and the second-order fractional shift can be calculated and compared, with a knowledge of λ_0, θ, and v_0. This provides a means to test the self-consistency between these shifts. It can be expected that the deviation of the sum $\lambda_R+\lambda_B$ from $2\lambda_0$ is quite small. By using a high-precision spectrograph, it has been measured that $\lambda_R = 661.8808$ and $\lambda_B = 650.7253$ (in nm) [78]. Meanwhile, it is known that $\lambda_0 = 656.2793$ and $\theta = 0.075$ (in rad). Then formulas (7.20) and (7.21) lead to $v_t^2/c^2 = 7.26 \times 10^{-5}$ and 7.24×10^{-5}, respectively, where the quadratic term v_0^2/c^2 is as small as 10^{-12} and hence is omitted. The agreement between the two data is quite good, since the discrepancy is as small as the round-off in the calculation.

According to the local-ether wave equation, the wavelength λ_0 corresponds to a transition frequency of a hydrogen atom stationary with respect to an ECI frame. On the other hand, it is reported that λ_0 is the wavelength of the H_α line of the Balmer series observed in a reference frame at rest with respect to the radiating atom [78]. The value of λ_0 could be actually measured from the atoms stationary in a geostationary laboratory. Thus the fractional discrepancy in λ_0 due to the difference in the reference frame is also of the order of the negligible quadratic term v_0^2/c^2. Therefore, with both the Doppler frequency shift and the quantum energy variation being taken into account, the local-ether wave equation is in accord with the Ives-Stilwell experiment by showing the self-consistency between the first- and the second-order frequency shift.

7.4.2 Output frequency from ammonia masers

Next, we consider the case where the source is moving in a direction transverse to the transmission path. In the ammonia maser, the molecular beam is split into the upper and the lower state by an electric system, and then the upper-state beam is injected into a cavity and emits microwave due to quantum state transition under stimulation [17, 33]. Then the output microwave passes through a waveguide which in turn is coupled to the cavity via a small aperture (see Fig. 8).

Suppose that the cavity and the receiver are stationary in the laboratory frame of velocity $\mathbf{v}_0$ and that the emitting ammonia molecular beam moves at a velocity $\mathbf{v}_t$ with respect to the cavity. Moreover, suppose that the output waveguide is thin and long and is positioned with its longitudinal axis being perpendicular to the direction of the molecular beam represented by $\mathbf{v}_t$. Thus the transmission path for the output microwave is virtually parallel to the longitudinal axis of

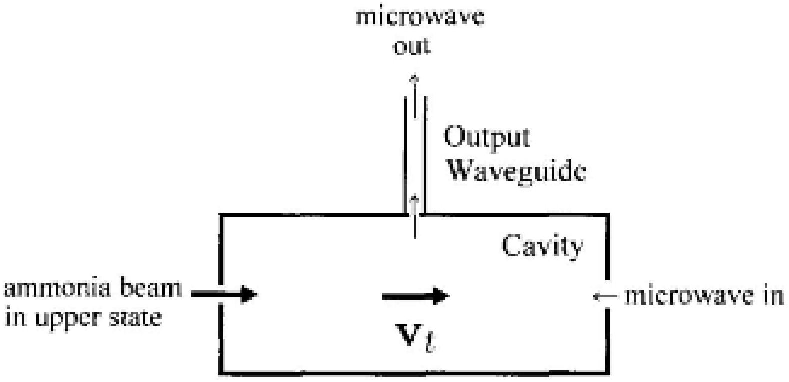

Fig. 8 Ammonia maser. The ammonia maser is formed by a cavity, an output waveguide, and an electric system (not shown) which splits the ammonia beam into the upper and the lower state and deflects the beam in the lower state away from entering the cavity.

the output waveguide and hence is transverse to the particle velocity, that is, $\mathbf{v}_t\cdot\hat{R}_t = 0$.

Thus, as in the Ives-Stilwell experiment, $\mathbf{v}_e = \mathbf{v}_0$, $\mathbf{a}_e = 0$, $\mathbf{v}_s = \mathbf{v}_t + \mathbf{v}_0$, and $\mathbf{v}_{es} = -\mathbf{v}_t$. But $u_{es} = 0$. Then the resonant-absorption condition (7.11) leads to

$$f_{0e}\sqrt{1 - v_0^2/c^2} = f_{0s}\sqrt{1 - (\mathbf{v}_t + \mathbf{v}_0)^2/c^2}\left\{1 + \mathbf{v}_0\cdot\mathbf{v}_t/c^2\right\}, \quad (7.22)$$

where the Doppler effect is represented by the dot-product term $\mathbf{v}_0\cdot\mathbf{v}_t$. By an expansion one immediately has

$$\frac{f_{0e}}{f_{0s}} = 1 - \frac{v_t^2}{2c^2}. \quad (7.23)$$

It is noted again that the dot-product term $\mathbf{v}_0\cdot\mathbf{v}_t$ appears both in the Doppler and in the quantum effect and then cancels out. It is seen that this frequency relation is even independent of the laboratory velocity $\mathbf{v}_0$.

In terms of the received frequency, the preceding formula becomes

$$\frac{f_r}{f_{0s}} = 1 - \frac{v_t^2 + v_0^2}{2c^2}. \quad (7.24)$$

This formula then represents the frequency at the output waveguide of the maser, by taking both the Doppler and the quantum effect into account. As the dot-product term $\mathbf{v}_0 \cdot \mathbf{v}_t$ cancels out, the output frequency from the maser is independent of the directions of the velocities $\mathbf{v}_t$ and $\mathbf{v}_0$. Therefore, the preceding frequency formula is in accord with the experiments where it has been demonstrated that the beat frequency between two masers with molecular beams moving in opposite directions is substantially zero and is almost independent of earth's motions [17].

If the clocks in the Hafele-Keating experiment are replaced by those of the ammonia maser with the clock rate being determined by the output frequency f_r, the preceding frequency relation also leads to a speed-dependence in the clock-rate difference. It is noted that this dependence is identical to that given in (6.26) for the cesium atomic clocks where the motion of the atoms with respect to the cavity is omitted for simplicity and thus the Doppler effect vanishes.

It is noticed that a term quite similar to the second-order Doppler effect in (7.22) has been derived alternatively from a classical approach, aside from the difference in the reference frame of the laboratory velocity [17, 33]. Then, with the use of a speed-dependent frequency based on the time dilation, a similar cancellation of the terms associated with $\mathbf{v}_0$ has been accounted for by combining such two entirely different approaches [18]. Anyway, with both the Doppler frequency shift and the quantum energy variation being taken into account, the local-ether wave equation is in accord with the experiments with ammonia masers.

7.4.3 Mössbauer rotor experiment

Then we consider the case where the absorber as well as the source is moving in the laboratory frame. The Mössbauer rotor experiment is based on the gamma-ray recoilless nuclear transition known as the Mössbauer effect [42, 19, 111, 97, 49], which leads to a narrow linewidth and thus has been used to measure the gravitational redshift in the Pound-Rebka experiment discussed in Chapter 5. In the rotor experiment the source and the absorber of gamma rays are placed separately on a rod rotating in a horizontal plane. Both the quantum energy variation of nuclear states and the Doppler effect with gamma-ray propagation cause the frequency shift. A frequency deviation from the resonant-absorption condition manifests itself as an increase in the scattering of gamma rays, which in turn can be measured by counters fixed at the laboratory or at the rod.

Suppose that the absorber and the source atom rotate about an axis with linear velocities $\mathbf{v}_r$ and $\mathbf{v}_t$, respectively, where the axis is stationary in a laboratory frame which in turn moves at a velocity $\mathbf{v}_0$

with respect to an ECI frame, and the minute contributions to $\mathbf{v}_r$ and $\mathbf{v}_t$ due to earth's rotation are neglected. In the rotor experiment, the directed path length $\mathbf{R}_t$ which points from the source to the absorber is always perpendicular both to $\mathbf{v}_r$ and to $\mathbf{v}_t$. Moreover, the path length R_t is fixed, while the direction of $\mathbf{R}_t$ is changing periodically with time. Thus $dR_t/dt = 0$ and $d\mathbf{R}_t/dt = \mathbf{v}_{rt}$, where $\mathbf{v}_{rt} = \mathbf{v}_r - \mathbf{v}_t$.

To the second order of normalized speed, the fractional Doppler frequency shift (7.16) due to the motions of the source and receiver then becomes

$$\frac{\triangle f_D}{f_r} = -\frac{d}{cdt}\left(R_t + \frac{1}{c}\mathbf{v}_0 \cdot \mathbf{R}_t\right) = -\frac{\mathbf{v}_0 \cdot \mathbf{v}_{rt}}{c^2}, \tag{7.25}$$

where the orthogonality $\mathbf{v}_r \cdot \mathbf{R}_t = 0$ is used and the derivative of $\mathbf{v}_0$ is omitted as earth's rotation rate is low. It is seen that this frequency shift depends on the laboratory velocity $\mathbf{v}_0$. It is noted that due to the path length R_t being fixed, the first-order term of normalized speed vanishes in the rotor experiment.

Consider the case where the source and the absorber have an identical rest transition frequency f_0. Thus the fractional frequency shift due to the quantum effect is

$$\frac{\triangle f_Q}{f_0} = \sqrt{1 - (\mathbf{v}_r + \mathbf{v}_0)^2/c^2} - \sqrt{1 - (\mathbf{v}_t + \mathbf{v}_0)^2/c^2}$$

$$\simeq \frac{1}{2c^2}\left(-2\mathbf{v}_{rt} \cdot \mathbf{v}_0 - v_r^2 + v_t^2\right). \tag{7.26}$$

It is noted that the dot-product term $\mathbf{v}_{rt} \cdot \mathbf{v}_0$ appears again.

Consequently, by taking both the Doppler and the quantum effect into account to the second order of normalized speed, the fractional frequency deviation from the resonant absorption is given by

$$\frac{\delta f}{f_0} = \frac{v_r^2 - v_t^2}{2c^2}, \tag{7.27}$$

where we have made use of the relation that $\triangle f_D/f_r$ given by (7.25) is identical to $\triangle f_D/f_0$ to the third order of normalized speed, since the discrepancy of f_r/f_0 from unity, as well as $\delta f/f_0$, is of the second order. It is noted that the term $\mathbf{v}_{rt} \cdot \mathbf{v}_0$ cancels out and hence the frequency deviation is independent of the directions of $\mathbf{v}_r$ and $\mathbf{v}_t$. This deviation is also independent of the laboratory velocity $\mathbf{v}_0$.

The preceding formula is in agreement with the one that has been demonstrated in experiments with various rotation rates and various positions of the source and the absorber at the rod [42, 19, 111]. Moreover, it has been found that between the two geostationary counters oriented to detect the gamma rays propagating south- and northward, respectively, there is no substantial difference in the measured frequency deviation [19]. Thus the deviation is expected to be independent of the orientation of the counter and then independent of the directions of the velocities $\mathbf{v}_r$ and $\mathbf{v}_t$. Therefore, the preceding frequency-deviation formula is in accord with the experiments.

It is noticed again that a term quite similar to the second-order Doppler effect in (7.25) has been derived alternatively from a classical approach, aside from the reference frame of the laboratory velocity [19, 97, 49]. Then a similar cancellation of the terms with $\mathbf{v}_0$ has been accounted for by combining different approaches, where a speed-dependent frequency based on the length contraction is used [97]. Anyway, with both the Doppler frequency shift and the quantum energy variation being taken into account, the local-ether wave equation is also in accord with the Mössbauer rotor experiment.

7.4.4 Spatial isotropy, terrestrial isotropy, Galilean relativity, and their breakdowns

According to the local-ether wave equation, the atom speed that determines the quantum states is referred uniquely to an ECI frame for earthbound atoms. Thus the associated quantum energy is entirely independent of earth's orbital motion around the Sun or others. Further, the quantum energy can even be invariant under earth's rotation, if the atom speed remains constant during the rotation. As discussed in Chapter 6, such a constant-speed condition is met by an atom or a molecule that is geostationary, or moves at a fixed ground velocity at a substantially fixed latitude, or moves in a circular satellite orbit around the Earth.

For an atom satisfying the constant-speed condition, the energies of quantum states and hence the transition frequency between two states are independent of the orientation and position of the Earth in space, whatever the dependence of quantum energy on the speed. Such a spatial isotropy in transition frequency with respect to earth's motions has been adopted in Chapter 6 to account for the hourly and daily frequency stability in the Hughes-Drever experiment [41] and for the high synchronism among the various GPS atomic clocks moving in circular orbits [69].

The applicability of the spatial isotropy can be extended to the cases where electromagnetic wave as well as matter wave is involved. According to the local-ether model, the results of an earthbound experiment are entirely independent of earth's orbital motion. Further, the results can be invariant under earth's rotation, so long as the atom speeds v_e and v_s together with the terms u_e, u_s, $\mathbf{v}_e \cdot \mathbf{v}_s$, and $\mathbf{a}_e \cdot \mathbf{R}_t$ are invariant under the rotation. Thereby, the frequency-variation formula (7.8), the propagation-range formula (7.2), and then the resonant-absorption condition (7.11) yield results which remain unchanged under earth's rotation, and hence the associated phenomena exhibit the spatial isotropy.

In the Ives-Stilwell experiment and the ammonia maser, it is seen that the speeds v_e and v_s are invariant under earth's rotation and the acceleration $\mathbf{a}_e$ is substantially zero. Moreover, the terms u_e, u_s, and $\mathbf{v}_e \cdot \mathbf{v}_s$ are invariant under the rotation, since the directions of $\mathbf{v}_e$, $\mathbf{v}_s$, and $\mathbf{R}_t$ all change in a coordinated way with earth's rotation. Thus the spatial isotropy can be expected in these experiments and has been demonstrated in the ammonia maser with the hourly and daily stability of its output frequency [17]. Similarly, the stability of the frequency deviation from the resonant absorption in the Mössbauer rotor experiment has been demonstrated experimentally [19]. On the contrary, when the source is located outside the earth local ether, the receiver velocity then incorporates earth's orbital motion. Thus the spatial isotropy can break down, as demonstrated in the seasonal variation in Roemer's observations and in the cosmic microwave background radiation discussed in Chapter 1.

The spatial isotropy with respect to earth's motions in space can be generalized with a step forward. When the particle velocities are written in the laboratory frame of velocity $\mathbf{v}_0$, the terms $\mathbf{v}_0 \cdot \mathbf{v}_r$, $\mathbf{v}_0 \cdot \mathbf{v}_t$, and v_0^2 will emerge in the relevant formulas. It has been pointed out that the dot-product term $\mathbf{v}_0 \cdot \mathbf{v}_r$ or $\mathbf{v}_0 \cdot \mathbf{v}_t$ can be common in the Doppler and the quantum effect and then cancels out. Moreover, the radial speeds u_0, u_r, and u_t emerge in the Doppler effect. However, the speed u_0 cancels out in the terms with the relative speed u_{es}, and the directions of $\mathbf{v}_r$, $\mathbf{v}_t$, and $\mathbf{R}_t$ also change in a coordinated way with the orientation of the setup. Consequently, the experimental results are independent of the setup orientation with respect to the ground. Thus the experiment possesses the terrestrial isotropy with respect to the setup orientation on the ground, in addition to the spatial isotropy with respect to earth's orientation in space.

This terrestrial isotropy is observed in the three experiments examined in this Chapter so far. Thus the output frequency from the ammonia maser is independent of the direction of the particle velocity and hence no observable beat frequency between masers with different orientations can be expected, as demonstrated experimentally in [17]. Moreover, the frequency deviation in the Mössbauer rotor experiment can be expected to be identical for counters with different orientations, as demonstrated experimentally in [19].

Further, the squared term v_0^2/c^2 in some frequency formulas cancels out or is too small to be detected. As a consequence, the experiments become independent of the laboratory velocity $\mathbf{v}_0$ and hence comply with Galilean relativity, in spite of the restriction on the reference frame of the particle and propagation velocities. Thus, when the whole experimental setup is put on a vehicle moving smoothly with respect to the ground, the measurement results will be independent of the ground velocity of the vehicle, as well as of the orientations of the setup and the Earth. Thereby, the possession of the terrestrial isotropy is generalized to the compliance with Galilean relativity. In this manner, it is seen that the Mössbauer rotor experiment complies with Galilean relativity. Moreover, Galilean relativity can also be observed in the Ives-Stilwell experiment and in the output frequency from the ammonia maser, as the minute squared term is difficult to detect. Anyway, these experiments preserve the isotropy with respect to the setup orientation and earth's motions.

However, when the measurement precision is improved so that higher-order effects can be detected, some minute terms may emerge to make Galilean relativity or even the isotropy break down. The just-mentioned squared term v_0^2/c^2 in the Ives-Stilwell experiment and the ammonia maser is an example. For another, we reexamine the Mössbauer rotor experiment to a higher order.

In order to derive the Doppler effect to the third order of normalized speed, the second-order propagation-range formula (7.2) is needed, which for the Mössbauer rotor experiment becomes

$$R(t) = R_t \left\{ 1 + \frac{1}{c} u_0 + \frac{1}{2c^2} \left[u_0^2 + \left(v_r^2 + v_0^2 + 2\mathbf{v}_r \cdot \mathbf{v}_0 \right) + \mathbf{a}_e \cdot \mathbf{R}_t \right] \right\}. \tag{7.28}$$

For a rotation at a fixed rate, the terms v_r and $\mathbf{a}_e \cdot \mathbf{R}_t$ as well as v_0 are invariant during the rotation. Thus the time rate of change in the propagation range R is given by

$$\frac{dR(t)}{dt} = R_t \frac{d}{dt} \left\{ \frac{1}{c} u_0 + \frac{1}{2c^2} \left[u_0^2 + 2\mathbf{v}_r \cdot \mathbf{v}_0 \right] \right\}. \tag{7.29}$$

Thereby, to the third order of normalized speed, the fractional Doppler frequency shift due to wave propagation can be given by

$$\frac{\triangle f_D}{f_0} = -\frac{1}{c^2} \mathbf{v}_{rt} \cdot \mathbf{v}_0 - \frac{1}{c^3} \left[\left(\mathbf{v}_{rt} \cdot \mathbf{v}_0 \right) u_0 - v_{rt} v_r u_0 \right], \tag{7.30}$$

where we have made use of (7.16) with $\triangle f_D/f_0 = \triangle f_D/f_r$ to the third order and of $d\mathbf{v}_r/dt = -\hat{R}_t v_r v_{rt}/R_t$. It is seen that $\triangle f_D = 0$ when the laboratory speed $v_0 = 0$.

On the other hand, the frequency-shift formula (7.26) for the quantum effect is expected to be valid to the third order. Thus, by taking both the Doppler and the quantum effect into account to the third order of normalized speed, the fractional frequency deviation from the resonant absorption is given by

$$\frac{\delta f}{f_0} = \frac{1}{2c^2}\left(v_r^2 - v_t^2\right) - \frac{1}{c^3}\left(\mathbf{v}_{rt}\cdot\mathbf{v}_0 - v_{rt}v_r\right)u_0. \tag{7.31}$$

It is noted that the dot-product term $\mathbf{v}_{rt}\cdot\mathbf{v}_0$ survives in the third-order effect, while it cancels out in the second-order one. The presence of this term or of the speed u_0 then makes the terrestrial isotropy with respect to the setup orientation and hence Galilean relativity break down, even though their effects appear quite small in magnitude. Accordingly, the frequency deviation tends to be different as measured in counters with different orientations with respect to the ground, when it can be measured to the third order. Thereby, the terrestrial anisotropy in the frequency deviation is predicted. Meanwhile, the spatial isotropy with respect to earth's rotational and orbital motions remains.

7.5 Summary

By taking both the Doppler frequency shift for electromagnetic wave and the quantum energy variation of matter wave into account, the resonant-absorption condition for the emitting and the absorbing atom in motion is presented to account for the Ives-Stilwell experiment, the output frequency from ammonia masers, and the Mössbauer rotor experiment in a consistent way. Based on the local-ether wave equation, it is obvious that earthbound phenomena do not at all depend on earth's orbital motion around the Sun or others. This immediately accounts for the null effect of the orbital motion in various terrestrial experiments. Further, for a geostationary setup, the experimental results can be invariant under earth's rotation. This corresponds to the spatial isotropy found in the stability of frequency in the Hughes-Drever experiment and the ammonia maser. The spatial isotropy also holds for the atomic clocks on board earth's satellites moving in circular orbits and hence accounts for the high synchronism among the various GPS atomic clocks.

Further, in the formulas for the Doppler and the quantum effect, it is seen that the major term associated with the laboratory velocity is a dot product of this velocity and the velocity of the emitting or the absorbing atom. This term appears both in the Doppler frequency shift and in the transition-frequency variation and then cancels out. Thus the experimental results become invariant with respect to the setup orientation, as well as to earth's motions. This terrestrial isotropy has been demonstrated in the ammonia maser where the output frequency is independent of the direction of the particle beam, and in the Mössbauer rotor experiment where the frequency deviation from the resonant absorption is independent of the orientation of the counter. Further, the frequency deviation is independent of the laboratory velocity and hence the Mössbauer rotor experiment complies with Galilean relativity.

However, the laboratory velocity may emerge in some situations to make Galilean relativity break down. Further, the aforementioned dot-product term with the laboratory velocity may emerge to make the terrestrial isotropy and hence Galilean relativity break down. By examining the resonant-absorption condition in the Mössbauer rotor experiment to the third order of normalized speed, such a breakdown is found. Thereby, it is expected that the frequency deviation tends to vary when measured in counters with different orientations. This predicted terrestrial anisotropy in the frequency deviation may provide a means to test the local-ether wave equation, if the measurement precision can be raised to the third order of normalized speed.

Chapter 8

Interference of Matter Wave

Based on the local-ether wave equation for free particles, the dispersion of matter wave is revisited. From the dispersion relation, the angular frequency and the wavelength of the associated matter wave are derived, which correspond to the quantum energy and the momentum of the particle, respectively. These formulas look like the postulates of de Broglie in conjunction with the Lorentz mass-variation law. However, the fundamental difference is that for terrestrial particles their speeds are referred specifically to a geocentric inertial frame and hence incorporate the speed due to earth's rotation. Thus the local-ether wave equation predicts an east-west directional anisotropy in mass and matter wavelength. As the phase variation of a particle beam is given by the propagation vector and the path length along the beam, a shift in either of these quantities then leads to a phase difference between two coherent beams. The derived phase-difference formulas consistently account for the matter-wave interference experiments demonstrating the Bragg reflection, the gravitational effect, and the Sagnac effect, in spite of the restriction on the reference frame. For electron wave, the effects of earth's rotation can be negligible and thus the derived Bragg angle is actually in accord with the Davisson-Germer experiment, as examined within the present precision. On the other hand, the local-ether wave equation leads to a terrestrial anisotropy due to earth's rotation in the Bragg angle in neutron diffraction. The predicted anisotropy then provides a means to test its validity.

8.1 Properties of Matter Wave

The concept of wave nature of matter is known to emanate from de Broglie who presented in 1924 the postulate that a particle is associated with a matter wave of which the angular frequency and the wavelength are related to the energy and the momentum of the particle, respectively [3, 26]. The energy and momentum in turn are associated with the speed-dependent mass given by the Lorentz mass-variation law. Shortly, in 1927, the matter wavelength was demonstrated in the Bragg reflection of electron beams from a crystal by Davisson and Germer [3]. Furthermore, based on the phase difference between two coherent beams of electrons, neutrons, or atoms, various matter-wave interference experiments have been reported to demonstrate the Bragg reflection, the double-slit diffraction, the gravitational effect, and the Sagnac effect.

In Chapter 1 we have presented the local-ether model of wave propagation. That is, electromagnetic wave can be viewed as propagating via a medium like the ether. However, the ether is not universal. It is supposed that in the region under a sufficient influence of the gravitation due to the Earth, the Sun, or another celestial body, there forms a local ether which in turn moves with the gravitational potential of the respective body. For earthbound waves, the medium is the earth local ether which as well as earth's gravitational potential is stationary in an earth-centered inertial (ECI) frame. This local-ether model has been adopted to account for a wide variety of propagation phenomena, including the Sagnac effect in the global positioning system and in the rotating-loop interferometer.

Further, matter wave is supposed to follow the local-ether propagation model. Thereby, we have presented in Chapters 5 and 6 a wave equation for a particle of charge q and natural frequency ω_0 in the presence of the gravitational and the electrical scalar potential. Under the ordinary condition of low particle speed, the local-ether wave equation has been shown to lead to a unified quantum theory of gravitational and electromagnetic forces. It also leads to the identity of gravitational and inertial mass, since both the gravitational mass and the inertial mass are found to originate from the natural frequency. Furthermore, the local-ether wave equation leads to the effect that the energy of quantum state of the matter wave bound in an atom decreases with the gravitational potential, and thus accounts for the gravitational redshift. When the restriction on particle speed is removed, the local-ether wave equation leads to the speed-dependence in mass and hence in quantum-state energy, which in turn leads to the east-west directional anisotropy in atomic clock rate, as an effect of earth's rotation on the bound matter wave. This terrestrial anisotropy has been shown to be in accord with the Hafele-Keating experiment with circumnavigation atomic clocks.

In this Chapter, based on the local-ether wave equation, we explore the property of matter wave associated with free particles, instead of those bound in atoms or molecules. For a wave packet composed of plane waves, the dispersion of matter wave is revisited. Then, from the dispersion relation, the angular frequency and wavelength of the matter wave and the associated speed-dependent mass of the particle are derived. According to the local-ether model, the velocity of earthbound particles that determines the mass and the wave properties is referred specifically to an ECI frame and hence incorporates the linear velocity due to earth's rotation. Thereby, the matter-wave interference experiments associated with the Bragg reflection, the gravitational effect, or with the Sagnac effect are reexamined, particularly for the roles of earth's rotational and orbital motions.

8.2 Local-Ether Wave Equation for Free Particle

It is supposed that a free particle is represented by a wavefunction Ψ which in turn is governed by the nonhomogeneous wave equation proposed to be

$$\left\{\nabla^2 - \frac{1}{c^2}\frac{\partial^2}{\partial t^2}\right\}\Psi(\mathbf{r},t) = \frac{\omega_0^2}{c^2}\Psi(\mathbf{r},t), \tag{8.1}$$

where c is the speed of light and ω_0 is the natural frequency of the particle. This equation is the prototype of the local-ether wave equation presented in Chapters 4-6 with the gravitational and the electric scalar potential being omitted, and made its debut in [138].

Since matter wave is supposed to follow the local-ether propagation model, the position vector and the time derivative in the proposed wave equation are referred specifically to the associated local-ether frame which is an ECI frame for earthbound phenomena. As the time derivative is referred to a specific frame, its value remains unchanged when observed in different reference frames. The preceding wave equation looks like the free-space Klein-Gordan equation [58, 12, 35, 105] and like the equation dealing with the spin (as an origin of mass) given in [11], aside from the fundamental difference in the reference frame.

The natural frequency is a constant and has been found to be the origin of rest mass of the particle associated with the wavefunction Ψ. In Chapters 4 and 5 it has been shown from the local-ether wave equation incorporating the gravitational and the electric scalar potential that the natural frequency ω_0 is related to the gravitational and inertial mass m_0 of a low-speed particle in the familiar form

$$m_0 = \hbar\omega_0/c^2, \tag{8.2}$$

where $\hbar$ is Planck's constant divided by 2π. This relation states that the rest mass of a particle is just its natural frequency, with $\hbar/c^2$ serving as the scaling factor.

From the wave equation, it is seen that the wavefunction Ψ oscillates at the natural frequency when its spatial variations vanish. As the wavefunction starts to vary spatially, its temporal variation will increase accordingly. Both the spatial and the temporal variation of a wavefunction are important characteristics of wave motion and are expected to play important roles in determining physical properties of the particle associated with the wavefunction.

8.3 Dispersion of Matter Wave

Suppose that the wavefunction Ψ is a wave packet composed of plane waves with a narrow bandwidth. Each component of the plane waves is of the form of a space-time harmonic like $e^{ikx}e^{-i\omega t}$, where ω is the angular frequency, k is the propagation constant, and x is referred to the local-ether frame. Then, for each harmonic component of such a wave, the local-ether wave equation reduces to the algebraic equation

$$\omega^2 - c^2k^2 = \omega_0^2. \tag{8.3}$$

It is seen that the angular frequency and the propagation constant are related to each other. Further, owing to the presence of the natural frequency ω_0, the relationship between ω and k becomes nonlinear and hence the matter wave is dispersive. For electromagnetic wave with a zero natural frequency, the dispersion then vanishes. On the other hand, the dispersion relation is important in determining the properties of a matter wave.

It is known that the peak of a wave packet moves at its group velocity. Thus the speed v of a particle can be given by the group speed v_g of the associated wave packet, that is, $v = v_g = d\omega/dk$, where the speeds and the frequency ω as well as the coordinate x

in the harmonic are referred specifically to the associated local-ether frame. From the preceding dispersion relation, one has $\omega d\omega = c^2 k dk$ which then yields the propagation constant-speed relation

$$k = \frac{\omega}{c^2} v. \tag{8.4}$$

It is noted that the propagation constant k is proportional to the speed v with the angular frequency ω serving as a proportionality. This relation states that the spatial rate of change and the group velocity of a wave packet are closely related properties of wave motion.

From the local-ether wave equation, a first-order time evolution equation similar to Schrödinger's equation has been derived, from which it has been shown in Chapter 6 that the velocity of a particle, defined as the time derivative of expectation value of the position operator, corresponds to the expectation value of the del operator. That is, $\mathbf{v} = (-ic^2/\omega) \langle \nabla \rangle_\Psi$, where the expectation value of an operator O is evaluated in terms of the wavefunction Ψ as $\langle O \rangle_\Psi = \int \Psi^* O \Psi dv$, and the particle velocity is referred to the local-ether frame. It is of interest to note that for a wave packet, the particle velocity derived from the evolution equation is just identical to the group velocity derived simply from the dispersion relation.

On substituting (8.4) back into the dispersion relation, it is seen as in Chapter 6 that the angular frequency ω depends on the particle speed v as

$$\omega = \omega_0 \frac{1}{\sqrt{1 - v^2/c^2}}. \tag{8.5}$$

In terms of the natural frequency ω_0, the propagation constant-speed relation becomes

$$k = \frac{\omega_0}{c^2} v \frac{1}{\sqrt{1 - v^2/c^2}}. \tag{8.6}$$

As wavelength is inversely proportional to propagation constant, the wavelength associated with a wave packet also depends on the particle speed.

In terms of the rest mass m_0, the angular frequency and the propagation constant take the forms

$$\hbar\omega = \frac{m_0 c^2}{\sqrt{1 - v^2/c^2}} \tag{8.7}$$

and

$$\hbar k = \frac{m_0 v}{\sqrt{1 - v^2/c^2}}, \tag{8.8}$$

respectively. It is of essence to note that the preceding two formulas look like the postulates of de Broglie. However, the fundamental difference is that based on the local-ether wave equation, the particle speed is referred specifically to an ECI frame for earthbound particles and hence remains unchanged in different frames. The Galilean invariance of the particle speed is consistent with the frame-invariance of the propagation constant and the wavelength. Ignoring this difference in reference frames, the famous postulates of de Broglie are then consequences derived from the dispersion of matter wave.

From the frequency-speed relation (8.5), one immediately has

$$v = c\sqrt{1 - \omega_0^2/\omega^2}. \tag{8.9}$$

It is seen that the particle speed v increases monotonically with the angular frequency ω. Meanwhile, the speed of a free particle is limited to the speed of light c, as referred to the associated local-ether frame. In that limit, k and ω are quite large and thus the natural frequency ω_0 in the dispersion relation is negligible. Then the propagation characteristics of such a matter wave are close to those of electromagnetic wave. For terrestrial high-energy electrons emitted spontaneously from radiative elements or accelerated in a synchrotron, the limiting speed is expected to be referred to an ECI frame. However, as the linear speed due to earth's rotation is relatively low, it makes no substantial difference if the particle speed is referred instead to a geostationary laboratory frame, as done tacitly in common practice.

A dispersion relation quite similar to (8.3) can be found in the electromagnetic wave propagating in a plasma, with the natural frequency ω_0 being replaced by the plasma frequency [95]. Another similar dispersion can be found in the guided mode propagating in a waveguide, with the natural frequency being replaced by the cutoff frequency [95]. Hence a frequency-speed relation similar to (8.5) or (8.9) can be found in a plasma and in a waveguide.

8.4 Mass, Energy, and Momentum

The formulas for the angular frequency and propagation constant can be written in a more compact way by the use of the speed-dependent mass m which is defined in terms of the rest mass m_0 in a familiar form

$$m = m_0 \frac{1}{\sqrt{1 - v^2/c^2}}. \tag{8.10}$$

Then one has the frequency-mass relation

$$\hbar\omega = mc^2 \tag{8.11}$$

and the propagation vector-velocity relation

$$\hbar\mathbf{k} = m\mathbf{v}. \tag{8.12}$$

The speed-dependent mass m looks like that given by the famous Lorentz mass-variation law. However, the fundamental difference is that the particle velocity in the preceding formulas is referred specifically to the local-ether frame, rather than a laboratory frame or any other. Thus, for terrestrial particles, the velocity incorporates the one due to earth's rotation, while the associated wave properties are entirely independent of earth's orbital motion around the Sun.

From the preceding relations, it is seen that the rest mass m_0 and the speed-dependent mass m of a particle are just the natural frequency and the angular frequency of the associated matter wave, respectively, aside from the common scaling factor $\hbar/c^2$. Thereby, based on the local-ether wave equation, mass originates from the temporal variation of matter wave. And the mass variation originates from the dispersion of matter wave, which in turn is due to the natural frequency.

On the other hand, it is noticed that the standard derivation of the mass variation is through a quite indirect way of dealing with an elastic or inelastic collision between two identical particles, where the Lorentz transformation of space and time is used [74, 49, 9, 37]. The speed-dependent mass was first introduced by Lorentz [71] and then by Einstein (in a somewhat different form) in his original paper on the special relativity [24].

For a high-speed terrestrial particle, it may make no substantial difference whether the particle speed is referred to an ECI frame or to the ground. Nevertheless, one consequence of the local-ether wave equation is that the speed-dependent mass m as well as the matter wavelength is expected to possess an east-west directional anisotropy due to earth's rotation. That is, for a given ground speed, the particles moving eastward have the highest speed with respect to an ECI frame and hence have the heaviest mass, while those moving westward, the lightest. This terrestrial anisotropy in mass in conjunction with the mass-dependence of quantum energy of the matter wave bound in an atom has been adopted in Chapter 6 to account for the east-west directional anisotropy in clock rate observed in the Hafele-Keating experiment with circumnavigation atomic clocks.

The *momentum* and the *energy* of a particle are defined in a quantum-mechanical way to be $\langle -i\hbar\nabla\rangle_\Psi$ and $\langle i\hbar\partial/\partial t\rangle_\Psi$, the expectation values associated with the spatial and the temporal derivative of Ψ, respectively, where the time derivative is referred to the local-ether frame. Thus, for a space-harmonic wave, the momentum is related to the propagation vector by $\mathbf{p} = \hbar\mathbf{k}$. Then, according to the propagation vector-velocity relation (8.12), the momentum becomes a familiar form $\mathbf{p} = m\mathbf{v}$. However, the particle velocity $\mathbf{v}$ is referred specifically to the local-ether frame.

Besides, for a local-ether time-harmonic wave, the energy is related to the angular frequency by $\mathcal{E} = \hbar\omega$. Then, according to the frequency-mass relation (8.11), the quantum energy becomes a familiar form

$$\mathcal{E} = mc^2. \tag{8.13}$$

Ignoring the difference in the reference frame of the particle speed, the preceding formula is just the famous mass-energy relation first introduced by Poincaré in 1900 [114, 85].

For a low-speed particle, the mass-variation law (8.10) leads to

$$\hbar\omega - \hbar\omega_0 = mc^2 - m_0c^2 = \frac{1}{2}m_0v^2. \tag{8.14}$$

Thus, due to the dispersion of matter wave, the variation in the angular frequency or in the mass corresponds to the *kinetic energy* of a low-speed particle. When the spatial variation of Ψ is weak, its temporal variation is close to the one of the harmonic $e^{-i\omega_0 t}$ and then the wavefunction can be given by $\Psi(\mathbf{r},t) = \psi(\mathbf{r},t)e^{-i\omega_0 t}$, where the temporal variation of the wavefunction ψ is weak. The aforementioned time evolution equation is just expressed in terms of the reduced wavefunction ψ. It is noted that the quantum energy and the kinetic energy are given by the expectation values of the operator $i\hbar\partial/\partial t$ evaluated in terms of Ψ and ψ, respectively.

As the particle velocity is referred to a specific frame, all the values of the angular frequency, the propagation vector, the quantum energy, the kinetic energy, and the momentum then remain unchanged when observed in different reference frames. For earthbound particles, the momentum and the kinetic energy are expected to be referred specifically to an ECI frame. This differs from the common understanding, since the conventional momentum and kinetic energy are not attached to a specific frame and hence tend to be different in different frames. However, in what follows we show that the local-ether momentum and kinetic energy can comply with the conservation laws for their conventional counterparts.

Consider the collision between two low-speed particles of rest masses m_1 and m_2. It is supposed that the sum of the propagation vectors and the one of the angular frequencies of the two particles remain fixed during the collision. Thus

$$m_1\mathbf{v}_1 + m_2\mathbf{v}_2 = m_1\mathbf{v}_3 + m_2\mathbf{v}_4 \tag{8.15}$$

and

$$m_1 v_1^2 + m_2 v_2^2 = m_1 v_3^2 + m_2 v_4^2, \tag{8.16}$$

where $\mathbf{v}_1$ and $\mathbf{v}_3$ are the velocities of the particle of m_1 before and after the collision, respectively, $\mathbf{v}_2$ and $\mathbf{v}_4$ are those of the particle of m_2, and all the velocities are referred to the local-ether frame.

Then, for an arbitrary velocity $\mathbf{v}_0$, one immediately has

$$m_1(\mathbf{v}_1 - \mathbf{v}_0) + m_2(\mathbf{v}_2 - \mathbf{v}_0) = m_1(\mathbf{v}_3 - \mathbf{v}_0) + m_2(\mathbf{v}_4 - \mathbf{v}_0). \tag{8.17}$$

Besides, by the use of (8.15), one has

$$m_1(\mathbf{v}_1 - \mathbf{v}_0)^2 + m_2(\mathbf{v}_2 - \mathbf{v}_0)^2 = m_1(\mathbf{v}_3 - \mathbf{v}_0)^2 + m_2(\mathbf{v}_4 - \mathbf{v}_0)^2. \tag{8.18}$$

These two relations can be interpreted in the way that based on Galilean transformations, the conventional momentum and kinetic energy conserve as observed in a laboratory frame moving at the velocity $\mathbf{v}_0$ with respect to the local-ether frame.

It is seen that these two important quantities conserve in an arbitrary laboratory frame, though their values of respective particles are different in different frames. In other words, the conservation laws for the conventional momentum and kinetic energy are invariant under Galilean transformations and no frames are preferred, as expected in classical mechanics. Therefore, in spite of the restriction on reference frames, the local-ether wave equation can be in accord with the conservation laws and with Galilean relativity under the low-speed condition.

For the case with $m_2 \gg m_1$ and $\mathbf{v}_2 = \mathbf{v}_0$, it is seen that $\mathbf{v}_4 \simeq \mathbf{v}_0$ and then $(\mathbf{v}_1 - \mathbf{v}_0)^2 = (\mathbf{v}_3 - \mathbf{v}_0)^2$. Thus the speed, the magnitude of momentum, and the kinetic energy of a particle remain substantially unchanged before and after its collision with a rigid plane, when observed in the laboratory frame in which the reflecting plane is stationary. Meanwhile, the particle speeds v_1 and v_3 tend to be different from each other as referred to the local-ether frame. Thus the wavelength of the reflected matter wave tends to be different from that of the incident one. Since the difference between $\mathbf{v}_3$ and

$\mathbf{v}_1$ is parallel to the unit normal $\hat{n}$ of the reflecting plane, one has

$$\mathbf{v}_3 = \mathbf{v}_1 - 2(\mathbf{v}_1 - \mathbf{v}_0) \cdot \hat{n}\hat{n}. \tag{8.19}$$

Then $(\mathbf{v}_3 - \mathbf{v}_0)\cdot\hat{n} = -(\mathbf{v}_1 - \mathbf{v}_0)\cdot\hat{n}$. It is seen that the particle speeds v_1 and v_3 become identical when $\mathbf{v}_0\cdot\hat{n} = 0$, namely, the reflecting plane is stationary or moves in a direction parallel to itself.

For the case where the reflecting point is fixed on a rigid plane, the direction of the beam formed by the incident particles or by the reflected ones is determined by the particle velocity referred specifically to the reflecting plane. Thereby, one obtains the consequence that the angle of reflection of the matter wave associated with a particle beam is equal to the angle of incidence. This relationship is simply analogous to the famous Snell's law of reflection in optics.

8.5 Reexamination of Matter-Wave Interference Experiments

In this section we discuss the matter-wave interferometry, where two matter waves are coherently split off from a particle beam, then propagate respectively along two separate paths, and then are combined to cause an interference depending on the phase difference between them. It is supposed that the phase variation ϕ of the matter wave associated with a particle beam over a differential path of directed length $d\mathbf{l}$ along the beam is given by

$$\phi = \mathbf{k} \cdot d\mathbf{l}. \tag{8.20}$$

The particle velocity $\mathbf{v}$ associated with the propagation vector $\mathbf{k}$ is referred uniquely to an ECI frame for the terrestrial experiments considered in this section, while the length $d\mathbf{l}$ is not with a particular frame. This expression is identical to that adopted in the literature [106, 68], except the reference frame of the involved particle velocity.

From the preceding phase-variation formula, it is seen that a shift either in the propagation vector or in the path length along the beam tends to result in a phase difference between the two coherent beams. The Bragg reflection and the double-slit diffraction are due to the difference in path length. Besides, the propagation vector can be changed directly by the gravity on the surface of the Earth or indirectly by the rotation of the Earth or of the interferometer. Thereby, we reexamine the associated matter-wave interference experiments reported in the literature, particularly for the reference frame of particle velocity and the effects of earth's motions.

8.5.1 Bragg reflection of matter wave

The Bragg reflection from a crystal is due to the constructive interference among various reflected waves from successive lattice planes in parallel. Analogous to the Bragg reflection of x rays from a crystal, the wavelength and the propagation constant of a matter wave can be determined from the scattering from the surface of lattice planes of a known spacing by measuring the Bragg angle θ_B, the reflection angle corresponding to the constructive interference.

For a crystal of lattice spacing d, the path-length difference between two matter waves incident upon, or reflected from, two consecutive lattice planes is $d\cos\theta'$, where θ' is the angle of incidence and reflection measured from the normal $\hat{n}$ of the reflecting lattice planes, and the aforementioned Snell's law of reflection is used. Then, according to the phase-variation formula (8.20), the Bragg condition of constructive reflection is given by

$$m(v_p + \mathbf{v}_0 \cdot \mathbf{t}) d \cos\theta' = n\pi\hbar, \tag{8.21}$$

where the involved particle velocity $\mathbf{v}_p = \mathbf{v} - \mathbf{v}_0$ is referred to the laboratory frame in which the crystal is stationary, $\mathbf{v}_0$ is the laboratory velocity with respect to an ECI frame, $\mathbf{t}$ is one half of the sum of the unit vectors $\hat{v}_p$ of the incident and the reflected beam as these vectors represent the beam directions, and n is a positive integer. It is noted that the direction of $\mathbf{t}$ is parallel to the lattice plane and its magnitude is equal to $\sin\theta'$. It is seen that the Bragg angle depends on the laboratory speed and on the orientation of the lattice plane with respect to the laboratory velocity.

As the particle speed is normally much lower than the speed of light, the speed-dependent mass is substantially identical to the rest mass. On the other hand, the particle speed is supposed to be high enough so that $v_0 \ll v_p \ll c$. Thus the Bragg condition becomes a simpler form

$$m_0 v_p d \cos\theta' = n\pi\hbar. \tag{8.22}$$

As the laboratory speed v_0 can be omitted, the Bragg reflection then complies with Galilean relativity. The preceding formula is identical to that given in the literature [26], as the matter wavelength therein is understood to be associated with the particle speed referred to the laboratory frame.

The matter wavelength has been demonstrated in the Davisson-Germer experiment, where the scattering of an accelerated electron beam from the surface of a metal crystal was measured. Similarly, the matter wavelength has also been demonstrated in the diffraction ring pattern of a high-speed electron beam passing through a thin foil of polycrystalline gold [26]. Moreover, evidence for matter wavelength can be provided by the diffraction from macroscopic objects, such as Young's double slit. As in optics, it is expected that the period of the interference fringe pattern is proportional to the wavelength and to the inverse of the slit separation. Single-, double-, and multiple-slit diffraction of matter wave have been demonstrated with the particle beam of electrons [52], neutrons [116], or atoms [16].

In these various experiments demonstrating the matter wavelength, the reference frame of the particle velocity is often not specified explicitly and is supposed to be a geostationary laboratory frame. In what follows, we address ourselves to the issue of the reference frame and the effects of earth's rotation. Consider the isotropic case where the speed of the particles with respect to the ground is independent of the beam direction, such as the speed gained electrostatically with a given voltage or the root-mean-square speed in thermal equilibrium at a certain temperature. However, due to earth's rotation the local-ether model immediately leads to the asymmetry that for a given ground speed, the terrestrial particles moving eastward have the shortest wavelength, while those moving westward have the longest one. The predicted anisotropy in matter wavelength tends to be much stronger than the one in mass, since the wavelength is proportional to the inverse of the particle speed aside from the common speed-dependent mass-variation factor.

Consider the terrestrial anisotropy associated with electron wave quantitatively. In order to have a matter wavelength of one angstrom (the order of lattice spacing), the speed for electrons is 7.4×10^6 m/s. This speed is much higher than that due to earth's rotation. Obviously, it makes no substantial difference whether the speed is referred to an ECI frame or to the ground. Thus, for this matter wave the predicted anisotropy in wavelength due to earth's rotation is difficult to detect. Therefore, the local-ether model is actually in accord with the Davisson-Germer experiment and others associated with electron wave, as examined within the present precision.

On the other hand, for heavier particles, such as neutrons and atoms, the effects of earth's rotation would be more appreciable. For example, in order to have a matter wavelength also of one angstrom, the speed for neutrons is 4×10^3 m/s, which is higher than the linear speed due to earth's rotation merely by a factor of about 10. In the Bragg reflection from a geostationary crystal, the ground speed of the reflected particles is identical to that of the incident ones.

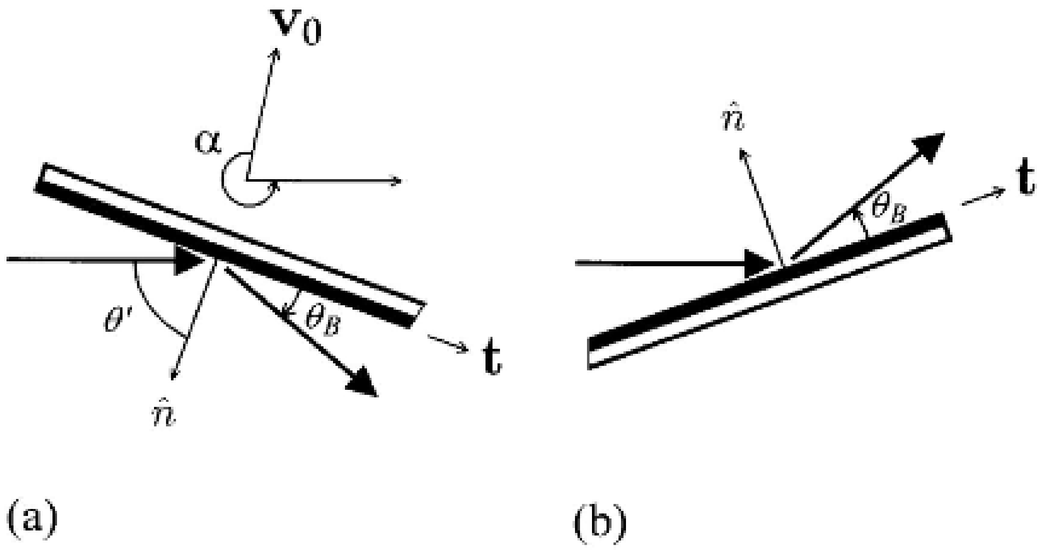

Fig. 9 Bragg reflection of matter wave. For a given particle beam incident upon a crystal slab rotatable about an axis perpendicular to the plane of incidence, there are two values for the Bragg angle θ_B, as shown in (a) $\theta_B < 0$ and (b) $\theta_B > 0$. The incident beam makes an angle of α from the laboratory velocity $\mathbf{v}_0$.

However, the wavelength of the reflected neutron beam is expected to be different from that of the incident one, except when the laboratory velocity is parallel to the lattice plane and thus $\mathbf{v}_0 \cdot \hat{n} = 0$ (such as in the case with a geostationary and horizontal lattice plane). Further, the Bragg angle and the fringe period in Young's slit diffraction are expected to depend on the orientation of the experimental setup with respect to the ground.

8.5.2 Predicted anisotropy in Bragg angle due to earth's rotation

We then proceed to examine the minute effect due to the laboratory velocity. Let the Bragg angle θ_B be measured from the lattice plane represented by the vector $\mathbf{t}$ to the direction of reflection. Then the deflection angle of the particle beam measured from incidence to reflection is $2\theta_B$. For a given particle beam incident upon a rotatable crystal slab, there are two values for the Bragg angle θ_B, one positive and one negative, which are associated with two orientations of the slab symmetric with respect to the incident beam if the anisotropy in matter wavelength is omitted (see Fig. 9).

Suppose that the laboratory velocity $\mathbf{v}_0$ lies in the plane of incidence and that the incident beam makes an angle of α from the direction of $\mathbf{v}_0$. Thus the vector $\mathbf{t}$ makes an angle of $\alpha + \theta_B$ from that direction. Then the Bragg condition (8.21) becomes

$$m_0 \{v_p + v_0 \cos(\alpha + \theta_B) \cos\theta_B\}\, d|\sin\theta_B| = n\pi\hbar, \tag{8.23}$$

where $\theta_B = \pm(\pi/2 - \theta')$ is used. The presence of $\mathbf{v}_0$ complicates the dependence on θ_B and makes Galilean relativity break down.

Consider the Bragg reflection of neutron wave from a pyrolytic graphite crystal briefly reported in [106], where the laboratory is geostationary, the plane of incidence is horizontal, and the incident neutron beam is directed due south ($\alpha = -90°$). Then the Bragg condition becomes

$$|\sin\theta_B|\, \{1 + (v_0/2v_p)\sin 2\theta_B\} = n\pi\hbar/m_0 v_p d. \tag{8.24}$$

The lattice constant is reported to be $d = 6.708$ angstroms with $n = 4$; the neutron wavelength is estimated to be $\lambda = 1.134$ angstroms and hence it is understood that $v_p = 3490$ m/s; and the laboratory is located at latitude 38.63° and hence $v_0 = 362$ m/s [106].

Then, according to the preceding formula, the predicted Bragg angles are $\theta_1 = -20.48°$ and $\theta_2 = 19.11°$. A positive or negative Bragg angle corresponds to the situation that the beam is reflected toward the east or west, respectively. It is noted that the beam reflected westward deflects more in magnitude than the one eastward. The difference in magnitude between the two Bragg angles is associated with the speed ratio v_0/v_p and represents an effect of earth's rotation. Physically, this anisotropy in the Bragg angle is a consequence of the rotation-induced anisotropy in matter wavelength.

The constructive reflection at the Bragg angle results in a minimum transmission through the crystal, which in turn can be detected by a counter. The measured results of the slab rotation angle for a minimum transmission are $\theta_3 = 19.14°$ and $\theta_4 = 159.63°$ [106], where the orientation corresponding to the starting value of the rotation angle is not specified explicitly. It is understood to correspond to the orientation with which the normal to the reflecting crystal surface is directed due west. And a rotation angle of 90° corresponds to the normal being directed due north. Thus θ_5 ($= -\theta_3$) and θ_6 ($= 180° - \theta_4 = 20.37°$) should be identical to θ_1 and θ_2, respectively.

It is seen that the two Bragg reflections are asymmetric, as predicted by the local-ether model. However, the agreement is not good quantitatively. This discrepancy in the Bragg angle deserves further study. Moreover, both Bragg angles are expected to depend on

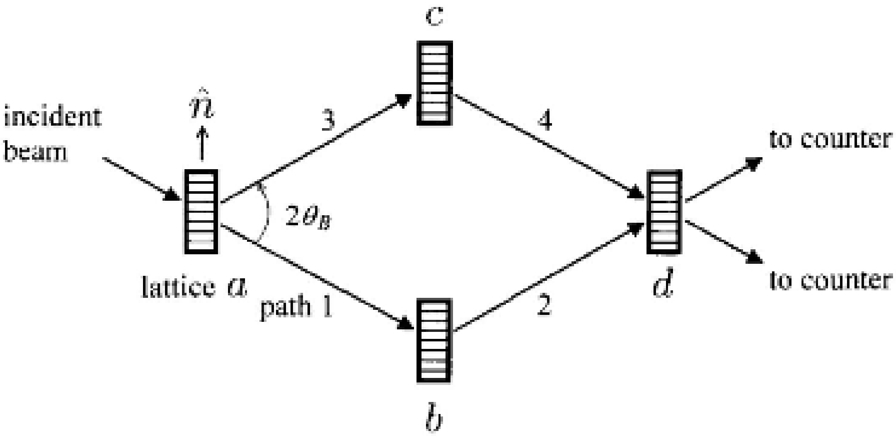

Fig. 10 Matter-wave interferometry. The neutron-wave loop interferometer is formed by four slabs of silicon crystal which support the Bragg reflection.

the incident direction represented by α. The predicted terrestrial anisotropy in the Bragg angle in neutron reflection due to earth's rotation provides a means to test the local-ether wave equation.

8.5.3 Effect of earth's gravity in neutron interferometry

By using the Bragg reflection from slabs of silicon crystal to form a closed path for the neutron beam, the loop interferometry of neutron wave has been achieved [106, 68]. As depicted in Fig. 10, part of the incident neutron beam is transmitted through a silicon slab (lattice a) to travel along path 1; meanwhile, the other part is reflected by this slab to travel along a different path 3. The angle of path 3 from path 1 is then $2\theta_B$. Thus the incident beam is split into two coherent beams along two separated paths.

Thereafter, the two beams are reflected by lattices b and c, respectively, and then are combined by another lattice d. The intensity of the combined neutron beam is measured by using counters to determine the phase difference between the beam along paths 1 and 2 and the one along paths 3 and 4. The four silicon slabs are parallel to each other and the four paths of directed length $\mathbf{l}_i$ form a closed path of parallelogram shape, where the index $i = 1, 2, 3, 4$. As the vector $\mathbf{t}$ for all the reflecting lattice planes is identical, the Bragg angle θ_B involved in the interferometry is identical in magnitude.

Suppose that the velocity of the neutron beam in path i is $\mathbf{v}_i$ and that the velocity of the laboratory frame in which the lattices are stationary is $\mathbf{v}_0$, all referred to an ECI frame. For a geostationary laboratory, the velocity $\mathbf{v}_0$ is due to earth's rotation alone. Then, from (8.19), it is seen that the collision of the particles with the rigid planes leads to $\mathbf{v}_4 = \mathbf{v}_1$ and

$$\mathbf{v}_2 = \mathbf{v}_3 = \mathbf{v}_1 - 2(\mathbf{v}_1 - \mathbf{v}_0) \cdot \hat{n}\hat{n}, \tag{8.25}$$

where the unit normal of all the reflecting lattice planes is given by $\hat{n} = (\hat{l}_2 - \hat{l}_1)/\sqrt{2 - 2\hat{l}_2 \cdot \hat{l}_1}$, $\hat{l}_i = \mathbf{l}_i/l_i$, and $l_i = |\mathbf{l}_i|$. It is noted that the particle speed v_p $(= |\mathbf{v}_i - \mathbf{v}_0|)$ with respect to the laboratory frame is identical in the four paths.

Further, as the phase variation ϕ of a matter wave over a linear path of directed length $\mathbf{l}$ along the particle beam is given by $\phi = \mathbf{k} \cdot \mathbf{l}$, the phase difference between the two coherent neutron beams along the paths is given by

$$\triangle\phi\hbar/m_0 = -\mathbf{v}_1 \cdot \mathbf{l}_1 - \mathbf{v}_2 \cdot \mathbf{l}_2 + \mathbf{v}_3 \cdot \mathbf{l}_3 + \mathbf{v}_4 \cdot \mathbf{l}_4, \tag{8.26}$$

where the particle speed v_i is low and hence the mass is given simply by the rest mass m_0. The direction of $\mathbf{v}_i$ tends to be different from that of $\mathbf{l}_i$. Anyway, due to the symmetry in the particle velocities ($\mathbf{v}_1 = \mathbf{v}_4$ and $\mathbf{v}_2 = \mathbf{v}_3$) and in the paths ($\mathbf{l}_1 = \mathbf{l}_4$ and $\mathbf{l}_2 = \mathbf{l}_3$), the phase difference becomes zero.

We then consider the case where earth's gravity is taken into account. Due to the acceleration of gravity $\mathbf{g}$, the particle velocity $\mathbf{v}_i$ tends to change continuously by an amount of $\mathbf{g}t$, where t is the time interval after the particle enters path i. (If the gravity $m_0\mathbf{g}$ is understood to be associated with the gravitational mass, then the identity of gravitational and inertial mass can be used, which is also a consequence derived from the local-ether wave equation as discussed in Chapter 5.) Thus, over path 1 or 4 or over path 2 or 3, this gravity term results in an additional phase variation (multiplied by $\hbar/m_0$) of $\mathbf{l}_1 \cdot \mathbf{g}\tau_1/2$ or $\mathbf{l}_2 \cdot \mathbf{g}\tau_2/2$, respectively, where τ_i is the traveling time over path i and is assumed to be short. It is noted that the traveling time is given by $\tau_i = l_i/v_p$, determined by the particle speed referred to the laboratory frame in which the paths are stationary.

Meanwhile, due to the collision with lattice b, the particle velocity $\mathbf{v}_2$ acquires an additional amount of $\tau_1(\mathbf{g} - 2\mathbf{g} \cdot \hat{n}\hat{n})$, since over path 1 $\mathbf{v}_1$ changes by $\mathbf{g}\tau_1$ immediately before the collision. Thus, over path 2, the total contribution to the phase variation due to the gravity is the sum $\mathbf{g} \cdot (\hat{l}_1 l_2 \tau_1 + \mathbf{l}_2 \tau_2/2)$, where the first term is associated with the collision and is a result of the relation $(\mathbf{g} - 2\mathbf{g} \cdot \hat{n}\hat{n}) \cdot \hat{l}_2 = \mathbf{g} \cdot \hat{l}_1$. Similarly, by taking the collision with lattice c into account, the phase variation over path 4 due to the gravity is the sum $\mathbf{g}\cdot(\hat{l}_2 l_1 \tau_2 + \mathbf{l}_1\tau_1/2)$. Thus the gravitation-induced phase difference becomes

$$\triangle\phi\hbar/m_0 = \mathbf{g}\cdot(\hat{l}_2 - \hat{l}_1)l_2 l_1/v_p. \tag{8.27}$$

It is noted that some of the terms due to the gravity cancel out and the surviving terms in the phase difference are associated with the collision of particles with the lattice planes.

It can be shown that if the just-mentioned collision associated with the gravity terms were omitted, the phase difference would happen to be the one given by the preceding formula with a change of sign. It will be shown later that the preceding formula leads to a gravitation-induced phase difference identical to the one given in [106, 68] which in turn is derived from an alternative approach based on the Hamiltonian and has been demonstrated experimentally. It is noted that unlike the Bragg condition, the preceding formula for matter-wave interference is independent of the laboratory velocity $\mathbf{v}_0$. This is a consequence of the situation that the paths in the interferometer form a loop and then the effect of $\mathbf{v}_0$ cancels out collectively. Thus, in spite of the restriction on the reference frame of the particle velocity $\mathbf{v}_i$, the gravitation-induced quantum interference complies with Galilean relativity.

8.5.4 Effect of earth's rotation in neutron interferometry

More precisely, owing to earth's rotation and the minute differences in geocentric position, the velocities of the various reflecting lattices tend to be different among themselves. Thus the lattice velocity $\mathbf{v}_l$ with respect to an ECI frame is not exactly equal to the laboratory velocity $\mathbf{v}_0$, but is given by $\mathbf{v}_l = \mathbf{v}_0 + \boldsymbol{\omega}_E \times (\mathbf{r} - \mathbf{r}_0)$, where $\mathbf{r}$ and $\mathbf{r}_0$ denote the position vector of the reflecting point on the lattice and of a suitable reference point at which the laboratory velocity is defined, respectively, and $\boldsymbol{\omega}_E$ is the directed rate of earth's rotation.

Hence the particle velocities $\mathbf{v}_2$ and $\mathbf{v}_3$ given in (8.25) together with $\mathbf{v}_4$ need some modifications. It is seen from (8.19) that due to the collision of particles with the rigid lattices b and a, the velocities $\mathbf{v}_2$ and $\mathbf{v}_3$ are given by (8.25) with $\mathbf{v}_0$ being replaced by the lattice velocities $\mathbf{v}_{lb}$ and $\mathbf{v}_{la}$, respectively. And it is easy to show that due to the collision with lattice a and then lattice c, the velocity $\mathbf{v}_4$ is given by

$$\mathbf{v}_4 = \mathbf{v}_1 - 2(\mathbf{v}_{la} - \mathbf{v}_{lc})\cdot\hat{n}\hat{n}, \tag{8.28}$$

where $\hat{n}$ is the normal given previously and the gravity is neglected for simplicity.

Then, due to the symmetry in the paths, the phase difference (8.26) becomes

$$\triangle\phi\hbar/m_0 = -2(\mathbf{v}_{la} - \mathbf{v}_{lc}) \cdot \hat{n}\hat{n} \cdot \mathbf{l}_1 + 2(\mathbf{v}_{la} - \mathbf{v}_{lb}) \cdot \hat{n}\hat{n} \cdot \mathbf{l}_2. \quad (8.29)$$

The velocity differences among the various lattices can be given by $\mathbf{v}_{la} - \mathbf{v}_{lb} = -\boldsymbol{\omega}_E \times \mathrm{l}_1$ and $\mathbf{v}_{la} - \mathbf{v}_{lc} = -\boldsymbol{\omega}_E \times \mathbf{l}_2$. By expressing the normal $\hat{n}$ in terms of $\hat{l}_1$ and $\hat{l}_2$, it is easy to show that the rotation-induced phase difference becomes

$$\triangle\phi\hbar/m_0 = 2\boldsymbol{\omega}_E \cdot \mathbf{S}, \quad (8.30)$$

where $\mathbf{S}$ $(= \mathbf{l}_2 \times \mathbf{l}_1)$ is the directed area of the loop formed by the paths and its magnitude $S = l_1 l_2 \sin 2\theta_B$.

This rotation-induced phase difference is identical to the one given in [106, 68] which is derived from the Hamiltonian approach and has been demonstrated experimentally. Again, it is seen that the preceding formula is independent of the laboratory velocity $\mathbf{v}_0$. Thus, in spite of the restriction on the reference frame of the particle velocity, the rotation-induced quantum interference also complies with Galilean relativity. The preceding formula is known to exhibit the matter-wave Sagnac effect, as it is similar to the one of the Sagnac effect for electromagnetic wave discussed in Chapters 1 and 3, though the latter effect is due to a different mechanism of the rotation-induced modification of the propagation length.

Specifically, consider the situation where paths 1 and 4 are positioned horizontally as that discussed in [106, 68]. The loop is rotated about a horizontal axis accommodating path 1 by a rotation angle α, where $\alpha = 0$ corresponds to the loop lying in a horizontal plane. The rotation axis is parallel to $\mathbf{l}_1$ or to the incident beam directed due south, so that path 4 is raised to a higher position than path 1 when $0 < \alpha < \pi$. Thus $\mathbf{g}\cdot\hat{l}_1 = 0$ and $\mathbf{g}\cdot\hat{l}_2 = -g \sin 2\theta_B \sin\alpha$. Then the phase difference due to earth's rotation and gravity becomes

$$\triangle\phi\hbar/m_0 = -2\omega_E S \cos\theta_L \cos\alpha - gS \sin\alpha/v_p, \quad (8.31)$$

where θ_L is the colatitude angle. This formula is identical to that given in [68].

Consider another specific situation where the loop is oriented in such a way that paths 1 and 4 are positioned vertically as that discussed in [106]. The loop is rotated about a vertical axis accommodating path 1 by a rotation angle α, where $\alpha = 0$ corresponds to the loop facing due west. The rotation axis is antiparallel to l_1

or to the incident beam directed upward, so that the loop faces due north or south when $\alpha = \pi/2$ or $3\pi/2$, respectively, and thus the directions follow those given in Fig. 21 in [106]. Thus $\mathbf{g}\cdot\hat{l}_1 = -g$ and $\mathbf{g}\cdot\hat{l}_2 = -g\cos 2\theta_B$. Then the phase difference due to earth's rotation and gravity becomes

$$\triangle\phi h/m_0 = 2\omega_E S\sin\theta_L\sin\alpha + gS\tan\theta_B/v_p. \tag{8.32}$$

Obviously, the phase difference due to the gravity is independent of α. Thus, as the loop is rotating around the axis with a changing α, the variation of the phase difference is due to earth's rotation alone.

The derivation of the effects of earth's rotation and gravity in the neutron interferometry adopted in [106, 68] is based on the Hamiltonian which is a function of space and incorporates the kinetic energy with the inertial mass, the gravitational energy with the gravitational mass, and an additional energy term with earth's rotation rate and the angular momentum. Then, from Hamilton's equations, the canonical momentum is derived, which incorporates the gravity term $\mathbf{g}t$, the linear velocity due to earth's rotation, and other minor terms. In the derivation, the gravitational mass is made equal to the inertial mass, by resorting to the principle of equivalence. Then the gravitation- and rotation-induced quantum interferences are derived, which apparently agree with those based on the local-ether wave equation and the collision with the lattices.

Another approach, somewhat similar to the presented one, has been given for the rotation-induced phase difference, where a Doppler effect on the propagation vectors of the waves reflected from moving lattices is used in the derivation for matter and optical waves [23]. In the Hamiltonian approach to the rotation-induced phase difference, it has been supposed tacitly that the effect of earth's rotation on the matter wave is a function of space and hence the propagation vector tends to change continuously during the traveling of the particles along the paths. On the other hand, in our collision approach or in [23], earth's rotation changes the properties of the matter wave merely at the instants when the particles collide with the lattices.

8.5.5 Matter-wave Sagnac effect in rotating loop

Further, we discuss the Sagnac effect for matter wave associated with the rotation of an interferometer that has a closed path formed by a series of reflecting planes of suitable orientations. For simplicity, the gravity is neglected and the particle velocity is supposed to be altered only by the collision with the planes. Consider two coherently split particle beams forming two paths L_1 and L_2 which in turn form a coplanar closed contour L of arbitrary shape. Suppose that the loop L is rotating about an axis at an arbitrary location with a directed rotation rate $\boldsymbol{\omega}_I$ with respect to the laboratory frame which in turn is rotating with the rate $\boldsymbol{\omega}_E$ in an ECI frame. Thus the velocities $\mathbf{v}_l$ of the various reflecting planes forming the path are not uniform and are given by $\mathbf{v}_l = \mathbf{v}_0 + (\boldsymbol{\omega}_I + \boldsymbol{\omega}_E) \times (\mathbf{r} - \mathbf{r}_0)$ with respect to an ECI frame, where the reference point $\mathbf{r}_0$ can be on the axis.

The direction of the particle beam in each path segment between two consecutive planes is determined by the propagation vector given by $\mathbf{k}_p = m\mathbf{v}_p/\hbar$, where $\mathbf{v}_p$ $(= \mathbf{v} - \mathbf{v}_l)$ is the particle velocity with respect to the associated reflecting plane. For the trivial case with $\omega_I = 0$, the lattice velocity $\mathbf{v}_l$ is substantially uniform among the planes, as earth's rotation rate is low. Thus the particle velocity $\mathbf{v}_p$, the propagation vector $\mathbf{k}_p$, and the particle beam in each path segment are all along the directed linear segment $\mathbf{l}$ connecting the reflecting point on one of the two consecutive planes and that on the other. Consequently, the term $\mathbf{k}_p \cdot \mathbf{l}$ incorporated in the phase variation $\mathbf{k} \cdot \mathbf{l}$ over the path segment $\mathbf{l}$ is then equal to the scalar product $k_p l$. Furthermore, the particle speed v_p is fixed while the particle beam is traveling along the various segments of paths L_1 and L_2.

However, for the case with $\omega_I \neq 0$, the lattice velocity $\mathbf{v}_l$ is varying among the planes. Thus the direction of the particle beam, as well as that of $\mathbf{v}_p$ and $\mathbf{k}_p$, tends to deviate from the direction of the segment l. Nevertheless, the effect of these deviations on the phase variation can be negligible if the rotation rate ω_I times the segment length l is much smaller than the particle speed v_p. Actually, it is merely of the second order of the speed ratio $\omega_I l/v_p$, since the difference in lattice velocity between two consecutive planes under rotation is perpendicular to the segment $\mathbf{l}$. Similarly, the fractional variation of the particle speed v_p among the various segments of paths L_1 and L_2 is also of this order.

The phase difference between the coherent beams along the two paths can be given by the path integral

$$\triangle\phi = -\int_{L_1} \mathbf{k} \cdot \hat{l}_1 dl \; + \; \int_{L_2} \mathbf{k} \cdot \hat{l}_2 dl = \oint_L \mathbf{k} \cdot d\mathbf{l}, \tag{8.33}$$

where $d\mathbf{l} = -\hat{l}_1 dl$ and $\hat{l}_2 dl$ for paths L_1 and L_2, respectively. For a loop that is formed by closely spaced reflecting planes or is undergoing a slow rotation so that the condition $\omega_I l \ll v_p$ is met for every segment, the differential phase variations $\mathbf{k}_p \cdot \hat{l}_1 dl$ and $\mathbf{k}_p \cdot \hat{l}_2 dl$ can then be given by $k_p dl$. Further, as the mass variation can be neglected, k_p as well as v_p remains a substantially fixed value in the various segments of the loop. Thereby, the phase difference becomes

$$\triangle\phi = k_p(l_2 - l_1) + \frac{m_0}{\hbar} \oint_L \mathbf{v}_l \cdot d\mathbf{l}, \tag{8.34}$$

where l_1 and l_2 are the lengths of paths L_1 and L_2, respectively.

For the case where the path is suitably constructed so that $l_1 = l_2$, the phase difference then takes the form

$$\triangle\phi = \frac{2\omega_0}{c^2}(\boldsymbol{\omega}_I + \boldsymbol{\omega}_E) \cdot \mathbf{S}, \tag{8.35}$$

where $\mathbf{S}$ $(= \frac{1}{2} \oint_L \mathbf{r} \times d\mathbf{l})$ denotes the directed area enclosed by the coplanar loop L, and we have made use of a vector identity and of the result that the integral of a constant vector $\mathbf{v}_0$ or $\mathbf{r}_0$ over an arbitrary loop is zero. It is noted that the phase difference is then independent of the particle speed and the matter wavelength. It is seen that both earth's rotation and the rotation of the loop with respect to the ground contribute to the phase difference, as the lattice velocity $\mathbf{v}_l$ is referred to an ECI frame.

The phase-difference formula (8.35) with either $\boldsymbol{\omega}_I$ or $\boldsymbol{\omega}_E$ agrees with the one for the matter-wave Sagnac effect derived from quite various approaches [87, 106, 23, 40]. The matter-wave Sagnac effect associated with the rotation-induced quantum interference has been demonstrated with a particle beam of electrons [40], atoms [65, 38], or of neutrons discussed previously. In these experiments, the loop can be rotating with a turntable [40, 65] or simply be geostationary with a variable orientation [106, 68].

It is noted that the phase difference given by (8.35) is identical to the one for optical wave discussed in Chapters 1 and 3 when the natural frequency ω_0 is replaced with the angular frequency of an optical wave, aside from a factor of 2 due to a difference in the path structure. As the natural frequency of matter wave is much higher than the optical frequency, the loop area required for a matter wave can be much smaller. It is noticed that in the aforementioned neutron interferometry for the detection of earth's rotation, the loop area is about 10^{-3} m^2 [106, 68], which is much smaller than 2×10^5 m^2 employed in the Michelson-Gale experiment for the same purpose with an optical wave [6]. By using a cesium atomic beam, the detection of earth's rotation has also been reported [38].

On the other hand, in as early as 1904 Michelson supposed that the Sagnac effect due to the orbital motion of the Earth around the Sun might be detectable [6], though the angular speed of the orbital motion is about 1/366 times that of the rotation. If this orbital effect does exist, it could be demonstrated with a matter wave of neutrons or atoms by constructing a path enclosing an area of 0.2 m^2 or smaller. However, the orbital effect is never observed in earthbound interferometers either with electromagnetic or with matter wave, to our knowledge. In some terrestrial experiments with electromagnetic wave, this effect has been assumed to be null by resorting to the principle of local Lorentz invariance [6].

Anyway, according to the local-ether propagation model, the particle velocity that determines the propagation vector $\mathbf{k}$ of an earthbound matter wave is referred uniquely to an earth-centered inertial frame, rather than to the ground, to a heliocentric inertial frame, or to any other. Thus earthbound experiments can depend on earth's rotation but are entirely independent of earth's orbital motion around the Sun or whatever. Thereby, the local-ether wave equation unambiguously predicts a discrepancy between the effects of earth's rotational and orbital motions in the Bragg reflection and in the loop interferometry, as well as in many other earthbound experiments discussed in previous Chapters, which then provides a means to test its validity. Moreover, the phase-difference formula (8.35) is not expected to hold for an interferometer with a high rotation rate, especially when the particle speed v_p is low. This restriction provides another means to test the local-ether wave equation.

8.6 Summary

The local-ether wave equation for free particles looks like the free-space Klein-Gordan equation, except the reference frame of the position vector and time derivative. By virtue of the natural frequency, the wave equation leads to the dispersion of matter wave. From the dispersion relation, the angular frequency and wavelength of a wave packet and the speed-dependent mass of a particle are derived. The formulas are identical to the postulates of de Broglie and the Lorentz mass-variation law, except the reference frame of the particle velocity. For a space- and time-harmonic matter wave, the angular frequency and the propagation vector correspond to the energy and the momentum of the particle, respectively, as the energy and the momentum are given by the expectation values associated with the temporal and the spatial derivative of the wavefunction, respectively.

As the phase variation of the matter wave representing a particle beam is given by the propagation vector and the path length along the beam, a shift in either of these quantities then leads to a phase difference between two coherent beams. From the difference in the path length in a crystal, the Bragg condition of constructive reflection is derived. Besides, from the shift in the propagation vector due to the gravity, earth's rotation, or a rotation of the interferometer, the phase differences in the loop interferometry are derived.

As the velocity that determines the properties of matter wave is referred uniquely to an ECI frame for earthbound particles, it is predicted that earth's rotation leads to an east-west directional anisotropy both in mass and in matter wavelength. Moreover, the particle velocity involved in earthbound matter-wave interference experiments incorporates the laboratory velocity with respect to an ECI frame. For electrons, the mass is light and the speed is normally high. The anisotropy due to earth's rotation or the effect associated with the laboratory velocity is then negligibly small. Thereby, the local-ether model for electron wave is actually in accord with the Davisson-Germer experiment and Young's slit diffraction as examined within the present precision. Further, the effect with the laboratory velocity can cancel out in a loop interferometer. Consequently, in spite of the restriction on the reference frame of particle velocity, the derived interference formulas for the Bragg reflection and the loop interferometry can be independent of the laboratory velocity and then comply with Galilean relativity.

On the other hand, for neutrons or atoms, the effects of earth's rotation on matter wavelength are expected to be more appreciable. It is predicted that the Bragg angle and the fringe period in Young's slit diffraction depend on the orientation of the experimental setup with respect to the ground. Thus the terrestrial isotropy and Galilean relativity break down. For a given incident neutron beam, it is inferred that the Bragg angle can deviate by an amount of about one degree between two orientations of the crystal. The predicted terrestrial anisotropy in the Bragg angle and in the fringe period, the slow-rotation restriction for the famous formula for the matter-wave Sagnac effect, and the discrepancy between the effects of earth's rotational and orbital motions provide different approaches to test the local-ether wave equation.

Epilogue

The theory of *Quantum Electromagnetics* is based on a local-ether wave equation which unifies quantum mechanics, electromagnetics, and gravitation, and accounts for a wide variety of experiments. This wave equation incorporates a natural frequency and leads to the speed-dependent frequency and wavelength of the matter wave of a free particle and to its speed-dependent mass. By incorporating the electric scalar potential, the wave equation leads to the speed-dependent quantum energy of the matter wave of a particle bound in an atom. With the electric scalar potential being connected with the augmentation operator, which is derived from the Laplace operator and the velocity of the source particles, a first-order time evolution equation is derived, which represents modifications of Schrödinger's equation. From this modified equation, an electromagnetic force law is derived, which represents modifications of the Lorentz force law. From the modified force law, relationships among the spatial and temporal derivatives of the electric and magnetic fields are derived, which represent modifications of Maxwell's equations. These modified equations are substantially identical to their counterparts observed in the matrix or atom frame as done tacitly in common practice. Furthermore, by refining the d'Alembert operator in the wave equation with a gravitational potential, the gravitational force is also derived. Thereby, the wave equation leads to a unified quantum theory of gravitational and electromagnetic forces in conjunction with the wave-motion origin and the identity of gravitational and inertial mass.

The groundwork of this wave equation is that both electromagnetic and matter waves are proposed to propagate according to the local-ether model. That is, the wave propagates via a medium like the ether. However, the ether is not universal. It is supposed that in the region under a sufficient influence of the gravitation due to the Earth, the Sun, or another celestial body, there forms a local ether which in turn comoves with the gravitational potential of the respective body. In this local-ether theory all the involved physical quantities of the position vectors, time derivatives, propagation velocity, particle velocities, and current density are referred specifically to their respective frames and hence remain unchanged in different frames under Galilean transformations.

In spite of such a restriction on reference frames, the consequences of this brand-new theory account for a spate of experiments associated with the propagation or interference of electromagnetic wave, and are in accord with a wide variety of experiments commonly ascribed to the special relativity, the general relativity, the Lorentz mass-variation law, or to the de Broglie matter wave. These experiments demonstrate various phenomena, including the Sagnac effect in the global positioning system (GPS), the intercontinental microwave link, the rotating-loop interferometer, and in the Michelson-Gale experiment; the round-trip Sagnac effect in the interplanetary radar; the apparently null effect in the Michelson-Morley experiment; the constancy of the speed of light with a moving source; the spatial isotropy with phase stability in the Kennedy-Thorndike experiment and the one-way fiber-link experiment; the Doppler effects and spatial anisotropy in Roemer's observations and the cosmic microwave background radiation; the effects of the moving medium in Fizeau's experiment and the Sagnac loop interferometry; the gravitational deflection of light by the Sun; the gravitational effect on the interplanetary radar echo time; the gravitational redshift in the Pound-Rebka experiment; the gravitation- and speed-dependent atomic clock rate in GPS, the Hafele-Keating experiment, and in the spacecraft microwave links; the spatial isotropy with frequency stability in the Hughes-Drever experiment and the cavity heterodyne experiment; the resonant absorption in the Ives-Stilwell experiment, the ammonia-maser experiment, and in the Mössbauer rotor experiment; the matter-wave Bragg reflection in the Davisson-Germer experiment; the matter-wave Sagnac effect; and the effects of earth's rotation and gravity in the neutron-wave loop interferometry. Moreover, in spite of the restriction on reference frames, many consequences of the local-ether wave equation can comply with Galilean relativity, including the magnetic force, the electric induction, the propagation and interference of electromagnetic wave, the interference of matter wave, the quantum effect in an atom, and the resonant absorption between atoms.

Meanwhile, this theory leads to some predictions, particularly those with the effects of earth's motions. Based on the round-trip Sagnac effect due to earth's rotation, we predict a quadrupole anisotropy in phase difference in the Michelson-Morley experiment and a like one in beat frequency in the cavity heterodyne experiment. Further, based on the one-way Sagnac effect due to earth's rotation, we propose the one-way-link rotor experiment, in which a strong first-order terrestrial anisotropy in phase variation is predicted. Moreover, in the radar tracking of low-earth-orbit satellites, a transverse Doppler shift is predicted; in the magnetic deflection an effect of the relative motion between the deflection yokes and the accelerating electrodes is predicted; in the Sagnac loop interferometry, various index-dependences among the phase-difference terms associated with the rotation rates of the Earth and the loop are predicted; in the interaction of atoms with electromagnetic radiation, a stronger second-order effect is predicted; in the gravitational redshift the quantum origin and the transition-dependence are predicted; in the stellar spectrum a gravitation-induced downshift depending on the mass of the star is predicted; in the interplanetary spacecraft microwave link, a constant deviation in frequency shift associated with the role of earth's orbital motion for the clock at the ground station is predicted; and in the neutron diffraction a terrestrial anisotropy in matter wavelength and the Bragg angle due to earth's rotation is predicted. These various predictions then provide different approaches to test the validity of the local-ether wave equation.

Appendix A

Derivation of Wave Equations for Potentials and of Lorenz Gauge

The electric scalar potential Φ due to a distribution of charge of density ρ is given by the integral over a volume containing all the charges

$$\Phi(\mathbf{r}, t) = \frac{1}{\epsilon_0} \int G(R) \rho(\mathbf{r}', t - R/c) dv', \tag{A.1}$$

where Green's function G is defined as

$$G(R) = \frac{1}{4\pi R}, \tag{A.2}$$

$R = |\mathbf{r} - \mathbf{r}'|$, c is the speed of light, and R/c represents the time retardation.

A.1 Poisson equation for Green's function

It is known that Green's function satisfies the Poisson equation [126]

$$\nabla^2 G(R) = -\delta(R), \tag{A.3}$$

where the delta function $\delta(R)$ is defined in the sense that its volume integral is equal to unity if the integration volume contains the point $R = 0$ ($\mathbf{r} = \mathbf{r}'$). The derivation is given in what follows.

As R approaches zero, then $\nabla^2 G$ becomes singular, but is still integrable. For a volume V being a sphere of radius a and centered at the source point, one has

$$\int_V \nabla^2 G(R) dv = \oint_S \nabla G \cdot d\mathbf{s} = 4\pi R^2 \left(\frac{-1}{4\pi R^2} \right) \Bigg|_{R=a} = -1, \tag{A.4}$$

where S is the enclosing surface of V and the direction of $d\mathbf{s}$ is normal to S. Here, as in common practice, the divergence theorem has been used. However, it is noticed that the divergence theorem is valid only for a vector function which and the first partial derivatives of which are continuous in a volume containing V, whereas Green's function and its derivatives are singular at the point $R = 0$. Nevertheless, the difficulty with the mathematical legitimacy can be avoided by using a physical argument associated with a regularization of Green's function, as discussed in [126].

A.2 Wave equations for potentials

By applying the Laplace operator to both sides of the integral formula for the retarded potential Φ, one has

$$\nabla^2\Phi(\mathbf{r},t) = \frac{1}{\epsilon_0}\int \nabla^2[G(R)\rho(\mathbf{r}',t-R/c)]dv'. \tag{A.5}$$

Then, by a direct expansion, the integrand becomes

$$\nabla^2[G\rho] = G\nabla^2\rho + 2\nabla G\cdot\nabla\rho + \rho\nabla^2 G. \tag{A.6}$$

It is noted that the gradient and the Laplacian of an arbitrary scalar function f of $(t-R/c)$ can be converted to its time derivatives. That is,

$$\nabla f(t-R/c) = \nabla(t-R/c)\frac{\partial f}{\partial t} = -\hat{R}\frac{1}{c}\frac{\partial f}{\partial t} \tag{A.7}$$

and

$$\nabla^2 f(t-R/c) = \frac{1}{c^2}\frac{\partial^2 f}{\partial t^2} - \frac{2}{R}\frac{1}{c}\frac{\partial f}{\partial t}, \tag{A.8}$$

where the unit vector $\hat{R} = (\mathbf{r}-\mathbf{r}')/R$ and we have made use of the identities $\nabla R = \hat{R}$ and $\nabla\cdot\hat{R} = 2/R$.

Thereby, the Laplacian can be rewritten as

$$\nabla^2\Phi(\mathbf{r},t) = \frac{1}{\epsilon_0}\int\left\{G(R)\frac{1}{c^2}\frac{\partial^2}{\partial t^2}\rho + \rho\nabla^2 G(R)\right\}dv', \tag{A.9}$$

where ρ stands for $\rho(\mathbf{r}',t-R/c)$. Then, by using the Poisson equation for Green's function and by noting

$$\int \rho(\mathbf{r}',t-R/c)\delta(R)dv' = \rho(\mathbf{r},t), \tag{A.10}$$

we obtain the wave equation for the electric scalar potential Φ

$$\nabla^2\Phi(\mathbf{r},t) - \frac{1}{c^2}\frac{\partial^2}{\partial t^2}\Phi(\mathbf{r},t) = -\frac{1}{\epsilon_0}\rho(\mathbf{r},t). \tag{A.11}$$

By the same way, for the magnetic vector potential **A** which is due to a distribution of current of density **J** and is given by

$$\mathbf{A}(\mathbf{r},t) = \mu_0 \int G(R)\mathbf{J}(\mathbf{r}', t - R/c)dv', \tag{A.12}$$

we have the wave equation for the potential **A**

$$\nabla^2 \mathbf{A}(\mathbf{r},t) - \frac{1}{c^2}\frac{\partial^2}{\partial t^2}\mathbf{A}(\mathbf{r},t) = -\mu_0 \mathbf{J}(\mathbf{r},t). \tag{A.13}$$

A.3 Lorenz gauge and continuity equation

As in a fluid, suppose that the current and charge densities are related to each other by the continuity equation

$$\nabla \cdot \mathbf{J}(\mathbf{r},t) = -\frac{\partial}{\partial t}\rho(\mathbf{r},t). \tag{A.14}$$

Then, by manipulating the wave equations for the two potentials according to the continuity equation, we have

$$\left\{\nabla^2 - \frac{1}{c^2}\frac{\partial^2}{\partial t^2}\right\}\left(\nabla \cdot \mathbf{A} + \mu_0\epsilon_0\frac{\partial}{\partial t}\Phi\right) = -\mu_0\left(\nabla \cdot \mathbf{J} + \frac{\partial}{\partial t}\rho\right) = 0. \tag{A.15}$$

Based on the physical intuition that a null source corresponds to a null initial condition for a potential and then to a null potential, it is supposed that the equality

$$\left\{\nabla^2 - \frac{1}{c^2}\frac{\partial^2}{\partial t^2}\right\} f(\mathbf{r},t) = 0 \tag{A.16}$$

for all space and time implies $f(\mathbf{r},t) = 0$ for all space and time.

Thus, based on the continuity equation, we arrive at the Lorenz gauge

$$\nabla \cdot \mathbf{A}(\mathbf{r},t) = -\mu_0\epsilon_0\frac{\partial}{\partial t}\Phi(\mathbf{r},t). \tag{A.17}$$

It is noted that there is a similarity between the Lorenz gauge and the continuity equation. Alternative derivations of this important gauge can be found in [114, 107].

Appendix B

Explicit Formula for Second-Order Round-Trip Propagation Time

Consider the round-trip propagation where a wave is emitted from a transceiver, reaches and is reflected back from a target, and then is received by the transceiver. Suppose that the target and the transceiver move at velocities $\mathbf{v}_a$ and $\mathbf{v}_b$ with accelerations $\mathbf{a}_a$ and $\mathbf{a}_b$, respectively. The round-trip propagation time τ is the sum of the propagation times for the forward and the backward path.

The propagation time τ_f for the forward path can be given in terms of the transmission-path length $R_t = |\mathbf{R}_t|$, where $\mathbf{R}_t$ is the directed distance from the transceiver to the target. To the second order of normalized speed, formula (1.6) can be used. Thus

$$\tau_f = \frac{R_t}{c}\left\{1 + \frac{u_a}{c} + \frac{1}{2c^2}\left(u_a^2 + v_a^2 + \mathbf{a}_a \cdot \mathbf{R}_t\right)\right\}, \qquad \text{(B.1)}$$

where $\mathbf{v}_a$, $\mathbf{a}_a$, and $\mathbf{R}_t$ are referred to the instant of wave emission from the transceiver, $u_a = \mathbf{v}_a \cdot \hat{R}_t$, and $\hat{R}_t = \mathbf{R}_t / R_t$.

Similarly, the backward propagation time τ_b can be given in terms of the path length $R_{tb} = |\mathbf{R}_{tb}|$, where $\mathbf{R}_{tb}$ is the directed distance from the target to the transceiver. That is,

$$\tau_b = \frac{R_{tb}}{c}\left\{1 + \frac{u_b}{c} + \frac{1}{2c^2}\left(u_b^2 + v_b^2 + \mathbf{a}_b \cdot \mathbf{R}_{tb}\right)\right\}, \qquad \text{(B.2)}$$

where $\mathbf{v}_b$, $\mathbf{a}_b$, and $\mathbf{R}_{tb}$ are referred to the instant of wave reflection from the target, $u_b = \mathbf{v}_b \cdot \hat{R}_{tb}$, and $\hat{R}_{tb} = \mathbf{R}_{tb} / R_{tb}$.

In order to make simpler the calculation of the round-trip propagation time, $\mathbf{v}_b$ and $\mathbf{a}_b$ in the preceding formula are expressed in terms of the corresponding ones referred to the instant of emission, as well as $\mathbf{v}_a$ and $\mathbf{a}_a$. Accordingly, the velocity of the transceiver at the instant of reflection is given by $\mathbf{v}_b + \mathbf{a}_b\tau_f$ and thus, to the second order of normalized speed, the backward propagation time τ_b becomes

$$\tau_b = \frac{R_{tb}}{c}\left\{1 + \frac{1}{c}\left(\mathbf{v}_b + \mathbf{a}_b\frac{R_t}{c}\right)\cdot\hat{R}_{tb} + \frac{1}{2c^2}\left[\left(\mathbf{v}_b\cdot\hat{R}_{tb}\right)^2 + v_b^2 + \mathbf{a}_b\cdot\mathbf{R}_{tb}\right]\right\}, \tag{B.3}$$

where $\mathbf{v}_b$ and $\mathbf{a}_b$ are then referred to the instant of emission, instead of the one of reflection.

Furthermore, it is of convenience to express R_{tb}, $\hat{R}_{tb}$, and $\mathbf{R}_{tb}$ in the preceding formula in terms of their forward counterparts, respectively. Due to the relative motion between the target and the transceiver during the forward propagation, $\mathbf{R}_{tb}$ tends to be different from $-\mathbf{R}_t$. To the second order, one has

$$\begin{aligned}\mathbf{R}_{tb} &= -(\mathbf{R}_t + \mathbf{v}_{ab}\tau_f + \mathbf{a}_{ab}\tau_f^2/2)\\ &= -R_t\left(\hat{R}_t + \frac{\mathbf{v}_{ab}}{c} + \frac{\mathbf{v}_{ab}u_a}{c^2} + \frac{\mathbf{a}_{ab}R_t}{2c^2}\right),\end{aligned} \tag{B.4}$$

where $\mathbf{v}_{ab} = \mathbf{v}_a - \mathbf{v}_b$ is the relative velocity between the target and the transceiver at the instant of emission and $\mathbf{a}_{ab} = \mathbf{a}_a - \mathbf{a}_b$.

Then, by using the binomial expansion to the second order, the preceding formula leads to

$$R_{tb} = R_t\left[1 + \frac{u_{ab}}{c} + \frac{1}{2c^2}\left(2u_{ab}u_a + \mathbf{a}_{ab}\cdot\mathbf{R}_t + v_{ab}^2 - u_{ab}^2\right)\right], \tag{B.5}$$

where the radial relative speed $u_{ab} = \mathbf{v}_{ab}\cdot\hat{R}_t$.

In (B.3), $\mathbf{R}_{tb}$ and $\hat{R}_{tb}$ appear in the second-order terms, for which it suffices to approximate them by $-\mathbf{R}_t$ and $-\hat{R}_t$, respectively. Meanwhile, $\hat{R}_{tb}$ also appears in the first-order term, for which it is approximated to the first order. This gives

$$\hat{R}_{tb} \simeq \frac{-R_t(\hat{R}_t + \mathbf{v}_{ab}/c)}{R_t(1 + u_{ab}/c)} \simeq -\hat{R}_t\left(1 - \frac{u_{ab}}{c}\right) - \frac{\mathbf{v}_{ab}}{c}. \tag{B.6}$$

By using the approximations of R_{tb}, $\hat{R}_{tb}$, and $\mathbf{R}_{tb}$, the backward propagation time τ_b, when given to the second order, becomes

$$\begin{aligned}\tau_b = {} & \frac{R_t}{c}\left[1+\frac{u_{ab}}{c}+\frac{1}{2c^2}\left(u_a^2-u_b^2+v_{ab}^2+\mathbf{a}_{ab}\cdot\mathbf{R}_t\right)\right] \\ & +\frac{R_t}{c}\left[1+\frac{u_{ab}}{c}\right]\frac{\mathbf{v}_b}{c}\cdot\left[-\hat{R}_t\left(1-\frac{u_{ab}}{c}\right)-\frac{\mathbf{v}_{ab}}{c}\right] \\ & +\frac{R_t}{c}\frac{1}{2c^2}\left[(-\mathbf{v}_b\cdot\hat{R}_t)^2+v_b^2-3\mathbf{a}_b\cdot\mathbf{R}_t\right]. \qquad \text{(B.7)}\end{aligned}$$

By a direct expansion to the second order, it is easy to show that

$$\begin{aligned}\tau_b = {} & \frac{R_t}{c}\left\{1+\frac{1}{c}\left(u_{ab}-u_b\right)\right. \\ & \left.+\frac{1}{2c^2}\left[u_a^2-v_a^2+2v_{ab}^2+2v_b^2+(\mathbf{a}_{ab}-3\mathbf{a}_b)\cdot\mathbf{R}_t\right]\right\}, \qquad \text{(B.8)}\end{aligned}$$

where $u_b = \mathbf{v}_b \cdot \hat{R}_t$, instead of $\mathbf{v}_b \cdot \hat{R}_{tb}$.

Thereby, to the second order of normalized speed, the round-trip propagation time is given explicitly by

$$\tau = \frac{2R_t}{c}\left\{1+\frac{1}{c}u_{ab}+\frac{1}{2c^2}\left[u_a^2+v_b^2+v_{ab}^2+(\mathbf{a}_{ab}-\mathbf{a}_b)\cdot\mathbf{R}_t\right]\right\}, \qquad \text{(B.9)}$$

where $\mathbf{R}_t$, $\mathbf{v}_a$, $\mathbf{v}_b$, $\mathbf{a}_a$, and $\mathbf{a}_b$ are all referred to the instant of wave emission from the transceiver. This equation reduces to the radar formula given in the literature [57, 102], if the various second-order terms are omitted. It is noted that the first-order term of the echo time is associated with the radial relative speed between the target and the transceiver. Meanwhile, the second-order terms are associated with the radial component of the individual velocity of the target, the individual speed of the transceiver, the relative speed, and the accelerations.

Appendix C

Deflection of Wave Propagating in Slowly-Varying Medium

Consider a time-harmonic electromagnetic wave at an angular frequency ω, which is propagating in a dielectric medium of refractive index n. It is known that in a source-free region the electric field is governed by the Helmholtz equation

$$\nabla^2\Psi(\mathbf{r}) + k_0^2 n^2 \Psi(\mathbf{r}) = 0, \tag{C.1}$$

where $k_0 = \omega/c$ and Ψ denotes a Cartesian component of the field.

In a homogeneous medium, a uniform plane wave given by the space harmonic $\Psi = e^{i\mathbf{k}\cdot\mathbf{r}}$ is obviously a solution of the preceding equation, where the propagation vector $\mathbf{k}$ determines the propagation direction and, by its magnitude $k = k_0 n$, the rate of phase variation. Without loss of generality, consider a plane wave of which the phase is a constant value ϕ_0 over the plane at $x = x_0$. That is,

$$\Psi(x_0, y, z) = \exp(i\phi_0). \tag{C.2}$$

As the phase has no variations over the y-z plane, the propagation vector has no components in that plane. That is, $\mathbf{k} = \hat{x}k$ which means that the wave is propagating in the x direction. Thus, over a neighboring plane (at $x = x_0 + \delta x$) parallel to the first one, the field is given by

$$\Psi(x_0 + \delta x, y, z) = \exp(i\phi_0 + ik\delta x). \tag{C.3}$$

Next, consider the case where the index n is a very weak function of space. For such a slowly-varying medium, it can be expected that the field is close to the space harmonic and the preceding phase distribution holds. Then, by applying the Taylor series expansion to the index along a transverse (say, z) direction, the field can be rewritten as

$$\begin{aligned}\Psi(x_0+\delta x, y, z) &= \exp\left\{i\phi_0 + ik_0\left[n + \tfrac{\partial n}{\partial z}(z-z_0)\right]\delta x\right\} \\ &= \exp\left\{i\phi_0 + ik\delta x + i\delta k_z(z-z_0)\right\}, \end{aligned} \qquad \text{(C.4)}$$

where $\delta k_z = (\partial k/\partial z)\delta x$ and the index and its derivative are taken at a suitable point $(x_0+\delta x, y, z_0)$ on the second plane.

It is noted that the phase then has a small variation along the transverse direction. That is, the index variation along a transverse z direction introduces a space harmonic $\exp(i\delta k_z z)$ in that direction to the phase distribution. As the propagation vector has no transverse components in the first plane, the rate of change of the transverse z component of the propagation vector is then given by

$$\frac{dk_z}{dx} = \frac{\partial k}{\partial z}. \qquad \text{(C.5)}$$

From the Helmholtz equation it is seen that the phase distribution (C.4) holds in a region with $|(z-z_0)\partial n/n\partial z| \ll 1$.

With the transverse harmonic $\exp(i\delta k_z z)$, the plane wave tends to deflect by a small angle of $\delta\alpha = \sin^{-1}(\delta k_z/k)$ toward the z direction. Thus the deflection per unit propagation length in the x direction is related to the partial derivative of the index in the z direction by

$$\frac{d\alpha}{dx} = \frac{1}{n}\frac{\partial n}{\partial z}. \qquad \text{(C.6)}$$

For the general case where a plane wave propagates in an arbitrary direction, the preceding equation implies that the deflection over a differential propagation length dl is equal to dl times the partial derivative of the index in a transverse direction divided by the index. It is noticed that this result agrees with the transverse component of the vector form of the differential equations of the light rays derived in geometric optics by using a different approach [13].

Bibliography

[1] Yu. N. Aleksandrov, B. I. Kuznetsov, G. M. Petrov, and O. N. Rzhiga, "Techniques of radar astrometry," *Sov. Astron.*, vol. 16, pp. 137–144, July 1972.

[2] D. W. Allan, M. A. Weiss, and N. Ashby, "Around-the-world relativistic Sagnac experiment," *Science*, vol. 228, pp. 69–70, Apr. 1985.

[3] M. Alonso and E. J. Finn, *Physics* (Wesley, New York, 1992), chs. 19, 23, 28, and 36.

[4] T. Alväger, F. J. M. Farley, J. Kjellman, and I. Wallin, "Test of the second postulate of special relativity in the GeV region," *Phys. Lett.*, vol. 12, pp. 260–262, Oct. 1964.

[5] J. D. Anderson, P. B. Esposito, W. Martin, C. L. Thornton, and D. O. Muhleman, "Experimental test of general relativity using time-delay data from *Mariner 6* and *Mariner 7*," *Astrophys. J.*, vol. 200, pp. 221–233, Aug. 1975.

[6] R. Anderson, H. R. Bilger, and G. E. Stedman, ""Sagnac" effect: A century of Earth-rotated interferometers," *Am. J. Phys.*, vol. 62, pp. 975–985, Nov. 1994.

[7] H. J. Arditty and H. C. Lefèvre, "Sagnac effect in fiber gyroscopes," *Opt. Lett.*, vol. 6, pp. 401–403, Aug. 1981.

[8] N. Ashby and J. J. Spilker Jr., "Introduction to relativistic effects on the global positioning system," in *The Global Positioning System: Theory and Applications*, B. W. Parkinson and J. J. Spilker Jr., eds. (American Institute of Aeronautics and

Astronautics, DC, 1996), vol. 1, ch. 18; N. Ashby, "Relativity in the future of engineering," *IEEE Trans. Instrum. Meas.*, vol. 43, pp. 505–514, Aug. 1994.

[9] L. C. Baird, "Relativistic mass," *Am. J. Phys.*, vol. 48, p. 779, Sept. 1980.

[10] L. E. Ballentine, *Quantum Mechanics* (Prentice-Hall, Englewood Cliffs, 1990), sect. 4-3.

[11] E. P. Battey-Pratt and T. J. Racey, "Geometric model for fundamental particles," *Int. J. Theoret. Phys.*, vol. 19, pp. 437–475, June 1980.

[12] J. D. Bjorken and S. D. Drell, *Relativistic Quantum Mechanics* (McGraw-Hill, New York, 1964), ch. 1.

[13] M. Born and E. Wolf, *Principles of Optics* (Pergamon, Oxford, 1980), ch. 3.

[14] K. Brecher, "Is the speed of light independent of the velocity of the source?" *Phys. Rev. Lett.*, vol. 39, pp. 1051–1054, Oct. 1977.

[15] A. Brillet and J. L. Hall, "Improved laser test of the isotropy of space," *Phys. Rev. Lett.*, vol. 42, pp. 549–552, Feb. 1979.

[16] O. Carnal and J. Mlynek, "Young's double-slit experiment with atoms: A simple atom interferometer," *Phys. Rev. Lett.*, vol. 66, pp. 2689–2692, May 1991.

[17] J. P. Cedarholm, G. F. Bland, B. L. Havens, and C. H. Townes, "New experimental test of special relativity," *Phys. Rev. Lett.*, vol. 1, pp. 342–343, Nov. 1958.

[18] J. P. Cedarholm and C. H. Townes, "A new experimental test of special relativity," *Nature,* vol. 184, pp. 1350–1351, Oct. 1959.

[19] D. C. Champeney, G. R. Isaak, and A. M. Khan, "An 'aether drift' experiment based on the Mössbauer effect," *Phys. Lett.*, vol. 7, pp. 241–243, Dec. 1963.

[20] T. E. Chupp, R. J. Hoare, R. A. Loveman, E. R. Oteiza, J. M. Richardson, M. E. Wagshul, and A. K. Thompson, "Results of a new test of local Lorentz invariance: A search for mass anisotropy in ^{21}Ne," *Phys. Rev. Lett.*, vol. 63, pp. 1541–1545, Oct. 1989.

[21] B. Culshaw and I. P. Giles, "Fibre optic gyroscopes," *J. Phys. E*, vol. 16, pp. 5–15, 1983.

[22] J. O. Dickey, P. L. Bender, J. E. Faller, X X Newhall, R. L. Ricklefs, J. G. Ries, P. J. Shelus, C. Veillet, A. L. Whipple, J. R. Wiant, J. G. Williams, and C. F. Yoder, "Lunar laser ranging: A continuing legacy of the Apollo program," *Science*, vol. 265, pp. 482–490, July 1994.

[23] M. Dresden and C. N. Yang, "Phase shift in a rotating neutron or optical interferometer," *Phys. Rev. D*, vol. 20, pp. 1846–1848, Oct. 1979.

[24] A. Einstein, "On the electrodynamics of moving bodies," in *The Principle of Relativity* (Dover, New York, 1952), pp. 37–65. (translated from an article of 1905)

[25] A. Einstein, "On the influence of gravitation on the propagation of light," in *The Principle of Relativity* (Dover, New York, 1952), pp. 99–108. (translated from an article of 1911)

[26] R. M. Eisberg, *Fundamentals of Modern Physics* (Wiley, New York, 1961), chs. 1, 3, 6, and 10.

[27] E. Eisner, "Aberration of light from binary stars – a paradox?" *Am. J. Phys.*, vol. 35, pp. 817–819, Sept. 1967.

[28] L. Essen, "A new aether-drift experiment," *Nature*, vol. 175, pp. 793–794, May 1955.

[29] J. V. Evans, R. A. Brockelman, J. C. Henry, G. M. Hyde, L. G. Kraft, W. A. Reid, and W. W. Smith, "Radio echo observations of Venus and Mercury at 23 cm wavelength," *Astron. J.*, vol. 70, pp. 486–501, Sept. 1965.

[30] S. Ezekiel, S. P. Smith, and F. Zarinetchi, "Basic principles of fiber-optic gyroscopes," in *Optical Fiber Rotation Sensing*, W. K. Burns, ed. (Academic, New York, 1994), ch. 1, pp. 4–7.

[31] D. J. Fixsen, E. S. Cheng, and D. T. Wilkinson, "Large-scale anisotropy in the 2.7-K radiation with a balloon-borne maser radiometer," *Phys. Rev. Lett.*, vol. 50, pp. 620–622, Feb. 1983.

[32] E. B. Fomalont and R. A. Sramek, "Measurements of the solar gravitational deflection of radio waves in agreement with general relativity," *Phys. Rev. Lett.*, vol. 36, pp. 1475–1478, June 1976.

[33] A. P. French, *Special Relativity* (Chapman & Hall, New York, 1968), chs. 2 and 5.

[34] I. A. Getting, "The global positioning system," *IEEE Spectrum*, pp. 36–47, Dec. 1993.

[35] F. Gross, *Relativistic Quantum Mechanics and Field Theory* (Wiley, New York, 1993), ch. 4.

[36] P. D. Gupta, "Exact derivation of the Doppler shift formula for a radar echo without using transformation equations," *Am. J. Phys.*, vol. 45, pp. 674–675, July 1977.

[37] P. D. Gupta, "Relativistic mass," *Am. J. Phys.*, vol. 49, p. 890, Sept. 1981.

[38] T. L. Gustavson, P. Bouyer, and M. A. Kasevich, "Precision rotation measurements with an atom interferometer gyroscope," *Phys. Rev. Lett.*, vol. 78, pp. 2046–2049, Mar. 1997.

[39] J. C. Hafele and R. E. Keating, "Around-the-world atomic clocks: Predicted relativistic time gains," *Science*, vol. 177, pp. 166–168, July 1972; "Around-the-world atomic clocks: Observed relativistic time gains," *Science*, vol. 177, pp. 168–170, July 1972.

[40] F. Hasselbach and M. Nicklaus, "Sagnac experiment with electrons: Observation of the rotational phase shift of electron waves in vacuum," *Phys. Rev. A*, vol. 48, pp. 143–151, July 1993.

[41] M. P. Haugan and C. M. Will, "Modern tests of special relativity," *Phys. Today*, vol. 40, pp. 69–76, May 1987.

[42] H. J. Hay, J. P. Schiffer, T. E. Cranshaw, and P. A. Egelstaff, "Measurement of the red shift in an accelerated system using the Mössbauer effect in Fe^{57}," *Phys. Rev. Lett.*, vol. 4, pp. 165–166, Feb. 1960.

[43] O. Heaviside, "On the electromagnetic effects due to the motion of electrification through a dielectric," *Philos. Mag.*, ser. 5, vol. 27, pp. 324–339, Apr. 1889.

[44] D. Hils and J. L. Hall, "Improved Kennedy-Thorndike experiment to test special relativity," *Phys. Rev. Lett.*, vol. 64, pp. 1697–1700, Apr. 1990.

[45] V. W. Hughes, H. G. Robinson, and V. Beltran-Lopez, "Upper limit for the anisotropy of inertial mass from nuclear resonance experiments," *Phys. Rev. Lett.*, vol. 4, pp. 342–344, Apr. 1960.

[46] H. E. Ives, "Light signals on moving bodies as measured by transported rods and clocks," *J. Opt. Soc. Am.*, vol. 27, pp. 263–273, July 1937.

[47] H. E. Ives and G. R. Stilwell, "An experimental study of the rate of a moving atomic clock," *J. Opt. Soc. Am.*, vol. 28, pp. 215–226, July 1938; "An experimental study of the rate of a moving atomic clock. II," *J. Opt. Soc. Am.*, vol. 31, pp. 369–374, May 1941.

[48] H. E. Ives, "Extrapolation from the Michelson-Morley experiment," *J. Opt. Soc. Am.*, vol. 40, pp. 185–191, Apr. 1950.

[49] J. D. Jackson, *Classical Electrodynamics* (Wiley, New York, 1999), chs. 6 and 11.

[50] J. D. Jackson and L. B. Okun, "Historical roots of gauge invariance," *Rev. Modern Phys.*, vol. 73, pp. 663–680, July 2001.

[51] T. S. Jaseja, A. Javan, J. Murray, and C. H. Townes, "Test of special relativity or of the isotropy of space by use of infrared masers," *Phys. Rev.*, vol. 133, pp. A1221–A1225, Mar. 1964.

[52] C. Jönsson, "Electron diffraction at multiple slits," *Am. J. Phys.*, vol. 42, pp. 4–11, Jan. 1974.

[53] E. D. Kaplan, J. L. Leva, and M. S. Pavloff, "Fundamentals of satellite navigation," in *Understanding GPS: Principles and Applications*, E. D. Kaplan, ed. (Artech, Boston, 1996), ch. 2.

[54] R. J. Kennedy and E. M. Thorndike, "Experimental establishment of the relativity of time," *Phys. Rev.*, vol. 42, pp. 400–418, Nov. 1932.

[55] I. R. Kenyon, *General Relativity* (Oxford, Oxford, 1990), ch. 8.

[56] D. Kleppner, R. F. C. Vessot, and N. F. Ramsey, "An orbiting clock experiment to determine the gravitational red shift," *Astrophys. Space Sci.*, vol. 6, pp. 13–32, 1970.

[57] C. M. Knop, "A note on Doppler-shifted signals," *Proc. IEEE*, vol. 54, pp. 807–808, May 1966.

[58] H. Kragh, "Equation with the many fathers. The Klein-Gordan equation in 1926," *Am. J. Phys.*, vol. 52, pp. 1024–1033, Nov. 1984.

[59] T. P. Krisher, J. D. Anderson, and J. K. Campbell, "Test of the gravitational redshift effect at Saturn," *Phys. Rev. Lett.*, vol. 64, pp. 1322–1325, Mar. 1990.

[60] T. P. Krisher, L. Maleki, G. F. Lutes, L. E. Primas, R. T. Logan, J. D. Anderson, and C. M. Will, "Test of the isotropy of the one-way speed of light using hydrogen-maser frequency standards," *Phys. Rev. D*, vol. 42, pp. 731–734, July 1990.

[61] T. P. Krisher, D. D. Morabito, and J. D. Anderson, "The Galileo solar redshift experiment," *Phys. Rev. Lett.*, vol. 70, pp. 2213–2216, Apr. 1993.

[62] S. K. Lamoreaux, J. P. Jacobs, B. R. Heckel, F. J. Raab, and E. N. Fortson, "New limits on spatial anisotropy from optically pumped ^{201}Hg and ^{199}Hg," *Phys. Rev. Lett.*, vol. 57, pp. 3125–3128, Dec. 1986.

[63] L. D. Landau and E. M. Lifshitz, *The Classical Theory of Fields* (Pergamon, Oxford, 1975), sect. 48.

[64] C. B. Lee, I. D. Jeon, N. S. Chung, T. Morikawa, C. Miki, and K. Yoshimura, "Time comparisons between KSRI and CRL via the geostationary meteorological satellite of Japan," *IEEE Trans. Instrum. Meas.*, vol. 38, pp. 658–660, Apr. 1989.

[65] A. Lenef, T. D. Hammond, E. T. Smith, M. S. Chapman, R. A. Rubenstein, and D. E. Pritchard, "Rotation sensing with an atom interferometer," *Phys. Rev. Lett.*, vol. 78, pp. 760–763, Feb. 1997.

[66] U. Leonhardt and P. Piwnicki, "Optics of nonuniformly moving media," *Phys. Rev. A*, vol. 60, pp. 4301–4312, Dec. 1999.

[67] J. L. Leva, M. Uijt de Haag, and K. Van Dyke, "Performance of standalone GPS," in *Understanding GPS: Principles and Applications*, E. D. Kaplan, ed. (Artech, Boston, 1996), ch. 7.

[68] K. C. Littrell, B. E. Allman, and S. A. Werner, "Two-wavelength-difference measurement of gravitationally induced quantum interference phases," *Phys. Rev. A*, vol. 56, pp. 1767–1780, Sept. 1997.

[69] T. Logsdon, *The NAVSTAR Global Positioning System* (Van Nostrand Reinhold, New York, 1992), chs. 2 and 11.

[70] A. A. Logunov and Yu. V. Chugreev, "Special theory of relativity and the Sagnac effect," *Sov. Phys. Usp.*, vol. 31, pp. 861–864, Sept. 1988.

[71] H. A. Lorentz, "Electromagnetic phenomena in a system moving with any velocity less than that of light," in *The Principle of Relativity* (Dover, New York, 1952), pp. 11–34. (reprinted from an article of 1904)

[72] H. A. Lorentz, *The Theory of Electrons* (Dover, New York, 1952), Arts. 7, 8, and 13, and Note 2. (reprinted from 2nd ed. of 1915)

[73] L. Lorenz, "On the identity of the vibrations of light with electrical currents," *Philos. Mag.*, ser. 4, vol. 34, pp. 287–301, Oct. 1867.

[74] P. Lorrain and D. R. Corson, *Electromagnetic Fields and Waves* (Freeman, San Francisco, 1970), chs. 5 and 6.

[75] P. Lubin, T. Villela, G. Epstein, and G. Smoot, "A map of the cosmic background radiation at 3 millimeters," *Astrophys. J.*, vol. 298, pp. L1–L5, Nov. 1985.

[76] D. Luckey and J. W. Weil, "The velocity of 170-Mev gamma-rays," *Phys. Rev.*, vol. 85, p. 1060, Mar. 1952.

[77] W. M. Macek, J. R. Schneider, and R. M. Salamon, "Measurement of Fresnel drag with the ring laser," *J. Appl. Phys.*, vol. 35, pp. 2556–2557, Aug. 1964.

[78] H. I. Mandelberg and L. Witten, "Experimental verification of the relativistic Doppler effect," *J. Opt. Soc. Am.*, vol. 52, pp. 529–536, May 1962.

[79] P. Marmet, "Stellar aberration and Einstein's relativity," *Phys. Essays*, vol. 9, pp. 96–99, Mar. 1996.

[80] J. C. Maxwell, *A Treatise on Electricity and Magnetism* (Oxford, Oxford, 1998), Arts. 295, 530, and 607. (reprinted from 3rd ed. of 1891)

[81] E. Merzbacher, *Quantum Mechanics* (Wiley, New York, 1998), chs. 12, 18, and 19.

[82] C. Møller, "On the possibility of terrestrial tests of the general theory of relativity," *Suppl. Nuovo Cimento*, vol. 6, pp. 381–398, 1957.

[83] D. O. Muhleman, D. B. Holdridge, and N. Block, "The astronomical unit determined by radar reflections from Venus," *Astron. J.*, vol. 67, pp. 191–203, May 1962.

[84] R. Nevels and C. S. Shin, "Lorenz, Lorentz, and the gauge," *IEEE Antennas Propagat. Mag.*, vol. 43, pp. 70–72, June 2001.

[85] L. B. Okun, "The concept of mass," *Phys. Today*, vol. 42, pp. 31–36, June 1989.

[86] S. J. Ostro, "Planetary radar astronomy," *Rev. Modern Phys.*, vol. 65, pp. 1235–1279, Oct. 1993.

[87] L. A. Page, "Effect of earth's rotation in neutron interferometry," *Phys. Rev. Lett.*, vol. 35, p. 543, Aug. 1975.

[88] L. Page and D. Wilkinson, "Cosmic microwave background radiation," *Rev. Modern Phys.*, vol. 71, pp. S173–S179, 1999.

[89] G. Petit and P. Wolf, "Relativistic theory for picosecond time transfer in the vicinity of the Earth," *Astron. Astrophys.*, vol. 286, pp. 971–977, June 1994.

[90] G. H. Pettengill, R. B. Dyce, and D. B. Campbell, "Radar measurements at 70 cm of Venus and Mercury," *Astron. J.*, vol. 72, pp. 330–337, Apr. 1967.

[91] E. J. Post, "Sagnac effect," *Rev. Modern Phys.*, vol. 39, pp. 475–493, Apr. 1967.

[92] R. V. Pound and G. A. Rebka, Jr., "Resonant absorption of the 14.4-kev γ ray from 0.10-μsec Fe^{57}," *Phys. Rev. Lett.*, vol. 3, pp. 554–556, Dec. 1959.

[93] R. V. Pound and G. A. Rebka, Jr., "Apparent weight of photons," *Phys. Rev. Lett.*, vol. 4, pp. 337–341, Apr. 1960; "Gravitational red-shift in nuclear resonance," *Phys. Rev. Lett.*, vol. 3, pp. 439–441, Nov. 1959.

[94] J. D. Prestage, J. J. Bollinger, W. M. Itano, and D. J. Wineland, "Limits for spatial anisotropy by use of nuclear-spin-polarized ^{9}Be$^+$ ions," *Phys. Rev. Lett.*, vol. 54, pp. 2387–2390, June 1985.

[95] S. Ramo, J. R. Whinnery, and T. Van Duzer, *Fields and Waves in Communication Electronics* (Wiley, New York, 1994), sects. 3.19, 8.3, and 13.3.

[96] R. D. Reasenberg, I. I. Shapiro, P. E. MacNeil, R. B. Goldstein, J. C. Breidenthal, J. P. Brenkle, D. L. Cain, T. M. Kaufman, T. A. Komarek, and A. I. Zygielbaum, "*Viking* relativity experiment: Verification of signal retardation by solar gravity," *Astrophys. J.*, vol. 234, pp. L219–L221, Dec. 1979.

[97] M. Ruderfer, "First-order terrestrial ether drift experiment using the Mössbauer radiation," *Phys. Rev. Lett.*, vol. 5, pp. 191–192, Sept. 1960; vol. 7, p. 361, Nov. 1961.

[98] Y. Saburi, M. Yamamoto, and K. Harada, "High-precision time comparison via satellite and observed discrepancy of synchronization," *IEEE Trans. Instrum. Meas.*, vol. 25, pp. 473–477, Dec. 1976.

[99] L. I. Schiff, *Quantum Mechanics* (McGraw-Hill, New York, 1968), sects. 24 and 44.

[100] R. S. Shankland, S. W. McCuskey, F. C. Leone, and G. Kuerti, "New analysis of the interferometer observations of Dayton C. Miller," *Rev. Modern Phys.*, vol. 27, pp. 167–178, Apr. 1955.

[101] I. I. Shapiro, M. E. Ash, R. P. Ingalls, W. B. Smith, D. B. Campbell, R. B. Dyce, R. F. Jurgens, and G. H. Pettengill, "Fourth test of general relativity: New radar result," *Phys. Rev. Lett.*, vol. 26, pp. 1132–1135, May 1971.

[102] M. I. Skolnik, *Introduction to Radar Systems* (McGraw-Hill, New York, 1980), p. 80.

[103] W. B. Smith, "Radar observations of Venus, 1961 and 1959," *Astron. J.*, vol. 68, pp. 15–21, Feb. 1963.

[104] G. F. Smoot, M. V. Gorenstein, and R. A. Muller, "Detection of anisotropy in the cosmic blackbody radiation," *Phys. Rev. Lett.*, vol. 39, pp. 898–901, Oct. 1977.

[105] A. A. Sokolov, I. M. Ternov, and V. Ch. Zhukovskii, *Quantum Mechanics* (Mir, Moscow, 1984), sect. 17.

[106] J.-L. Staudenmann, S. A. Werner, R. Colella, and A. W. Overhauser, "Gravity and inertia in quantum mechanics," *Phys. Rev. A*, vol. 21, pp. 1419–1438, May 1980.

[107] J. A. Stratton, *Electromagnetic Theory* (McGraw-Hill, New York, 1941), sects. 1.3 and 8.2.

[108] C. T. Tai, "On the presentation of Maxwell's theory," *Proc. IEEE*, vol. 60, pp. 936–945, Aug. 1972.

[109] C. L. Temes, "Relativistic consideration of Doppler shift," *IRE Trans.*, vol. ANE-6, p. 37, Mar. 1959.

[110] J. J. Thomson, "On the electric and magnetic effects produced by the motion of electrified bodies," *Philos. Mag.*, ser. 5, vol. 11, pp. 229–249, Apr. 1881.

[111] K. C. Turner and H. A. Hill, "New experimental limit on velocity-dependent interactions of clocks and distant matter," *Phys. Rev.*, vol. 134, pp. B252–B256, Apr. 1964.

[112] R. F. C. Vessot and M. W. Levine, “A test of the equivalence principle using a space-borne clock,” *Gen. Relativ. Gravit.*, vol. 10, pp. 181–204, Feb. 1979.

[113] R. F. C. Vessot, M. W. Levine, E. M. Mattison, E. L. Blomberg, T. E. Hoffman, G. U. Nystrom, B. F. Farrel, R. Decher, P. B. Eby, C. R. Baugher, J. W. Watts, D. L. Teuber, and F. D. Wills, “Test of relativistic gravitation with a space-borne hydrogen maser,” *Phys. Rev. Lett.*, vol. 45, pp. 2081–2084, Dec. 1980.

[114] E. T. Whittaker, *A History of the Theories of Aether and Electricity* (American Institute of Physics, New York, 1987), vol. 1, ch. 8 and vol. 2, ch. 2.

[115] P. Wolf and G. Petit, “Satellite test of special relativity using the global positioning system,” *Phys. Rev. A*, vol. 56, pp. 4405–4409, Dec. 1997.

[116] A. Zeilinger, R. Gähler, C. G. Shull, W. Treimer, and W. Mampe, “Single- and double-slit diffraction of neutrons,” *Rev. Modern Phys.*, vol. 60, pp. 1067–1073, Oct. 1988.

[117] C.C. Su, “A local-ether model of propagation of electromagnetic wave,” *Eur. Phys. J. C*, vol. 21, pp. 701–715, July 2001.

[118] C.C. Su, “Reinterpretation of the Michelson-Morley experiment based on the GPS Sagnac correction,” *Europhys. Lett.*, vol. 56, pp. 170–174, Oct. 2001.

[119] C.C. Su, “Reinterpretation of Fizeau’s experiment with moving medium in accord with the Sagnac effect due to earth’s rotation,” *J. Electromagnetic Waves Applicat.*, vol. 19, pp. 559–567, Apr. 2005.

[120] C.C. Su, “A local-ether wave equation and the consequent electromagnetic force law,” *J. Electromagnetic Waves Applicat.*, vol. 16, pp. 1275–1290, Sept. 2002.

[121] C.C. Su, “A local-ether wave equation unifying gravitational and electromagnetic forces,” *J. Electromagnetic Waves Applicat.*, vol. 16, pp. 403–410, Mar. 2002.

[122] C.C. Su, "A wave-propagation model for gravitational effects on light deflection and radar echo time," *J. Electromagnetic Waves Applicat.*, vol. 15, pp. 259–268, Feb. 2001.

[123] C.C. Su, "A local-ether wave equation and speed-dependent mass and quantum energy," *Eur. Phys. J. B*, vol. 24, pp. 231–239, Nov. 2001.

[124] C.C. Su, "Reinterpretation of the effects of earth's rotation and gravity on the neutron-interferometry experiment," *Europhys. Lett.*, vol. 60, pp. 1–6, Oct. 2002.

[125] C.C. Su, "Explicit definitions of electric and magnetic fields in potentials and derivation of Maxwell's equations," *Eur. J. Phys.*, vol. 22, pp. L5–L8, May 2001.

[126] C.C. Su, "On the singularity of the static Green's function and the derivations of equations associated with potentials," *J. Electromagnetic Waves Applicat.*, vol. 14, pp. 1251–1259, Sept. 2000.

[127] C.C. Su, "An explicit second-order formula for radar echo time," *J. Electromagnetic Waves Applicat.*, vol. 14, pp. 1525–1531, Nov. 2000.

[128] C.C. Su, "Generalisation of radar Doppler shift for target of arbitrary velocity relative to transceiver," *Electron. Lett.*, vol. 36, pp. 1812–1813, Oct. 2000.

[129] C.C. Su, "A local-ether model of wave propagation complying with the Sagnac correction in the global positioning system," in *IEEE Antennas Propagat. Soc. Int. Symp. Dig.* (July 2000), vol. 3, pp. 1570–1573; in *Bull. Am. Phys. Soc.* (Mar. 2000), p. 637.

[130] C.C. Su, "Modifications of the Lorentz force law complying with Galilean transformations and the local-ether propagation model," `http://arXiv.org/physics/0211019`; in *IEEE Antennas Propagat. Soc. Int. Symp. Dig.* (July 2001), vol. 1, pp. 208–211; in *Bull. Am. Phys. Soc.* (Mar. 2001), p. 1144.

[131] C.C. Su, "Modifications of Maxwell's equations invariant under Galilean transformations," in *IEEE Antennas Propagat. Soc. Int. Symp. Dig.* (July 2001), vol. 1, pp. 212–215.

[132] C.C. Su, "Local-ether wave equation of electric field and interferometry experiments with moving medium and path," `http://arXiv.org/physics/0208082`.

[133] C.C. Su, "A local-ether wave equation and the Galilean-invariant electromagnetic force law," in *IEEE Antennas Propagat. Soc. Int. Symp. Dig.* (July 2001), vol. 1, pp. 216–219; in *Bull. Am. Phys. Soc.* (Mar. 2001), p. 1144.

[134] C.C. Su, "Modifications of Schrödinger's equation complying with the effect of earth's rotation on quantum energy in atoms and with the electromagnetic force," `http://arXiv.org/physics/0208083`.

[135] C.C. Su, "A quantum theory of gravity based on the local-ether wave equation," in *Bull. Am. Phys. Soc.* (Mar. 2001), pp. 1143-1144.

[136] C.C. Su, "A quantum-mechanical wave equation complying with the experiment of circumnavigation atomic clocks," in *Bull. Am. Phys. Soc.* (Apr. 2000), p. 61.

[137] C.C. Su, "Resonant absorption between moving atoms due to Doppler frequency shift and quantum energy variation," `http://arXiv.org/physics/0208084`; in *Bull. Am. Phys. Soc.* (Apr. 2001), p. 99.

[138] C.C. Su, "A quantum-mechanical origin of the mass-variation law," in *Bull. Am. Phys. Soc.* (Apr. 2000), p. 59.

[139] C.C. Su, "Reinterpretation of matter-wave interference experiments based on the local-ether wave equation," `http://arXiv.org/physics/0208085`.

Index

Aberration, stellar, 50
  annual, 50
  diurnal, 50
Acceleration, 23, 106, 124, 146
  and natural frequency, 106
  electrostatic, 67, 107, 170
  evaluated in expectation value, 106, 111, 127
  gravitational, 127
Altitude, effect with, 131, 136, 153, 154
Ammonia maser, output frequency from, 172
  Galilean relativity in, *see* Galilean relativity
  reinterpretation of, *see* Local-ether interpretation
Ampère's law, 2
  modifications of, *see* Modifications
Angular frequency, *see* Electromagnetic wave, Matter wave
  and mass, *see* Mass
Anisotropy, spatial, 49
Anisotropy, terrestrial, 44, 46, 178, 191
  in atomic clock rate, 141, 153
  in Bragg angle, 193, 194
  in cavity resonant frequency, 40
  in mass, 186
  in matter wavelength, 191, 193
  in phase variation, 46, 52, 88
Antenna, 27, 69, 70
Antenna temperature, 47
Atomic clock, 24, 26, 137, 141, 152, 153, 166
Atomic clock rate, 152
  adjustment of, *see* Global positioning system
  and transition frequency, 150, 162
  anisotropy in, *see* Anisotropy, terrestrial
  gravitation-dependence of, 153, 154
  speed-dependence of, 141, 150, 153, 154, 161, 165
  synchronism in, *see* Global positioning system
Augmentation operator, 110–112, 116, 117, 128, 135
  definition of, 108
Augmented scalar potential, *see* Potential
Augmented vector potential, *see* Potential

Beat frequency, 40, 45, 173, 176
Binary stars, 44, 51
Blackbody radiation, 47
Blackbody temperature, 47

Bragg angle, 190, 192, 194
  anisotropy in, *see* Anisotropy, terrestrial
Bragg reflection, 181, 190, 193, 194
  of electron wave, 190, 191
  of neutron wave, 193
Breakdown
  of Galilean relativity, *see* Galilean relativity
  of spatial isotropy, *see* Spatial isotropy
  of terrestrial isotropy, *see* Terrestrial isotropy
Bucherer's experiment, 8, 141

Cathode-ray tube, 67
  Galilean relativity in, *see* Galilean relativity, in magnetic force
Causality, 155
Charge, 2, 9, 61, 94, 103, 107, 124, 126, 142
  conservation of, 4, 78
  of electron, 107
  polarization, 69, 80, 82, 84
Charge density, 2, 3
  matrix, 63, 76, 79, 114
  net, 63, 79, 81, 114
  polarization, 80
  source, 60, 63, 76, 78, 113, 114
Classical propagation model, 21, 30
Clock-rate adjustment, *see* Global positioning system
Collision, in neutron interference, 195, 196, 198
Conservation, *see* Charge, Energy, Momentum
Constant-speed condition, 157, 158, 175
Continuity equation, 4, 209
  for potentials, 79, 209
  matrix-frame, 79
Cosmic microwave background radiation (CMBR), 47
  anisotropy in, 49
Coulomb gauge, 115
Current
  conduction, 10, 58, 63, 64, 68, 74, 95, 101, 114
    Galilean relativity in, *see* Galilean relativity
  convection, 3, 7, 57, 58, 74
  magnetization, 81, 95
  polarization, 81, 83
Current density, 2, 3, 74
  magnetization, 80
  neutralized, 58, 63, 75, 78, 79, 81, 94, 114
    and conduction current, 64
  polarization, 80

Davisson-Germer experiment, 181, 190
de Broglie postulates, for matter wave, 147, 181, 185
de Broglie wavelength, *see* Matter wave
Delta function, 207
Dielectric, 80, 85, 129, 213
Dispersion, of matter wave, 143, 144, 146, 147, 183–187
Doppler effect, 46, 47, 136, 137, 150, 161, 163
  first-order, 47, 48
  round-trip, 52
  second-order, 8, 52, 161, 164
  third-order, 177
  transverse, 53
Double-slit diffraction, *see* Interference, of matter wave

Drift velocity, *see* Velocity
Dufour-Prunier experiment, 90
  index-dependence of phase difference in, 90
  reinterpretation of, *see* Local-ether interpretation

Earth's orbital motion, effect of, 25, 26, 43
  in CMBR, 48
  in interplanetary microwave link, 157
  in interplanetary radar, 32
  in Michelson-Morley experiment, 19, 39
  in Roemer's observations, 19
  in stellar aberration, 50
Earth's rotation, effect of, 32, 40, 44, 48, 50–52, 85, 87, 97, 169, 170, 185, 186, 191, 198
  in global positioning system, 25, 26, 154
  in Hafele-Keating experiment, 141, 153
  in interplanetary radar, 32
  in Michelson-Gale experiment, 41, 43
  in Michelson-Morley experiment, 19, 39
  in microwave-link experiment, 26
  in Sagnac interferometry, 43, 90, 197, 200
  see also Interference, of matter wave
Earth's rotation rate, 25, 43, 87, 88, 196
  detection of, 43, 200
Earth-centered earth-fixed (ECEF) frame, *see* Frame
Earth-centered inertial (ECI) frame, *see* Frame
Effector, 102, 126
  definition of, 60
Ehrenfest's theorem, 127
  generalization of, 10, 110
Einstein, A., 6, 39, 57, 58, 74, 132, 147, 161, 186
Electric field, *see* Field
Electric induction force, *see* Electromagnetic force
Electric scalar potential, *see* Potential
Electromagnetic force, 10, 65, 114
  and augmented potentials, 61, 62, 112
  derivation of, from local-ether wave equation, 112
  electric force, 57, 94
    electric induction force, 3, 65, 66
    electrostatic force, 3, 65, 70, 71, 106
  magnetic force, 3, 57, 58, 66, 67, 71, 74
    magnetic induction force, 65
    magnetostatic force, 65
  proposed model of, 61
Electromagnetic wave
  angular frequency of, 82, 83, 136
  gamma ray, 44, 136, 137, 173
  microwave, 24, 26, 27, 47, 49, 130, 133, 150, 154, 155, 171
  optical wave, 39, 90, 133
    in moving medium, *see* Moving medium
  propagation vector of, 82,

85, 213
  short wave, 50, 131
  x ray, 190
Electromotive force, 71
Electrostatic acceleration, 67, 107, 170
Electrostatic force, *see* Electromagnetic force
Energy
  and angular frequency, 134, 149, 151, 187
  and mass, 187
  conservation of, 5, 188
  gravitational, 126, 134, 198
  kinetic, 187, 198
  potential, 107, 126
  quantum, 134, 149, 151, 187
  quantum-state, 9, 107, 135, 149, 166
  rest, 134
Ether, 21, 34, 57, 84
  local, 11, 34, 35
    CMBR, 48
    earth, 35, 36, 50, 51
    galaxy, 35
    sun, 35, 50
  universal, 19, 20, 49
Expectation value, 9, 105, 133, 145, 151

Faraday's law, 2, 96
  modifications of, *see* Modifications
Fiber gyroscope, 89
Fiber-link experiment, one-way, 44, 86
  reinterpretation of, *see* Local-ether interpretation
  spatial isotropy in, *see* Spatial isotropy
Field
  electric, 2, 94
    definition of, 3, 66, 76
  magnetic, 2, 67, 94
    definition of, 3, 66, 76
Fine-structure constant, 107
Fizeau's experiment, with moving medium, 90
  reinterpretation of, *see* Local-ether interpretation
Force, *see* Electromagnetic force, Gravitational force
Frame
  atom, 116–119, 148, 149, 165
  ECEF, 25, 29
  ECI, 25, 26, 35, 61, 78, 88, 130, 141, 143, 152–154, 156, 161, 175, 185, 199, 201
  effector, 61, 65, 111, 114
  galaxy, 25, 29
  heliocentric inertial, 25, 28, 29, 36, 50, 130, 141, 143, 156
  laboratory, 30, 66–68, 95, 169, 185, 188, 190, 194, 195
  local-ether, 61, 66, 78, 79, 93, 103, 104, 108, 109, 115–117, 125, 143, 148, 188
  matrix, 64–66, 68, 71, 77–80, 83, 93–96, 114, 115
  propagation, *see* Propagation frame
  tacitly adopted, 68, 77, 92, 96, 118, 149
Frame-invariance, 21, 28, 32, 57, 58, 64, 77
Frequency
  angular, *see* Electromagnetic wave, Matter wave
  beat, *see* Beat frequency

cutoff, 185
natural, *see* Natural frequency
plasma, 185
resonant, 40, 41, 45, 149
transition, *see* Transition frequency
Frequency shift, 48, 53, 155–157, 161, 167, 168, 170, 171, 173, 174
atom speed-dependent, *see* Transition frequency
Doppler, *see* Doppler effect
gravitation-dependent, *see* Transition frequency, Gravitational effect, in redshift
stellar, *see* Stellar frequency shift
Fresnel drag effect, 84
reinterpretation of, *see* Local-ether interpretation

Galilean invariance, *see* Invariance
Galilean relativity, 67, 177, 188
breakdown of, 119, 178, 193
in ammonia maser, 177
in Bragg reflection, 190
in conduction current, 10, 64, 77
in Doppler effect, 47
in electric induction, 95
in inductor, 95
in transformer, 95
in Ives-Stilwell experiment, 177
in magnetic force, 68
in cathode-ray tube, 68
in motor, 68
in Mössbauer rotor experiment, 177
in neutron interferometry, 196, 197
in optical interferometry, 92
in quantum effects, 119, 149
in radar, 38
Galilean transformations, 5, 57, 58, 65, 75, 81, 83, 101, 114, 116, 117, 148, 188
Gauge, *see* Coulomb gauge, Lorenz gauge
Gauss's law
for electric field, 2
modifications of, *see* Modifications
for magnetic field, 2
General relativity, 49, 122, 128, 130, 132, 133, 136, 153, 155
Geocentric inertial frame, *see* Frame, ECI
Global positioning system (GPS), 24
clock synchronism in, 153, 175
clock-rate adjustment in, 154
Doppler effect in, 47
gravitation-dependent clock rate in, 154
gravitation-dependent propagation time in, 49, 130
pseudorange in, 25
Sagnac pseudorange correction in, 25, 26
speed-dependent clock rate in, 154
Gravitational constant, 49, 125, 143
Gravitational effect
in atomic spectrum, 137
in clock rate, *see* Atomic clock rate
in deflection of light, 50,

    122, 131, 132
  in GPS, *see* Global positioning system
  in neutron interference, 196–198
  in precession of perihelion, 128
  in radar echo time, 49, 122, 130, 131
  in redshift, 122, 135–137
  in transition frequency, *see* Transition frequency
  on quantum energy, 134, 151
  on speed of light, 49, 125, 129, 131, 132
Gravitational force, 128
  derivation of, from local-ether wave equation, 127
Gravitational index, 49, 129, 131, 134, 143
  definition of, 125
Gravitational mass, *see* Mass
  derivation of, from local-ether wave equation, 127
Gravitational potential, *see* Potential
Gravitational redshift, *see* Gravitational effect
  transition-dependence of, 138
Gravity, 195
  acceleration of, 127, 128, 136, 195
Green's function, 207
  singularity in, 208

Hafele-Keating experiment, 141, 152, 166
  anisotropy in atomic clock rate in, 153
  reinterpretation of, *see* Local-ether interpretation
Hamiltonian, 110, 126, 198
Harzer experiment, 89
  and fiber gyroscope, 89
  index-dependence of phase difference in, 89
  reinterpretation of, *see* Local-ether interpretation
Heaviside, O., 57, 74
Heliocentric inertial frame, *see* Frame
Helmholtz equation, 149, 213
Heterodyne experiment, cavity, 40, 45
Hidden restrictions
  for Lorentz force law, 68, 115
  for Maxwell's equations, 96
  for phase speed in moving medium, 84
  for Schrödinger's equation, 119
Hughes-Drever experiment, 157
  reinterpretation of, *see* Local-ether interpretation
  spatial isotropy in, *see* Spatial isotropy
Hydrogen maser, 44, 86, 156
Hyperfine splitting, 137

Identity, of inertial and gravitational mass, *see* Mass
Induction force, *see* Electromagnetic force
Inductor, 95, 96
  Galilean relativity in, *see* Galilean relativity, in electric induction
Inertial mass, *see* Mass
  derivation of, from local-ether wave equation, 106
Initial condition, 2, 79, 80, 209

Interference, of electromagnetic wave
  effect of earth's rotation in, 39–41, 92
  in Michelson-Morley-type experiment, 39, 40
  in Sagnac interferometry, 41, 89, 90
  with moving medium, 88, 90
Interference, of matter wave, 181
  effect of earth's gravity in, 196–198
  effect of earth's rotation in, 193, 194, 197, 198
  in Bragg reflection, 190, 193
  in double-slit diffraction, 191
  in Sagnac interferometry, 200
  loop interferometer for, 194, 198
Interplanetary radar, *see* Radar
Interplanetary wave propagation, *see* Propagation, wave
Interstellar wave propagation, *see* Propagation, wave
Invariance
  Galilean, 5, 6, 57–59, 77, 105, 111, 188
    see also Galilean relativity
  local Lorentz, 32, 44, 158, 201
  Lorentz, 7, 8, 58, 74
Inverse square law, 128
Isotropy, *see* Spatial isotropy, Terrestrial isotropy
Ives-Stilwell experiment, 168
  Galilean relativity in, *see* Galilean relativity
  reinterpretation of, *see* Local-ether interpretation

Kennedy-Thorndike experiment, 45
  reinterpretation of, *see* Local-ether interpretation
Kinetic energy, *see* Energy
Klein-Gordan equation, 103, 182

Laboratory velocity, *see* Velocity
Latitude, effect with, 41, 52, 87, 153, 154, 193, 197
Length contraction, *see* Special relativity
Local ether, *see* Ether
Local-ether frame, *see* Frame
Local-ether interpretation
  of ammonia maser, 173
  of clock-rate adjustment in GPS, 155
  of Dufour-Prunier experiment, 90
  of Fizeau's experiment, 91, 92
  of Fresnel drag effect, 84
  of gravitational redshift, 136, 152, 155
  of gravity-induced neutron interference, 195, 196
  of Hafele-Keating experiment, 153
  of Harzer experiment, 89
  of Hughes-Drever experiment, 158
  of Ives-Stilwell experiment, 171
  of Kennedy-Thorndike experiment, 45
  of matter-wave Sagnac effect, 200

    of Michelson-Gale experiment, 43
    of Michelson-Morley experiment, 39
    of microwave-link experiment
      earthbound, 156
      interplanetary, 156, 157
    of Mössbauer rotor experiment, 175
    of one-way fiber-link experiment, 45
    of rotation-induced neutron interference, 197
Local-ether propagation model, 78, 102, 157, 163
    definition of, 34
Local-ether wave equation, *see* Wave equation
Local Lorentz invariance, *see* Invariance
Longitude, effect with, 26
Lorentz force law, 2, 57, 68, 74, 101, 115
    hidden restrictions for, 68, 115
    modifications of, *see* Modifications
Lorentz invariance, *see* Invariance
Lorentz mass-variation law, 8, 147, 161, 186
Lorentz transformation, 6, 10, 30, 58, 74, 82, 84, 101, 147, 161, 186
Lorentz, H. A., 2–4, 6, 8, 57, 74, 147, 186
Lorenz gauge, 4, 79
    and Coulomb gauge, 115
    derivation of, 209
Lorenz retarded potential, *see* Potential
Lorenz, L. V., 3, 4
Low-speed condition, 61, 69–71, 96, 97, 106, 109, 112, 114, 116, 118, 119, 127, 134, 144, 151, 187, 188, 195
    definition of, 64
Lunar laser ranging, 36

Magnet, 68
Magnetic deflection, 57, 67
Magnetic field, *see* Field
Magnetic force, *see* Electromagnetic force
    Galilean relativity in, *see* Galilean relativity
Magnetic vector potential, *see* Potential
Magnetization current, *see* Current
Magnetization vector, 80
Mass
    and angular frequency, 147, 186
    and energy, 187
    and natural frequency, *see* Natural frequency
    anisotropy in, *see* Anisotropy, terrestrial
    derivation of, from local-ether wave equation, 106, 127
    gravitational, 128, 198
    identity of inertial and gravitational, 15, 128, 195, 198
    inertial, 106, 107, 112, 124, 127, 128, 198
    of electron, 107, 161
    origin of, 107, 128, 147, 182
    rest, 8, 9, 106–109, 112, 124, 126, 127, 146, 184, 185

    speed-dependent, 8, 16, 147–149, 185
Mass-variation factor, 8, 16, 148–150, 152, 161, 162, 165
Matrix, *see* Neutralizing matrix
Matrix-frame continuity equation, *see* Continuity equation
Matrix-frame wave equation, *see* Wave equation
Matter wave
    angular frequency of, 133, 134, 143, 146, 147, 151, 183, 184, 186
    of electron, 191
    of neutron, 193
    propagation vector of, 116, 143, 146, 147, 183, 184, 186, 189, 201
    wavelength of, 147, 184, 186, 190–192
Matter-wave interference, *see* Interference, of matter wave
Maxwell's equations, 2, 74
    derivation of, 4
    hidden restrictions for, 96
    modifications of, *see* Modifications
Maxwell, J. C., 3, 57, 74
Michelson-Gale experiment, 41, 43, 200
    reinterpretation of, *see* Local-ether interpretation
Michelson-Morley experiment, 32, 38
    reinterpretation of, *see* Local-ether interpretation
Microwave link
    intercontinental, 26
    interplanetary, 156
    satellite, 26
    spacecraft, 33, 155, 156
Modifications
    of Ampère's law, 93, 94
    of Faraday's law, 92, 95
    of Gauss's law for electric field, 93
    of Lorentz force law, 13, 66, 114
    of Maxwell's equations, 14, 94
    of Schrödinger's equation, 14, 16, 109
Momentum, 8, 108, 187
    and propagation vector, 187
    canonical, 198
    conservation of, 5, 188
Momentum operator, 9, 108, 110, 111, 127
Mössbauer effect, 137, 173
Mössbauer rotor experiment, 173
    Galilean relativity in, *see* Galilean relativity
    reinterpretation of, *see* Local-ether interpretation
Motor, 68
    Galilean relativity in, *see* Galilean relativity, in magnetic force
Moving medium, 82
    and Fresnel drag effect, 84
    effect of polarization in, 84
    Fizeau's experiment with, 90
    interference with, 90
    phase speed in, 83, 84
    propagation constant in, 82, 85

Natural frequency, 12, 107, 116, 123, 126, 134, 142, 143, 146, 182, 186, 200
    and acceleration, 106, 146

    and dispersion, 143, 183
    and rest mass, 106, 124, 128, 146
    definition of, 103
    of electron, 107
Net charge density, *see* Charge density
Neutralization, 58, 63, 65, 68–70, 95, 115, 117, 119
Neutralized current density, *see* Current density
Neutralizing matrix, 58, 63, 67, 94, 114
Neutron interference, 193, 194, 198
Newton's laws of motion, 4
    second of, 106, 112, 127
    third of, 69
Nuclear magnetic interaction, 158

Open-circuit voltage, 94, 95
Orbital motion, effect of
    of earth, *see* Earth's orbital motion
    of Sun, 29, 32, 36, 48

Permeability, 3, 80, 107
Permittivity, 3, 80, 84, 104, 107
Perturbation method, 118, 133, 134, 151
Phase variation
    of electromagnetic wave, 46, 85–90
    of matter wave, 189, 195
Planck's constant, 107, 108, 124
    origin of, 103, 107
Plasma, 71, 185
Poincaré, J. H., 6, 74, 187
Polarization charge, *see* Charge
Polarization current, *see* Current
Polarization vector, 80
Position operator, 9, 105, 110, 127, 145
Position vector, 21, 84, 103, 105, 115, 117, 124, 143, 148, 182
Potential
    augmented scalar, 60, 62–64, 111–114
    augmented vector, 61, 63, 65, 110, 112–114
    electric scalar, 2, 9, 63, 77, 78, 102, 106–117, 123, 126, 133, 134, 142, 148
        definition of, 103
    gravitational, 35, 49, 125, 126, 133, 134, 142
    magnetic vector, 2, 9, 63, 65, 77, 109, 114, 115, 117
    retarded, 3, 208
Pound-Rebka experiment, 136, 137
    gravitational redshift in, 136
        reinterpretation of, *see* Local-ether interpretation
Principle of relativity, *see* Relativity, principle of
Propagation delay time, 3, 21, 25, 45, 60, 61, 69, 77, 78, 95, 103, 129
    round-trip, 19, 23, 27, 38–40, 130, 210
Propagation frame, unique, 21, 24, 26, 29
    for mechanical wave, 103
    proposed for electromagnetic wave, 34, 59
    proposed for matter wave, 102
    switchability of, 34, 130, 141, 156, 157

Propagation model, *see* Classical propagation model, Local-ether propagation model
Propagation range, 22, 23, 25, 27, 46, 60, 66, 67, 103, 129, 163, 164, 177
  and transmission path, 21
  apparent, 30, 67
  definition of, 21
  path-velocity modification of, 85
  receiver-velocity modification of, 22, 163
Propagation vector, *see* Electromagnetic wave, Matter wave
Propagation velocity, 21, 23, 59, 112
  in dielectric medium, 83
  in gravitational potential, 49, 129, 131
  in magnetic medium, 80
  in moving medium, 80, 83
  see also Speed of light
Propagation, wave
  earthbound, 24–26, 38, 51, 129
  interplanetary, 27, 47, 130
  interstellar, 48, 50
Pseudorange, *see* Global positioning system
Pseudorange correction, *see* Global positioning system

Quadratic term, omitted, 64, 82, 116, 118, 119, 128, 170, 171, 177
Quantum energy, *see* Energy
Quantum energy variation
  atom speed-induced, 151
  gravitation-induced, 134, 151
Quasi-static case, 60, 77, 94, 113

Radar
  Doppler frequency shift, 52
  earthbound, 37, 52
  echo time, 27, 212
  interplanetary, 27, 130
Reference frame, *see* Frame
Refractive index, 82, 129, 213
  effect of, 86, 89, 91, 131
Relative velocity, 6, 28
  Newtonian, 23, 24, 47, 61, 64, 69, 86, 105, 113, 164
  non-simultaneous, 61
Relativistic mass, *see* Mass, speed-dependent
Relativity, *see* Galilean relativity, Special relativity, General relativity
Relativity, principle of, 4, 6, 10, 30, 37, 38, 47
  see also Galilean relativity
Resonance, 133, 149
Resonant absorption, 136, 137, 150
  condition of, 167, 168, 172
  deviation from, 136, 167, 173, 174, 178
Resonant cavity, 40, 45
Resonant frequency, 40, 41, 45, 149
Rest energy, 134
Rest mass, *see* Mass
  origin of, 106
Rest transition frequency, *see* Transition frequency
Retarded potential, *see* Potential
Roemer's observations, 19, 47
Rotation, effect with, 174

  - of earth, *see* Earth's rotation
  - of interferometer, 42, 88, 199

- Sagnac effect, for electromagnetic wave, 21, 22, 30, 66, 163
  - due to earth's orbital motion, 32, 36
  - due to earth's rotation, 25, 26, 32, 36, 40, 41, 45, 51, 92
  - due to moving path, 40, 41, 85
  - due to moving receiver, 21
  - in fiber-link experiment, 45
  - in global positioning system, *see* Global positioning system
  - in interplanetary radar, 28
  - in Michelson-Gale experiment, 41
  - in Michelson-Morley experiment, 38
  - in microwave-link experiment, 26
  - in rotating interferometer, 41, 88
  - one-way, 23, 24, 44, 51
  - round-trip, 24, 38, 40
- Sagnac effect, for matter wave, 197, 200
- Sagnac-effect deviation, 30, 31, 67, 68, 118
- Satellite
  - geostationary, 26, 155
  - half-synchronous, 24, 153
  - low-earth-orbit, 53
- Scattering, 69
  - of gamma ray, 136, 173
  - of matter wave, 190
- Schrödinger's equation, 9, 107, 115, 149
  - hidden restrictions for, 119
  - modifications of, *see* Modifications
  - time-independent, 149
- Self-adjoint operator, 105, 110, 133
- Semistable particle, radiation from, 44
- Snell's law of reflection, 189, 190
- Spatial anisotropy, 49
- Spatial isotropy, 8, 175
  - breakdown of, 176
  - in ammonia maser, 176
  - in cavity heterodyne experiment, 45
  - in Hughes-Drever experiment, 157, 175
  - in Kennedy-Thorndike experiment, 45
  - in Mössbauer rotor experiment, 176
  - in one-way fiber-link experiment, 45, 87
- Special relativity, 6, 30, 39, 58, 84, 141, 153, 155, 161, 186
  - Doppler effect in, 161
  - four-vector in, 168
  - length contraction in, 30, 150, 166, 175
  - time dilation in, 8, 30, 141, 150, 166, 168, 173
  - velocity addition in, 8, 83
- Spectrograph, 161, 168, 169, 171
- Spectroscopy, 107
- Spectrum, atomic, 9, 47, 137
  - gravitation-dependence of, 137
- Speed of light, 3, 19, 21, 25,

27, 34, 47, 49, 59, 78, 80, 103, 141, 185
    constancy of, 30, 44
    gravitation-dependent, *see* Gravitational effect
Speed, limit of, 185
Speed-dependence
    of angular frequency, 146, 184
    of clock rate, *see* Atomic clock rate
    of mass, *see* Mass
    of quantum energy, 149, 151
    of quantum-state energy, 149
    of transition frequency, *see* Transition frequency
Spin, 135, 138, 158, 182
Spin-spin interaction, 135, 137, 152
Stellar frequency shift, 47, 137
    due to Doppler effect, 137
    due to gravitational effect, 137
Synchrotron, 185
    radiation from, 44

Terrestrial anisotropy, *see* Anisotropy, terrestrial
Terrestrial isotropy, 68, 95, 176
    breakdown of, 178
Test of local-ether wave equation, 44, 46, 49, 53, 90, 118, 137, 138, 157, 201
    with Bragg reflection, 194
    with cavity heterodyne experiment, 41
    with magnetic deflection, 68
    with Michelson-Morley experiment, 39
    with one-way-link rotor experiment, 52, 88
Thomson, J. J., 57, 62
Time comparison, 26
    synchronization error in, 26
Time derivative, 96, 115
    atom-frame, 117, 148
    effector-frame, 61, 62, 65, 111, 114
    local ether-frame, 81, 103, 105, 108, 117, 148, 187
    matrix-frame, 65, 66, 78, 79, 81, 94, 96, 114
Time dilation, *see* Special relativity
Time evolution equation, 104, 117, 124, 126, 144, 146, 148
    and Schrödinger's equation, 107, 109, 118, 147
Total internal reflection, 50, 131
Transformation, of space and time coordinates, *see* Galilean transformations, Lorentz transformation
Transformer, 94
    Galilean relativity in, *see* Galilean relativity, in electric induction
Transition frequency, 9, 135, 149
    atom speed-dependent, 150–154, 156, 161, 165
    gravitation-dependent, 135, 136, 151–154
    rest, 150, 152, 165–167, 174
Transmission path, 20, 40, 163, 169, 171
    and propagation range, 21
    length of, 20, 44, 66, 163, 174, 210
Transverse Doppler shift, *see* Doppler effect

Unified quantum theory, of electromagnetic and grav-

itational forces, 15, 127, 128
Uniqueness and switchability, of propagation frame, 34, 157

Velocity
  atom, 116, 119, 148–150, 152, 161, 165
  drift, 58, 64, 71, 78, 79, 95, 114, 117, 118
  effector, 60, 62, 65, 69, 105, 106, 110, 112, 127
  evaluated in expectation value, 9, 105, 106, 110, 127, 145, 184
  ground, 68, 95, 153
  group, 183, 184
  individual, 37, 86
  laboratory, 31, 67, 68, 82, 84, 88, 91, 92, 95, 119, 170–176, 178, 190, 192–197
  lattice, 196, 199
  matrix, 63, 81, 82, 90, 97, 114
  path, 85, 88, 92
  phase, 83, 84
  propagation, *see* Propagation velocity
  receiver, 22, 163
  relative, *see* Relative velocity
  source, 60, 108, 110, 163
Velocity addition, *see* Special relativity

Wave equation
  d'Alembert operator in, 7, 78, 125
  for fields, 79
  for potentials, 3, 78, 208
  local-ether, 12, 14, 15, 78–81, 103, 108, 116, 124–126, 129, 133, 143, 182
  matrix-frame, 81–83
  proposed for matter wave, 103
Wave motion, effect of, 70, 96, 107, 128, 146, 147, 184
Wave-operator deviation, 93, 94, 96
  and Sagnac-effect deviation, 97
Wavefunction, 9, 102, 107, 124, 133, 142, 145
  reduced, 104, 105, 109, 116, 126, 144, 147
Waveguide, 69, 171, 185
Weak-potential condition, 70, 106, 109, 112, 118, 119, 126, 134, 144, 151
  definition of, 104, 125

Young's slit diffraction, *see* Interference, of matter wave

Zeeman splitting, 158

ISBN 957-41-1097-4
90000
9 789574 110971

http://academic.nthu.edu.tw/publish/